Bioplastic-eating animals: Polyhydroxyalkanoate degrading enzymes in a chemosymbiotic worm

Dissertation

zur Erlangung des Grades eines

Doktors der Naturwissenschaften

– Dr. rer. nat.-

dem Fachbereich Biologie/Chemie

der Universität Bremen

vorgelegt von

Caroline Zeidler

Bremen, Oktober 2023

Die vorliegende Arbeit wurde in der Zeit von Mai 2019 bis Oktober 2023 in der Abteilung Symbiose am Max-Planck-Institut für Marine Mikrobiologie in Bremen unter der Leitung von Prof. Dr. Nicole Dubilier und direkter Betreuung durch Dr. E. Maggie Sogin durchgeführt.

The research presented in this thesis was conducted from May 2019 to October 2023 in the Department of Symbiosis at the Max-Planck Institute for Marine Microbiology in Bremen under the leadership of Prof. Dr. Nicole Dubilier and direct supervision by Dr. E. Maggie Sogin.

Gutachterinnen / Reviewers

Frau Prof. Dr. Nicole Dubilier

Herr Prof. Dr. Tilmann Harder

Frau Assoz.-Prof. Dr. Jillian Petersen

Tag des Promotionskolloquium / Date of the doctoral defense 11th of December 2023

"**All our dreams can come true, if we have the courage to pursue them**."

-Walt Disney-

Table of Contents

Summary 1

Zusammenfassung 3

Introduction 5

Aims of the dissertation 31

Chapter I | Animals degrade the bioplastic polyhydroxyalkanoate 51

Chapter II | Can Chromatiales bacteria degrade their own PHA? 136

Chapter III | Earthworms degrade the bioplastic polyhydroxyalkanoate 191

Discussion 228

Acknowledgements 247

Contributions to manuscripts and co-authorships 250

Insurance in Lieu of oath 252

Summary

Bacteria and halophilic archaea synthesize the bioplastic polyhydroxyalkanoate (PHA). PHA represents an important carbon and energy storage compound build up under nutrient limitation. PHA can make up to 90% of the microorganism's dry weight. When growth conditions are lifted, the microorganisms degrade PHA into their monomers, dimers or a mix of oligomers. Microorganism will metabolize the resulting degradation products to yield CO_2, CH_4, H_2O and energy. To degrade PHA, microorganisms, including bacteria, archaea, fungi and a few protist species, use a PHA depolymerase enzyme (PHAD). Until now, it was largely thought that animals were unable to produce the PHAD enzyme to breakdown PHA.

In **Chapter I** of my dissertation, I identified the first animal PHAD in the gutless worm *Olavius algarvensis*. I characterized the enzyme structure, function and expression pattern. The host PHAD degrades extracellular PHA and expresses all genes needed to generate energy from PHA degradation, which likely indicates that the worm benefits from the PHA degradation. Surprisingly, I discovered that additional 67 metazoan species from nine distinct animal phyla encode for at least one PHAD. All of the animal species that encode for a PHAD access PHA through their diet. My in-depth analysis of the earthworm PHAD in **Chapter III** contradicted my hypothesis that animals encode for a PHAD to meet their nutritional requirements. Using immunohistochemistry assays, I found that the *Lumbricus rubellus* PHAD was localized in the epidermis. One possible explanation for my findings is that the PHAD degrades PHA of invading bacteria. Alternatively, earthworms might excrete their PHADs to their habitat to target extracellular PHA in the soil. Therefore, I predict that animal PHADs might have multiple benefits for metazoans.

PHADs degrade PHA either intracellularly or extracellularly. Intracellular PHADs function on native PHA inside the cell. In contrast, extracellular PHADs function on denatured PHA that occurs outside the cell. The affinity of the PHAD for either intracellular or extracellular PHA is reflected in the enzymes structure. PHADs are typically classified based on sequence homology of the predicted protein. In **Chapter II** of my dissertation, I showed that the classification of PHADs from the gammaproteobacterial group Chromatiales is often misleading. One challenge is that there is less known about the protein structure of intracellular PHADs, which makes predicting the type of PHAD by sequence homology alone uncertain. Using AlphaFold2

to generate and compare PHAD models from multiple Chromatiales PHAD enzymes, I showed that true intracellular PHADs lack a signal peptide and have an altered substrate binding site. Enzyme assays on selected Chromatiales species, including *Thiocapsa rosea*, confirmed the initial hypothesis. Experimental evidence is thus crucial to reveal the true functions of PHADs. It is important to correctly classify the type of PHAD because it alters our interpretation of PHA degradation in natural ecosystems and consequently our understanding of carbon cycling.

In conclusion, my dissertation adds new data to the field of PHA degradation. I revealed that experimental evidence is needed to classify PHADs. Additionally, I identified a novel group of PHADs that likely function after lysis of microbial species. Significantly, I showed that PHA degradation is not limited to bacteria, fungi, archaea, protists but that the ability to degrade PHA is widespread in animals.

Zusammenfassung

Bakterien und halophile Archaeen synthetisieren den Biokunststoff Polyhydroxyalkanoat (PHA). PHA ist eine wichtige Kohlenstoff- und Energiespeicherverbindung, die während Nährstofflimitierung aufgebaut wird. PHA kann bis zu 90% des Trockengewichts der Mikroorganismen ausmachen. Wenn die Wachstumsbedingungen aufgehoben werden, bauen die Mikroorganismen PHA in ihre Monomere, Dimere oder eine Mischung von Oligomeren ab. Die Mikroorganismen verstoffwechseln die entstehenden Abbauprodukte und produzieren dabei CO_2, CH_4, H_2O und gewinnen Energie. Um PHA abzubauen, verwenden Mikroorganismen, darunter Bakterien, Archaeen, Pilze und einige Protisten, ein PHA-Depolymerase-Enzym (PHAD). Bislang ging man weitgehend davon aus, dass Tiere das PHAD-Enzym zum Abbau von PHA nicht produzieren können.

In **Kapitel I** meiner Dissertation identifizierte ich die erste tierische PHAD in dem darmlosen Wurm *Olavius algarvensis*. Ich charakterisierte die Struktur und Funktion des Enzyms sowie die Expressionsmuster. Der Wirt baut tatsächlich extrazelluläres PHA ab und exprimiert Gene die es ermöglichen Energie von PHA zu gewinnen, was wahrscheinlich darauf hindeutet, dass der Wurm vom PHA-Abbau profitiert. Überraschenderweise entdeckte ich, dass weitere 67 Metazoen aus neun verschiedenen Phyla für mindestens eine PHAD kodieren. Alle Tierarten, die für die PHAD kodieren, nehmen PHA über ihre Nahrung auf. Meine eingehende Analyse der PHAD des Regenwurms in **Kapitel III** widerlegte meine Hypothese, dass Tiere für eine PHAD kodieren, um ihren Nahrungsbedarf zu decken. Mit Hilfe von immunhistochemischen Tests habe ich festgestellt, dass die *Lumbricus rubellus* PHAD in der Epidermis lokalisiert ist. Eine mögliche Erklärung für meine Ergebnisse ist, dass die PHAD das PHA von eindringenden Bakterien abbaut. Alternativ dazu könnten Regenwürmer ihre PHADs in ihren Lebensraum ausscheiden, um extrazelluläre PHA im Boden zu nutzen. Daher gehe ich davon aus, dass tierische PHADs verschiedene Nutzen für Metazoen haben könnten.

PHADs bauen PHA entweder intrazellulär oder extrazellulär ab. Intrazelluläre PHADs wirken auf natives PHA innerhalb der Zelle. Im Gegensatz dazu wirken extrazelluläre PHADs auf denaturiertes PHA, dass außerhalb der Zelle vorkommt. Die Affinität der PHADs für intrazelluläres oder extrazelluläres PHA spiegelt sich in der Struktur des Enzyms wider. PHADs werden in der Regel anhand von Sequenzhomologie des

Proteins klassifiziert. In **Kapitel II** meiner Dissertation habe ich gezeigt, dass die Klassifizierung von PHADs aus der Gruppe der Gammaproteobakterien Chromatiales oft irreführend ist. Eine Herausforderung besteht darin, dass weniger über die Proteinstruktur intrazellulärer PHADs bekannt ist, was die Vorhersage des PHAD-Typs allein durch Sequenzhomologie unsicher macht. Mithilfe von AlphaFold2 zur Erstellung und zum Vergleich von PHAD-Modellen mehrerer Chromatiales-PHADs konnte ich zeigen, dass echten intrazellulären PHADs ein Signalpeptid fehlt und sie eine veränderte Substratbindungsstelle aufweisen. Enzymtests an ausgewählten Chromatiales-Arten, darunter *Thiocapsa rosea*, bestätigten die ursprüngliche Hypothese und sind daher entscheidend für die Entdeckung der wahren Funktionen von PHADs. Es ist wichtig, die Art von PHADs richtig zu klassifizieren, da dies unsere Interpretation des PHA-Abbaus in natürlichen Ökosystemen und damit unser Verständnis des Kohlenstoffkreislaufs verändert.

Zusammenfassend lässt sich sagen, dass meine Dissertation neue Daten auf dem Gebiet des PHA-Abbaus liefert. Ich habe gezeigt, dass experimentelle Nachweise erforderlich sind, um PHADs zu klassifizieren. Außerdem habe ich eine neue Gruppe von PHADs identifiziert, die wahrscheinlich nach der Lyse mikrobieller Spezies funktionieren. Wichtig ist, dass ich gezeigt habe, dass der PHA-Abbau nicht auf Bakterien, Pilze, Archaeen und Protisten beschränkt ist, sondern dass die Fähigkeit zum PHA-Abbau auch bei Tieren weit verbreitet ist.

Introduction

Storage compounds and their function

All living organisms require energy for their survival. However, energy can often be scarce due to limiting conditions. Storage compounds enable organisms to overcome unfavorable conditions by decoupling the use of excessive compounds from immediate use, providing adaptability to environmental fluctuations[1, 2]. Under high-nutrient availability of one nutrient, such as carbon, nitrogen or phosphate, but the limitation of another nutrient, organisms lock up the excessive nutrient into compartmentalized storage molecules. Once the nutrient-limiting conditions are lifted, the organisms can tap into these compounds to jump-start their metabolism[3-5]. Storage compounds must therefore be easy to degrade to allow quick mobilization of resources. The advantage that is derived from storage compounds comes not only with their quick remobilization. Storage compounds help to overcome stress. For example, the Antarctic species *Pseudomonas* sp. has an enhanced cold shock survival due to carbon storage[6]. Storage compounds are thus an important mechanism to allow species to survive.

Organisms build up storage compounds either inside or outside of the cell from carbon, nitrogen and phosphate (Figure 1). **Polyphosphate (PolyP)** is a phosphate storage compound that accumulates in granules or acidocalcisomes inside the cell[7-9]. Bacteria accumulate PolyP once phosphate is in excess but nitrogen is limiting in the environment [10]. PolyP can serve as an alternative to ATP in several enzymatic reactions[11]. **Extracellular polymeric substances (EPS)** are extracellular storage compounds[12]. EPS are high-molecular weight polymers. Microbial aggregates facilitate the binding of cells, with for example polysaccharides and proteins, forming the polymer[13]. The most common form of storage are carbon storage compounds. These range from **Triacylglycerols (TAGs)** and **wax esters (WEs)**, which are lipid inclusions[14, 15] to, **glycogen**, which is a high molecular weight polymer composed of glucose monomers[16, 17]. Additionally, **polyhydroxyalkanoates (PHAs**; **see Section:** "PHA as a microbial storage compound") play an important role as an intracellular and extracellular carbon storage.

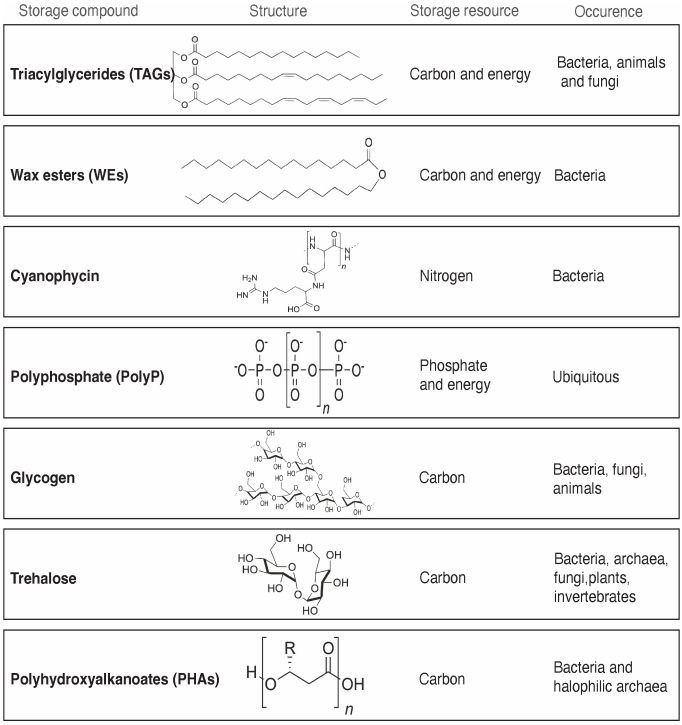

Figure 1 | Overview of intracellular macromolecules that serves as storage compounds. Various organisms synthesize storage compounds. Storage compounds exist for carbon, energy, nitrogen and phosphate. The molecular structures of the storage compounds are quite diverse, ranging from glycosidic bonds in glycogen and trehalose to phosphoanhydride bonds in PolyP. Figure adapted from Mason-Jones et al., 2022[18].

PHAs as microbial storage compounds

PHAs are carbon and energy stores synthesized by bacteria and halophilic archaea in various environments[19-25]. Microorganisms synthesize PHA under unbalanced growth conditions, meaning when certain nutrients, such as nitrogen, phosphate or oxygen, are limited but carbon is abundantly available. The carbon is stored as intracellular insoluble granules in the cytoplasm, making up to 90% of the organism's dry weight[26, 27]. Furthermore, PHA serves as an electron sink for reducing powers[22]. The stored energy and carbon can be utilized for the organism's metabolism once nutrient limiting

conditions are lifted[28-31]. Consequently, PHA serves as a constant carbon reserve, playing an important role for the organism's survival[32].

Chemically, PHAs are biopolyesters formed by (R)-3-hydroxy fatty acid monomers (Figure 1)[26, 33]. PHAs have an ester bond between the carboxyl group of one monomer and the hydroxyl group of the neighboring monomer[34]. Over 150 known hydroxyalkanoates can be the monomeric units of PHAs[35]. There are three major groups, defined by the number of carbon atoms in the hydroxyalkanoic monomers [32]:

1. PHAs with three to five carbon atoms in their monomeric backbone, referred to as short chain length PHAs (PHAscl).
2. PHAs with more than six carbon atoms in their carbon backbone are medium chain length PHAs (PHAmcl).
3. Lastly, several bacteria synthesize a combination of several short chain and medium chain length PHAs.

Length variation of PHA monomers can result not only from the carbon backbone but also from side chain extension at the third carbon atom or beta position (Figure 2a). These differences in PHA structures arise from the specific PHA synthases that connect the hydroxyalkanoates to form the polymer chain[36, 37]. The PHA synthase of *Alcaligenes eutrophus* functions on short chain length hydroxyalkanoates. In contrast, the *Pseudomonas oleovorans* PHA synthase acts on medium chain length hydroxyalkanoates. The monomeric unit can be extended into an alkyl group, ranging from methyl to aromatic side chains[38-42]. The structural variability of PHAs enables the design and creation of biopolymers with different physical properties (**see section:** "PHA as a biosynthesized and biodegradable plastic")[36, 37].

Microorganisms that synthesize PHA have been discovered in various ecosystems (**see section:** "PHA degradation in the terrestrial world" and "PHA degradation in the marine world"). Examples of such environments include: activated sludges, wastewater treatment plants and natural habitats such terrestrial, marine and freshwater ecosystems[43, 44]. Over 300 taxonomically and physiologically distinct bacteria and archaea were shown to store PHA[22, 43, 45, 46].

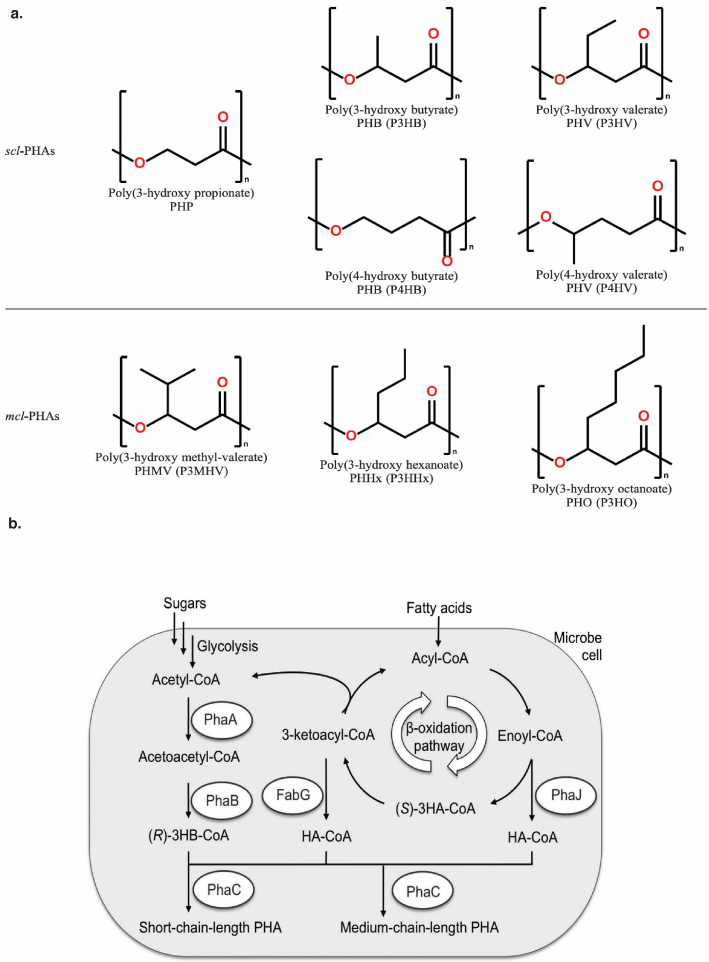

Figure 2 | Up to 150 hydroxyalkanoic monomers can form the PHA polymer chain that is polymerized by the PHA synthase (PhaC) – the key enzyme of the PHA synthesis pathway. a. PHAs are defined by the carbon backbone of their monomeric compounds. PHAs of three to five carbon atoms are short chain PHAs (PHAscl), while medium chain length PHAs (PHAmcl) have 6 to 14 carbon atoms in their monomeric carbon backbone. Figure taken from Luef et al., 2015 [47] **b.** PHAs are synthesized from acetyl-CoA that is converted to acetoacetyl-CoA by the enzyme PhaA. Acetoacetyl-CoA is then formed into the PHA monomers by PhaB which are polymerized by the PHA synthase (PhaC). PHA can also be formed from enoyl-CoA. Figure taken from Numata et al., 2013[48].

PHA synthases are the key enzyme to build up PHA

The most common used PHA synthesis pathway (Figure 2b) is mediated by the enzyme PHA synthase (PhaC, EC 2.3.1) that polymerizes the PHA chain. PHA synthesis begins with the reaction of two acetyl-coenzyme A (acetyl-CoA) molecules to acetoacetyl-CoA, facilitated by a beta-ketoacyl-CoA-thiolase (PhaA, EC 2.3.1.9). Acetoacetyl-CoA is then reduced into CoA-bound PHA monomers, such as (R)-3- hydroxybutyryl-CoA (3HB-CoA) by an acetoacetyl-CoA reductase (PhaB, EC 1.1.1.36). The PHA monomers are then polymerized by the PHA synthase (PhaC, EC 2.3.1)[33, 45, 49, 50]. PHA synthases form four groups according to the type of PHA they produce. Class I (EC 2.3.1.B2) and Class III (EC 2.3.1.B4) use hydroxyalkanoates with three to five carbon atoms such as the one from *Cupriavidus necator*[51] or *Allochromatium vinosum*[52, 53]. Class II (EC 2.3.1.B3) and IV (EC 2.3.1.B5) use hydroxyalkanoates with more than six carbon atoms such as the one from *Pseudomonas* spp.[52-54].

There are additional PHA synthesis pathways. These pathways lead to the synthesis of different PHA types. The PHA source polyhydroxybutyrate (PHB) can be synthesized from sugars and fatty acids via de novo fatty acid biosynthesis and β-oxidation[55]. In the case of medium chain length PHA (PHAmcl), the PHA synthesis can involve intermediates of fatty acid biosynthetic pathway by forming (R)-3-hydroxyacyl-CoA from (R)-3-hydroxyfatty acids catalyzed by a (R)-3-hydroxydecanoyl-ACP:CoA transacylase (PhaG; EC 2.4.1.)[56-58]. Additionally, *Aeromonas caviae,* that synthesizes the PHA copolymer Poly(3-hydroxybutyrate-co-3-hydroxyhexanoate), uses a specific enoyl-CoA hydratase to build up PHA (PhaJ; EC 4.2.1.119). Enoyl-CoA is used in β-oxidation forming the PHA monomers[59]. In all pathways the PHA synthase polymerizes the PHA chain from the monomers[48]. The PHA synthesis pathway is thus diverse with the key enzyme being the PHA synthase.

Once the PHA synthase build up the polymer chain, PHA accumulates as light refracting insoluble granules within the cell's cytoplasm[60, 61]. The size and number of these accumulated granules varies among species[37]. Each granule is enclosed by a phospholipid membrane that separates the granule from the cell lumen[62-64]. The surrounding protein layer harbors the PHA synthase, phasin proteins and PHA regulators[65-67]. Phasin proteins play a role in coating, and stabilizing the granules by preventing them from aggregating, while also regulating the genes for PHA synthesis[34,

[60, 61, 68-71]. These findings are summarized in the budding model[67, 72, 73]. According to it the enzymes that degrade intracellular PHA are also located on the surface of the granule[74].

PHA is degraded by the enzyme PHAD

PHA depolymerases (PHADs; EC 3.1.1.75, EC 3.1.1.76) degrade PHA. PHADs are carboxylesterases of the alpha/beta hydrolase family[32]. So, far there are 35 PHADs whose function has been experimentally verified[75, 76]. In cultivation-based studies, PHA-degrading organisms were isolated from soil, composts, sewage sludges and aquatic environments[77-79]. In cultivation-independent studies PHA-degrading organisms were identified across all known ecosystems. The PHADs identified in these habitats belong to ten bacteria phyla, six haloarchaea species and several fungal genus[75]. Additionally, two protist species, *Acanthamoeba castellanii* and *Dictyostelium discoideum,* encode for a PHAD[80]. PHADs are thus found in almost all ecosystem and are described to be present in all domains of life, with exceptions in them such as metazoans and plants.

Extracellular versus intracellular PHA degradation

PHA found in the environment is either degraded intracellularly or extracellularly. Thus, PHA stored within microorganisms and those found in the surrounding is mobilized[32, 78, 81-83]. Both intracellular and extracellular PHA degradation results in the cleavage of the polymer chain into its monomeric or dimeric hydroxyalkanoates which can be further metabolized to energy, carbon dioxide (CO_2), water (H_2O), or methane (CH_4)[84-86]. Intracellular PHA degradation occurs once nutrient limiting conditions are lifted, allowing the organism to jump start their metabolism[45]. Extracellular PHA degradation enables organisms to use PHA produced by other organisms, which are usually released to the environment after cell death or lysis[32]. In both cases, the degradation of PHA releases carbon and energy that is essential for the survival of the organism.

Key factors influencing PHA degradation are the size of the monomeric unit and the surface structure of PHA (Figure 3a)[32, 45, 87]. PHA exists in its native state (nPHA) in

an amorphous form with a surface layer consisting of proteins and phospholipids[74]. Extracellular PHA (dPHA) is partially crystalline because the surface structure of the granule is disrupted once the PHA granule is released after cell death or lysis[32]. PHADs are adapted to degrade either intracellular or extracellular PHA and to PHA monomers of a specific size (**see Section**: "PHA as a microbial storage compound"). The adaptation of PHADs for a specific substrate is also reflected in their primary enzyme structure (Figure 3a).

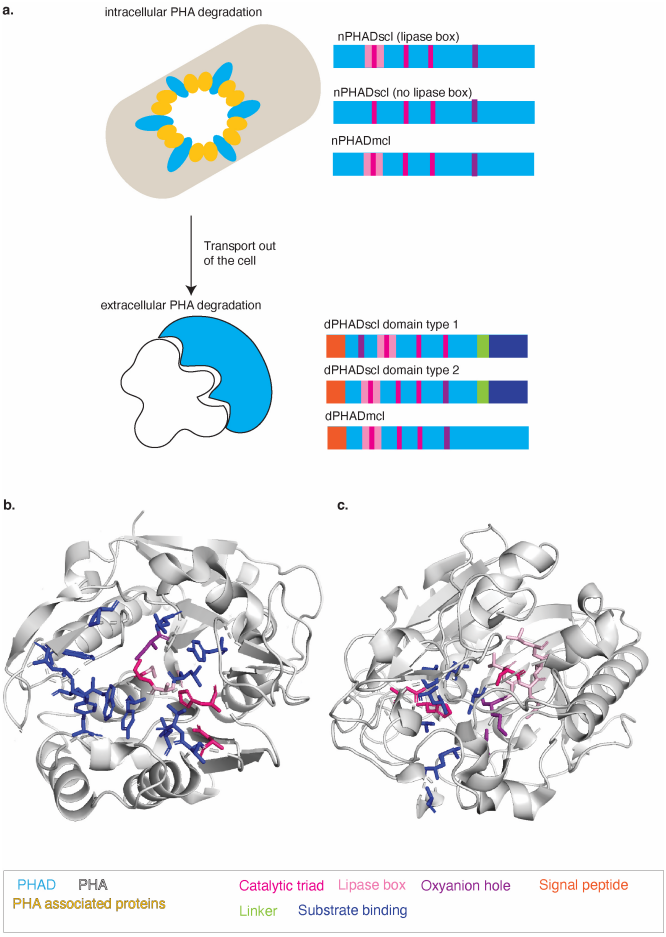

Figure 3 | Extracellular PHADs are clearly differentiated by their structure from intracellular PHADs. a. Intracellular PHADs degrade native PHA with an intact surface layer. Intracellular PHADs show conservation of the catalytic triad (pink) and oxyanion hole (purple). Some of the intracellular PHADs lack a lipase box motif (light pink). In comparison to extracellular PHADs, intracellular PHADs lack a substrate binding site (blue), signal peptide (orange) and linker (green). Extracellular PHADs degrade partially crystalline PHA outside the cell. Taken from Chapter 2. **b.** Crystal structure of the PHAD from *Penecillium funiculousm* (pdb 2d81) shows conservation of the catalytic triad (pink), oxyanion hole (purple), lipase box (light pink) and substrate binding site (blue). **c.** Crystal structure of the PHADs from *Paucimonas lemoignei* (pdb 2x76) shows conservation of the catalytic triad (pink), oxyanion hole (purple), lipase box (light pink) and substrate binding site (blue).

Intracellular and extracellular PHADs share a common catalytic domain (Figure 3a). Like extracellular PHADs, intracellular PHADs have a catalytic triad formed by a serine-histidine-asparagine motif. The catalytic serine residue lies in a lipase box motif. The catalytic triad together with a second histidine, that functions as an oxyanion hole, form the catalytic domain. What differentiates intracellular PHADs from extracellular PHADs is the well-known enzyme structure of extracellular PHADs. Extracellular PHADs that degrade short chain PHA (dPHADscl) have a common domain structure composed of a N-terminal signal peptide, a N- terminal catalytic domain, a linker domain and a C-terminal substrate binding domain. There are two types of extracellular PHADs degrading short chain PHA. The two types are differentiated by the position of the lipase box. Domain type 1 extracellular PHADs have the lipase box located after the oxyanion hole. Domain type 2 extracellular PHADs have the lipase box located before the oxyanion hole[32, 88-90]. In contrast, extracellular PHADs degrading medium chain length PHAs (dPHADmcl) lack an identified substrate binding site. It is likely that the N- terminal functions to bind to the polymer chain[32, 88-90]. In general, 16 bacterial taxa[75] and 95 genera of fungi[91] across ecosystems encode for extracellular PHADs.

Intracellular PHADs degrading short chain (nPHADscl) or medium chain length PHA (nPHADmcl) are less characterized. To date, there is no identified substrate binding domain. Additionally, intracellular PHADs do not have a signal peptide. This clearly differentiates them from extracellular PHADs[76]. Additionally, some intracellular PHADs lack the lipase box in the catalytic domain. These intracellular PHADs instead have a cysteine residue replacing the catalytic serine residue[29]. Due to limited

knowledge of the protein structure of intracellular PHADs, their characterization is often misleading.

The sequence homology that differentiates extracellular and intracellular PHADs serves as the basis for the classification in the PHAD engineering database (DED)[76]. The DED was constructed using 28 seed sequences from all four described PHAD classes that were experimentally validated. PHADs were classified into eight superfamilies comprising 38 homology classes. The database contains 735 PHADs. Extracellular PHADs are split into 24 homology groups, including 16 homology groups for extracellular PHADs degrading short chain PHA with the lipase box after the oxyanion hole and eight homology classes with the lipase box before the oxyanion hole. Intracellular PHADs formed two superfamilies: with and without a lipase box. Intracellular PHADs lacking a lipase box split into nine homology classes. Intracellular PHADs with a lipase box only represented 20 proteins[76]. The DED composition highlights the predominance of extracellular PHADs degrading short chain PHA, which may be due to the higher interest and easier classification based on their well-described primary protein structure.

Extracellular PHAD of the fungus *Penicillum funiculosum*

The crystal structure of the PHAD from the fungus *Penicillium funiculosum* (basionym *Talaromyces funiculosus*) is to the best of my knowledge the only eukaryotic crystalized PHAD structure deposited in the PDB-database. Therefore, I used it throughout my dissertation as a comparison to the metazoan PHADs. *P. funiculosum* encodes for an extracellular PHAD with the typical alpha/beta-type structure. The enzyme was crystalized with a resolution of 1.7 Ångstrom (pdb: 2d81; Figure 3b), resulting in the structure of a globular molecule with the dimensions 52Å X 48Å X 41Å[92]. The PHAD of *P. funiculosum* shows characteristics of extracellular PHADs such as the conservation of the catalytic site and substrate binding site[92]. The sequence comparison with other extracellular PHADs revealed that *P. funiculosum's* PHAD is an extracellular PHAD that degrades short chain PHA. The catalytic triad consists of the residues Ser_{39}, Asp_{121}, and His_{155}. The catalytic residues form a nucleophilic elbow. The lipase box is located before the oxyanion hole. The oxyanion hole and catalytic triad are in a crevice formed at the surface of the PHAD that serves as the substrate binding site. The crevice has the space to fit a single chain of PHA (length 15 Å and width 6 Å).

The *P. funiculosum* PHAD has a different substrate binding site in comparison to other multidomain extracellular PHADs[93-97]. The fungal PHAD has in contrast a region of surface hydrophobic residues. These threonine rich residues (e.g. Thr_{122} and Thr_{173},) are found around the catalytic crevice and fulfill the function of the attachment of the PHA chain. The hydrophobic residues interact with the PHA chain at three subsites. The first is formed by Tyr_{43}, Val_{124} and Trp_{307}, the second by Trp_{307}, Tyr_{76}, Val_{308} and Trp_{310} and the third with Tyr_{76}, Leu_{298}, Pro_{301} and Trp_{310}. The first two hydrophobic pocket subsites allow the binding of PHA-monomers with side-chains smaller than an ethyl group. The third subsite is located to the outside of the enzyme. Thus, exposed to the solvent. As PHA is not water-soluble, the PHA substrate needs to attach for longer time to the surface. The altered substrate binding site allows the PHAD from *P. funiculosum* to bind efficiently to the PHB substrates[92].

Bacterial PHADs – The example of *Paucimonas lemoignei*

The bacteria *Paucimonas lemoignei* and *Raslstonia pickettii* (formerly *Pseudomonas,* then *Burkholderia, pickettii*) are model organisms for PHA degradation[98, 99]. *P. lemoignei* has at least seven PHADs. The first six PHADs (PhaZ1-PhaZ6) are extracellular PHADs. The seventh PHAD (PhaZ7) is an extracellular PHAD that functions on amorphous PHA[100, 101]. Due to the function of the PhaZ7 from *P. lemoignei*, I used it as a comparison to the identified Chromatiales PHADs throughout my dissertation.

The PhaZ7 from *P. lemoignei* is a single globular domain PHAD (pdb: 2x76; Figure 3c)[102]. The crystal structure of the *P. lemoignei* PHAD was determined with a resolution of 1.45 Å. A serine-asparagine-histidine motif forms the catalytic triad[103]. Similarly, to all other described PHADs the catalytic serine residue nucleophillically attacks the polymer chain. The substrate binding site is composed of water molecules that shape a channel to the surface of the protein. A loop formed by the amino acid residues 249 to 257 on one site and on the opposite site by the amino acid residues 238 to 243 form the entrance of the channel. The water molecules of the residues surrounding the channel are used for the docking of the PHA chain. The residues that especially lead to the interaction are Gly_{164} Gly_{239}, Cys_{255}, Gly_{163} and Ala_{162}. The guidance allows the attachment of the PHA chain, facilitating the PHA degradation[103].

PHA degradation mechanisms for energy generation

PHADs degrade PHA into their monomeric or dimeric hydroxyalkanoates which can be used for energy generation. PHA degradation is a two-step process. The substrate binding domain of the enzyme first recognizes PHA, followed by PHA hydrolysis by the catalytic domain[104]. PHA hydrolysis involves a nucleophilic attack. The catalytic serine residue reacts with the carbonyl carbon atom of PHA by the oxygen atoms of its side chain[81]. The other two residues of the catalytic triad (asparagine and histidine) enhance the nucleophilicity[81, 92]. The oxyanion hole further stabilizes the reaction through its amide group. The PHA chain is cleaved as a result, releasing an intermediate product with a hydroxyl group. The oxyanion hole stabilizes the rearrangement of the catalytic site. PHA is further degrade to an intermediate chain with a carboxyl group[92]. From this intermediate the monomers and dimers of the PHA hydroxyalkanoic units are released[105].

The released monomeric and dimeric hydroxyalkanoates are further broken down into intermediates of the citric acid cycle used for energy generation. The oligomers of PHAs are first broken down to their monomers by a hydroxybutyrate-dimer hydrolase (EC 3.1.1.22). The hydroxyalkanoic monomers are further degraded to acetoacetate by a beta-hydroxybutyrate dehydrogenase (EC 1.1.1.30). Acetoacetate is then oxidized to acetyl-CoA. Acetyl-CoA, is likely used in the citric acid cycle to generate energy[106, 107]. During intracellular PHA degradation, the PHA monomers are often coenzyme-A bound. The organisms can thus quickly recycle the monomers for PHA synthesis or degrade them to acetyl-CoA for energy generation by a 3- hydroxybutyryl-CoA dehydrogenase (EC 1.1.1.157)[108]. The degradation of PHA thus yields carbon compounds that can be used to re-build PHA or to produce energy for the organism.

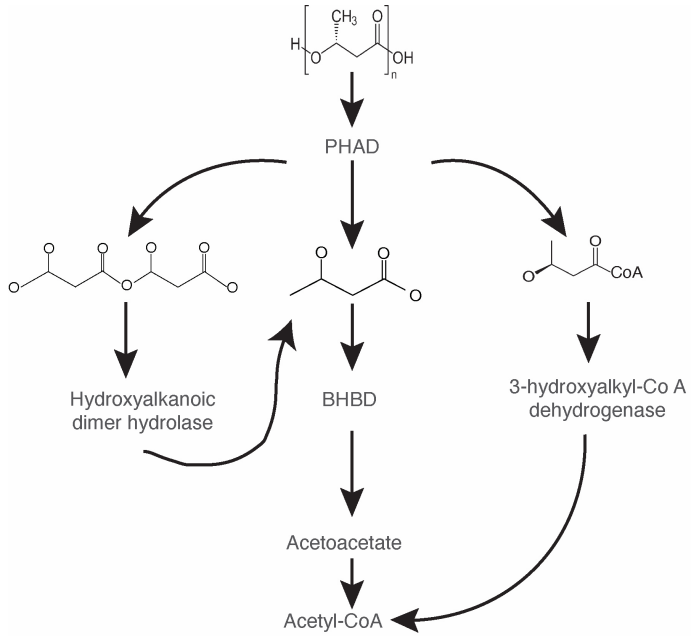

Figure 4 | PHA degradation results in Acetyl-CoA formation used in the citric acid cycle for energy generation. PHADs degrade PHA either to their dimers or monomers. The dimers are further degraded by hydroxyalkanoic dimer hydrolase to monomers. The monomers are degraded to acetoacetate by the enzyme BHBD. Intracellular PHA degradation often results in CoA-bound monomers. A 3-hydroxyalkyl-CoA dehydrogenase degrades the CoA-bound monomers to acetyl-CoA. The resulting acetyl-CoA is likely used in the citric acid circle for energy generation. Figure created using references presented in "PHA degradation mechanisms for energy generation".

PHA in the marine world

PHA-synthesizing organisms are found in various marine environments, either free-living in the water column, sediments, deep sea, or in association with marine invertebrates, such as shrimps, tunicates, sponges (Figure 5a). Marine PHA-synthesizers belong to the bacteria phyla Proteobacteria, Firmicutes, and Actinobacteria. These bacteria use various carbon sources to build up PHA[109]. For example, the species *Burkholderia* sp. AIU M5M02, found in shallow sea muds, synthesizes PHA from mannitol derived from seaweed[110]. *Halomonas hydrothermalis,*

a coastal water bacterium, instead uses glycerol to build up PHA[111]. Aerobic anoxygenic phototrophs from the bacterial genera *Dinoroseobacter, Roseobacter, Labrenzia*, and *Erythrobacter* synthesize PHA from sugars and organic acids. PHA producing bacteria are also found living inside marine animals. For example, *Photobacterium phosphoreum* found in the light organ and intestine of fish[112] or *Halomonas profundus* AT1214 isolated from a hydrothermal vent shrimp[113]. While the exact concentrations of PHA is yet to be determined in marine systems, the examples suggest that PHA serves as a valuable carbon and energy source in marine environments.

Extracellular PHA degradation is as widespread across marine habitats as PHA synthesis[109] (Figure 5a). For example, PHA degrading organisms were identified in coastal seawater in Japan[114], in the deep sea[115], and marine sediments[116]. Marine PHADs share a common structure that differentiates them from terrestrial PHADs (**see Section:** "PHA degradation in the terrestrial world"). All marine PHADs have the lipase box motif located behind the oxyanion hole. A fibronectin type III [Fn(III)], or a cadherin (Cad) domain form the linker. Marine PHADs have two substrate binding domains and one catalytic domain (References in Suzuki et al., 2021[109] e.g. Zadjelovic et al., 2020[117]; Kita et al., 1995[118]; Ma et al., 2011[119]; Kasuya et al., 2000[115]; Kita et al., 1997[120]; Kasuya et al., 2003[121]; Ohura et al., 1999[90]). The two substrate binding domains of marine PHADs might account for the weak binding in comparison to terrestrial PHADs (K = 1.0 ml/µg for terrestrial PHADs and 0.2ml/µg for marine PHADs)[122]. Nevertheless, marine and terrestrial PHADs contribute to the release from carbon and energy to the global carbon cycle.

PHA in the terrestrial world

PHA-synthesizing species such as *Pseudomonas* spp. or *Bacillus* spp. are found in soil ecosystems (Figure 5b). Among 73 soil isolates, 23 soil bacteria synthesize PHA[24]. PHA concentration in soil ranges between 1-4 µg C/g soil and depends on the soil type. Agricultural soils have a PHA content of 4.3 µg C/g soil, while temperate zone forest soils have a PHA content of 1.2 µg C/g soil. Contributing to 2.5% to 4.2% of the microbial carbon pool[18, 123]. Addition of glucose enhanced PHA production[123, 124], suggesting that PHA content in soil is responsive to carbon inputs. The addition of glucose further increased the nitrogen limitation, leading to unbalanced growth

conditions and thus triggering PHA synthesis[123]. PHA represents an important carbon reservoir in soils to overcome fluctuating conditions[125].

PHA synthesis in soils plays a significant role in the rhizosphere, which is the soil adjacent to plant roots[126]. The rhizosphere of several plants, such as sugar beets, wheat and rapeseed harbors PHA-synthesizing organisms[127]. Plants excrete organic compounds but use up essential nutrients. PHA production is thus enhanced due to nutrient limitation[127-130]. However, there is an ongoing discussion whether PHA synthesizing organisms are more abundant in bulk soils or in the rhizosphere. For example, PHA synthesizing organisms were more abundant in the rhizosphere of rice plants than in the adjacent soil[131]. In contrast, the bulk soil in sugarcane fields was richer in PHA synthesizing organisms[129, 130]. The role of PHA-producing bacteria thus needs to be elucidated. It seems likely that PHA production plays a role in the cycling of nutrients between plants and bacteria (**see section**: "The plant root symbiosis").

The degradation rates of PHA in terrestrial systems are not known[44]. Terrestrial PHA-degraders use PHA as a carbon source for biomass production and growth[22] (Figure 5b). The differences in the primary structure of terrestrial PHADs and marine PHADs might be linked to the efficiency of the PHA degradation. PHA degradation in soil is faster than those in marine environments[109, 132]. Thus, terrestrial environments might account for a large fraction of released carbon from extracellular PHA degradation.

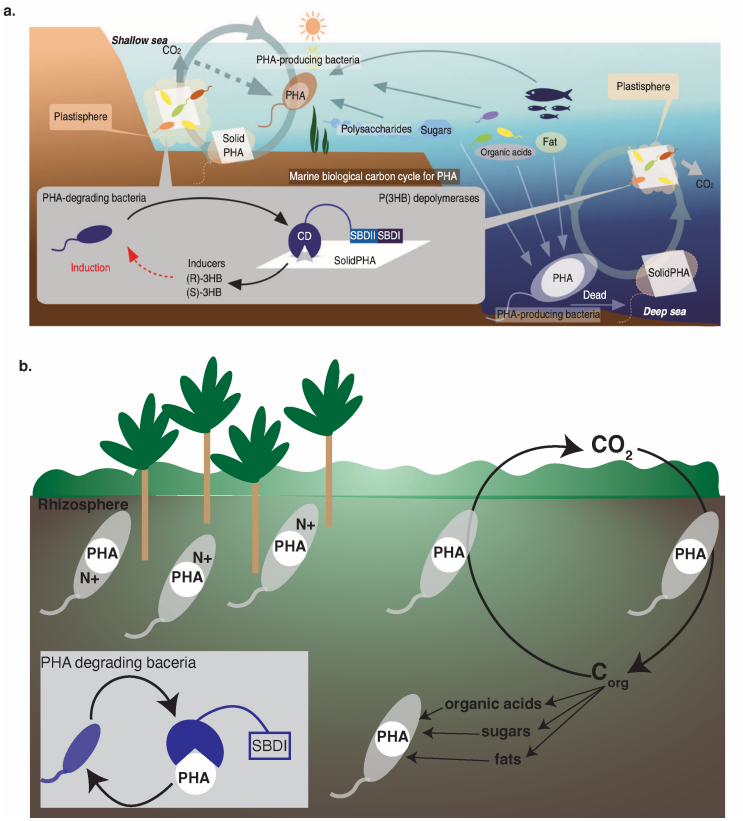

Figure 5 | Role and degradation of PHA in marine and terrestrial environments. a. Model of the incorporation of PHA in the marine carbon cycle. Marine microorganisms synthesize PHA across marine habitats, including shallow water systems and the deep sea. In all habitats PHA-synthesizers store PHA. PHADs, that have two substrate binding domains (SBD), degrade PHA. Additionally, bacteria form a plastisphere by colonizing PHA. Figure taken from Suzuki et al., 2021[109]. **b**. PHA is also synthesized in terrestrial environments. As soil systems influence the global carbon cycle, PHA synthesis leads to storage of carbon. Terrestrial organisms usually have a PHAD with one substrate binding site that degrades PHA, leading to carbon release. PHA-synthesis is suggested to be coupled to nitrogen fixation, as the latter might create unbalanced growth conditions in the rhizosphere. Figure drawn based on references indicated in "PHA degradation in the terrestrial world".

PHA as a biosynthesized and biodegradable plastic

Why are bioplastics a good alternative to petroleum-based plastics?

The widespread use of plastics by humans poses a challenge in ecosystems worldwide (e.g. Dris et al., 2015[133]; Lebreton et al., 2017[134]; Brandon et al., 2019[135]; Hurley et al., 2020[136]). Petroleum-based plastics accumulate in the environment, gradually breaking down into microplastics that enter the food chain[137-142]. The use of conventional plastics threatens thus not only ecosystems, but also affects the human population. For example, up to 12.7 million tons of conventional recalcitrant plastics accumulate every year in the ocean[143]. The production of petrochemical-based plastics is predicted to increase annually by 4%. The increase in plastic production will not only lead to accumulation of plastics but deplete natural products and fossil-based resources[44].

The problems associated with conventional plastics lead to a higher interest in bio-based plastics. Bio-based plastics can either be synthesized by microorganisms from e.g. vegetable fats, oils etc., or degraded by microbial activity[144]. Bio-degradable plastics are completely mineralized to inorganic substances such as CO_2 and CH_4[84-86, 109, 145]. The main backbone of the bio-degradable polymer is first hydrolyzed into smaller compounds by microbial activity. In the second step, microorganisms take up the degradation products. Microorganisms then catabolize the taken up degradation products, releasing CO_2, CH_4 and water[146]. The complete remineralization makes bio-degradable plastics attractive as it helps to overcome the problems of plastic accumulation and microplastic formation. Considering the advances in current research on PHA-based plastics, they show great potential as an alternative to petrochemical-based plastics.

PHAs biosynthesized and biodegradable plastics

High molecular weight PHAs share numerous characteristics with thermoplastics. In contrast, PHA-based plastics are both synthesized and degraded by microorganisms. Thus, PHA is an attractive alternative to petroleum-based plastics[147-150]. PHA

bioplastics are directly extracted from PHA synthesizing bacteria after incubation in the presence of a rich carbon source[151]. Potential carbon sources are food waste products such as whey or fermentative feedstocks[152-155]. PHA-production does thus not rely on fossil resources[45]. PHADs encoded by bacteria, fungi, archaea and protists degrade PHA-based plastics[32, 75, 80, 82, 83]. PHAs are the only biodegradable plastic with a specific enzyme that hydrolyses the polymer chain. In contrast, polylactic acid (PLA), produced via chemical synthesis, is degraded by both lipases and cutinases[88, 109, 156-161]. These non-specific enzymes for PLA degradation influence the rate of the plastic degradation. PHA-based plastic degradation is much faster than that of other biodegradable plastics[109, 162-164]. Degradation rates of PHA-based bottles were estimated to be 10-20 mg/d resulting in a lifespan of 5-10 years after depositing them in the Swiss Lake Lugano for 250 days[165]. In marine habitats PHA films decreased in thickness by 60% in the first six to eight weeks[166-169]. The degradation of PHA produces non-toxic compounds. Microorganisms metabolize the degradation products, releasing CO_2, CH_4 and H_2O[84-86]. PHA-based plastics do not require specific conditions for the hydrolysis by enzymatic reaction. PHA-based plastics are degraded across all environments under both aerobic and anaerobic conditions[84-87]. The combination of the characteristics of thermoplastics but with complete biodegradability, make PHA one of the best alternatives to conventional plastics.

PHA-based plastics share similarities with thermoplastics in terms of moldability and resistance to UV radiation[44, 170]. These properties make them well-suited for single-use plastic products such as packaging, hygiene products and containers for food[37, 45, 170-173]. PHAs are highly attractable for biotechnology due to their potential as a source for the production of biodegradable plastics[132, 147-151, 174, 175]. The benefit of PHA as a biodegradable plastic comes from the versatility in their structure. The monomeric composition facilitates the high adaptability of PHA-based plastics. For example, PHB (Polyhydroxybutyrate) is a hard to brittle material with a high crystallinity, making it comparable to polypropylene[26]. PHB copolymerized with larger hydroxyalkanoates, e.g. forming Poly(3-hydroxybutyrate-*co*-3-hydroxyhexanoate) (P(3HB-*co*-3HHx)), decreases the crystallinity from 60 to 29[49, 109, 176]. These examples highlight that the type of copolymerization tailors PHA from hard to brittle material to a flexible material.

One of the major problems concerning the production of PHA-based plastics is the efficiency and ability to produce PHA large scale. The problems lead to high production costs, hindering the use of PHA-based plastics[34, 132, 177, 178]. In 2022, 2.22 million tons

plastic were produced, 48.5% being bio-based plastics and 51.5% bio-degradable plastics. PHA accounted for 3.9% of the total amount of plastics. The relative amount of PHA-based plastics is expected to increase to 8.9% until 2027 (https://www.european-bioplastics.org/market/). Since PHAs are the only available biosynthesized and biodegradable plastics, their market share should be increased to match the United Nations agreement to end plastic pollution (https://www.un.org/en/climatechange/nations-agree-end-plastic-pollution).

Role of PHA for eukaryote-microbe interactions

What is symbiosis?

All life depends on the interactions with other organisms. A concept summarized by the term "symbiosis", coming from the Greek word "living together". The concept was initially described by Anton de Bary who defined symbiosis based on three criteria: (1) two symbiotic partners must be dissimilar, (2) they must be in physical contact and (3) they must live together over a long period of time[179]. This definition does not consider the relationship between the symbiotic partners. In a symbiotic relationship both partners can derive benefits from each other (**mutualistic**), only one of the partners gains a benefit without harming the other partner (**communalistic**), or one partner harms the other partner for its own benefit (**parasitic**)[180, 181]. Boundaries between these concepts can be fluid because temporal changes might affect the symbiosis[182, 183]. In this thesis, the term "symbiosis" is used to describe the mutualistic association between eukaryotic hosts and their bacterial symbionts.

Symbiosis serves as a source for novel metabolic and physiological adaptations for both the eukaryotic host and the bacterial symbionts. For example, symbiosis enables the degradation of lignocellulose by termites[184], generation of energy from denitrification[185], or the use of chemical energy for biomass production for the eukaryotic host[186] (**see Section:** "PHA and its role in chemosynthetic symbiosis"). Novel metabolic capabilities allow the eukaryotic host to inhabit new environments and lifestyles, ultimately leading to its evolutionary diversification[187]. Mutualistic associations can impact the nutrition, morphology and immune responses of the host (e.g. Baumann, 2005[188]; Hosseini et al., 2021[189]; Gross et al., 2009[190]). For this

reason, the following section focuses on the role of PHA for (1) nutrition and (2) stress response in mutualistic symbioses.

PHA and its role in stress response in the bean bug *Riptortus pedestris*

The bean bug *Riptortus pedestris* is in a beneficial and specific symbiosis with a Betaproteobacterium of the genus *Burkholderia* (Figure 6a). Nymphs get the symbionts from the environment through their oral cavity in each generation. In adult bean bugs, the symbionts sit in crypts in the posterior midgut[191-193]. The symbionts produce PHA granules in larger size than the free-living state of the symbionts. Gas chromatography mass spectrometry analysis revealed that the symbionts synthesize PHB. PHA represents a carbon and energy source, leading to the investigation of the role of PHA in the symbiosis of *R. pedestris*[194].

Mutants of the symbionts were created, each lacking one of the PHA synthesis genes, namely *pha*A, *pha*B, *pha*C and *pha*P. When grown under nutrient limiting conditions, the wild type produced PHA, while the mutants produced less PHA. The mutants were given orally to the nymphs of *R. pedestris*. Analysis of the colonization pattern of the mutants, suggested that Δ*pha*B and Δ*pha*A mutants colonized the crypts less frequently. The crypts appeared thinner and translucent, similar to the ones found in non-symbiotic crypts. The lack of PHA of the symbiont mutants affected the host not in its survival but the hosts needed longer time until adulthood. Additionally, the body length of males and females were shorter. Females had a lower body weight in comparison to the wild types. The results indicate that hosts with Δ*pha*A and Δ*pha*B mutants had lower fitness compared to the wild types. The data suggests that PHA plays a role in the symbiont colonization and proliferation. Wild type symbionts appeared to be better in colonizing the host, even under nutrient limitations or other stresses[194].

The plant root symbiosis

Many bacteria of the genus *Rhizobium, Bradyrhizobium*, and *Azorhizobium* synthesize PHA both in their free-living state but also in symbiosis with root nodules (Figure 6b).

PHA likely plays a role in nitrogen fixation in the root nodule symbiosis of *Vicia faba* and *Lupinus* because the bacteria are limited in nutrients by the plant[195-198]. *Bradyrhizobium japonicum* simultaneously fixes nitrogen and builds up PHA[195]. PHA synthesis might also contribute to the extension of nitrogen-fixation during darkness in soybean root nodules[199]. Lastly, the role of PHA synthesis and nitrogen fixation might be related to the partitioning of energy and reducing powers[200].

Other studies suggested that PHA synthesis is not essential for root nodule symbiosis[201]. PHA-mutants of rhizobial symbionts showed increased nitrogen production and improved host fitness, potentially due to a reallocation of energy and reducing powers during nitrogen fixation [202-204]. A possible explanation for this discrepancy, could be that PHA synthesis is not directly linked to nitrogen fixation but rather increases the growth of the bacteria and the colonization efficiency of the root nodules[205, 206], similar as suggested for the bean bug symbiosis of *R. pedestris*.

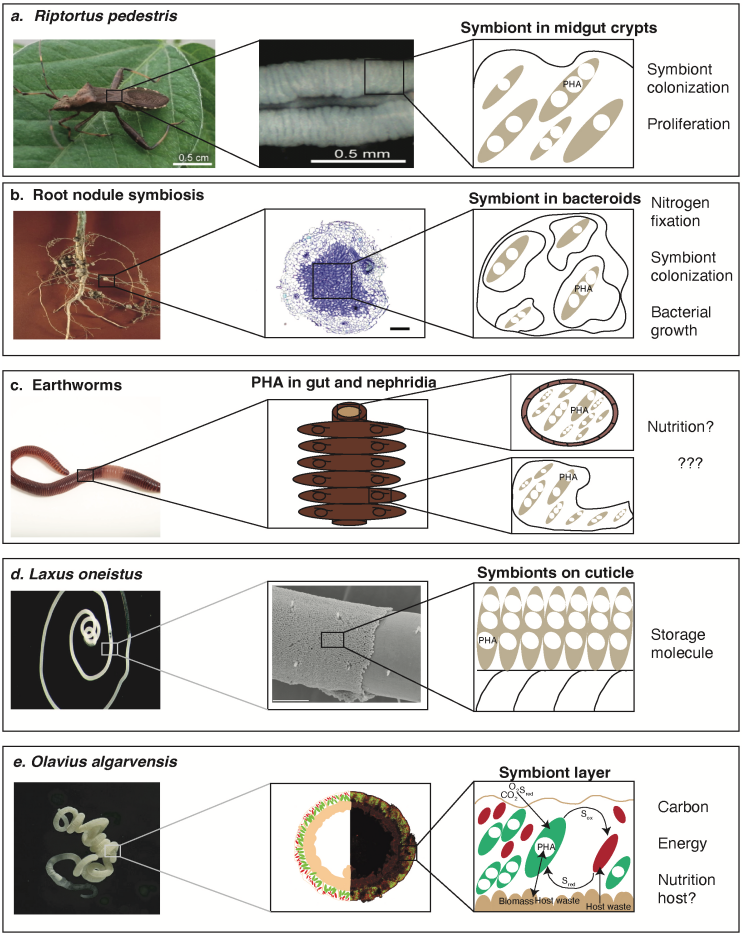
a. Riptortus pedestris
0.5 cm
0.5 mm
Symbiont in midgut crypts
PHA
Symbiont colonization
Proliferation
b. Root nodule symbiosis
Symbiont in bacteroids
PHA
Nitrogen fixation
Symbiont colonization
Bacterial growth
c. Earthworms
PHA in gut and nephridia
PHA
PHA
Nutrition?
???
d. Laxus oneistus
Symbionts on cuticle
PHA
Storage molecule
e. Olavius algarvensis
Symbiont layer
PHA
Biomass
Host waste
Host waste
Carbon
Energy
Nutrition host?

Figure 6 | Role of PHA in host-microbe interactions. a. The symbionts of the bean bug *R. pedestris* are located in crypts in the posterior midgut. They produce PHA which might function to enhance symbiont colonization. Images taken from Kim et al., 2013[194] **b.** Rhizobial symbionts in root nodules build up PHA. PHA is linked to nitrogen fixation, symbiont growth and colonization. Images taken from Yokota et al., 2009[207]; Surridge, et al., 2021[208] **c.** Earthworms take up PHA with their diet. They also have nephridial symbionts that synthesize PHA. Both PHA sources could be of nutritional value for the earthworm. Image taken from https://www.nationalgeographic.com/animals/invertebrates/facts/common-earthworm **d.** *Laxus oneistus* is in symbiosis with *Ca*. Thiosymbion oneisti that sits on its cuticle building up PHA as a storage molecule. Images taken from https://news.univie.ac.at/uniview/forschung/detailansicht/artikel/einmal-anders-zur-perfekten-symbiose/ & Schmidt, 2013[209] **e.** *Olavius algarvensis* lacks a digestive system and relies on its symbionts for nutrition that sit underneath its cuticle and above the epidermis. The primary symbiont *Ca*. Thiosymbion algarvensis fixes CO_2 to build up biomass. The symbiont uses host waste products for PHA synthesis. PHA might thus play a nutritional role for the host. *Ca*. Thiosymbion algarvensis is in synthrophy with Deltaproteobacteria for sulfur compounds. Image courtesy to Alexander Gruhl. Figure adapted from Dubilier et al., 2001[210]& Kleiner et al., 2012[211].

PHA as a potential nutritional source in earthworms

Earthworms influence soil ecosystems due to their role in carbon storage and release[212]. They contribute to soil aggregation which stabilizes soil carbon. Additionally, they transform plant materials to be usable substrates for microorganisms[212]. Earthworms are generally considered to be bioindicators and ecosystem engineers[213, 214].

In soil habitats, earthworms have access to PHA-producing organisms. Soil PHA concentrations range between 1- 4 µg C/g soil[18, 123]. PHA synthesizing organisms were found in the earthworm's gut[215] (Figure 6c), suggesting that PHA might play a nutritional role for earthworms. Moreover, earthworms are also considered to play a role in plastic degradation. Earthworms partially break down commercial plastics, leading to the accumulation of microplastics in the earthworm's gut[216-218]. Although, the contribution of earthworms to the degradation of bio-degradable plastics is not known, earthworms likely enhance the activity of microorganisms in soils and thereby stimulating the degradation of PHA[219]. However, it is unclear if earthworms actively degrade PHA.

Besides PHA found in the environment, earthworms harbor symbionts of the genus *Verminephrobacter* that synthesize PHA. *Verminephrobacter* sp. are commonly found in earthworms nephridia which are excretory organs found in pairs and excrete

nitrogenous waste products[220, 221]. Nephridial symbionts are host specific forming a monophyletic clade[222]. 19 out of 23 earthworm species, including *Lumbricus terrestris,* harbor *Verminephrobacter* symbionts. The symbionts are species-specific, meaning that distinct earthworm species have different symbiont genotypes, while the same species found in different habitats have more closely related symbiont genotypes[223]. All symbionts synthesize PHA by having a PHA synthase (PhaC)[224-226]. Future research is needed to determine if PHA synthesized by the symbionts might play a role for the earthworm. Additionally, future work should determine if PHA synthesized by the symbionts or taken up by the earthworm's nutrition leads to an advantage for earthworms.

PHA and its role in chemosynthetic symbiosis

Chemosynthesis is a process similar to photosynthesis. Inorganic compounds, such as sulfide, methane, carbon monoxide or hydrogen, are oxidized and used as an energy source for the fixation of CO_2[211, 227-232]. The symbionts fix the carbon compounds used for biomass production for the eukaryotic host, representing thus a nutritional association. Two modes have been described for how the hosts gain nutrition from their symbionts. The first, "milking", describes the direct transfer of nutrients to the host. The second mode, "farming", refers to the direct eating of the symbionts. The second mode seems to be the main mode of nutrient transfer, suggested by for example gutless worms such as *Riftia* and *Olavius* [231].

Chemosynthetic symbioses were first discovered in the tube worm *Riftia pachyptila* at hydrothermal vents in the deep sea[233]. Since the discovery, chemosynthetic symbioses were found in several eukaryotic hosts. Chemosynthetic symbioses evolved multiple times in a wide variety of invertebrate hosts and some protists. Alphaproteobacteria, Gammaproteobacteria, and Campylobacteria (formerly Epsilonproteobacteria) are in chemosynthetic symbioses[231, 234]. Chemosymbioses occurs in almost all marine environments ranging from shallow-water habitats to coral reef sediments to the deep sea[186, 231, 234]. Chemosynthetic symbionts provide the host with new metabolic abilities allowing them to access new ecological niches.

Many chemosynthetic symbioses involve sulfur-oxidizing chemoautotrophic symbionts. These thioautotrophic symbionts fix CO_2 using reduced sulfur compounds

as electron donors and oxygen as an electron acceptor[235, 236]. Therefore, thioautotrophic symbioses are generally found at the interface between oxic and anoxic zones, such as at hydrothermal vents and shallow-water sediments[186, 235].

PHA in the symbiosis of the *Stilbonematinae*

Stilbonematinae nematodes form a stable association with sulfur-oxidizing chemoautotrophic symbionts in shallow-water sediments[235, 237]. The chemosynthetic symbiont found in *Stilbonematinae* nematodes is the gammaproteobacterium "*Candidatus* Thiosymbion sp.". The symbiont belongs to the family of *Chromatiaceae*, which are purple sulfur bacteria. *Candidatus* Thiosymbion oneisti lives on the cuticle of the marine nematode *Laxus oneistus*, forming a single layer (Figure 6d). The symbiont and host form a specific association[238-244]. Similar to other marine nematodes, *L. oneistus* shuttles the symbiont to the oxic and anoxic sediment layers[245].

Ca. T. oneisti builds up PHA as a storage molecule under oxic conditions. The symbiont uses glyoxylate, acetate, and propionate for the synthesis of PHA by the partial 3- hydroxypropionate cycle. Genes involved in PHA synthesis, such as the acetyl-CoA acetyltransferase (*pha*A) and a class III PHA synthase subunit (*pha*C) seem to be more expressed under oxic conditions. Conversely, *Ca.* T. oneisti upregulated the PHAD under anoxic conditions, leading to lower PHA content under anoxic conditions. The most likely explanation is that in the presence of oxygen *Ca.* T. oneisti switches to mixothrophy, using simultaneously inorganic and organic carbon. The excess of carbon could thus be stored in form of PHA[245], serving as a storage molecule for carbon.

Nutritional role of PHA for gutless worms

Gutless oligochaetes form an obligate symbiosis with sulfur-oxidizing chemoautotrophic symbionts (Figure 6e). Marine gutless oligochaetes belong to a monophyletic group in the phylum Annelida divided into two distinct genera *Olavius* and *Inanidrilus*, with 100 described species[246-248]. Gutless oligochaetes live in the interstitial water of marine sediments in shallow water habitats[249]. Individual tubificied worms are 15 to 25 mm long with a diameter of 0.1 to 0.3 mm[250]. All gutless

oligochaetes lack a digestive system consisting of a mouth, gut, anus and nephridial organs[210, 251]. Consequently, the hosts depend on their extracellular symbionts for their nutrition and waste management[210].

The symbionts form a thick layer underneath the cuticle and above the epidermis, representing ~25% of the worm's biomass[252, 253]. The primary symbiont belongs to the same genus of *Ca.* Thiosymbion sp. as the one described for nematodes[241]. The symbionts fix CO_2 via the Calvin−Benson−Bassham (CBB) cycle by oxidation of reduced sulfur compounds to sulfate. As terminal electron acceptors the symbionts use oxygen[210, 229]. The gutless oligochaete *Olavius algarvensis* also harbors Deltaproteobacteria that live in syntrophy with *Ca.* Thiosymbion algarvensis. The Deltaproteobacteria symbionts reduce the produced sulfate to sulfide and use the energy to metabolize host waste products, such as succinate and other fatty acids[211, 229, 230]. The gutless oligochaetes harbor several other symbionts such as spirochaetes and Alphaproteobacteria. The symbiont community varies among different host species although *Ca.* Thiosymbion sp. is present in almost all identified host species[254].

The primary symbiont *Ca*. T. algarvensis expressed a putative PHA synthase and phasin enzyme under anaerobic conditions[211]. PHA serves as a valuable carbon storage, using excessive carbon and reducing equivalents[211]. *Ca.* T. algarvensis stores PHA as a copolymer of polyhydroxybutyrate (PHB), polyhydroxyvalerate (PHV) and polyhydroxymethylvalerate (PHMV). Notably, PHA makes up to 42% of the symbiont's internal carbon storage (Kleiner et al., unpublished). Thus, PHA clearly represents an important nutritional compound in the symbiosis from gutless worms.

The eukaryotic host gains most of its nutrition, if not all, from its symbionts. The suggested primary mode of nutrient transfer is by symbiont digestion[252]. Many aspects of the gutless oligochaete symbiosis have already been characterized in the past. However, little is known about the role of PHA as a nutritional compound in the symbiosis. Especially, considering that the host might gain access to the PHA by symbiont digestion. The question remains if *O. algarvensis* and other gutless oligochaetes express functional PHADs? However, PHADs are not described in animals. As PHA represents a valuable carbon and energy compound across ecosystems[19-25], it would be intriguing if not only gutless oligochaetes but other metazoan species could use PHA as a nutritional source.

Aims of the dissertation

PHA is an important carbon and energy source synthesized as a storage compound by many bacteria and archaea[21-23, 25, 125]. Given the high carbon and energy contents of PHA, metazoans would profit from being able to degrade PHA to support their growth and reproduction. Until now, only bacteria, fungi and a few protist and archaea species are thought to be able to use PHA for their metabolism by encoding a PHAD enzyme[75, 80]. Therefore, the aim of this thesis was to look into the ability of animal species to degrade PHA by encoding a PHAD. Throughout my thesis, I used several techniques ranging from metatranscriptomic analysis, AlphaFold2 modelling, phylogenetic analyses, wet-lab experiments such as enzyme overexpression, functional assays and fluorescent labelling of the enzyme. The obtained data allowed me to identify that PHADs are widespread in the animal kingdom. Animal species across ecosystems can use PHA as a carbon and energy resource (**Chapter I & III**). Furthermore, my analyses allowed me to identify that the classification of PHADs is often misleading, exemplified at the misclassified Chromatiales PHADs (**Chapter II**).

Chapter I | Animals degrade the bioplastic polyhydroxyalkanoate

Until now, it was assumed that only bacteria, fungi, archaea and protists degrade PHA[75, 80]. In the symbiosis of the gutless oligochaetes *O. algarvensis*, PHA likely plays an important nutritional role. Especially as the host lacks a digestive system and relies on its symbionts, that produce PHA, for nutrition[210, 211, 251]. The aim of the first chapter was to identify if *O. algarvensis* can degrade PHA. I used metagenomic and metatranscriptomic analysis to identify the host PHAD. I was indeed able to identify the first animal PHAD in *O. algarvensis*. AlphaFold2 modelling and enzyme assays suggest that the *O. algarvensis* PHAD degrades extracellular short chain PHA, showing a potential adaptation to PHA produced by the symbionts. The metatranscriptomic analysis showed that the host expressed needed enzymes to further degrade PHA for energy generation. By zooming out, I identified that *O. algarvensis* is not the only gutless oligochaete species with a PHAD but that nine other gutless worms have the ability to generate energy from PHA degradation. The identified gutless oligochaete PHADs allowed me to identify 195 PHAD homologs in 67 animal species spanning nine metazoan phyla across diverse ecological niches. The metazoan PHADs

formed a monophyletic clade, branching off from a clade of bacterial predators of the genus *Bdellovibrio* and protists. The phylogenetic analysis suggested that the animal PHADs were evolutionary conserved. Taken together, the identification of animal PHADs suggests that animals can degrade PHA, likely obtaining a nutritional benefit. Given that microbial produced PHA is widespread across ecosystems, the ability of animals to degrade PHA likely influences carbon budgets.

Chapter II | Can Chromatiales bacteria degrade their own PHA?

PHADs show substrate affinity for the size and the surface structure of PHA. The protein sequence reflects the substrate affinity. While the protein structure of extracellular PHADs is well-described, little is known about intracellular PHADs[32, 76]. Thus, homology-based classification of PHADs is often misleading. While grouping Chromatiales PHADs with sequences of the PHAD engineering database[76], all Chromatiales PHADs fell into an extracellular PHAD clade. Given that some Chromatiales species, including *Ca.* Thiosymbion algarvensis, synthesize PHA, it seems likely that the classification was incorrect. Therefore, the aim of this chapter was to analyze if Chromatiales species can use their own PHA resource. I further aimed to identify protein characteristics that separate intracellular PHADs from extracellular PHADs. I applied AlphaFold2 modelling, primary structure analysis together with phylogenetic analysis to characterize Chromatiales PHADs. Functional PHA assays, showed that Chromatiales species such as *Rheinheimera aquimaris,* degrade extracellular PHA. Other Chromatiales species such as *Thiocapsa rosea* and *Allochromatium vinosum* were not able to degrade extracellular PHA, contradicting their classification. Therefore, the experimental validation of PHADs is crucial. My analysis confirmed the hypothesis that PHADs are differentiated by the signal peptide and substrate binding site. If those are missing or different, the PHAD is suggested to degrade intracellular PHA. Based on this I hypothesized that *Ca.* T. algarvensis can *in vivo* degrade its own PHA. The heterologous expressed *Ca.* T. algarvensis PHAD showed activity on extracellular PHA but lacked a signal peptide, suggesting that the enzyme *in vivo* cannot be transported outside.

Chapter III | Earthworms degrade the bioplastic polyhdroxyalkanoate

PHAs are important storage compounds found in terrestrial soils[18, 123]. I previously identified PHADs in three globally distributed earthworm species, suggesting that earthworms influence PHA degradation (**Chapter I**). I hypothesized that PHA plays an important nutritional role for animals. The aim of this chapter was to characterize the earthworm PHADs and to identify if earthworms gain a benefit from PHA degradation. I used AlphaFold2 modeling, primary structure analysis and enzyme assays to characterize the earthworm PHADs. I combined the characterization with laboratory work to localize the PHAD protein by immunohistochemistry. Lastly, I supplemented PHA to the earthworm's diet to identify if they gain a nutritional benefit from PHA. Contradicting my initial hypothesis that PHA degradation plays a nutritional role for earthworms, I localized the PHAD protein in the worm's epidermis. Potentially, the earthworm might excrete the PHAD through its gland cells. The PHAD could thus act on PHA after degrading invading bacteria. Alternatively, the PHAD could be excreted to degrade extracellular PHA found in the earthworm's casts. The PHA degradation products likely stimulate the microbial community, improving the ecosystem health. Based on this, I hypothesized that future studies should focus on the benefits of PHA degradation by animals.

References

1. Varpe, Ø., *Life history adaptations to seasonality.* Integrative and Comparative Biology, 2017. **57**(5): p. 943-960.
2. Fischer, B., U. Dieckmann and B. Taborsky, *When to store energy in a stochastic environment.* Evolution, 2011. **65**(5): p. 1221-1232.
3. Pond, C., *Storage.* Physiological Ecology, 1981: p. 190-219.
4. Millard, P., *The accumulation and storage of nitrogen by herbaceous plants.* Plant, Cell & Environment, 1988. **11**(1): p. 1-8.
5. Chapin III, F.S., E. Schulze and H.A. Mooney, *The ecology and economics of storage in plants.* Annual Review of Ecology and Systematics, 1990. **21**(1): p. 423-447.
6. Ayub, N.D., P.M. Tribelli and N.I. López, *Polyhydroxyalkanoates are essential for maintenance of redox state in the Antarctic bacterium* Pseudomonas *sp. 14-3 during low temperature adaptation.* Extremophiles, 2009. **13**: p. 59-66.
7. Albi, T. and A. Serrano, *Inorganic polyphosphate in the microbial world. Emerging roles for a multifaceted biopolymer.* World Journal of Microbiology and Biotechnology, 2016. **32**: p. 1-12.
8. Rao, N.N., M.R. Gómez-García and A. Kornberg, *Inorganic polyphosphate: essential for growth and survival.* Annual Review of Biochemistry, 2009. **78**: p. 605-647.
9. Denoncourt, A. and M. Downey, *Model systems for studying polyphosphate biology: a focus on microorganisms.* Current Genetics, 2021. **67**(3): p. 331-346.
10. Kuroda, A. and H. Ohtake, *Molecular analysis of polyphosphate accumulation in bacteria.* Biochemistry C/C of Biokhimila, 2000. **65**(3): p. 304-308.
11. Reusch, R.N. and H.L. Sadoff, *Putative structure and functions of a poly-beta-hydroxybutyrate/calcium polyphosphate channel in bacterial plasma membranes.* Proceedings of the National Academy of Sciences, 1988. **85**(12): p. 4176-4180.
12. Flemming, H.-C. and J. Wingender, *The biofilm matrix.* Nature Reviews Microbiology, 2010. **8**(9): p. 623-633.
13. Wingender, J., T.R. Neu and H.-C. Flemming, *What are bacterial extracellular polymeric substances?* 1999: Springer.
14. Murphy, D.J., *The dynamic roles of intracellular lipid droplets: from archaea to mammals.* Protoplasma, 2012. **249**: p. 541-585.
15. Alvarez, H.M., *Triacylglycerol and wax ester-accumulating machinery in prokaryotes.* Biochimie, 2016. **120**: p. 28-39.
16. Roach, P.J., A.A. Depaoli-Roach, T.D. Hurley and V.S. Tagliabracci, *Glycogen and its metabolism: some new developments and old themes.* Biochemical Journal, 2012. **441**(3): p. 763-787.
17. Wang, L., M. Wang, M.J. Wise, Q. Liu, T. Yang, Z. Zhu, C. Li, X. Tan, D. Tang and W. Wang, *Recent progress in the structure of glycogen serving as a durable energy reserve in bacteria.* World Journal of Microbiology and Biotechnology, 2020. **36**: p. 1-12.
18. Mason-Jones, K., S.L. Robinson, G. Veen, S. Manzoni and W.H. van der Putten, *Microbial storage and its implications for soil ecology.* The ISME Journal, 2022. **16**(3): p. 617-629.

19. Koller, M., L. Maršálek, M.M. de Sousa Dias and G. Braunegg, *Producing microbial polyhydroxyalkanoate (PHA) biopolyesters in a sustainable manner.* New Biotechnology, 2017. **37**: p. 24-38.
20. Obruca, S., P. Sedlacek, E. Slaninova, I. Fritz, C. Daffert, K. Meixner, Z. Sedrlova and M. Koller, *Novel unexpected functions of PHA granules.* Applied Microbiology and Biotechnology, 2020. **104**: p. 4795-4810.
21. Fernandez-Castillo, R., F. Rodriguez-Valera, J. Gonzalez-Ramos and F. Ruiz-Berraquero, *Accumulation of poly (β-hydroxybutyrate) by halobacteria.* Applied and Environmental Microbiology, 1986. **51**(1): p. 214-216.
22. Steinbüchel, A. and H. Schlegel, *Physiology and molecular genetics of poly (β-hydroxyalkanoic acid) synthesis in* Alcaligenes eutrophus. Molecular Microbiology, 1991. **5**(3): p. 535-542.
23. Arun, A., R. Arthi, V. Shanmugabalaji and M. Eyini, *Microbial production of poly-β-hydroxybutyrate by marine microbes isolated from various marine environments.* Bioresource Technology, 2009. **100**(7): p. 2320-2323.
24. Wang, J. and L.R. Bakken, *Screening of soil bacteria for poly-β-hydroxybutyric acid production and its role in the survival of starvation.* Microbial Ecology, 1998. **35**: p. 94-101.
25. Khardenavis, A., P. Guha, M.S. Kumar, S. Mudliar and T. Chakrabarti, *Activated sludge is a potential source for production of biodegradable plastics from wastewater.* Environmental Technology, 2005. **26**(5): p. 545-552.
26. Madison, L.L. and G.W. Huisman, *Metabolic engineering of poly (3-hydroxyalkanoates): from DNA to plastic.* Microbiology and Molecular Biology Reviews, 1999. **63**(1): p. 21-53.
27. Müller, H.M. and D. Seebach, *Poly (hydroxyalkanoates): a fifth class of physiologically important organic biopolymers?* Angewandte Chemie International Edition in English, 1993. **32**(4): p. 477-502.
28. Anderson, A.J., G.W. Haywood and E.A. Dawes, *Biosynthesis and composition of bacterial poly (hydroxyalkanoates).* International Journal of Biological Macromolecules, 1990. **12**(2): p. 102-105.
29. Handrick, R., S. Reinhardt and D. Jendrossek, *Mobilization of poly (3-hydroxybutyrate) in* Ralstonia eutropha. Journal of Bacteriology, 2000. **182**(20): p. 5916-5918.
30. Kawaguchi, Y. and Y. Doi, *Kinetics and mechanism of synthesis and degradation of poly (3-hydroxybutyrate) in* Alcaligenes eutrophus. Macromolecules, 1992. **25**(9): p. 2324-2329.
31. Ruiz, J.A., N.I. López, R.O. Fernández and B.S. Méndez, *Polyhydroxyalkanoate degradation is associated with nucleotide accumulation and enhances stress resistance and survival of* Pseudomonas oleovorans *in natural water microcosms.* Applied and Environmental Microbiology, 2001. **67**(1): p. 225-230.
32. Jendrossek, D. and R. Handrick, *Microbial degradation of polyhydroxyalkanoates.* Annual Review of Microbiology, 2002. **56**: p. 403.
33. Rehm, B.H., *Genetics and biochemistry of polyhydroxyalkanoate granule self-assembly: the key role of polyester synthases.* Biotechnology Letters, 2006. **28**: p. 207-213.
34. Zinn, M., B. Witholt and T. Egli, *Occurrence, synthesis and medical application of bacterial polyhydroxyalkanoate.* Advanced Drug Delivery Reviews, 2001. **53**(1): p. 5-21.

35. Steinbüchel, A. and H.E. Valentin, *Diversity of bacterial polyhydroxyalkanoic acids.* FEMS Microbiology Letters, 1995. **128**(3): p. 219-228.
36. Haywood, G., A. Anderson and E. Dawes, *The importance of PHB-synthase substrate specificity in polyhydroxyalkanoate synthesis by A*lcaligenes eutrophus. FEMS Microbiology Letters, 1989. **57**(1): p. 1-6.
37. Anderson, A.J. and E. Dawes, *Occurrence, metabolism, metabolic role, and industrial uses of bacterial polyhydroxyalkanoates.* Microbiological Reviews, 1990. **54**(4): p. 450-472.
38. Doi, Y. and C. Abe, *Biosynthesis and characterization of a new bacterial copolyester of 3-hydroxyalkanoates and 3-hydroxy-omega.-chloroalkanoates.* Macromolecules, 1990. **23**(15): p. 3705-3707.
39. Fritzsche, K., R.W. Lenz and R.C. Fuller, *An unusual bacterial polyester with a phenyl pendant group.* Die Makromolekulare Chemie: Macromolecular Chemistry and Physics, 1990. **191**(8): p. 1957-1965.
40. Fritzsche, K., R.W. Lenz and R.C. Fuller, *Bacterial polyesters containing branched poly (β-hydroxyalkanoate) units.* International Journal of Biological Macromolecules, 1990. **12**(2): p. 92-101.
41. Fritzsche, K., R.W. Lenz and R.C. Fuller, *Production of unsaturated polyesters by* Pseudomonas oleovorans. International Journal of Biological Macromolecules, 1990. **12**(2): p. 85-91.
42. Kim, B.S., S.Y. Lee and H.N. Chang, *Production of poly-β-hydroxybutyrate by fed-batch culture of recombinant* Escherichia coli. Biotechnology Letters, 1992. **14**: p. 811-816.
43. Berlanga, M., M.T. Montero, J. Fernández-Borrell and R. Guerrero, *Rapid spectrofluorometric screening of poly-hydroxyalkanoate-producing bacteria from microbial mats.* International Microbiology, 2006. **9**(2): p. 95.
44. Muhammadi, Shabina, M. Afzal and S. Hameed, *Bacterial polyhydroxyalkanoates-eco-friendly next generation plastic: production, biocompatibility, biodegradation, physical properties and applications.* Green Chemistry Letters and Reviews, 2015. **8**(3-4): p. 56-77.
45. Ojumu, T., J. Yu and a. Solomon, *Production of polyhydroxyalkanoates, a bacterial biodegradable polymers.* African Journal of Biotechnology, 2004. **3**(1): p. 18-24.
46. Ciesielski, S., A. Cydzik-Kwiatkowska, T. Pokoj and E. Klimiuk, *Molecular detection and diversity of medium-chain-length polyhydroxyalkanoates-producing bacteria enriched from activated sludge.* Journal of Applied Microbiology, 2006. **101**(1): p. 190-199.
47. Luef, K.P., F. Stelzer and F. Wiesbrock, *Poly (hydroxy alkanoate)s in medical applications.* Chemical and Biochemical Engineering Quarterly, 2015. **29**(2): p. 287-297.
48. Numata, K., K. Morisaki, S. Tomizawa, M. Ohtani, T. Demura, M. Miyazaki, Y. Nogi and S. Deguchi, *Synthesis of poly- and oligo (hydroxyalkanoate)s by deep-sea bacteria,* Colwellia *spp.,* Moritella *spp., and* Shewanella *spp.* Polymer Journal, 2013. **45**(10): p. 1094-1100.
49. Suriyamongkol, P., R. Weselake, S. Narine, M. Moloney and S. Shah, *Biotechnological approaches for the production of polyhydroxyalkanoates in microorganisms and plants—a review.* Biotechnology Advances, 2007. **25**(2): p. 148-175.
50. Huisman, G.W., E. Wonink, R. Meima, B. Kazemier, P. Terpstra and B. Witholt, *Metabolism of poly (3-hydroxyalkanoates)(PHAs) by* Pseudomonas oleovorans. *Identification and sequences of genes and function of the*

encoded proteins in the synthesis and degradation of PHA. Journal of Biological Chemistry, 1991. **266**(4): p. 2191-2198.

51. Chek, M.F., S.-Y. Kim, T. Mori, H. Arsad, M.R. Samian, K. Sudesh and T. Hakoshima, *Structure of polyhydroxyalkanoate (PHA) synthase* Pha*C from* Chromobacterium *sp. USM2, producing biodegradable plastics.* Scientific Reports, 2017. **7**(1): p. 5312.
52. Rehm, B.H., *Polyester synthases: natural catalysts for plastics.* Biochemical Journal, 2003. **376**(1): p. 15-33.
53. Tsuge, T., M. Hyakutake and K. Mizuno, *Class IV polyhydroxyalkanoate (PHA) synthases and PHA-producing* Bacillus. Applied Microbiology and Biotechnology, 2015. **99**: p. 6231-6240.
54. Mezzolla, V., O.F. D'Urso and P. Poltronieri, *Role of* Pha*C type I and type II enzymes during PHA biosynthesis.* Polymers, 2018. **10**(8): p. 910.
55. Aldor, I.S. and J.D. Keasling, *Process design for microbial plastic factories: metabolic engineering of polyhydroxyalkanoates.* Current Opinion in Biotechnology, 2003. **14**(5): p. 475-483.
56. Rehm, B.H., N. Kruger and A. Steinbuchel, *A New Metabolic Link between Fatty Acid de NovoSynthesis and Polyhydroxyalkanoic Acid Synthesis: The* pha*G gene from* Pseudomonas putida *KT2440 encodes a 3-hydroxyacil-acyl carriere protein-coenzymeA transferase.* Journal of Biological Chemistry, 1998. **273**(37): p. 24044-24051.
57. Rehm, B.H., T.A. Mitsky and A. Steinbüchel, *Role of fatty acid* de novo *biosynthesis in polyhydroxyalkanoic acid (PHA) and rhamnolipid synthesis by* Pseudomonads*: establishment of the transacylase (*Pha*G)-mediated pathway for PHA biosynthesis in* Escherichia coli. Applied and Environmental Microbiology, 2001. **67**(7): p. 3102-3109.
58. Hoffmann, N., A.A. Amara, B.B. Beermann, Q. Qi, H.-J. Hinz and B.H. Rehm, *Biochemical characterization of the* Pseudomonas putida *3-hydroxyacyl ACP: CoA transacylase, which diverts intermediates of fatty acid de novo biosynthesis.* Journal of Biological Chemistry, 2002. **277**(45): p. 42926-42936.
59. Fukui, T., N. Shiomi and Y. Doi, *Expression and characterization of (R)-specific enoyl coenzyme A hydratase involved in polyhydroxyalkanoate biosynthesis by* Aeromonas caviae. Journal of Bacteriology, 1998. **180**(3): p. 667-673.
60. Fuller, R.C., *Microbial inclusions with special reference to PHA inclusions and intracellular boundary envelopes.* International Journal of Biological Macromolecules, 1999. **25**(1-3): p. 21-29.
61. Mezzina, M.P., D.E. Wetzler, M.V. Catone, H. Bucci, M. Di Paola and M.J. Pettinari, *A phasin with many faces: structural insights on* Pha*P from* Azotobacter *sp. FA8.* PLoS One, 2014. **9**(7): p. e103012.
62. Griebel, R., Z. Smith and J. Merrick, *Metabolism of poly (β-hydroxybutyrate). I. Purification, composition, and properties of native poly (β-hydroxybutyrate) granules from* Bacillus megaterium. Biochemistry, 1968. **7**(10): p. 3676-3681.
63. Stuart, E., A. Tehrani, H.E. Valentin, D. Dennis, R.W. Lenz and R.C. Fuller, *Protein organization on the PHA inclusion cytoplasmic boundary.* Journal of Biotechnology, 1998. **64**(2-3): p. 137-144.
64. Stuart, E.S., R.C. Fuller and R.W. Lenz, *The ordered macromolecular surface of polyester inclusion bodies in* Pseudomonas oleovotans. Canadian Journal of Microbiology, 1995. **41**(13): p. 84-93.

65. Gerngross, T., P. Reilly, J. Stubbe, A. Sinskey and O. Peoples, *Immunocytochemical analysis of poly-beta-hydroxybutyrate (PHB) synthase in* Alcaligenes eutrophus *H16: localization of the synthase enzyme at the surface of PHB granules.* Journal of Bacteriology, 1993. **175**(16): p. 5289-5293.
66. Pieper-Fürst, U., M.H. Madkour, F. Mayer and A. Steinbüchel, *Identification of the region of a 14-kilodalton protein of* Rhodococcus ruber *that is responsible for the binding of this phasin to polyhydroxyalkanoic acid granules.* Journal of Bacteriology, 1995. **177**(9): p. 2513-2523.
67. Grage, K., A.C. Jahns, N. Parlane, R. Palanisamy, I.A. Rasiah, J.A. Atwood and B.H. Rehm, *Bacterial polyhydroxyalkanoate granules: biogenesis, structure, and potential use as nano-/micro-beads in biotechnological and biomedical applications.* Biomacromolecules, 2009. **10**(4): p. 660-669.
68. Foster, L.J.R., R.W. Lenz and R. Clinton Fuller, *Quantitative determination of intracellular depolymerase activity in* Pseudomonas oleovorans *inclusions containing poly-3-hydroxyalkanoates with long alkyl substituents.* FEMS Microbiology Letters, 1994. **118**(3): p. 279-282.
69. Prieto, M.A., B. Bühler, K. Jung, B. Witholt and B. Kessler, *PhaF, a polyhydroxyalkanoate-granule-associated protein of P*seudomonas oleovorans GPo*1 involved in the regulatory expression system for* pha *genes.* Journal of Bacteriology, 1999. **181**(3): p. 858-868.
70. Potter, M., H. Muller, F. Reinecke, R. Wieczorek, F. Fricke, B. Bowien, B. Friedrich and A. Steinbuchel, *The complex structure of polyhydroxybutyrate (PHB) granules: four orthologous and paralogous phasins occur in* Ralstonia eutropha*.* Microbiology, 2004. **150**(7): p. 2301-2311.
71. Potter, M., H. Muller and A. Steinbuchel, *Influence of homologous phasins (*Pha*P) on PHA accumulation and regulation of their expression by the transcriptional repressor* Pha*R in* Ralstonia eutropha *H16.* Microbiology, 2005. **151**(3): p. 825-833.
72. Dunlop, W.F. and A. Robards, *Ultrastructural study of poly-β-hydroxybutyrate granules from* Bacillus cereus*.* Journal of Bacteriology, 1973. **114**(3): p. 1271-1280.
73. Mayer, F., M.H. Madkour, U. Pieper-fürst, R. Wieczorek, M. Liebergesell and A. Steinbüchel, *Electron microscopic observations on the macromolecular organization of the boundary layer of bacterial PHA inclusion bodies.* The Journal of General and Applied Microbiology, 1996. **42**(6): p. 445-455.
74. Amor, S.R., T. Rayment and J.K. Sanders, *Poly (hydroxybutyrate)* in vivo*: NMR and x-ray characterization of the elastomeric state.* Macromolecules, 1991. **24**(16): p. 4583-4588.
75. Viljakainen, V. and L. Hug, *The phylogenetic and global distribution of bacterial polyhydroxyalkanoate bioplastic-degrading genes.* Environmental Microbiology, 2021. **23**(3): p. 1717-1731.
76. Knoll, M., T.M. Hamm, F. Wagner, V. Martinez and J. Pleiss, *The PHA depolymerase engineering database: a systematic analysis tool for the diverse family of polyhydroxyalkanoate (PHA) depolymerases.* BMC Bioinformatics, 2009. **10**: p. 1-8.
77. Nishida, H. and Y. Tokiwa, *Distribution of poly (β-hydroxybutyrate) and poly (ε-caprolactone) aerobic degrading microorganisms in different environments.* Journal of Environmental Polymer Degradation, 1993. **1**: p. 227-233.

78. Jendrossek, D., *Extracellular polyhydroxyalkanoate depolymerases: the key enzymes of PHA degradation.* Biopolymers. Polyesters, 2002: p. 41-83.
79. Calabia, B.P. and Y. Tokiwa, *Microbial degradation of poly (D-3-hydroxybutyrate) by a new thermophilic* Streptomyces *isolate.* Biotechnology Letters, 2004. **26**: p. 15-19.
80. Anderson, I.J., R.F. Watkins, J. Samuelson, D.F. Spencer, W.H. Majoros, M.W. Gray and B.J. Loftus, *Gene discovery in the* Acanthamoeba castellanii *genome.* Protist, 2005. **156**(2): p. 203-14.
81. Jendrossek, D., A. Schirmer and H. Schlegel, *Biodegradation of polyhydroxyalkanoic acids.* Applied Microbiology and Biotechnology, 1996. **46**(5): p. 451-463.
82. Gonda, K., D. Jendrossek and H.-P. Molitoris, *Fungal degradation of the thermoplastic polymer poly-ß-hydroxybutyric acid (PHB) under simulated deep sea pressure*, in *Life at Interfaces and Under Extreme Conditions*. 2000, Springer. p. 173-183.
83. Kim, D. and Y. Rhee, *Biodegradation of microbial and synthetic polyesters by fungi.* Applied microbiology and biotechnology, 2003. **61**(4): p. 300-308.
84. Lee, S.Y. and J.-i. Choi, *Production and degradation of polyhydroxyalkanoates in waste environment.* Waste Management, 1999. **19**(2): p. 133-139.
85. Jendrossek, D., *Extracellular polyhydroxyalkanoate (PHA) depolymerases: the key enzymes of PHA degradation.* Biopolymers Online: Biology Chemistry Biotechnology Applications, 2005. **3**.
86. Volova, T., A. Boyandin, A. Vasiliev, V. Karpov, S. Prudnikova, O. Mishukova, U. Boyarskikh, M. Filipenko, V. Rudnev and B.B. Xuân, *Biodegradation of polyhydroxyalkanoates (PHAs) in tropical coastal waters and identification of PHA-degrading bacteria.* Polymer degradation and stability, 2010. **95**(12): p. 2350-2359.
87. Boyandin, A.N., S.V. Prudnikova, V.A. Karpov, V.N. Ivonin, N.L. Đỗ, T.H. Nguyễn, T.M.H. Lê, N.L. Filichev, A.L. Levin and M.L. Filipenko, *Microbial degradation of polyhydroxyalkanoates in tropical soils.* International Biodeterioration & Biodegradation, 2013. **83**: p. 77-84.
88. Jaeger, K.-E., A. Steinbüchel and D. Jendrossek, *Substrate specificities of bacterial polyhydroxyalkanoate depolymerases and lipases: bacterial lipases hydrolyze poly (omega-hydroxyalkanoates).* Applied and Environmental Microbiology, 1995. **61**(8): p. 3113-3118.
89. Behrends, A., B. Klingbeil and D. Jendrossek, *Poly (3-hydroxybutyrate) depolymerases bind to their substrate by a C-terminal located substrate binding site.* FEMS Microbiology Letters, 1996. **143**(2-3): p. 191-194.
90. Ohura, T., K.-I. Kasuya and Y. Doi, *Cloning and characterization of the polyhydroxybutyrate depolymerase gene of* Pseudomonas stutzeri *and analysis of the function of substrate-binding domains.* Applied and Environmental Microbiology, 1999. **65**(1): p. 189-197.
91. Neumeier, S., *Abbau thermoplastischer Biopolymere auf Poly-ß-Hydroxyalkanoat-Basis durch terrestrische und marine Pilze*. 1994, Diplomarbeit, Universität Regensburg: 99 pp.
92. Hisano, T., K. Kasuya, Y. Tezuka, N. Ishii, T. Kobayashi, M. Shiraki, E. Oroudjev, H. Hansma, T. Iwata, Y. Doi, T. Saito and K. Miki, *The crystal structure of polyhydroxybutyrate depolymerase from* Penicillium funiculosum *provides insights into the recognition and degradation of biopolyesters.* Journal of Molecular Biology, 2006. **356**(4): p. 993-1004.

93. Murase, T., T. Iwata and Y. Doi, *Atomic force microscopy investigation of poly [(R)-3-hydroxybutyrate] lamellar single crystals: Relationship between molecular weight and enzymatic degradation behavior.* Macromolecular Bioscience, 2001. **1**(7): p. 275-281.

94. Murase, T., Y. Suzuki, Y. Doi and T. Iwata, *Nonhydrolytic fragmentation of a poly [(R)-3-hydroxybutyrate] single crystal revealed by use of a mutant of polyhydroxybutyrate depolymerase.* Biomacromolecules, 2002. **3**(2): p. 312-317.

95. Nobes, G., R. Marchessault, H. Chanzy, B. Briese and D. Jendrossek, *Splintering of poly (3-hydroxybutyrate) single crystals by PHB-depolymerase A from* Pseudomonas lemoignei. Macromolecules, 1996. **29**(26): p. 8330-8333.

96. Iwata, T., Y. Doi, K.-i. Kasuya and Y. Inoue, *Visualization of enzymatic degradation of poly [(R)-3-hydroxybutyrate] single crystals by an extracellular PHB depolymerase.* Macromolecules, 1997. **30**(4): p. 833-839.

97. Iwata, T., Y. Doi, T. Tanaka, T. Akehata, M. Shiromo and S. Teramachi, *Enzymatic degradation and adsorption on poly [(R)-3-hydroxybutyrate] single crystals with two types of extracellular PHB depolymerases from* Comamonas acidovorans *YM1609 and* Alcaligenes faecalis *T1.* Macromolecules, 1997. **30**(18): p. 5290-5296.

98. Hiraishi, T., Y. Hirahara, Y. Doi, M. Maeda and S. Taguchi, *Effects of mutations in the substrate-binding domain of poly [(R)-3-hydroxybutyrate](PHB) depolymerase from* Ralstonia pickettii *T1 on PHB degradation.* Applied and Environmental Microbiology, 2006. **72**(11): p. 7331-7338.

99. Saito, T., K. Suzuki, J. Yamamoto, T. Fukui, K. Miwa, K. Tomita, S. Nakanishi, S. Odani, J.-l. Suzuki and K. Ishikawa, *Cloning, nucleotide sequence, and expression in* Escherichia coli *of the gene for poly (3-hydroxybutyrate) depolymerase from* Alcaligenes faecalis. Journal of Bacteriology, 1989. **171**(1): p. 184-189.

100. Handrick, R., S. Reinhardt, M.L. Focarete, M. Scandola, G. Adamus, M. Kowalczuk and D. Jendrossek, *A new type of thermoalkalophilic hydrolase of* Paucimonas lemoignei *with high specificity for amorphous polyesters of short chain-length hydroxyalkanoic acids.* Journal of Biological Chemistry, 2001. **276**(39): p. 36215-36224.

101. Reinhardt, S., R. Handrick and D. Jendrossek, *The "PHB Depolymerase Inhibitor" of* Paucimonas lemoignei *Is a PHB Depolymerase.* Biomacromolecules, 2002. **3**(4): p. 823-827.

102. Wakadkar, S., S. Hermawan, D. Jendrossek and A.C. Papageorgiou, *The structure of* PhaZ*7 at atomic (1.2 Å) resolution reveals details of the active site and suggests a substrate-binding mode.* Acta Crystallographica Section F: Structural Biology and Crystallization Communications, 2010. **66**(6): p. 648-654.

103. Papageorgiou, A.C., S. Hermawan, C.B. Singh and D. Jendrossek, *Structural basis of poly (3-hydroxybutyrate) hydrolysis by* PhaZ*7 depolymerase from* Paucimonas lemoignei. Journal of Molecular Biology, 2008. **382**(5): p. 1184-1194.

104. Hiraishi, T. and S. Taguchi, *Protein engineering of enzymes involved in bioplastic metabolism.* Protein Engineering - Technology and Application, InTech, Rijeka, Croatia, 2013: p. 133-165.

105. Shirakura, Y., T. Fukui, T. Tanio, K. Nakayama, R. Matsuno and K. Tomita, *An extracellular D (−)-3-hydroxybutyrate oligomer hydrolase from* Alcaligenes faecalis. Biochimica et Biophysica Acta (BBA)-Protein Structure and Molecular Enzymology, 1983. **748**(2): p. 331-339.
106. Senior, P.J. and E.A. Dawes, *The regulation of poly-beta-hydroxybutyrate metabolism in* Azotobacter beijerinckii. Biochemical Journal, 1973. **134**(1): p. 225-38.
107. Kobayashi, T. and T. Saito, *Catalytic triad of intracellular poly (3-hydroxybutyrate) depolymerase (*PhaZ*1) in* Ralstonia eutropha *H16.* Journal of Bioscience and Bioengineering, 2003. **96**(5): p. 487-492.
108. Eggers, J. and A. Steinbüchel, *Poly (3-hydroxybutyrate) degradation in* Ralstonia eutropha *H16 is mediated stereoselectively to (S)-3-hydroxybutyryl coenzyme A (CoA) via crotonyl-CoA.* Journal of Bacteriology, 2013. **195**(14): p. 3213-3223.
109. Suzuki, M., Y. Tachibana and K.-i. Kasuya, *Biodegradability of poly (3-hydroxyalkanoate) and poly (ε-caprolactone) via biological carbon cycles in marine environments.* Polymer Journal, 2021. **53**(1): p. 47-66.
110. Yamada, M., A. Yukita, Y. Hanazumi, Y. Yamahata, H. Moriya, M. Miyazaki, T. Yamashita and H. Shimoi, *Poly (3-hydroxybutyrate) production using mannitol as a sole carbon source by* Burkholderia *sp. AIU M5M02 isolated from a marine environment.* Fisheries Science, 2018. **84**: p. 405-412.
111. Shrivastav, A., S.K. Mishra, B. Shethia, I. Pancha, D. Jain and S. Mishra, *Isolation of promising bacterial strains from soil and marine environment for polyhydroxyalkanoates (PHAs) production utilizing Jatropha biodiesel byproduct.* International Journal of Biological Macromolecules, 2010. **47**(2): p. 283-287.
112. Boyandin, A., G. Kalacheva, E. Rodicheva and T. Volova, *Synthesis of reserve polyhydroxyalkanoates by luminescent bacteria.* Microbiology, 2008. **77**: p. 318-323.
113. Simon-Colin, C., G. Raguénès, J. Cozien and J. Guezennec, Halomonas profundus *sp. nov., a new PHA-producing bacterium isolated from a deep-sea hydrothermal vent shrimp.* Journal of Applied Microbiology, 2008. **104**(5): p. 1425-1432.
114. Uefuji, M., K.-i. Kasuya and Y. Doi, *Enzymatic degradation of poly [(R)-3-hydroxybutyrate]: secretion and properties of PHB depolymerase from* Pseudomonas stutzeri. Polymer Degradation and Stability, 1997. **58**(3): p. 275-281.
115. Kasuya, K.-i., H. Mitomo, M. Nakahara, A. Akiba, T. Kudo and Y. Doi, *Identification of a Marine Benthic P(3HB)-Degrading Bacterium Isolate and Characterization of its P(3HB) Depolymerase.* Biomacromolecules, 2000. **1**(2): p. 194-201.
116. Doronina, N.V., Y.A. Trotsenko and T.P. Tourova, Methylarcula marina *gen. nov., sp. nov. and* Methylarcula terricola *sp. nov.: novel aerobic, moderately halophilic, facultatively methylotrophic bacteria from coastal saline environments.* International Journal of Systematic and Evololutionary Microbiology, 2000. **50 Pt 5**: p. 1849-1859.
117. Zadjelovic, V., A. Chhun, M. Quareshy, E. Silvano, J.R. Hernandez-Fernaud, M.M. Aguilo-Ferretjans, R. Bosch, C. Dorador, M.I. Gibson and J.A. Christie-Oleza, *Beyond oil degradation: enzymatic potential of* Alcanivorax *to degrade natural and synthetic polyesters.* Environmental Microbiology, 2020. **22**(4): p. 1356-1369.

118. Kita, K., K. Ishimaru, M. Teraoka, H. Yanase and N. Kato, *Properties of poly(3-hydroxybutyrate) depolymerase from a marine bacterium,* Alcaligenes faecalis *AE122.* Applied Environmental Microbioly, 1995. **61**(5): p. 1727-30.
119. Ma, W.T., J.H. Lin, H.J. Chen, S.Y. Chen and G.C. Shaw, *Identification and characterization of a novel class of extracellular poly(3-hydroxybutyrate) depolymerase from* Bacillus *sp. strain NRRL B-14911.* Applied Environmental Microbioly, 2011. **77**(22): p. 7924-32.
120. Kita, K., S. Mashiba, M. Nagita, K. Ishimaru, K. Okamoto, H. Yanase and N. Kato, *Cloning of poly(3-hydroxybutyrate) depolymerase from a marine bacterium,* Alcaligenes faecalis *AE122, and characterization of its gene product.* Biochimica et Biophysica Acta (BBA)-Gene Structure and Expression, 1997. **1352**(1): p. 113-22.
121. Kasuya, K., T. Takano, Y. Tezuka, W.C. Hsieh, H. Mitomo and Y. Doi, *Cloning, expression and characterization of a poly(3-hydroxybutyrate) depolymerase from* Marinobacter *sp. NK-1.* International Journal of Biological Macromolecules, 2003. **33**(4-5): p. 221-6.
122. Kasuya, K.-i., T. Ohura, K. Masuda and Y. Doi, *Substrate and binding specificities of bacterial polyhydroxybutyrate depolymerases.* International Journal of Biological Macromolecules, 1999. **24**(4): p. 329-336.
123. Mason-Jones, K., C.C. Banfield and M.A. Dippold, *Compound-specific 13C stable isotope probing confirms synthesis of polyhydroxybutyrate by soil bacteria.* Rapid Communications in Mass Spectrometry, 2019. **33**(8): p. 795-802.
124. Hanzlíkova, A., A. Jandera and F. Kunc, *Formation of poly-3-hydroxybutyrate by a soil microbial community during batch and heterocontinuous cultivation.* Folia microbiologica, 1984. **29**: p. 233-241.
125. Wang, J. and L. Bakken, *Screening of soil bacteria for poly-β-hydroxybutyric acid production and its role in the survival of starvation.* Microbial Ecology, 1998. **35**(1): p. 94-101.
126. Berg, G. and K. Smalla, *Plant species and soil type cooperatively shape the structure and function of microbial communities in the rhizosphere.* FEMS Microbiology Ecology, 2009. **68**(1): p. 1-13.
127. Gasser, I., H. Müller and G. Berg, *Ecology and characterization of polyhydroxyalkanoate-producing microorganisms on and in plants.* FEMS Microbiology Ecology, 2009. **70**(1): p. 142-150.
128. Flores, H.E., J.M. Vivanco and V.M. Loyola-Vargas, *'Radicle' biochemistry: the biology of root-specific metabolism.* Trends Plant Sciences, 1999. **4**(6): p. 220-226.
129. Revelo Romo, D.M., M.V. Grosso, N.C. Moreno Solano and D. Montoya Castaño, *A most effective method for selecting a broad range of short and medium-chain-length polyhidroxyalcanoate producing microorganisms.* Electronic Journal of Biotechnology, 2007. **10**(3): p. 348-357.
130. Lima, T.C.S.d., B.M. Grisi and M.C.M. Bonato, *Bacteria isolated from a sugarcane agroecosystem: their potential production of polyhydroxyalcanoates and resistance to antibiotics.* Revista de Microbiologia, 1999. **30**: p. 214-224.
131. Reichardt, W., G. Mascarina, B. Padre and J. Doll, *Microbial communities of continuously cropped, irrigated rice fields.* Applied and Environmental Microbiology, 1997. **63**(1): p. 233-238.
132. Lee, S.Y., *Bacterial polyhydroxyalkanoates.* Biotechnology and Bioengineering, 1996. **49**(1): p. 1-14.

133. Dris, R., H. Imhof, W. Sanchez, J. Gasperi, F. Galgani, B. Tassin and C. Laforsch, *Beyond the ocean: contamination of freshwater ecosystems with (micro-) plastic particles.* Environmental Chemistry, 2015. **12**(5): p. 539-550.
134. Lebreton, L.C., J. Van Der Zwet, J.-W. Damsteeg, B. Slat, A. Andrady and J. Reisser, *River plastic emissions to the world's oceans.* Nature Communications, 2017. **8**(1): p. 15611.
135. Brandon, J.A., W. Jones and M.D. Ohman, *Multidecadal increase in plastic particles in coastal ocean sediments.* Science Advances, 2019. **5**(9): p. eaax0587.
136. Hurley, R., A. Horton, A. Lusher and L. Nizzetto, *Plastic waste in the terrestrial environment*, in *Plastic Waste and Recycling*. 2020, Elsevier. p. 163-193.
137. Steinmetz, Z., C. Wollmann, M. Schaefer, C. Buchmann, J. David, J. Tröger, K. Muñoz, O. Frör and G.E. Schaumann, *Plastic mulching in agriculture. Trading short-term agronomic benefits for long-term soil degradation?* Science of the Total Environment, 2016. **550**: p. 690-705.
138. Ammala, A., S. Bateman, K. Dean, E. Petinakis, P. Sangwan, S. Wong, Q. Yuan, L. Yu, C. Patrick and K. Leong, *An overview of degradable and biodegradable polyolefins.* Progress in Polymer Science, 2011. **36**(8): p. 1015-1049.
139. Laycock, B., M. Nikolić, J.M. Colwell, E. Gauthier, P. Halley, S. Bottle and G. George, *Lifetime prediction of biodegradable polymers.* Progress in Polymer Science, 2017. **71**: p. 144-189.
140. Qi, R., D.L. Jones, Z. Li, Q. Liu and C. Yan, *Behavior of microplastics and plastic film residues in the soil environment: A critical review.* Science of the Total Environment, 2020. **703**: p. 134722.
141. Qian, J., S. Tang, P. Wang, B. Lu, K. Li, W. Jin and X. He, *From source to sink: Review and prospects of microplastics in wetland ecosystems.* Science of the Total Environment, 2021. **758**: p. 143633.
142. Rillig, M.C., *Microplastic in terrestrial ecosystems and the soil?* 2012, ACS Publications.
143. Jambeck, J.R., R. Geyer, C. Wilcox, T.R. Siegler, M. Perryman, A. Andrady, R. Narayan and K.L. Law, *Plastic waste inputs from land into the ocean.* Science, 2015. **347**(6223): p. 768-771.
144. Rodríguez, T., D. Represas and E.V. Carral, *Ecotoxicity of Single-Use Plastics to Earthworms.* Environments, 2023. **10**(3): p. 41.
145. Censi, V., F. Saiano, D. Bongiorno, S. Indelicato, A. Napoli and D. Piazzese, *Bioplastics: A new analytical challenge.* Frontiers in Chemistry, 2022. **10**: p. 971792.
146. Lucas, N., C. Bienaime, C. Belloy, M. Queneudec, F. Silvestre and J.-E. Nava-Saucedo, *Polymer biodegradation: Mechanisms and estimation techniques–A review.* Chemosphere, 2008. **73**(4): p. 429-442.
147. Steinbüchel, A. and T. Lütke-Eversloh, *Metabolic engineering and pathway construction for biotechnological production of relevant polyhydroxyalkanoates in microorganisms.* Biochemical Engineering Journal, 2003. **16**(2): p. 81-96.
148. Snell, K.D. and O.P. Peoples, *PHA bioplastic: A value-added coproduct for biomass biorefineries.* Biofuels, Bioproducts and Biorefining: Innovation for a Sustainable Economy, 2009. **3**(4): p. 456-467.
149. Keshavarz, T. and I. Roy, *Polyhydroxyalkanoates: bioplastics with a green agenda.* Current Opinion in Microbiology, 2010. **13**(3): p. 321-326.

150. Pratt, S., L.-J. Vandi, D. Gapes, A. Werker, A. Oehmen and B. Laycock, *Polyhydroxyalkanoate (PHA) bioplastics from organic waste.* Biorefinery: Integrated Sustainable Processes for Biomass Conversion to Biomaterials, Biofuels, and Fertilizers, 2019: p. 615-638.
151. Holmes, P., *Applications of PHB - a microbially produced biodegradable thermoplastic.* Physics in Technology, 1985. **16**(1): p. 32.
152. Amaro, T.M., D. Rosa, G. Comi and L. Iacumin, *Prospects for the use of whey for polyhydroxyalkanoate (PHA) production.* Frontiers in Microbiology, 2019. **10**: p. 992.
153. Nielsen, C., A. Rahman, A.U. Rehman, M.K. Walsh and C.D. Miller, *Food waste conversion to microbial polyhydroxyalkanoates.* Microbial Biotechnology, 2017. **10**(6): p. 1338-1352.
154. Doi, Y., *Synthesis and properties of biodegradable polymers and plastics*, in *Superconductors, Surfaces and Superlattices*. 1994, Elsevier. p. 1057-1060.
155. Page, W.J., *Production of polyhydroxyalkanoates by* Azotobacter vinelandii *UWD in beet molasses culture.* FEMS Microbiology Reviews, 1992. **9**(2-4): p. 149-157.
156. Tokiwa, Y. and T. Suzuki, *Hydrolysis of polyesters by lipases.* Nature, 1977. **270**(5632): p. 76-78.
157. Murphy, C.A., J. Cameron, S.J. Huang and R.T. Vinopal, Fusarium *polycaprolactone depolymerase is cutinase.* Applied and Environmental microbiology, 1996. **62**(2): p. 456-460.
158. Labet, M. and W. Thielemans, *Synthesis of polycaprolactone: a review.* Chemical Society Reviews, 2009. **38**(12): p. 3484-3504.
159. Tserki, V., P. Matzinos, E. Pavlidou, D. Vachliotis and C. Panayiotou, *Biodegradable aliphatic polyesters. Part I. Properties and biodegradation of poly (butylene succinate-co-butylene adipate).* Polymer Degradation and Stability, 2006. **91**(2): p. 367-376.
160. Nampoothiri, K.M., N.R. Nair and R.P. John, *An overview of the recent developments in polylactide (PLA) research.* Bioresource Technology, 2010. **101**(22): p. 8493-8501.
161. Ku, H., H. Wang, N. Pattarachaiyakoop and M. Trada, *A review on the tensile properties of natural fiber reinforced polymer composites.* Composites Part B: Engineering, 2011. **42**(4): p. 856-873.
162. Nakayama, A., N. Yamano and N. Kawasaki, *Biodegradation in seawater of aliphatic polyesters.* Polymer Degradation and Stability, 2019. **166**: p. 290-299.
163. Luzier, W.D., *Materials derived from biomass/biodegradable materials.* Proceedings of the National Academy of Sciences, 1992. **89**(3): p. 839-842.
164. Kasuya, K.-i., K.-i. Takagi, S.-i. Ishiwatari, Y. Yoshida and Y. Doi, *Biodegradabilities of various aliphatic polyesters in natural waters.* Polymer Degradation and Stability, 1998. **59**(1-3): p. 327-332.
165. Brandl, H. and P. Püchner, *Biodegradation of plastic bottles made from 'Biopol'in an aquatic ecosystem under in situ conditions.* Biodegradation, 1991. **2**: p. 237-243.
166. Doi, Y., Y. Kanesawa, N. Tanahashi and Y. Kumagai, *Biodegradation of microbial polyesters in the marine environment.* Polymer Degradation and Stability, 1992. **36**(2): p. 173-177.
167. Tsuji, H. and K. Suzuyoshi, *Environmental degradation of biodegradable polyesters 1. Poly (ε-caprolactone), poly [(R)-3-hydroxybutyrate], and poly*

(L-lactide) films in controlled static seawater. Polymer Degradation and Stability, 2002. **75**(2): p. 347-355.

168. Rutkowska, M., K. Krasowska, A. Heimowska, G. Adamus, M. Sobota, M. Musioł, H. Janeczek, W. Sikorska, A. Krzan and E. Žagar, *Environmental degradation of blends of atactic poly [(R, S)-3-hydroxybutyrate] with natural PHBV in Baltic sea water and compost with activated sludge.* Journal of Polymers and the Environment, 2008. **16**: p. 183-191.
169. Thellen, C., M. Coyne, D. Froio, M. Auerbach, C. Wirsen and J.A. Ratto, *A processing, characterization and marine biodegradation study of melt-extruded polyhydroxyalkanoate (PHA) films.* Journal of Polymers and the Environment, 2008. **16**: p. 1-11.
170. Bugnicourt, E., P. Cinelli, A. Lazzeri and V.A. Alvarez, *Polyhydroxyalkanoate (PHA): Review of synthesis, characteristics, processing and potential applications in packaging.* Express Polymer Letters, 2014.
171. Poirier, Y., *Green chemistry yields a better plastic.* Nature Biotechnology, 1999. **17**(10): p. 960-961.
172. Poirier, Y., C. Nawrath and C. Somerville, *Production of polyhydroxyalkanoates, a family of biodegradable plastics and elastomers, in bacteria and plants.* Bio/technology, 1995. **13**(2): p. 142-150.
173. Steinbüchel, A., *Perspectives for biotechnological production and utilization of biopolymers: metabolic engineering of polyhydroxyalkanoate biosynthesis pathways as a successful example.* Macromolecular Bioscience, 2001. **1**(1): p. 1-24.
174. Ivanov, V., V. Stabnikov, Z. Ahmed, S. Dobrenko and A. Saliuk, *Production and applications of crude polyhydroxyalkanoate-containing bioplastic from the organic fraction of municipal solid waste.* International Journal of Environmental Science and Technology, 2015. **12**: p. 725-738.
175. Cox, M., *Properties and applications of polyhydroxyalkanoates*, in *Studies in Polymer Science*. 1994, Elsevier. p. 120-135.
176. Doi, Y., S. Kitamura and H. Abe, *Microbial synthesis and characterization of poly (3-hydroxybutyrate-co-3-hydroxyhexanoate).* Macromolecules, 1995. **28**(14): p. 4822-4828.
177. Steinbüchel, A. and B. Füchtenbusch, *Bacterial and other biological systems for polyester production.* Trends in Biotechnology, 1998. **16**(10): p. 419-427.
178. Riedel, S.L., C.J. Brigham, C.F. Budde, J. Bader, C. Rha, U. Stahl and A.J. Sinskey, *Recovery of poly (3-hydroxybutyrate-co-3-hydroxyhexanoate) from* Ralstonia eutropha *cultures with non-halogenated solvents.* Biotechnology and Bioengineering, 2013. **110**(2): p. 461-470.
179. De Bary, A., *Die erscheinung der symbiose: Vortrag gehalten auf der versammlung deutscher naturforscher und aerzte zu cassel*. Trübner, 1879.
180. Starr, M., *A generalized scheme for classifying organismic associations.* Symposia of the Society for Experimental Biology, 1975.(29),1-20.
181. Margulis, L., *Words as battle cries: symbiogenesis and the new field of endocytobiology.* Bioscience, 1990. **40**(9): p. 673-677.
182. Mushegian, A.A. and D. Ebert, *Rethinking "mutualism" in diverse host-symbiont communities.* BioEssays, 2016. **38**(1): p. 100-108.
183. Pérez-Brocal, V., A. Latorre and A. Moya, *Symbionts and pathogens: what is the difference?* Between Pathogenicity and Commensalism, 2011: p. 215-243.

184. Brune, A. and M. Ohkuma, *Role of the termite gut microbiota in symbiotic digestion.* Biology of Termites: A Modern Synthesis, 2011: p. 439-475.
185. Graf, J.S., S. Schorn, K. Kitzinger, S. Ahmerkamp, C. Woehle, B. Huettel, C.J. Schubert, M.M. Kuypers and J. Milucka, *Anaerobic endosymbiont generates energy for ciliate host by denitrification.* Nature, 2021. **591**(7850): p. 445-450.
186. Dubilier, N., C. Bergin and C. Lott, *Symbiotic diversity in marine animals: the art of harnessing chemosynthesis.* Nature Reviews Microbiology, 2008. **6**(10): p. 725-740.
187. Douglas, A.E., *The molecular basis of bacterial–insect symbiosis.* Journal of Molecular Biology, 2014. **426**(23): p. 3830-3837.
188. Baumann, P., *Biology of bacteriocyte-associated endosymbionts of plant sap-sucking insects.* Annual Reviews in Microbiology, 2005. **59**: p. 155-189.
189. Hosseini Faradonbeh, N., E. Izadi Darbandi, H. Karimmojeni and A. Nezami, *The morphological and physiological traits of* Cucumis sativus-Phelipanche aegyptiaca *association affected by arbuscular mycorrhizal fungi symbiosis.* Journal of Crop Protection, 2021. **10**(4): p. 669-684.
190. Gross, R., F. Vavre, A. Heddi, G.D. Hurst, E. Zchori-Fein and K. Bourtzis, *Immunity and symbiosis.* Molecular Microbiology, 2009. **73**(5): p. 751-759.
191. Kikuchi, Y., T. Hosokawa and T. Fukatsu, *Specific developmental window for establishment of an insect-microbe gut symbiosis.* Applied and Environmental Microbiology, 2011. **77**(12): p. 4075-4081.
192. Kikuchi, Y., T. Hosokawa and T. Fukatsu, *Insect-microbe mutualism without vertical transmission: a stinkbug acquires a beneficial gut symbiont from the environment every generation.* Applied and Environmental Microbiology, 2007. **73**(13): p. 4308-4316.
193. Kikuchi, Y., X.-Y. Meng and T. Fukatsu, *Gut symbiotic bacteria of the genus* Burkholderia *in the broad-headed bugs* Riptortus clavatus *and* Leptocorisa chinensis *(*Heteroptera: Alydidae*).* Applied and Environmental Microbiology, 2005. **71**(7): p. 4035-4043.
194. Kim, J.K., Y.J. Won, N. Nikoh, H. Nakayama, S.H. Han, Y. Kikuchi, Y.H. Rhee, H.Y. Park, J.Y. Kwon and K. Kurokawa, *Polyester synthesis genes associated with stress resistance are involved in an insect–bacterium symbiosis.* Proceedings of the National Academy of Sciences, 2013. **110**(26): p. E2381-E2389.
195. Wong, P.P. and H.J. Evans, *Poly-β-hydroxybutyrate utilization by soybean (*Glycine max Merr.*) nodules and assessment of its role in maintenance of nitrogenase activity.* Plant Physiology, 1971. **47**(6): p. 750-755.
196. Kretovich, W., V. Romanov, L. Yushkova, V. Shramko and N. Fedulova, *Nitrogen fixation and poly-β-hydroxybutyric acid content in bacteroids of* Rhizobium lupini *and* Rhizobium leguminosarum*.* Plant and Soil, 1977. **48**: p. 291-302.
197. Romanov, V., N. Fedulova, I. Tchermenskaya, V. Shramko, M. Molchanov and W. Kretovich, *Metabolism of poly-hydroxybutyric acid in bacteroids of* Rhizobium lupini *in connection with nitrogen fixation and photosynthesis.* Plant and Soil, 1980. **56**: p. 379-390.
198. Gerson, T., J. Patel and M. Wong, *The effects of age, darkness and nitrate on poly-β-hydroxybutyrate levels and nitrogen-fixing ability of* Rhizobium *in* Lupinus angustifolius*.* Physiologia Plantarum, 1978. **42**(4): p. 420-424.

199. Bergersen, F., M. Peoples and G. Turner, *A role for poly-β-hydroxybutyrate in bacteroids of soybean root nodules.* Proceedings of the Royal Society of London. Series B: Biological Sciences, 1991. **245**(1312): p. 59-64.
200. Bergersen, F.J. and G. Turner, *Bacteroids from soybean root nodules: accumulation of poly-β-hydroxybutyrate during supply of malate and succinate in relation to N2 fixation in flow-chamber reactions.* Proceedings of the Royal Society of London. B. Biological Sciences, 1990. **240**(1297): p. 39-59.
201. Tombolini, R. and M. Nuti, *Poly (β-hydroxyalkanoate) biosynthesis and accumulation by different* Rhizobium *species.* FEMS Microbiology Letters, 1989. **60**(3): p. 299-304.
202. Peralta, H., Y. Mora, E. Salazar, S. Encarnación, R. Palacios and J. Mora, *Engineering the* nif*H promoter region and abolishing poly-β-hydroxybutyrate accumulation in* Rhizobium etli *enhance nitrogen fixation in symbiosis with* Phaseolus vulgaris. Applied and Environmental Microbiology, 2004. **70**(6): p. 3272-3281.
203. Cevallos, M.A., S. Encarnación, A. Leija, Y. Mora and J. Mora, *Genetic and physiological characterization of a* Rhizobium etli *mutant strain unable to synthesize poly-beta-hydroxybutyrate.* Journal of Bacteriology, 1996. **178**(6): p. 1646-1654.
204. Lodwig, E., M. Leonard, S. Marroqui, T. Wheeler, K. Findlay, J. Downie and P. Poole, *Role of polyhydroxybutyrate and glycogen as carbon storage compounds in pea and bean bacteroids.* Molecular Plant-Microbe Interactions, 2005. **18**(1): p. 67-74.
205. Willis, L.B. and G.C. Walker, *The* phb*C (poly-β-hydroxybutyrate synthase) gene of* Rhizobium (Sinorhizobium) meliloti *and characterization of* phb*C mutants.* Canadian Journal of Microbiology, 1998. **44**(6): p. 554-564.
206. Aneja, P., A. Zachertowska and T. Charles, *Comparison of the symbiotic and competition phenotypes of* Sinorhizobium meliloti *PHB synthesis and degradation pathway mutants.* Canadian Journal of Microbiology, 2005. **51**(7): p. 599-604.
207. Yokota, K., E. Fukai, L.H. Madsen, A. Jurkiewicz, P. Rueda, S. Radutoiu, M. Held, M.S. Hossain, K. Szczyglowski and G. Morieri, *Rearrangement of actin cytoskeleton mediates invasion of* Lotus japonicus *roots by* Mesorhizobium loti. The Plant Cell, 2009. **21**(1): p. 267-284.
208. Surridge, C., *Light regulation of nodulation.* Nature Plants, 2021. **7**(11): p. 1437-1437.
209. Schmidt, A., *Morphological and molecular analysis of* Laxus oneistus *juveniles and their bacterial ectosymbiont.* Diplomarbeit Universität Wien, 2013, 10.25365/thesis.29923.
210. Dubilier, N., C. Mülders, T. Ferdelman, D. de Beer, A. Pernthaler, M. Klein, M. Wagner, C. Erséus, F. Thiermann and J. Krieger, *Endosymbiotic sulphate-reducing and sulphide-oxidizing bacteria in an oligochaete worm.* Nature, 2001. **411**(6835): p. 298-302.
211. Kleiner, M., C. Wentrup, C. Lott, H. Teeling, S. Wetzel, J. Young, Y.-J. Chang, M. Shah, N.C. VerBerkmoes and J. Zarzycki, *Metaproteomics of a gutless marine worm and its symbiotic microbial community reveal unusual pathways for carbon and energy use.* Proceedings of the National Academy of Sciences, 2012. **109**(19): p. E1173-E1182.
212. Angst, G., C.W. Mueller, I. Prater, Š. Angst, J. Frouz, V. Jílková, F. Peterse and K.G. Nierop, *Earthworms act as biochemical reactors to convert labile*

plant compounds into stabilized soil microbial necromass. Communications Biology, 2019. **2**(1): p. 441.

213. Jones, C.G., J.H. Lawton and M. Shachak, *Organisms as ecosystem engineers.* Oikos, 1994: p. 373-386.
214. Fusaro, S., F. Gavinelli, F. Lazzarini and M.G. Paoletti, *Soil Biological Quality Index based on earthworms (QBS-e). A new way to use earthworms as bioindicators in agroecosystems.* Ecological Indicators, 2018. **93**: p. 1276-1292.
215. Ponnusamy, S., S. Viswanathan, A. Periyasamy and S. Rajaiah, *Production and characterization of PHB-HV copolymer by* Bacillus thuringiensis *isolated from* Eisenia foetida. Biotechnology and Applied Biochemistry, 2019. **66**(3): p. 340-352.
216. Rodriguez-Seijo, A., J. Lourenço, T. Rocha-Santos, J. Da Costa, A. Duarte, H. Vala and R. Pereira, *Histopathological and molecular effects of microplastics in* Eisenia andrei *Bouché.* Environmental Pollution, 2017. **220**: p. 495-503.
217. Kim, H., *A study on the utilization of the earthworms* Eisenia fetida *and* Eisenia andrei *for the disposal of polymers.* International Journal of Environmental Science and Development, 2016. **7**(5): p. 355-358.
218. Lwanga, E.H., B. Thapa, X. Yang, H. Gertsen, T. Salánki, V. Geissen and P. Garbeva, *Decay of low-density polyethylene by bacteria extracted from earthworm's guts: A potential for soil restoration.* Science of the Total Environment, 2018. **624**: p. 753-757.
219. Sanchez-Hernandez, J.C., Y. Capowiez and K.S. Ro, *Potential use of earthworms to enhance decaying of biodegradable plastics.* ACS Sustainable Chemistry & Engineering, 2020. **8**(11): p. 4292-4316.
220. Knop, J. and J. Knop, *Bakterien und Bakteroiden bei Oligochaeten:* Inaugural-Dissertation zur Erlangung der Doktorwürde der Hohen Philosophischen Fakultät der Universität zu Greifswald. 1926: Springer.
221. Edwards, C. and P. Bohlen, *Biology and Ecology of Earthworms*. Volume 3 Spinger Science & Business Media, 1996. 426 p.
222. Pinel, N., S.K. Davidson and D.A. Stahl, Verminephrobacter eiseniae *gen. nov., sp. nov., a nephridial symbiont of the earthworm* Eisenia foetida *(Savigny).* International Journal of Systematic and Evolutionary Microbiology, 2008. **58**(9): p. 2147-2157.
223. Schramm, A., S.K. Davidson, J.A. Dodsworth, H.L. Drake, D.A. Stahl and N. Dubilier, *Acidovorax-like symbionts in the nephridia of earthworms.* Environmental Microbiology, 2003. **5**(9): p. 804-809.
224. Cheema, S., M. Bassas-Galia, P.M. Sarma, B. Lal and S. Arias, *Exploiting metagenomic diversity for novel polyhydroxyalkanoate synthases: production of a terpolymer poly (3-hydroxybutyrate-co-3-hydroxyhexanoate-co-3-hydroxyoctanoate) with a recombinant* Pseudomonas putida *strain.* Bioresource Technology, 2012. **103**(1): p. 322-328.
225. Lund, M.B., M.F. Mogensen, I.P. Marshall, M. Albertsen, F. Viana and A. Schramm, *Genomic insights into the Agromyces-like symbiont of earthworms and its distribution among host species.* FEMS Microbiology Ecology, 2018. **94**(6): p. fiy068.
226. Møller, P., M.B. Lund and A. Schramm, *Evolution of the tripartite symbiosis between earthworms,* Verminephrobacter *and* Flexibacter-*like bacteria.* Frontiers in Microbiology, 2015. **6**: p. 529.

227. Childress, J.J., C. Fisher, J. Brooks, M. Kennicutt, R. Bidigare and A. Anderson, *A methanotrophic marine molluscan (Bivalvia, Mytilidae) symbiosis: mussels fueled by gas.* Science, 1986. **233**(4770): p. 1306-1308.
228. Petersen, J.M., F.U. Zielinski, T. Pape, R. Seifert, C. Moraru, R. Amann, S. Hourdez, P.R. Girguis, S.D. Wankel and V. Barbe, *Hydrogen is an energy source for hydrothermal vent symbioses.* Nature, 2011. **476**(7359): p. 176-180.
229. Kleiner, M., J.M. Petersen and N. Dubilier, *Convergent and divergent evolution of metabolism in sulfur-oxidizing symbionts and the role of horizontal gene transfer.* Current Opinion in Microbiology, 2012. **15**(5): p. 621-631.
230. Kleiner, M., C. Wentrup, T. Holler, G. Lavik, J. Harder, C. Lott, S. Littmann, M.M. Kuypers and N. Dubilier, *Use of carbon monoxide and hydrogen by a bacteria–animal symbiosis from seagrass sediments.* Environmental Microbiology, 2015. **17**(12): p. 5023-5035.
231. Sogin, E.M., N. Leisch and N. Dubilier, *Chemosynthetic symbioses.* Current Biology, 2020. **30**(19): p. R1137-R1142.
232. Jannasch, H.W. and C.O. Wirsen, *Chemosynthetic primary production at East Pacific sea floor spreading centers.* Bioscience, 1979. **29**(10): p. 592-598.
233. Cavanaugh, C.M., S.L. Gardiner, M.L. Jones, H.W. Jannasch and J.B. Waterbury, *Prokaryotic cells in the hydrothermal vent tube worm* Riftia pachyptila *Jones: possible chemoautotrophic symbionts.* Science, 1981. **213**(4505): p. 340-342.
234. Sogin, E.M., M. Kleiner, C. Borowski, H.R. Gruber-Vodicka and N. Dubilier, *Life in the dark: phylogenetic and physiological diversity of chemosynthetic symbioses.* Annual Review of Microbiology, 2021. **75**: p. 695-718.
235. Ott, J., M. Bright and S. Bulgheresi, *Marine microbial thiotrophic ectosymbioses.* Oceanographic and Marine Biology: An Annual Review, 2004. **42**: p. 95-118.
236. Stewart, F.J., I.L. Newton and C.M. Cavanaugh, *Form I and II Rubisco and δ13C values in chemosynthetic symbioses.* Trends in Microbiology, 2005. **9**(13): p. 439-448.
237. Ott, J. and R. Novak, *Living at an interface: Meiofauna at the oxygen/sulfide boundary of marine sediments.* J. S. Ryland and P. A. Tyler, Eds., Reproduction, Genetics and Distribution of Marine Organisms, Olsen & Olsen, Fredensborg, 1989, pp. 415-422.
238. Polz, M.F., D.L. Distel, B. Zarda, R. Amann, H. Felbeck, J.A. Ott and C.M. Cavanaugh, *Phylogenetic analysis of a highly specific association between ectosymbiotic, sulfur-oxidizing bacteria and a marine nematode.* Applied and Environmental Microbiology, 1994. **60**(12): p. 4461-4467.
239. Bayer, C., N.R. Heindl, C. Rinke, S. Lücker, J.A. Ott and S. Bulgheresi, *Molecular characterization of the symbionts associated with marine nematodes of the genus* Robbea. Environmental Microbiology Reports, 2009. **1**(2): p. 136-144.
240. Pende, N., N. Leisch, H.R. Gruber-Vodicka, N.R. Heindl, J. Ott, T. Den Blaauwen and S. Bulgheresi, *Size-independent symmetric division in extraordinarily long cells.* Nature Communications, 2014. **5**(1): p. 4803.
241. Zimmermann, J., C. Wentrup, M. Sadowski, A. Blazejak, H.R. Gruber-Vodicka, M. Kleiner, J.A. Ott, B. Cronholm, P. De Wit and C. Erséus, *Closely coupled evolutionary history of ecto-and endosymbionts from two*

distantly related animal phyla. Molecular Ecology, 2016. **25**(13): p. 3203-3223.

242. Leisch, N., N. Pende, P.M. Weber, H.R. Gruber-Vodicka, J. Verheul, N.O. Vischer, S.S. Abby, B. Geier, T. Den Blaauwen and S. Bulgheresi, *Asynchronous division by non-ring FtsZ in the gammaproteobacterial symbiont of* Robbea hypermnestra. Nature Microbiology, 2016. **2**(1): p. 1-5.
243. Leisch, N., J. Verheul, N.R. Heindl, H.R. Gruber-Vodicka, N. Pende, T. den Blaauwen and S. Bulgheresi, *Growth in width and FtsZ ring longitudinal positioning in a gammaproteobacterial symbiont.* Current Biology, 2012. **22**(19): p. R831-R832.
244. Pende, N., J. Wang, P.M. Weber, J. Verheul, E. Kuru, K.-M.R. Simon, N. Leisch, M.S. VanNieuwenhze, Y.V. Brun and T. den Blaauwen, *Host-polarized cell growth in animal symbionts.* Current Biology, 2018. **28**(7): p. 1039-1051. e5.
245. Paredes, G.F., T. Viehboeck, R. Lee, M. Palatinszky, M.A. Mausz, S. Reipert, A. Schintlmeister, A. Maier, J.-M. Volland and C. Hirschfeld, *Anaerobic sulfur oxidation underlies adaptation of a chemosynthetic symbiont to oxic-anoxic interfaces.* Msystems, 2021. **6**(3): p. 10.1128/msystems. 01186-20.
246. Nylander, J.A., C. Erséus and M. Källersjö, *A test of monophyly of the gutless* Phallodrilinae *(Oligochaeta, Tubificidae) and the use of a 573-bp region of the mitochondrial cytochrome oxidase I gene in analysis of annelid phylogeny.* Zoologica Scripta, 1999. **28**(3-4): p. 305-313.
247. Erséus, C., *Taxonomy and phylogeny of the gutless Phallodrilinae (Oligochaeta, Tubificidae), with descriptions of one new genus and twenty-two new species.* Zoologica Scripta, 1984. **13**(4): p. 239-272.
248. Erséus, C., Inanidrilus bulbosus *gen. et sp. n., a marine tubificid (Oligochaeta) from Florida, USA.* Zoologica Scripta, 1979. **8**(1-4): p. 209-210.
249. Blazejak, A., C. Erséus, R. Amann and N. Dubilier, *Coexistence of bacterial sulfide oxidizers, sulfate reducers, and spirochetes in a gutless worm (Oligochaeta) from the Peru margin.* Applied and Environmental Microbiology, 2005. **71**(3): p. 1553-1561.
250. Giere, O., C. Erséus and F. Stuhlmacher, *A new species of* Olavius *(Tubificidae) from the Algarve coast in Portugal, the first East Atlantic gutless oligochaete with symbiotic bacteria.* Zoologischer Anzeiger, 1998. **237**(2): p. 209-214.
251. Felbeck, H., G. Liebezeit, R. Dawson and O. Giere, *CO 2 fixation in tissues of marine oligochaetes (*Phallodrilus leukodermatus *and* P. planus*) containing symbiotic, chemoautotrophic bacteria.* Marine Biology, 1983. **75**: p. 187-191.
252. Giere, O., C. Nieser, R. Windoffer and C. Erséus, *A comparative structural study on bacterial symbioses of Caribbean gutless Tubificidae (Annelida, Oligochaeta).* Acta zoologica, 1995. **76**(4): p. 281-290.
253. Giere, O., *The gutless marine oligochaete* Phallodrilus leukodermatus. *Structural studies on an aberrant tubificid associated with bacteria.* Marine Ecology Progress Series, 1981. **5**(3): p. 353-357.
254. Mankowski, A., M. Kleiner, C. Erséus, N. Leisch, Y. Sato, J.-M. Volland, B. Huettel, C. Wentrup, T. Woyke, J. Wippler, N. Dubilier and H. Gruber-Vodicka, *Highly variable fidelity drives symbiont community composition in an obligate symbiosis*. BioRxiv, 2021.

Chapter I

Animals degrade the bioplastic polyhydroxyalkanoate

Chapter I | Animals degrade the bioplastic polyhydroxyalkanoate

Caroline Zeidler[1], Anna Carlotta Kück[1], Tristan Wagner[1], Manuel Kleiner[2], Marlene Violette[2], Alexander Gruhl[1], Juliane Wippler[1], Manuel Liebeke[1,3], Dolma Michellod[1], Harald Gruber-Vodicka[1,3], Nicole Dubilier[1*], Maggie Sogin[1, 5*]

[1]Max-Planck Institute for Marine Microbiology, Celsiusstraße 1, 28359 Bremen, Germany

[2] Department of Plant and Microbial Biology NC State University, Raleigh, NC 27695, USA

[3] Zoologisches Institut, University of Kiel, 24118 Kiel, Germany

[5] University of California at Merced, Merced, CA 95343, USA

*corresponding authors: esogin@ucmerced.edu , ndubilie@mpi-bremen.de

[+] The manuscript is in preparation and has not been revised by all authors.

[+] Author contribution: C.Z, E.S. and N.D conceived the study. C.Z. collected, processed and analyzed the metatranscriptomic, metagenomic samples and protein models. A.C.K. helped to assemble the metatranscriptomes. Protein models were interpreted with the help from T.W. C.Z. performed HCR FISH. C.Z and D.M preformed the heterologous gene expression. C.Z. performed the enzyme assay and analyzed the data. C.Z. collected the databases used in this study and calculated the phylogenetic tree. Interpretation of the phylogenetic tree were done by C.Z. with guidance from E.S. and H.GV. C.Z. wrote the manuscript, with support from E.S and N.D.

Summary

Many bacteria and archaea synthesize the bioplastic polyhydroxyalkanoate (PHA) to store excess carbon and energy. Microorganisms degrade PHAs using PHA depolymerases (PHADs). Until now, it has been assumed that only bacteria and fungi have PHADs. We show here that animals also have PHADs. We first discovered an animal PHAD in the genome of the gutless marine worm *Olavius algarvensis*. Enzyme assays and protein modeling revealed that *O. algarvensis* degrades the PHA synthesized by its bacterial symbionts. *O. algarvensis* relies on digesting its bacterial symbionts to gain nutrition. PHA makes up 42% of the stored carbon of the primary symbiont *Candidatus* Thiosymbion algarvensis, representing a valuable nutritional source for the host. We discovered homologs of animal PHADs in 67 animal species from nine phylogenetically distinct phyla, indicating that PHADs were evolutionary conserved. Animal PHADs branched off from PHADs of the genus *Bdellovibrio* that obtain PHA from bacterial prey. All of the animal species obtain PHA through their diet, suggesting that all animals gain a nutritional advantage from PHA degradation. Given that microbially produced PHAs serve as a carbon storage in soil and sediment habitats, our discovery suggests that animals re-mineralize this carbon storage to produce CO_2, thus altering carbon budgets.

Introduction

Polyhydroxyalkanoates (PHAs) are natural biopolymers produced by prokaryotes in a wide range of ecosystems such as soils, activated sludge and marine sediments[1-5]. Only bacteria and archaea synthesize PHAs, which they use as storage and energy compounds when carbon compounds are available, but other conditions for growth are limiting, such as a lack of oxygen or essential nutrients like nitrogen and phosphate. PHA is stored intracellularly in the form of granules and can make up to 90% of the microorganism's dry weight[2, 4, 6-10]. When conditions become amendable again, microorganisms degrade the PHA into their monomers, dimers or a mix of hydroxyalkanoate oligomers which are metabolized in the cell to yield CO_2, H_2O and CH_4, promoting their growth and reproduction[11-17]. Considering how widespread PHA-synthesizing microorganisms are in both terrestrial and aquatic environments[1-4], PHA

likely contributes to carbon cycling by serving as both a reservoir and a resource for carbon and reducing equivalents[10, 13-19]. Moreover, because PHAs are biodegradable, commercial PHA production of bioplastics is on the uprise, and may contribute to a considerable increase in PHA in the environment[20, 21].

The enzymes that degrade PHAs in nature are PHA depolymerases (PHADs; EC 3.1.1.75, EC 3.1.1.76). Although widespread in bacteria and possibly some archaea, PHADs in eukaryotes are only known from fungi and two protists[11, 22-27]. PHADs are carboxylesterases from the alpha/beta-hydrolase protein family that either degrade PHA intracellularly or extracellularly. While intracellular PHADs break down intact, native PHA granules inside bacterial cells, extracellular PHADs only degrade excreted PHA, which lacks the surface associated proteins and phospholipids that are characteristic of intracellular PHA[11, 28]. Both intracellular and extracellular PHADs cleave the PHA polymer chain to release water-soluble hydroxyalkanoic acid monomers and oligomers, which are then further degraded to produce energy and biomass[10, 13-19]. Given the high carbon and energy contents of PHA, animals, particularly those in nutrient poor environments, would profit from being able to degrade PHA, but have so far been assumed to not have PHADs.

Here, we show that an animal, the gutless marine oligochaete, *Olavius algarvensis*, encodes and expresses a PHAD that degrades extracellular PHA produced by its symbiotic bacteria. *O. algarvensis* does not have a gut, mouth or anus, and relies on digesting its bacterial symbionts to gain nutrition. *O. algarvensis'* primary symbiont, *Candidatus* Thiosymbion algarvensis, is a sulfur oxidizing gammaproteobacterium that chemoautotrophically fixes CO_2 to build biomass[29, 30]. Under oxygen-limiting conditions, for example when the worm moves to deeper sediment layers, the worm switches to an anaerobic metabolism and produces waste products such as acetate and propionate[31, 32]. These waste products are used by *Ca.* T. algarvensis to synthesize PHA, which the symbiont stores as a copolymer of polyhydroxybutyrate (PHB), polyhydroxyvalerate (PHV) and polyhydroxymethylvalerate (PHMV). These PHA polymers make up as much as 42% of the symbiont's carbon stores (Kleiner et al., unpublished)[32]. We discovered homologs of PHADs in 67 animal species from nine distantly related phyla. Our results indicate that there is a selective advantage for animals to produce a functional PHAD. Animal PHADs branched off a clade of *Bdellovibrio* sp. PHADs. *Bdellovibrio* species lyse their bacterial prey to degrade PHA gaining a fitness advantage[33-35]. All animals with a PHAD take up PHA with their diet,

suggesting that animals gain carbon and energy from PHA degradation. Given that PHA degradation releases carbon to the atmosphere, our discovery suggests that animals can tap into microbial stored PHA found in various environments influencing carbon cycles.

Results and Discussion

The gutless marine worm *O. algarvensis* encodes and expresses a PHAD

The PHAD gene, *pha*Z, of *O. algarvensis* spanned a 19,000 bp region in the animal's genome and was separated into 10 exons and 9 introns (Figure 1a). This distinct exon-intron structure confirms the eukaryotic origin of the *pha*Z, and excludes that it originated from bacterial contamination[36]. Moreover, the *O. algarvensis* PHAD had less than 10.2% amino acid similarity to the PHAD of its bacterial symbiont *Ca*. T. algarvensis, a different structural alignment, and was phylogenetically distinct from that of its symbionts (Figure 1b, Extended Figure 1). The *O. algarvensis* PHAD fell in a clade of PHADs that contained extracellular PHADs, and this classification was supported by the presence of a predicted signal peptide at the N-terminal end of the protein (Supplementary Text 1, Supplementary Figure 1 & Supplementary Table 1). The catalytic and substrate binding site of the *O. algarvensis* PHAD aligned well with those of the well characterized, purified and crystallized extracellular PHAD from the fungus *Penicillium funiculosum* (basionym *Talaromyces funiculosus*; pdb 2d81)[37] (93.4% coverage, 31.2% identity; RMSD 0.773; Figure 1b and c; Supplementary Figure 1 & 2; Supplementary Text 1), indicating that the PHAD of *O. algarvensis* has the enzymatic ability to degrade extracellular PHA. Finally, the *pha*Z gene was expressed, based on metatranscriptomic analyses, in 16 out of 19 *O. algarvensis* individuals collected over six years.

To confirm that the *O. algarvensis* PHAD degrades PHA, we heterologously expressed the PHAD in *E. coli*. Spot assays of the purified enzyme on plates that contained denatured short-chain PHAs, either as polyhydroxybutyrate (PHB) or a mixture of 97% polyhydroxybutyrate and 3% polyhydroxyvalerate (PHB/PHV) showed a clearance zone after 24 h (Extended Figure 2). These results suggest that the PHAD of *O. algarvensis* is able to degrade extracellular PHB, and possibly PHV.

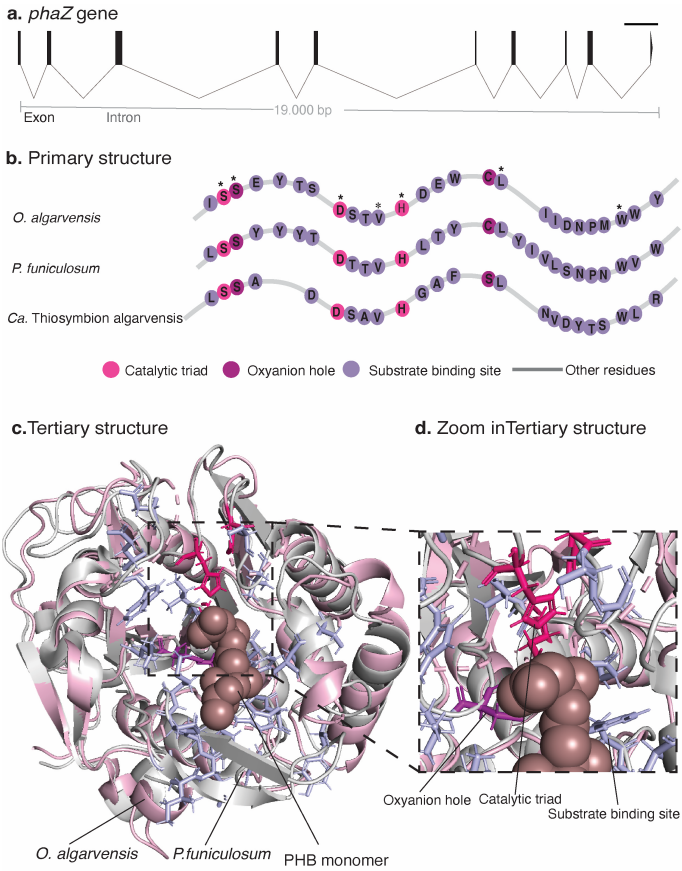
a. phaZ gene
Exon
Intron
19.000 bp
b. Primary structure
O. algarvensis
P. funiculosum
Ca. Thiosymbion algarvensis
Catalytic triad
Oxyanion hole
Substrate binding site
Other residues
c.Tertiary structure
d. Zoom inTertiary structure
Oxyanion hole
Catalytic triad
Substrate binding site
O. algarvensis
P.funiculosum
PHB monomer

Figure 1| *O. algarvensis* has a PHAD that is predicted to cleave extracellular short chain PHAs a, A *phaZ* gene was recovered from the *O. algarvensis'* draft genome (Michellod et al., 2023)[38]. The gene spans 19,000 bp and was split into 10 different exons (black bars). Scale bar=1000bp. **b**, The primary structure of the *pha*Z gene encodes for a 333 amino acid long protein. Using MAFFT[39] to align the newly recovered PHAD with that of homologs from *P. funiculsoum* (pdb 2d81) and *Ca.* T. algarvensis showed 100% conservation of the catalytic site across all three protein sequences. The *O. algarvensis*' enzyme had 31.6% identity and 89.2% coverage to the *P. funiculsoum* and 10.2% identity and 95.8% coverage to the *Ca.* T. algarvensis PHAD, suggesting that the gutless oligochaete's enzyme is of eukaryotic origin. Colored circles marked with an asterisk show the conserved residues of the catalytic triad (pink), substrate binding site (light purple) and oxyanion hole (purple). The regions between the circles represents all other residues **c,** AlphaFold2[40, 41] was used to predict the structure of the *O. algarvensis'* PHAD, which was then aligned to the PHAD crystal structure from *P. funiculosum* in PyMOL. The alignment suggested that the structures of animal and fungal homologs are similar (RMSD 0.773 Å). **d,** We aligned a monomer of PHB to the catalytic triad and oxyanion hole of the *O. algarvensis'* PHAD to identify its fitting in the catalytic pocket. The interaction of the catalytic site with the PHB monomer suggest that PHB could be degraded by the *O. algarvensis* PHAD. Pink colored residues show the catalytic triad, purple colored residues the oxyanion hole and light purple residues the substrate binding domain.

We visualized where the PHADs of *O. algarvensis* and its symbionts are expressed using whole mount hybridization chain reaction – fluorescence in situ hybridization (HCR-FISH) with probes specific to the mRNA of the host and symbionts *pha*Z (Figure 2). The probe specific to the *Ca.* T. algarvensis PHAD hybridized in the symbiont region just below the worm's cuticle and above its epidermal cells. The *O. algarvensis* PHAD probe hybridized in the same region but the signal was not overlapping with the *Ca.* T. algarvensis PHAD. In this epidermal layer, the host digests its symbionts through phago-lysosomal digestion[42, 43], indicating that the host expresses its PHAD in the cells that digest its symbionts.

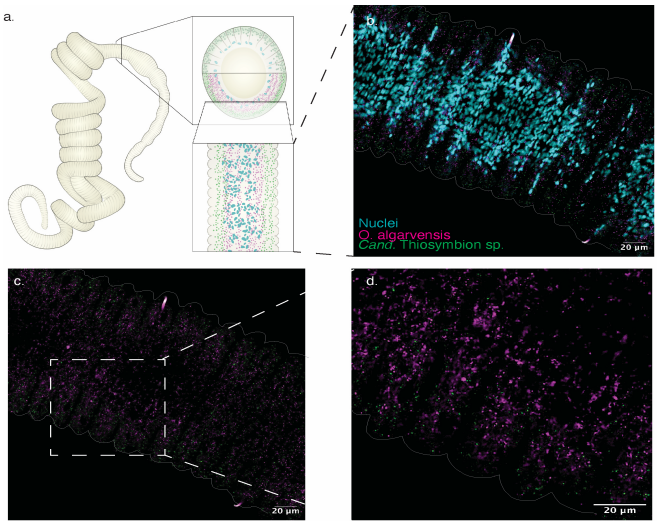

Figure 2 | Transcripts encoding for the animal and symbiont PHADs were localized not overlapping in the *O. algarvensis'* symbiont layer. a, Schematic overview of the position of the identified signal. We identified the HCR-FISH labels in the symbiont layer that is located underneath the worm's cuticle and above the epidermis. This region harbors all symbionts, including *Ca.* T. algarvensis that synthesizes PHA. The host nuclei are drawn in cyan, the host PHAD in pink and the symbiont PHAD in green. Image courtesy of Rebekka Janke. **b,** Whole mount images of HCR-FISH labeled *O. algarvensis'* (pink) and *Ca.* T. algarvensis' (green) PHAD transcripts within a single worm. Nuclei are shown in cyan. **c,d,** Image overlays indicate that the host and symbiont signal are not overlapping. No-label controls shown Supplementary Figure 3.

To gain energy and carbon from PHA degradation, bacteria use a hydroxybutyrate-dimer hydrolase (EC 3.1.1.22) to break down PHA-derived oligomers to monomers, and a beta-hydroxybutyrate dehydrogenase (EC 1.1.1.30) to transform the monomers into acetoacetate. Acetoacetate is then oxidized to acetyl-coenzyme A (acetyl-CoA), which is a key component in the citric acid cycle. Acetyl-CoA is oxidized in the citric acid cycle to release CO_2, water and under anaerobic conditions CH_4 together with reducing equivalents used for energy generation (Supplementary Figure 4)[10, 12-19, 44, 45]. While we did not identify a hydroxybutyrate-dimer hydrolase in *O. algarvensis*, the BHBD gene was present in the transcriptomes of 4 out of 9 *O. algarvensis* individuals investigated, and expressed at similar levels as the PHAD (Figure 3). Moreover, PHAD

and BHBD were expressed at similar levels as the digestive enzymes used by *O. algarvensis* to gain nutrition from its symbionts via phago-lysosomal digestion in the epidermal cells, indicating that these hosts use the PHA-derived monomers to gain energy and carbon.

Genes for degrading PHA are common to gutless oligochaetes

We next hypothesized that other gutless oligochaete species encode the genes needed for degrading PHA, given the nutritional advantage PHA degradation would likely provide. For PHAD, we recovered *pha*Z transcripts from all 10 gutless oligochaete species investigated, with 1 – 5 transcripts with high sequence homology (25% to 80%) to the *pha*Z gene from *O. algarvensis* (Figure 3; Supplementary Figure 1 & 2; Supplementary Table 2). Like *O. algarvensis*, the PHADs of other gutless oligochaetes encoded a signal peptide, their catalytic and substrate binding sites aligned to the crystal structure of *P. funiculosum*, and their sequences were phylogenetically distinct from their symbiont's PHAD (Extended Figure 1; Supplementary Text 1; Supplementary Figure 1 & 2; Supplementary Table 1). Seven gutless oligochaete species had at least two and as many as five PHAD homologs. Bacteria with multiple PHAD isoforms are able to degrade different types of PHA, such as PHB or PHV, thereby gaining metabolic flexibility (Supplementary Text 3)[46-51]. Similarly, gutless oligochaetes with multiple PHAD homologs may use these to digest different types of PHA such as PHB, PHV and PHMV produced by their symbiotic bacteria (Kleiner et al., unpublished).

For BHBD, we recovered transcripts from eight gutless oligochaete species, and these genes were present at similar levels as PHADs (Figure 3). The presence and expression of PHADs and BHBDs in all ten gutless oligochaetes investigated, which belong to two genera, and come from different habitats (seagrass and coral reef sediments) and two oceans (Mediterranean and Atlantic), indicates that these genes are widespread across all gutless oligochaetes, and provides these hosts with the ability to metabolize the PHA produced by their symbionts.

Surprisingly, while *Ca.* Thiosymbion symbionts of all ten gutless oligochaete species investigated in this study expressed the genes for synthesizing PHA, they appear to lack the genes for transforming the breakdown products of PHADs, hydroxyalkanoic monomers and oligomers, into acetoacetate. All three genes involved, BHBD,

hydroxybutyrate-dimer hydrolase, and 3- hydroxybutyryl-coenzyme A dehydrogenase (EC 1.1.1.157) were not found in the transcriptomes of all ten *Ca*. Thiosymbion species. At least one of these genes must be expressed to catabolize PHA completely to CO_2, CH_4 and H_2O yielding energy in form of reducing equivalents[10, 13-18], indicating that *Ca*. Thiosymbion sp. has lost the ability to metabolize the PHA it synthesizes. If true, this suggests that gutless oligochaetes do not compete with their symbionts for PHA-derived carbon, and can instead use all the PHA their symbiont produce for their own nutrition.

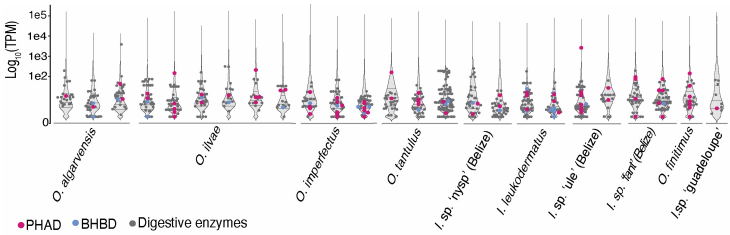

Figure 3 | Gutless oligochaetes expressed an animal specific PHAD and BHBD in their transcriptome. Violin plots representing assembled transcriptomes of single individuals from each of the 10 gutless oligochaete species showed the range in normalized transcription (log10(TPM)) per individual worm. At least one individual from each species expressed the host-specific PHAD (pink points) and BHBD (blue points) enzymes. The PHAD and BHBD were expressed within a similar range as other digestive enzymes (gray points) found within the host transcriptome. In order to estimate the transcript expression, we assembled per species one reference assembly to which we mapped the raw reads of each library representing one individual to obtain the kallisto transcript abundances[52].

Animals from nine phyla encode PHADs

We next asked if other animals besides gutless oligochaetes have PHADs, as these enzymes would be nutritionally advantageous to animals that feed on soil, sediments or other substrates with PHA-synthesizing organisms. Our searches of homologs of the gutless oligochaete PHADs in the NCBI non-redundant protein database[53], ENSEMBL[54], LumbriBASE[55] and UNIPROT[56] databases revealed 195 PHADs distributed across 67 animal species spanning nine metazoan phyla (Supplementary Table 2). We also expanded the known diversity of protist PHADs from 2 to 48

homologs in 18 protist species representing five phyla (for more details on the protist enzymes see Supplementary Text 2; Supplementary Table 3). The majority of the animal PHADs encoded the oxyanion hole (85%), the catalytic triad (100%) and a substrate binding site that aligned well with the fungal model (67%-93% coverage, 22-42% identity). The majority of the animal PHADs also had a signal peptide (75%), indicating that these are secreted (Supplementary Figure 5-10; Supplementary Table 1).

Our phylogenetic analysis revealed that all metazoan PHADs fell into a monophyletic clade that formed a sister clade to all protist PHADs (Figure 4). The exceptions were two sequences of the protist *Nibbleromonas* sp., which formed an early branching clade to the animal subclades III and IV, however without statistical support (bootstrap value of 57.4%). The other exception were PHADs from bdelloid rotifers that formed a sister clade to PHAD sequences from fungi and bacteria (Supplementary Figure 11). Given that four different species of rotifers have PHADs, that these cluster with each other and are distinct from bacterial and fungal PHADs, it is likely that rotifers recently acquired their PHADs through horizontal gene transfer, which is common in bdelloid rotifers[57]. In contrast, all other metazoan PHADs were likely acquired vertically by the last common ancestor of animals (discussed below).

The phylogeny of metazoan PHADs within most phyla corresponded largely to their phylogenetic classification (Figure 4; Supplementary Figure 12). For example, all PHADs from Mollusca formed a monophyletic clade, with subclades consisting of PHADs from molluscan classes Bivalvia and Gastropoda (Supplementary Figure 13). The exceptions were Chordata, with PHADs from the Chordata subphyla Tunicata, Craniata and Cephalochordata (Supplementary Figure 14) falling on disparate branches, and a single arthropod PHAD from a crayfish (*Procambarus clarkii*) that was most closely related to PHADs from Rotifera (Figure 14). Across phyla, the PHAD tree could either not be resolved or was not congruent with branching patterns between animal phyla (Figure 4; Supplementary Figures 11-17).

The sister group relationship between protist and metazoan PHADs suggests that PHADs were present in the last common ancestor of animals (LCA). This conclusion is further supported by the phylogenetic position of the PHAD from the sponge *Amphimedon queenslandica* as the sister branch to PHADs from all bilaterian animals (Figure 4). We therefore hypothesize that one or more PHAD homologs were vertically transferred from protists (which have multiple PHAD homologs) to the LCA of

animals. Metazoan PHADs then diversified within many animal lineages, with losses of the gene in other lineages.

To understand the adaptive forces that shaped the retention and diversification of PHAD homologs in metazoans, we classified the feeding strategies of all 77 animal species with PHADs. For gutless oligochaetes, the advantage of gaining nutrition from their PHA-synthesizing symbionts is obvious. For all other 67 animal species with PHAD homologs, we observed that these gain their nutrition by filter-feeding or ingesting soil, sediment, or detritus (Figure 4; Supplementary Figure 18 & Table 2). These food sources all contain microorganisms, of which many likely produce PHA. For example, earthworms ingest soil particles that contain between 1.2 and 4.3 µg C/g (soil) of native PHB, likely occurring within microbial cells[1]. Similarly, springtails (Collembola) also feed on soil and detritus rich in PHA producing microorganisms[58], and encode as many as 14 PHAD homologs, for example *Folsomia candida*. While most Arthropoda PHAD homologs grouped according to their subclass, those from Collembola were spread across multiple branches throughout the Arthropoda PHAD clade (Supplementary Figure 14), indicating diversification of these genes in these insects. As argued above for gutless oligochaetes, multiple PHAD isoforms may allow springtails to gain nutrition from different types and mixtures of PHAs in their environment (Supplementary Text 3).

The link between having PHADs and a microbial feeding ecology is also visible in the clade that groups PHADs from Bdellovibrionata bacteria and Provora protists, which are both microbial predators[35, 59], with a large group of protists known to feed on microorganisms, such as the amoeba *Acanthamoeba castelanii* (Figure 4, Supplementary Figure 19)[60]. Given the phylogenetic clustering of the protist and Bdellovibrionata PHADs with those of metazoans, we propose that this clade be named 'microvorus' PHADs.

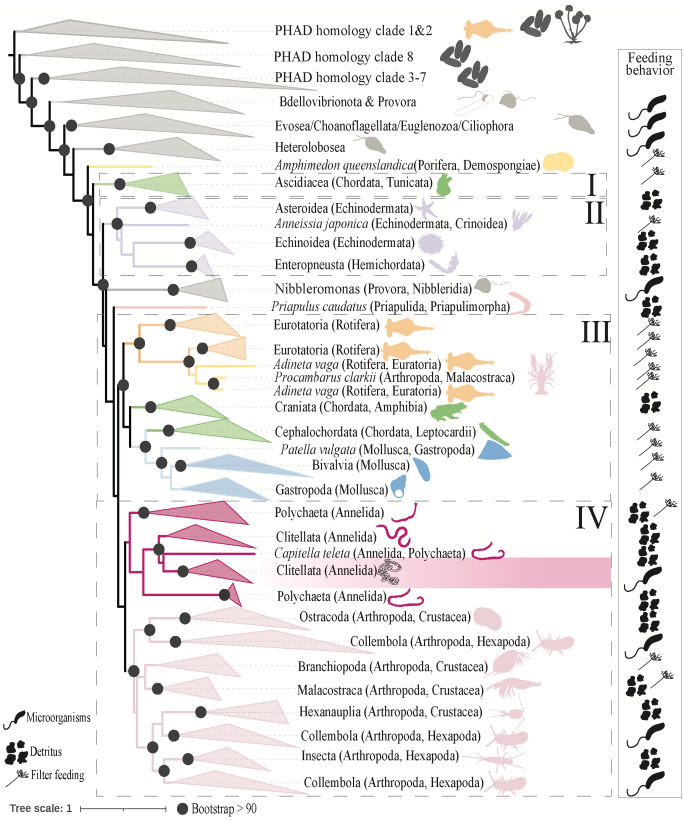

Figure 4 | Animals, protists and predatory bacteria form a new "microvorus" clade of PHADs. A maximum likelihood tree (IQ TREE[61] using ultrafast bootstrap support) built from extracellular PHAD protein sequences showed that PHA degradation likely occurs across fungal, protist and animal lineages. The tree indicates that the newly discovered animal PHADs belong to the extracellular PHADs of domain type 2, which target the degradation of short chain PHAs. Reconstruction of the feeding ecology indicated that all animals and protists that encode for a PHAD gain their nutrition by feeding either partially or completely on microbial communities.

Conclusions

PHA is known to occur in a broad range of microorganisms in habitats around the world[1-6, 22-27], but data on PHA concentrations and degradation rates in natural environments are sparse, particularly in marine habitats. Moreover, intracellular storage of carbon compounds like PHA is often overlooked in estimates of microbial biomass[62]. As so many bacteria, fungi and protist have the enzymes to degrade PHA[11, 24-26], these carbon and energy sources likely play a valuable role in supporting microbial populations and contributing to nutrient recycling. In soil habitats, PHB concentrations range between 1.2 to 4.3 µg C/g of soil[1, 63], which corresponds to 0.001% of the forest soil organic carbon (SOC) and 0.025 - 0.16% of the agricultural SOC[64, 65]. The degradation rates of PHAs and their influence to the carbon budget in natural habitats has yet to be quantified[66], but laboratory tests on PHA pieces suggest that homopolymers and copolymers lose up to 93% of their initial weight after 200 days at 28°C[67]. While it was previously assumed that only bacteria, fungi, archaea and protists are involved in the degradation of PHA[22-27], our study shows that animals from nine phyla can also degrade PHA. Animal PHA degradation would result in a net release of CO_2, and their contribution to carbon cycling needs to be considered in future studies.

One of the many pressing problems in the current Anthropocene is the enormous contamination of natural habitats with plastics, which have now been found in every known ecosystem on Earth[68-71]. PHA is the only bioplastic that can be both synthesized and degraded by microorganisms[72-75], and the global market for PHA is expected to double in value by 2027 to 81 million US dollars (https://www.statista.com/statistics/1010383/global-polyhydroxyalkanoate-market-size/). With the knowledge that animals in terrestrial and marine environments can also contribute to PHA degradation, industries together with governments should consider increasing the relative share of PHA in bioplastic production, which currently only accounts for less than 4% (https://www.european-bioplastics.org/market/) of the global bioplastic market. As an example, earthworms are considered to play a crucial role in the nutrient recycling of many terrestrial environments because their ingestion of tremendous amounts of decaying material breaks down organic matter and fertilizes soils[76]. The ability of earthworms to degrade plastics has therefore garnered considerable interest, although research is still in its infancy[77, 78]. While earthworms ingest plastics and bioplastics like polylactic acid[79], only the size of plastics was

reduced, but they were never fully degraded[80]. Our discovery that earthworms express a PHAD indicate that earthworms may be able to remove PHA-based plastics entirely from soil habitats.

In conclusion, this study highlights how expanding research beyond the limited number of model organisms that have been traditionally studied to non-model organisms like gutless marine oligochaetes, can lead to the discovery of a new group of enzymes that influences our understanding of the role of PHA for carbon cycling and the use of bioplastics in biotechnology.

Acknowledgements

We would like to thank Silke Wetzel, Miriam Sadowski, Wiebke Ruschmeier and Martina Meyer for the help in the lab. We also thank Bruno Huettel (Max Planck Genome Center) for his support with sequencing. We also thank colleagues in the Departments of Symbiosis (MPI-MM) for helpful discussions. We thank Miriam Weber, Christian Lott and the HYDRA team for their sampling support. This work was funded by the Max-Planck Society through Prof. N. Dubilier.

Code and data availability

Raw metagenomic and polyA metatranscriptomic sequences are published along the study by Michellod et al., 2023. Total RNA libraries, PHAD sequences and phylogenetic trees will be made publicly available upon peer-review submission and are currently available upon request.

Extended Data Figures

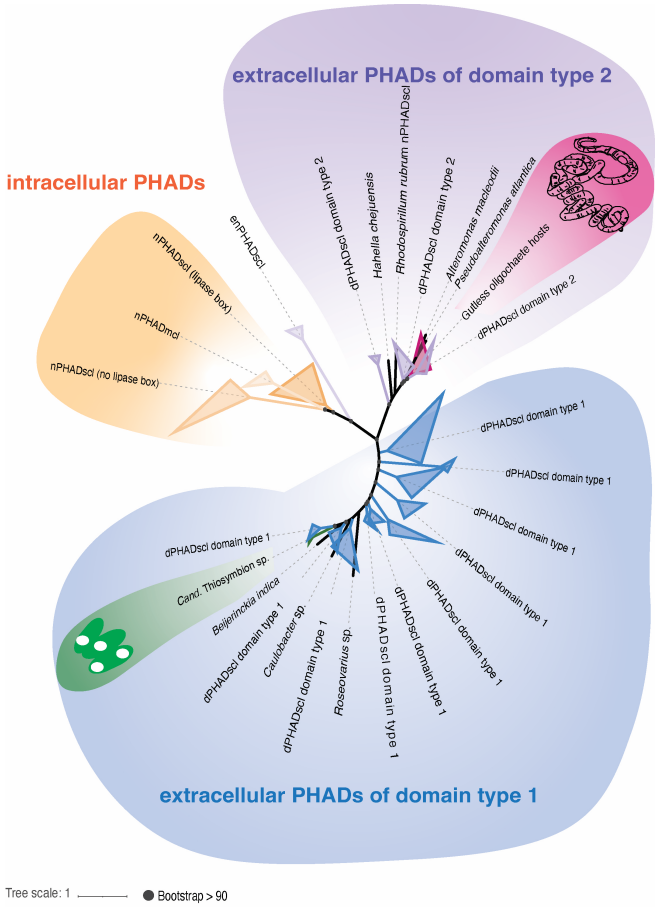

Extended Figure 1 | Gutless oligochaete PHADs form a separate cluster from their symbiont enzymes. The unrooted maximum likelihood tree[61] (IQ TREE, ultrafast bootstraps) of all known PHADs of the PHAD engineering database[81] showed that the animal enzyme are distinct from that of their bacterial symbionts. While the animal PHADs clustered within the clade of extracellular PHADs degrading short chain PHA of domain type 2, the *Ca*. Thiosymbion sp. PHADs clustered with extracellular PHADs degrading short chain PHA of domain type 1.

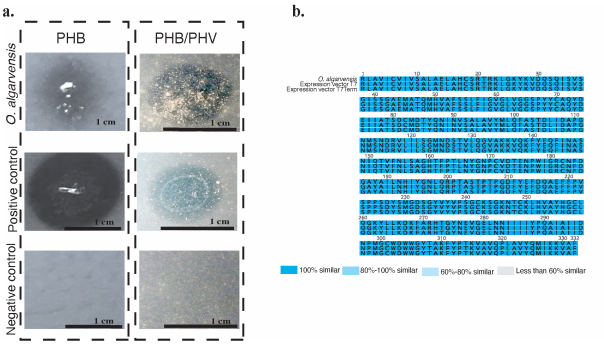

Extended Figure 2 | *O. algarvensis'* PHAD was active on PHB and PHB/PHV substrates. **a**. Using PHB and PHB/PHV assay plates, spot assays showed that the heterologously expressed PHAD from *O. algarvensis* broke down the PHA substrate after 24 hours. The clearance zone of the animal PHAD was not as strong as the positive control (a heterologously expressed PHAD from the bacterium *Paucimonas lemoignei*), probably due to a lower protein concentration obtained after purification. We were able to eliminate activity through heat inactivation (negative control). **b.** Plasmid sequencing of *E. coli* clones used for the heterologously expression of the enzyme provided confirmation that the expressed vector was indeed for the PHAD from *O. algarvensis* shown by a 100% similarity and coverage alignment.

Materials and Methods

Metatranscriptomic analysis

Sampling, Extraction and sequencing. To generate the metatranscriptomes used in this study, scuba divers collected 14 different gutless oligochaete species from their natural habitats between 2015 and 2021 (Supplementary Table 5). We manually sorted the worms from the sediment and directly fixed them in RNAlater (Thermo Fisher Scientific, Waltham, MA, US). Samples were stored at -80 °C until DNA/RNA extraction. We extracted RNA from individual worms using either Qiagen's AllPrep DNA/RNA/Protein Mini Kit or AllPrep DNA/RNA Mini Kit (Qiagen; Supplementary Table 5) using the following adjustments to the manufacturer's protocol: bead beating was performed using a sterilized mixture of small (approximately 20 1.2 mm ZY-S Silibeads) and large (5 2mm beads ZY-SSilibeads) silicon beads in addition to Matrix B silicon sand (MP Biosystems), β-mercaptoethanol was replaced by 20 µl of 2 M DTT and 1 µl of Reagent DX (Qiagen 19088), and tissues were disrupted by beat beating using a FastPrep (MP Biomedicals™) instrument set for two cycles of at 4 m/s for 40 seconds with 5 minutes resting of samples on ice. RNA samples were eluted in 40 µl of DEPC-treated water and stored at -80 °C until library preparation.

Extracted RNA was sent to the Max Planck Genome Centre (Cologne, Germany) for library generation and sequencing. PolyA enriched libraries were made with the NEBNext® Single Cell/Low Input RNA Library Prep Kit for Illumina® (NEB). Total RNA libraries were generated with the NEBNext® Ultra™ II Directional RNA Library Prep Kit for Illumina® (NEB). All metatranscriptomic libraries were sequenced on an Illumina HiSeq3000 by sequencing-by-synthesis and paired-end read mode, resulting in approximately 6639581 reads per library.

Identification of gutless oligochaete PHADs in metatranscriptomes. First, raw transcriptomic reads were trimmed of their adapters and quality filtered using BBDuk[82, 83] (BBMap version 38.90; parameters: mink= 11, minlength=36, trimq=2, hdist=1). Subsequently, we mapped the rRNA out by SortMeRNA[84] (version 4.3.4) using the SILVA_138_SSURef_NR99_tax_silva database. Further, to obtain enriched host fractions, we mapped the *O. algarvensis* and *O. ilvae* reads to the partial host genome assembly obtained from Michellod et al., 2023[38] and extracted them using BBMap[85]

(version 39.00) with a mapping threshold of 98 %. For the other gutless oligochaetes libraries, we mapped them to symbiont bins generated in the study by Mankowski et al., 2021[86] using the same parameters as described above to obtain host enriched reads due to the lack of high complete host genome assemblies. We then *de novo* assembled the separated host and symbiont reads using Trinity[87] (Trinity-v2.5.1; parameters: --max_memory 250G --normalize_reads --verbose). We assessed the quality of the host assemblies by calculating the N50 values[87] (TrinityStats.pl; Trinity-v2.5.1) and by using BUSCO[88](BUSCO 4.1.4) against the metazoan database (metazoa_odb10). Further, we predicted the coding sequences with Transdecoder (TransDecoder.Predict 5.5.0, TransDecoder.LongOrfs 5.5.0; https://github.com/TransDecoder/TransDecoder/).

We identified the *O. algarvensis* and symbiont PHAD sequences by a BLASTp search[89](e- value 1; version Protein-Protein BLAST 2.11.0) of the obtained coding sequences and the metatranscriptomes published by Wippler et al., 2016[42] using the PHAD engineering database[81] as a reference. Using BLASTp, we cross-checked the identified sequences against the non-redundant protein database on NCBI[53]. Recovered sequences were then used as the reference to identify the host and symbiont PHADs in the other gutless oligochaete datasets by the same method as described above.

PHAD identification in metagenomes. In order to identify the animal PHAD in the genome, we analyzed the partial host metagenome from the gutless oligochaete species *O. algarvensis* from the study by Michellod et al.(2023)[38] for the presence of the PHAD. We used the protein sequences of the identified PHAD from the metatranscriptomes from *O. algarvensis* as the reference for a TBLASTN[89] search against the metagenomes of the species (e-value 1, version Protein Query-Translated Subject BLAST 2.11.0+). We predicted the intron and exon structure of the PHAD gene using the online version of SPLIGN[90] against the cDNA obtained from the metatranscriptomes with the options for low identity. Gene structure of the PHAD was visualized by Exon-Intron Graphic Maker (version 4; http://wormweb.org/exonintron)

Sequence comparison

Primary structure analysis. To identify the conservation of the recovered gutless oligochaete PHADs, we aligned the putative PHAD sequences to the amino acid sequence of the PHAD from the fungus *Penicillium funiculosum* (basionym *Talaromyces funiculosus*; pdb 2d80; 2d81) using the local pair alignment in MAFFT[39](version v7.407 (2018/Jul/23) and visualized the alignment using the MSAviewer[91]. We based our analysis on the paper from Hisano *et al*. (2006)[37]. The same analysis was repeated for selected animal, PHADs (Supplementary Figure 4-10). Additionally, we predicted the signal peptides of individual enzymes using SignalP 6.0[92].

Phylogenetic reconstruction. To identify the phylogenetic relationship of the animal and symbiont PHADs we calculated an unrooted maximum likelihood tree. Therefore, we aligned the identified animal and symbiont PHADs with sequences of the PHAD engineering database[81] using the local pair alignment in MAFFT[39] (version v7.407 (2018/Jul/23)). The aligned sequences were used to calculate a maximum likelihood tree with ultrafast bootstrap support values using IQ TREE[61]. We visualized the calculated tree in iTOL[93] and Adobe Inc. Illustrator.

Functionality

Homologous modeling. To identify the structural conservation of the animal PHADs, we modeled all of the identified gutless oligochaete and selected metazoan PHADs using the monomer prediction against the full AlphaFold2 database[40, 41]. The generated enzyme models were analyzed and visualized using PyMOL (version 2.4.0.; The PyMOL Molecular Graphics System, Version 2.0 Schrödinger, LLC). First, we determined the quality of the models by visualizing the results of the predicted local distance difference test (pLDDT) saved in the beta-spectrum during the AlphaFold2 prediction. Then, to assess the structural conservation of the animal PHADs, we aligned the AlphaFold2 models to the crystal structure of the PHAD from the fungus *Penicillium funiculosum* (basionym *Talaromyces funiculosus*; pdb 2d81) and calculated the root-mean-square deviation (RMSD).

Heterologous gene expression and enzyme purification. To determine the functionality of the putative host PHAD, we expressed the *O. algarvensis* PHAD and an extracellular PHAD from *Paucimons lemoignei* (accession: P52090) as the positive control in *E. coli*. Therefore, Genscript (Genscript®) generated pet28a(+) vectors with the sequences of interest inserted between the restriction sites NheI/XhoI. We transformed the *O. algarvensis* PHAD vector by heat shock in *E. coli* BL21 competent cells (DE2; Thermo Fisher). The *P. lemoignei* vector was transformed into BL21 rosetta competent cells (DE3; Merck). For the enzyme overexpression and purification we followed the method described by Becker *et al.* (2018)[94]. The success of the enzyme overexpression was checked by SDS PAGE (TGX FastCast 12%, Biorad). For the reason that the *O. algarvensis* PHAD was expressed in inclusion bodies, we included a refolding step following Qi *et al.* (2015)[95], with the modification that we allowed thorough freezing overnight. Following the refolding step, the *O. algarvensis* PHAD was purified in the same way as the PHAD from *P. lemoignei* with the change of the protocol that we exchanged the buffer by an overnight dialysis using 6-8 kDa dialysis bags against SEC buffer (20 mM Tris, 0.5 M NaCl) at 4 °C stirred at 150 rpm. To determine if we successfully expressed the *O. algarvensis* PHAD, we sent samples of the *E. coli* clones for plasmid extraction and Sanger sequencing (Microsynth AG) and checked for the *O. algarvensis* and *P. lemoignei* PHAD sequences for successful insertion of the plasmids in *E. coli* (Extended Figure 2b).

Enzyme assays. To test enzyme activity, we used spot assays according to the method described by Briese *et al.* (1994)[96]. We modified the protocol and prepared polymer plates containing 0.5 mg/ml of the homopolymer PHB (Merck) and the copolymer PHB/PHV (Merck). We brought the polymers in a stable suspension in a 100 mM Tris HCl (Sigma-Aldrich) solution by sonication at maximum intensity for 3 h at 42°C. To the polymer suspension, 7 g / 500 ml agar was added (Becton Dickinson). The enzyme activity was tested by adding 10 µl of the purified *O. algarvensis* PHAD to the plate. We incubated the plates at 36°C for 24 h. The activity of the enzyme was determined by a clearance zone. As a positive control we used the purified PHAD of *P. lemoignei* and as a negative control we used a heat-denatured 1:1 enzyme mix (95 °C for 15 min) of the purified enzymes.

Expression analysis

Hybridization chain reaction-fluorescent *in situ* hybridization (HCR-FISH) to label PHAD expression. For the HCR-FISH analysis, we fixed *O. algarvensis* worms in batches of six individuals in 4% Paraformaldehyde (Electron Microscopy Sciences) in PBS (Phosphate Buffered Saline) for 4 hours at 4 °C and stored them at -20 °C in methanol. In order to visualize the animal and symbiont PHAD transcripts we designed specific HCR-FISH probes (Supplementary Table 6; Molecular Instruments Inc). For the whole mount *in situ* hybridizations, we followed the protocol for chicken embryos by Choi *et al.*, 2016[97] with the following modifications: We dissected the worms in pieces following the rehydration in PBS and digested them with 0.05 mg/ml proteinaseK (Thermo Fisher Scientific) to allow better penetration of the probes. The reaction was stopped by washing the worm pieces twice for 5 minutes in 2 mg/ml glycine in PBST (Phosphate Buffered Saline buffer with Tween). Subsequently, worms were re-fixed in 4% PFA for 60 min at room temperature to keep structural integrity. We pre-hybridized the worms firstly for 15 min in 30% hybridization buffer (30% formamide, 5x sodium chloride sodium citrate, 9mM citric acid, 0.1% Tween-20, 50µg/ml heparin, 1x Denhardts solution, 10% Dextran sulfate) on ice, then for 5 minutes at room temperature and finally for 30 min at 37 °C. Probes were added in a final concentration of 8 nmol in 30 % hybridization buffer to the samples. Samples were incubated overnight at 37 °C to allow binding of the probes. The probes were washed off in 30% wash buffer (30% formamide, 5x sodium chloride sodium citrate, 9mM citric acid, 0.1% Tween-20, 50µg/ml heparin) at 37°C for two times 15 min, 30 min and 60 min. We pre-amplified the samples for two times 30 min in amplification buffer (5x sodium chloride sodium citrate, 0.1% Tween-20, 10% Dextran sulfate) before adding the hairpins in a final concentration of 30 pmol to the amplification buffer. For the animal PHAD we used a B1 initiator sequence for the hairpin with the fluorophore 546 and for the *Ca.* Thiosymbion algarvensis PHAD we used a B3 initiator sequence for the hairpin with the fluorophore 647. For the negative control we choose to either leave out the probe or the hairpin (Supplementary Figure 3). The excess hairpins were washed off in 5 x SSCT (5x sodium chloride sodium citrate with 0.1% Tween-20) for two times 5 min, two times 30 min and 5 min. Before mounting the samples in Electron Microscopy Sciences Citifluor™, we counterstained the samples with 2 µM DAPI. We visualized the hybridizations using confocal microscopy (Zeiss LSM 780 with Airyscan and ELYRA PS.1).

PHAD expression and its further degradation. We used a hmmsearch[98](version HMMER 3.1b2 (February 2015)) to search all gutless oligochaete metatranscriptomes for the BHBD and other PHA degradation genes to identify potential transcripts that makes further use of PHA. Subsequently, we estimated transcript expression of the PHAD and BHBD using kallisto[52] (version 0.46.0). We mapped the raw reads of each individual worm library to a co-assembly generated from each library per species. The transcripts per kilobase million values (tpm) of all transcripts were plotted as violin plots on a log10 scale using ggplot2[99]. The median and upper and lower quartile of tpm-values of all host transcripts was plotted as a line.

Animal PHADs

Identification of animal PHADs. In order to recover more animal PHADs we screened publicly available databases. Therefore, we used the *O. algarvensis* PHAD sequence as a seed to BLAST (BLASTp) it against non-redundant protein database on NCBI[53, 89] and UNIPROT[56]. To recover more sequences, we used the putative animal PHAD with the lowest identity to the *O. algarvensis* PHAD as a new seed and BLASTed it in the same way. This step was repeated at least 10 times. Additionally, we manually searched the LumbriBASE annelid transcriptome database (earthworms.org v4.0)[55] and the ENSEMBL genome browser[54, 100]. In order to exclude duplicated sequences, we ran the BBMap script dedupe.sh[82, 83] (version BBMap version 38.90). We aligned the deduplicated sequences using the local pair alignment in MAFFT[39] (version v7.407 (2018/Jul/23)) and checked for the conservation of the catalytic site and other PHAD identifiers such as the substrate binding site. Animal sequences that had conservation of the catalytic site were defined as animal PHADs and further used in this study.

Phylogenetic reconstruction. In order to resolve the metazoan PHAD phylogeny, the identified metazoan PHADs, protist PHADs and extracellular PHADs degrading short chain PHA of the PHAD engineering database[81] were aligned using the local pair alignment in MAFFT[39] (version v7.407 (2018/Jul/23)). The aligned sequences were used to calculate a maximum likelihood tree with ultrafast bootstrap support values using IQ TREE[61]. We visualized the calculated tree in iTOL[93] and Adobe Inc. Illustrator.

Reference

1. Mason-Jones, K., C.C. Banfield and M.A. Dippold, *Compound-specific 13C stable isotope probing confirms synthesis of polyhydroxybutyrate by soil bacteria.* Rapid Communications in Mass Spectrometry, 2019. **33**(8): p. 795-802.
2. Wang, J. and L. Bakken, *Screening of soil bacteria for poly-β-hydroxybutyric acid production and its role in the survival of starvation.* Microbial Ecology, 1998. **35**(1): p. 94-101.
3. Khardenavis, A., P. Guha, M.S. Kumar, S. Mudliar and T. Chakrabarti, *Activated sludge is a potential source for production of biodegradable plastics from wastewater.* Environmental Technology, 2005. **26**(5): p. 545-552.
4. Arun, A., R. Arthi, V. Shanmugabalaji and M. Eyini, *Microbial production of poly-β-hydroxybutyrate by marine microbes isolated from various marine environments.* Bioresource Technology, 2009. **100**(7): p. 2320-2323.
5. Santhanam, A. and S. Sasidharan, *Microbial production of polyhydroxy alkanotes (PHA) from* Alcaligens *spp. and* Pseudomonas oleovorans *using different carbon sources.* African Journal of Biotechnology, 2010. **9**(21): p. 3144-3150.
6. Doudoroff, M. and R. Stanier, *Role of poly-β-hydroxybutyric acid in the assimilation of organic carbon by bacteria.* Nature, 1959. **183**(4673): p. 1440-1442.
7. Fernandez-Castillo, R., F. Rodriguez-Valera, J. Gonzalez-Ramos and F. Ruiz-Berraquero, *Accumulation of poly (β-hydroxybutyrate) by halobacteria.* Applied and Environmental Microbiology, 1986. **51**(1): p. 214-216.
8. Steinbüchel, A. and H. Schlegel, *Physiology and molecular genetics of poly (β-hydroxyalkanoic acid) synthesis in* Alcaligenes eutrophus. Molecular Microbiology, 1991. **5**(3): p. 535-542.
9. Müller, H.M. and D. Seebach, *Poly (hydroxyalkanoates): a fifth class of physiologically important organic biopolymers?* Angewandte Chemie International Edition in English, 1993. **32**(4): p. 477-502.
10. Madison, L.L. and G.W. Huisman, *Metabolic engineering of poly (3-hydroxyalkanoates): from DNA to plastic.* Microbiology and Molecular Biology Reviews, 1999. **63**(1): p. 21-53.
11. Jendrossek, D. and R. Handrick, *Microbial degradation of polyhydroxyalkanoates.* Annual Review of Microbiology, 2002. **56**: p. 403.
12. Senior, P.J. and E.A. Dawes, *The regulation of poly-beta-hydroxybutyrate metabolism in* Azotobacter beijerinckii. Biochemical Journal, 1973. **134**(1): p. 225-38.
13. Jendrossek, D., I. Knoke, R.B. Habibian, A. Steinbüchel and H.G. Schlegel, *Degradation of poly (3-hydroxybutyrate), PHB, by bacteria and purification of a novel PHB depolymerase from* Comamonas *sp.* Journal of Environmental Polymer Degradation, 1993. **1**(1): p. 53-63.
14. Schirmer, A., D. Jendrossek and H.G. Schlegel, *Degradation of poly (3-hydroxyoctanoic acid)[P (3HO)] by bacteria: purification and properties of a P (3HO) depolymerase from* Pseudomonas fluorescens *GK13.* Applied and Environmental Microbiology, 1993. **59**(4): p. 1220-1227.
15. Nakayama, K., T. Saito, T. Fukui, Y. Shirakura and K. Tomita, *Purification and properties of extracellular poly (3-hydroxybutyrate) depolymerases*

from Pseudomonas lemoignei. Biochimica et Biophysica Acta (BBA)-Protein Structure and Molecular Enzymology, 1985. **827**(1): p. 63-72.

16. Shirakura, Y., T. Fukui, T. Tanio, K. Nakayama, R. Matsuno and K. Tomita, *An extracellular D (−)-3-hydroxybutyrate oligomer hydrolase from* Alcaligenes faecalis. Biochimica et Biophysica Acta (BBA)-Protein Structure and Molecular Enzymology, 1983. **748**(2): p. 331-339.
17. Delafield, F., K.E. Cooksey and M. Doudoroff, *β-Hydroxybutyric dehydrogenase and dimer hydrolase of* Pseudomonas lemoignei. Journal of Biological Chemistry, 1965. **240**(10): p. 4023-4028.
18. Prieto, M.A., L.I.d. Eugenio, B. Galán, J.M. Luengo and B. Witholt, *Synthesis and degradation of polyhydroxyalkanoates*, in Pseudomonas. 2007, Springer. p. 397-428.
19. Doi, Y., Y. Kawaguchi, N. Koyama, S. Nakamura, M. Hiramitsu, Y. Yoshida and H. Kimura, *Synthesis and degradation of polyhydroxyalkanoates in* Alcaligenes eutrophus. FEMS Microbiology Reviews, 1992. **9**(2-4): p. 103-108.
20. Vicente, D., D.N. Proença and P.V. Morais, *The Role of Bacterial Polyhydroalkanoate (PHA) in a Sustainable Future: A Review on the Biological Diversity.* International Journal of Environmental Research and Public Health, 2023. **20**(4).
21. Koller, M. and A. Mukherjee, *A New Wave of Industrialization of PHA Biopolyesters.* Bioengineering (Basel), 2022. **9**(2).
22. Jendrossek, D., *Microbial degradation of polyesters: a review on extracellular poly (hydroxyalkanoic acid) depolymerases.* Polymer Degradation and Stability, 1998. **59**(1-3): p. 317-325.
23. Jendrossek, D., A. Schirmer and H. Schlegel, *Biodegradation of polyhydroxyalkanoic acids.* Applied Microbiology and Biotechnology, 1996. **46**(5): p. 451-463.
24. Gonda, K., D. Jendrossek and H.-P. Molitoris, *Fungal degradation of the thermoplastic polymer poly-β-hydroxybutyric acid (PHB) under simulated deep sea pressure*, in *Life at Interfaces and Under Extreme Conditions*. 2000, Springer. p. 173-183.
25. Kim, D. and Y. Rhee, *Biodegradation of microbial and synthetic polyesters by fungi.* Applied Microbiology and Biotechnology, 2003. **61**(4): p. 300-308.
26. Anderson, I.J., R.F. Watkins, J. Samuelson, D.F. Spencer, W.H. Majoros, M.W. Gray and B.J. Loftus, *Gene discovery in the* Acanthamoeba castellanii *genome.* Protist, 2005. **156**(2): p. 203-14.
27. Viljakainen, V. and L. Hug, *The phylogenetic and global distribution of bacterial polyhydroxyalkanoate bioplastic-degrading genes.* Environmental Microbiology, 2021. **23**(3): p. 1717-1731.
28. De Koning, G. and P. Lemstra, *The amorphous state of bacterial poly [(R)-3-hydroxyalkanoate] in vivo.* Polymer, 1992. **33**(15): p. 3292-3294.
29. Dubilier, N., O. Giere, D.L. Distel and C.M. Cavanaugh, *Characterization of chemoautotrophic bacterial symbionts in a gutless marine worm Oligochaeta, Annelida) by phylogenetic 16S rRNA sequence analysis and* in situ *hybridization.* Applied and Environmental Microbiology, 1995. **61**(6): p. 2346-2350.
30. Ruehland, C., A. Blazejak, C. Lott, A. Loy, C. Erséus and N. Dubilier, *Multiple bacterial symbionts in two species of co-occurring gutless oligochaete worms from Mediterranean sea grass sediments.* Environmental Microbiology, 2008. **10**(12): p. 3404-3416.

31. Woyke, T., H. Teeling, N.N. Ivanova, M. Huntemann, M. Richter, F.O. Gloeckner, D. Boffelli, I.J. Anderson, K.W. Barry and H.J. Shapiro, *Symbiosis insights through metagenomic analysis of a microbial consortium.* Nature, 2006. **443**(7114): p. 950-955.
32. Kleiner, M., C. Wentrup, C. Lott, H. Teeling, S. Wetzel, J. Young, Y.-J. Chang, M. Shah, N.C. VerBerkmoes and J. Zarzycki, *Metaproteomics of a gutless marine worm and its symbiotic microbial community reveal unusual pathways for carbon and energy use.* Proceedings of the National Academy of Sciences, 2012. **109**(19): p. E1173-E1182.
33. Jurkevitch, E. and Y. Davidov, *Phylogenetic diversity and evolution of predatory prokaryotes*, in *Predatory prokaryotes*. 2006, Springer. p. 11-56.
34. Martínez, V., E. Jurkevitch, J.L. García and M.A. Prieto, *Reward for* Bdellovibrio bacteriovorus *for preying on a polyhydroxyalkanoate producer.* Environmental Microbiology, 2013. **15**(4): p. 1204-1215.
35. Sockett, R.E., *Predatory lifestyle of* Bdellovibrio bacteriovorus. Annual Review of Microbiology, 2009. **63**: p. 523-539.
36. Lynch, M., *The origins of eukaryotic gene structure.* Molecular Biology and Evolution, 2006. **23**(2): p. 450-468.
37. Hisano, T., K. Kasuya, Y. Tezuka, N. Ishii, T. Kobayashi, M. Shiraki, E. Oroudjev, H. Hansma, T. Iwata, Y. Doi, T. Saito and K. Miki, *The crystal structure of polyhydroxybutyrate depolymerase from* Penicillium funiculosum *provides insights into the recognition and degradation of biopolyesters.* Journal of Molecular Biology, 2006. **356**(4): p. 993-1004.
38. Michellod, D., T. Bien, D. Birgel, M. Violette, M. Kleiner, S. Fearn, C. Zeidler, H.R. Gruber-Vodicka, N. Dubilier and M. Liebeke, De novo *phytosterol synthesis in animals.* Science, 2023. **380**(6644): p. 520-526.
39. Katoh, K. and D.M. Standley, *MAFFT multiple sequence alignment software version 7: improvements in performance and usability.* Molecular Biology and Evolution, 2013. **30**(4): p. 772-780.
40. Evans, R., M. O'Neill, A. Pritzel, N. Antropova, A. Senior, T. Green, A. Žídek, R. Bates, S. Blackwell and J. Yim, *Protein complex prediction with AlphaFold-Multimer.* BioRxiv, 2021: p. 2021.10. 04.463034.
41. Jumper, J., R. Evans, A. Pritzel, T. Green, M. Figurnov, O. Ronneberger, K. Tunyasuvunakool, R. Bates, A. Žídek, A. Potapenko, A. Bridgland, C. Meyer, S.A.A. Kohl, A.J. Ballard, A. Cowie, B. Romera-Paredes, S. Nikolov, R. Jain, J. Adler, T. Back, S. Petersen, D. Reiman, E. Clancy, M. Zielinski, M. Steinegger, M. Pacholska, T. Berghammer, S. Bodenstein, D. Silver, O. Vinyals, A.W. Senior, K. Kavukcuoglu, P. Kohli and D. Hassabis, *Highly accurate protein structure prediction with AlphaFold.* Nature, 2021. **596**(7873): p. 583-589.
42. Wippler, J., M. Kleiner, C. Lott, A. Gruhl, P.E. Abraham, R.J. Giannone, J.C. Young, R.L. Hettich and N. Dubilier, *Transcriptomic and proteomic insights into innate immunity and adaptations to a symbiotic lifestyle in the gutless marine worm* Olavius algarvensis. BMC Genomics, 2016. **17**(1): p. 1-19.
43. Giere, O. and C. Langheld, *Structural organisation, transfer and biological fate of endosymbiotic bacteria in gutless oligochaetes.* Marine Biology, 1987. **93**: p. 641-650.
44. Tanio, T., T. Fukui, Y. Shirakura, T. Saito, K. Tomita, T. Kahio and S. Masamune, *An extracellular poly (3-hydroxybutyrate) depolymerase from* Alcaligenes faecalis. European Journal of Biochemistry, 1982. **124**(1): p. 71-77.

45. Stuart, J., E. Ooi, J. McLeod, A. Bourns and J. Ballantyne, *D-and L-β-hydroxybutyrate dehydrogenases and the evolution of ketone body metabolism in gastropod molluscs.* The Biological Bulletin, 1998. **195**(1): p. 12-16.
46. Uchino, K., T. Saito, B. Gebauer and D. Jendrossek, *Isolated poly (3-hydroxybutyrate)(PHB) granules are complex bacterial organelles catalyzing formation of PHB from acetyl coenzyme A (CoA) and degradation of PHB to acetyl-CoA.* Journal of Bacteriology, 2007. **189**(22): p. 8250-8256.
47. Eggers, J. and A. Steinbüchel, *Poly (3-hydroxybutyrate) degradation in* Ralstonia eutropha *H16 is mediated stereoselectively to (S)-3-hydroxybutyryl coenzyme A (CoA) via crotonyl-CoA.* Journal of Bacteriology, 2013. **195**(14): p. 3213-3223.
48. Kobayashi, T. and T. Saito, *Catalytic triad of intracellular poly (3-hydroxybutyrate) depolymerase (*Pha*Z1) in* Ralstonia eutropha *H16.* Journal of Bioscience and Bioengineering, 2003. **96**(5): p. 487-492.
49. Abe, T., T. Kobayashi and T. Saito, *Properties of a novel intracellular poly (3-hydroxybutyrate) depolymerase with high specific activity (*Pha*Zd) in* Wautersia eutropha *H16.* Journal of Bacteriology, 2005. **187**(20): p. 6982-6990.
50. Uchino, K., T. Saito and D. Jendrossek, *Poly (3-hydroxybutyrate)(PHB) depolymerase* Pha*Za1 is involved in mobilization of accumulated PHB in* Ralstonia eutropha *H16.* Applied and Environmental Microbiology, 2008. **74**(4): p. 1058-1063.
51. Sznajder, A. and D. Jendrossek, *To be or not to be a poly (3-hydroxybutyrate)(PHB) depolymerase:* Pha*Zd1 (*Pha*Z6) and* Pha*Zd2 (*Pha*Z7) of* Ralstonia eutropha*, highly active PHB depolymerases with no detectable role in mobilization of accumulated PHB.* Applied and Environmental Microbiology, 2014. **80**(16): p. 4936-4946.
52. Bray, N.L., H. Pimentel, P. Melsted and L. Pachter, *Near-optimal probabilistic RNA-seq quantification.* Nature Biotechnology, 2016. **34**(5): p. 525-527.
53. Sayers, E.W., M. Cavanaugh, K. Clark, K.D. Pruitt, C.L. Schoch, S.T. Sherry and I. Karsch-Mizrachi, *GenBank.* Nucleic Acids Research, 2022. **50**(D1): p. D161.
54. Hubbard, T., D. Barker, E. Birney, G. Cameron, Y. Chen, L. Clark, T. Cox, J. Cuff, V. Curwen and T. Down, *The Ensembl genome database project.* Nucleic Acids Research, 2002. **30**(1): p. 38-41.
55. Owen, J., B.A. Hedley, C. Svendsen, J. Wren, M.J. Jonker, P.K. Hankard, L.J. Lister, S.R. Stürzenbaum, A.J. Morgan and D.J. Spurgeon, *Transcriptome profiling of developmental and xenobiotic responses in a keystone soil animal, the oligochaete annelid* Lumbricus rubellus*.* BMC Genomics, 2008. **9**: p. 1-21.
56. Consortium, U., *UniProt: a hub for protein information.* Nucleic Acids Research, 2015. **43**(D1): p. D204-D212.
57. Eyres, I., C. Boschetti, A. Crisp, T.P. Smith, D. Fontaneto, A. Tunnacliffe and T.G. Barraclough, *Horizontal gene transfer in bdelloid rotifers is ancient, ongoing and more frequent in species from desiccating habitats.* BMC Biology, 2015. **13**(1): p. 1-17.
58. Rusek, J., *Biodiversity of Collembola and their functional role in the ecosystem.* Biodiversity & Conservation, 1998. **7**: p. 1207-1219.

59. Tikhonenkov, D.V., K.V. Mikhailov, R.M. Gawryluk, A.O. Belyaev, V. Mathur, S.A. Karpov, D.G. Zagumyonnyi, A.S. Borodina, K.I. Prokina and A.P. Mylnikov, *Microbial predators form a new supergroup of eukaryotes.* Nature, 2022. **612**(7941): p. 714-719.
60. Weekers, P.H., P.L. Bodelier, J.P. Wijen and G.D. Vogels, *Effects of grazing by the free-living soil amoebae* Acanthamoeba castellanii, Acanthamoeba polyphaga, *and* Hartmannella vermiformis *on various bacteria.* Applied and Environmental Microbiology, 1993. **59**(7): p. 2317-2319.
61. Minh, B.Q., H.A. Schmidt, O. Chernomor, D. Schrempf, M.D. Woodhams, A. von Haeseler and R. Lanfear, *IQ-TREE 2: New Models and Efficient Methods for Phylogenetic Inference in the Genomic Era.* Molecular Biology and Evolution, 2020. **37**(5): p. 1530-1534.
62. Mason-Jones, K., A. Breidenbach, J. Dyckmans, C.C. Banfield and M.A. Dippold, *Intracellular carbon storage by microorganisms is an overlooked pathway of biomass growth.* Nature Communications, 2023. **14**(1): p. 2240.
63. Hanzlíkova, A., A. Jandera and F. Kunc, *Formation of poly-3-hydroxybutyrate by a soil microbial community during batch and heterocontinuous cultivation.* Folia Microbiologica, 1984. **29**: p. 233-241.
64. Spielvogel, S., J. Prietzel and I. Kögel-Knabner, *Soil organic matter stabilization in acidic forest soils is preferential and soil type-specific.* European Journal of Soil Science, 2008. **59**(4): p. 674-692.
65. Drexler, S., G. Broll, H. Flessa and A. Don, *Benchmarking soil organic carbon to support agricultural carbon management: A German case study.* Journal of Plant Nutrition and Soil Science, 2022. **185**(3): p. 427-440.
66. Mason-Jones, K., S.L. Robinson, G. Veen, S. Manzoni and W.H. van der Putten, *Microbial storage and its implications for soil ecology.* The ISME Journal, 2022. **16**(3): p. 617-629.
67. Mergaert, J., C. Anderson, A. Wouters, J. Swings and K. Kersters, *Biodegradation of polyhydroxyalkanoates.* FEMS Microbiology Reviews, 1992. **9**(2-4): p. 317-321.
68. Dris, R., H. Imhof, W. Sanchez, J. Gasperi, F. Galgani, B. Tassin and C. Laforsch, *Beyond the ocean: contamination of freshwater ecosystems with (micro-) plastic particles.* Environmental Chemistry, 2015. **12**(5): p. 539-550.
69. Lebreton, L.C., J. Van Der Zwet, J.-W. Damsteeg, B. Slat, A. Andrady and J. Reisser, *River plastic emissions to the world's oceans.* Nature Communications, 2017. **8**(1): p. 15611.
70. Brandon, J.A., W. Jones and M.D. Ohman, *Multidecadal increase in plastic particles in coastal ocean sediments.* Science Advances, 2019. **5**(9): p. eaax0587.
71. Hurley, R., A. Horton, A. Lusher and L. Nizzetto, *Plastic waste in the terrestrial environment*, in *Plastic Waste and Recycling*. 2020, Elsevier. p. 163-193.
72. Steinbüchel, A. and T. Lütke-Eversloh, *Metabolic engineering and pathway construction for biotechnological production of relevant polyhydroxyalkanoates in microorganisms.* Biochemical Engineering Journal, 2003. **16**(2): p. 81-96.
73. Snell, K.D. and O.P. Peoples, *PHA bioplastic: A value-added coproduct for biomass biorefineries.* Biofuels, Bioproducts and Biorefining: Innovation for a Sustainable Economy, 2009. **3**(4): p. 456-467.
74. Keshavarz, T. and I. Roy, *Polyhydroxyalkanoates: bioplastics with a green agenda.* Current Opinion in Microbiology, 2010. **13**(3): p. 321-326.

75. Pratt, S., L.-J. Vandi, D. Gapes, A. Werker, A. Oehmen and B. Laycock, *Polyhydroxyalkanoate (PHA) bioplastics from organic waste.* Biorefinery: Integrated Sustainable Processes for Biomass Conversion to Biomaterials, Biofuels, and Fertilizers, 2019: p. 615-638.
76. Phillips, H.R., E.M. Bach, M.L. Bartz, J.M. Bennett, R. Beugnon, M.J. Briones, G.G. Brown, O. Ferlian, K.B. Gongalsky and C.A. Guerra, *Global data on earthworm abundance, biomass, diversity and corresponding environmental properties.* Scientific Data, 2021. **8**(1): p. 136.
77. Li, Y., Q. Liu, M. Junaid, G. Chen and J. Wang, *Distribution, sources, transportation and biodegradation of microplastics in the soil environment.* TrAC Trends in Analytical Chemistry, 2023: p. 117106.
78. Meng, K., E.H. Lwanga, M. van der Zee, D.R. Munhoz and V. Geissen, *Fragmentation and depolymerization of microplastics in the earthworm gut: A potential for microplastic bioremediation?* Journal of Hazardous Materials, 2023. **447**: p. 130765.
79. Kim, H., *A study on the utilization of the earthworms* Eisenia fetida *and* Eisenia andrei *for the disposal of polymers.* International Journal of Environmental Science and Development, 2016. **7**(5): p. 355-358.
80. Lwanga, E.H., B. Thapa, X. Yang, H. Gertsen, T. Salánki, V. Geissen and P. Garbeva, *Decay of low-density polyethylene by bacteria extracted from earthworm's guts: A potential for soil restoration.* Science of the Total Environment, 2018. **624**: p. 753-757.
81. Knoll, M., T.M. Hamm, F. Wagner, V. Martinez and J. Pleiss, *The PHA depolymerase engineering database: a systematic analysis tool for the diverse family of polyhydroxyalkanoate (PHA) depolymerases.* BMC Bioinformatics, 2009. **10**: p. 1-8.
82. Nordberg, H., M. Cantor, S. Dusheyko, S. Hua, A. Poliakov, I. Shabalov, T. Smirnova, I.V. Grigoriev and I. Dubchak, *The genome portal of the Department of Energy Joint Genome Institute: 2014 updates.* Nucleic Acids Research, 2014. **42**(D1): p. D26-D31.
83. Grigoriev, I.V., H. Nordberg, I. Shabalov, A. Aerts, M. Cantor, D. Goodstein, A. Kuo, S. Minovitsky, R. Nikitin, R.A. Ohm, R. Otillar, A. Poliakov, I. Ratnere, R. Riley, T. Smirnova, D. Rokhsar and I. Dubchak, *The Genome Portal of the Department of Energy Joint Genome Institute.* Nucleic Acids Research, 2011. **40**(D1): p. D26-D32.
84. Kopylova, E., L. Noé and H. Touzet, *SortMeRNA: fast and accurate filtering of ribosomal RNAs in metatranscriptomic data.* Bioinformatics, 2012. **28**(24): p. 3211-3217.
85. Bushnell, B., *BBMap: a fast, accurate, splice-aware aligner.* 2014, Lawrence Berkeley National Lab.(LBNL), Berkeley, CA (United States).
86. Mankowski, A., M. Kleiner, C. Erséus, N. Leisch, Y. Sato, J.-M. Volland, B. Huettel, C. Wentrup, T. Woyke, J. Wippler, N. Dubilier and H. Gruber-Vodicka, *Highly variable fidelity drives symbiont community composition in an obligate symbiosis*. BioRxiv, 2021.
87. Haas, B.J., A. Papanicolaou, M. Yassour, M. Grabherr, P.D. Blood, J. Bowden, M.B. Couger, D. Eccles, B. Li and M. Lieber, De novo *transcript sequence reconstruction from RNA-seq using the Trinity platform for reference generation and analysis.* Nature Protocols, 2013. **8**(8): p. 1494-1512.
88. Seppey, M., M. Manni and E.M. Zdobnov, *BUSCO: assessing genome assembly and annotation completeness.* Gene prediction: methods and Protocols, 2019: p. 227-245.

89. Altschul, S.F., W. Gish, W. Miller, E.W. Myers and D.J. Lipman, *Basic local alignment search tool.* Journal of Molecular Biology, 1990. **215**(3): p. 403-410.
90. Kapustin, Y., A. Souvorov, T. Tatusova and D. Lipman, *Splign: algorithms for computing spliced alignments with identification of paralogs.* Biology Direct, 2008. **3**: p. 1-13.
91. Yachdav, G., S. Wilzbach, B. Rauscher, R. Sheridan, I. Sillitoe, J. Procter, S.E. Lewis, B. Rost and T. Goldberg, *MSAViewer: interactive JavaScript visualization of multiple sequence alignments.* Bioinformatics, 2016. **32**(22): p. 3501-3503.
92. Teufel, F., J.J. Almagro Armenteros, A.R. Johansen, M.H. Gíslason, S.I. Pihl, K.D. Tsirigos, O. Winther, S. Brunak, G. von Heijne and H. Nielsen, *SignalP 6.0 predicts all five types of signal peptides using protein language models.* Nature Biotechnology, 2022. **40**(7): p. 1023-1025.
93. Letunic, I. and P. Bork, *Interactive Tree Of Life (iTOL) v5: an online tool for phylogenetic tree display and annotation.* Nucleic Acids Research, 2021. **49**(W1): p. W293-W296.
94. Becker, S. and J.-H. Hehemann, *Laminarin quantification in microalgae with enzymes from marine microbes.* Bio-Protocol, 2018. **8**(8): p. e2666-e2666.
95. Qi, X., Y. Sun and S. Xiong, *A single freeze-thawing cycle for highly efficient solubilization of inclusion body proteins and its refolding into bioactive form.* Microbial Cell Factories, 2015. **14**: p. 1-12.
96. Briese, B.H., B. Schmidt and D. Jendrossek, Pseudomonas lemoignei *has five poly (hydroxyalkanoic acid)(PHA) depolymerase genes: a comparative study of bacterial and eukaryotic PHA depolymerases.* Journal of Environmental Polymer Degradation, 1994. **2**: p. 75-87.
97. Choi, H.M., C.R. Calvert, N. Husain, D. Huss, J.C. Barsi, B.E. Deverman, R.C. Hunter, M. Kato, S.M. Lee and A.C. Abelin, *Mapping a multiplexed zoo of mRNA expression.* Development, 2016. **143**(19): p. 3632-3637.
98. Eddy, S.R., *Accelerated profile HMM searches.* PLoS Computational Biology, 2011. **7**(10): p. e1002195.
99. Wickham, H., W. Chang and M.H. Wickham, *Package 'ggplot2'.* Create Elegant Data Visualisations Using the Grammar of Graphics. Version, 2016. **2**(1): p. 1-189.
100. Cunningham, F., J.E. Allen, J. Allen, J. Alvarez-Jarreta, M.R. Amode, I.M. Armean, O. Austine-Orimoloye, A.G. Azov, I. Barnes and R. Bennett, *Ensembl 2022.* Nucleic Acids Research, 2022. **50**(D1): p. D988-D995.

Chapter I

Supplementary Text, Figures and Tables

Supplementary Text

Supplementary Text 1 | *O. algarvensis* PHAD degrades short chain PHAs

Using AlphaFold2[1-3], we generated a model of *O. algarvensis'* PHAD (predicted local distance difference test (pLDDT) = 94; Figure 1c; Supplementary Figure 2) by comparing it to the crystal structure of a fungal homolog derived from *P. funiculosum* (pdb 2d81)[4]. Although the protein sequence between the animal PHAD and the fungal homolog was relatively low (31.6 %), AlphaFold2's prediction of the animal enzyme indicated that the superposition between the proteins was accurate and strong (root-mean-square deviation (RMSD) of 0.736 Å based on 236 Cα; DALI Z = 45.8). Because the two enzymes demonstrated high levels of structural homology, we explored their structural similarities. Like the fungal PHAD, the animal protein is predicted to fold into a single domain enzyme. Within the core of the enzyme, our prediction revealed that the animal PHAD is composed of an active site that includes a catalytic triad consisting of S_{27}-D_{128} and H_{161} residues and an oxyanion hole made up of S_{28} and C_{257}. The residues making up the active site of the animal protein aligned closely with that of the fungal homolog (RMSD score from 0.047-0.127 Å), suggesting that the animal enzyme, like other PHADs, cleaves PHA via a nucleophilic attack on the ester bond between the hydroxyalkanoate monomeric units[4, 5]. While the protein sequence of the substrate binding region of the animal enzyme only shared 28.6 % sequence homology to the same region of fungal homolog, the structure of the protein was highly conserved (RMSD score from 0.081-0.393 Å). Specifically, the positions of the residue W_{304}, which stabilizes the polymer chain, and V_{129} and P_{298}, which are located around the catalytic crevice and attract the substrate, were fully conserved. Additionally, we identified a signal peptide forming the first 19 amino acids of the enzyme's primary structure. This signal peptide is predicted to export the animal PHAD likely to the symbiont region underneath the worm's cuticle following the *SEC1* pathway (SignalP 6.0)[6]. All of the Alphafold2 models (pLDDT = 85-96; Supplementary Figure 2) from the gutless oligochaete PHADs revealed the same tertiary protein structure: complete conservation of the active site and critical residues of the substrate binding domain, and presence of the signal peptide (Supplementary Figure 1 & 2). Taken together, the domain structure of the worms PHADs indicates that they will bind denatured extracellular PHA produced by the symbiont and degrade it.

Based on our AlphaFold2 models, we sought to explore the specificity of the enzyme in binding symbiont produced PHA. Our analysis revealed that the animal PHADs have a reduced beta-sheet between D_{265} and G_{318} in comparison to the fungal homolog. Instead, the model predicts that there is a loop between I_{291} and A_{292}. This loop opens the catalytic pocket, allowing the substrate to enter through a tunnel in the protein structure. Within the catalytic crevice of the *O. algarvensis* PHAD, Y_{42} is substituted by E_{44}, which enlarges the crevice. We observed the same substitutions for most of the gutless oligochaetes PHADs (22/32). Based on these results, we propose that the catalytic site of gutless oligochaetes PHADs is larger in comparison to the fungal homolog, and therefore allows for the binding of a broad range of PHAs, including polyhydroxybutyrate (PHB), polyhydroxyvalerate (PHV) and polyhydroxymethylvalerate (PHMV). Considering that *O. algarvensis* symbionts produce a copolymer of PHB, PHV and PHMV (Kleiner et al., unpublished), our modeling results across gutless oligochaete enzymes suggest that the gutless oligochaete PHADs are likely adapted to the PHA source synthesized by the symbionts.

Supplementary Text 2 | Protist PHADs

Adding to our discovery that PHADs are widespread in animals, we also found homologs in 21 protist species representing five protist phyla (Supplementary Table 3). Previously, PHAD sequences were only known to be encoded by the Amoebozoa species, *Acanthamoeba castellanii,* and the Evasoa species, *Dictyostelium discoideum*[7]. Our analysis revealed that PHADs were also present in Choanoflagellates, Euglenozoa, Ciliophora, and Heterolobosea. PHADs from Ciliophora formed a sisterclade to Evosea PHADs and to a clade that is formed by individual species sequences from Evosea, Choanoflagellate and Euglenozoa (Supplementary Figure 19). Considering that Choanoflagellate PHADs formed a sister clade to the PHAD from *A. castellanii* (Amoebozoa) and not to metazoan PHADs, that clustered with PHADs from Heterolobosea species, the phylogeny of protist PHADs does not reflect the protist phylogeny. Possibly this grouping is influenced by the undersampling of protist PHADs, especially as there are many PHADs from a single species per phyla. Protists generally form a paraphyletic group and it is still debated what are major protist clades[8] which could also be reflected in the protist PHAD clades.

Alternatively, the protist PHADs underwent many loses and diversification that might have shaped the protist PHAD phylogeny.

Supplement Text 3 | Higher metabolic flexibility

PHA degradation in bacteria can lead to different products depending on the PHAD activity. For example the Betaproteobacteria *Ralstonia eutropha* has nine different intracellular PHADs that either release Co-A-bound monomers[9, 10], or hydrolyze PHA either into its hydroxycarboxylic monomers[11, 12] or oligomers[13, 14]. Considering that multiple PHAD copies allow the bacterium to use different metabolic pathways to make use of the PHA, we speculate that animal genomes which encode for multiple versions of the PHAD enzyme have a higher degree of metabolic flexibility in their ability to degrade various PHA compounds present in their environments.

To explore the hypothesis that having a diverse repertoire of PHAD enzymes could bind different types of PHAs and allow the individual to produce different degradation products, we choose to model each of *D. magna's* PHADs using AlphaFold2 to explore structural similarities across all homologs. The catalytic triad, oxyanion hole and $W_{302/317/336}$ residue that holds the polymer chain in place were fully conserved in all copies of *D. magna* PHAD in comparison to the fungal homolog, suggesting that the *D. magna*'s enzymes work to degrade PHA. Similar to the gutless oligochaete PHADs, the primary differences across *D. magna*'s PHAD copies are located at the substrate binding region, where we observed that each of the distinct copies of the protein have single amino acid substitutions that likely impact the type of PHA they can bind. For example, the two amino acids of the substrate binding site that follow the catalytic asparagine are substituted by either $SV_{140\text{-}141}$ or $ST_{124\text{-}125/158\text{-}159}$. The variation in the substrate binding region shifts the absolute size of the catalytic triad from 3.8 x 2.5 x 7.0 Å to 4.7 x 4.4 x 8.5 Å. Given the variation in size of the catalytic triad, we hypothesize that *D. magna's* different PHAD copies allow the enzyme to bind with different sized PHA substrates which could result in the production of diverse degradation products[9-13, 15]. While this has been shown for bacterial PHADs, further activity assays are needed to explore our hypothesis.

Supplementary Figures

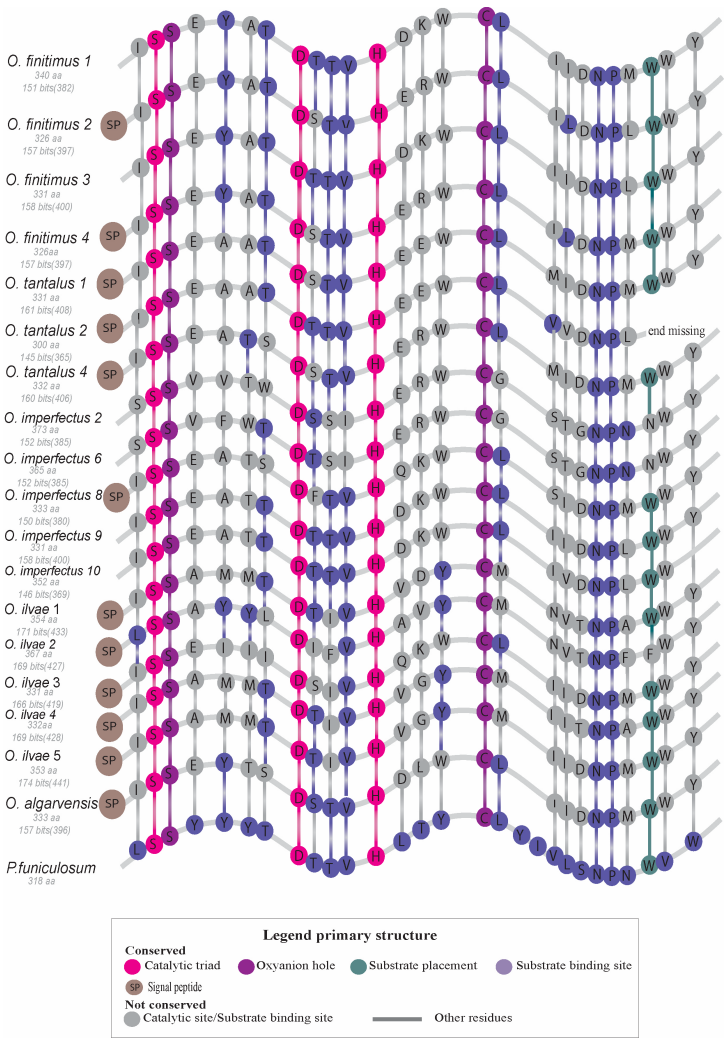

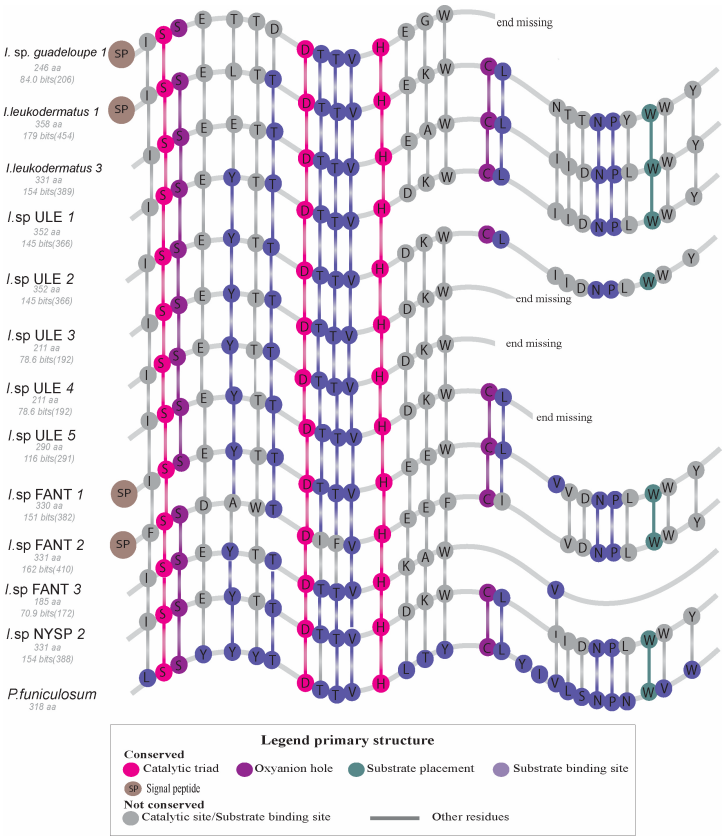

Supplementary Figure 1| Gutless oligochaete PHADs are predicted to cleave short chain PHAs extracellularly. The primary structure of the *phaZ* gene of gutless oligochaetes encoded for a 211 to 367 amino acid long protein. Using MAFFT[16] to align the gutless oligochaete PHADs with that of the homolog from *P. funiculsoum* (pdb 2d81) showed 100% conservation of the catalytic site across all protein sequences. Most gutless oligochaete PHADs were predicted to have a signal peptide (Supplementary Table 1). The *gutless oligochaete* enzymes had 14.5% to 33.8% identity and 65.9% to 95.3% coverage to the *P. funiculsoum* PHAD, suggesting that the gutless oligochaete PHADs function in the same way as the fungal homolog – namely to degrade PHA extracellularly. Colored circles show the conserved residues of the catalytic triad (pink), substrate binding site (light purple) and oxyanion hole (purple). Teal colored circles represent the residue that holds the polymer chain in place for cleavage. The regions between the circles represent all other residues. Gray circles represent non-conserved residues.

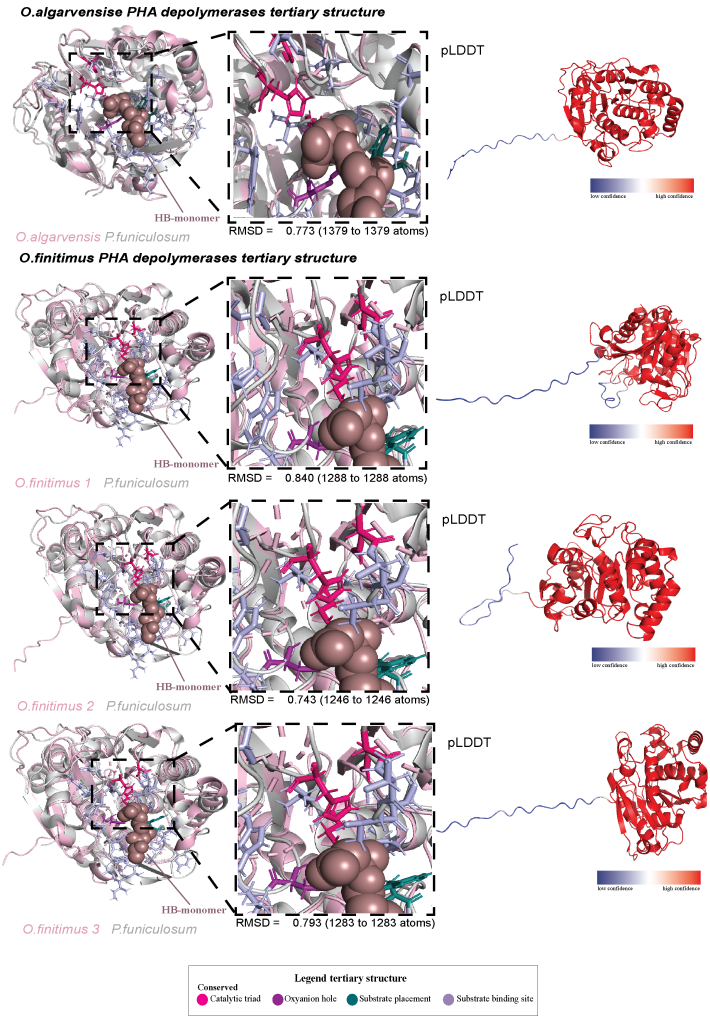
O.algarvensise PHA depolymerases tertiary structure
pLDDT
HB-monomer
O.algarvensis P.funiculosum
RMSD = 0.773 (1379 to 1379 atoms)
low confidence
high confidence
O.finitimus PHA depolymerases tertiary structure
pLDDT
HB-monomer
O.finitimus 1 P.funiculosum
RMSD = 0.840 (1288 to 1288 atoms)
low confidence
high confidence
pLDDT
HB-monomer
O.finitimus 2 P.funiculosum
RMSD = 0.743 (1246 to 1246 atoms)
low confidence
high confidence
pLDDT
HB-monomer
O.finitimus 3 P.funiculosum
RMSD = 0.793 (1283 to 1283 atoms)
low confidence
high confidence
Legend tertiary structure
Conserved
Catalytic triad
Oxyanion hole
Substrate placement
Substrate binding site

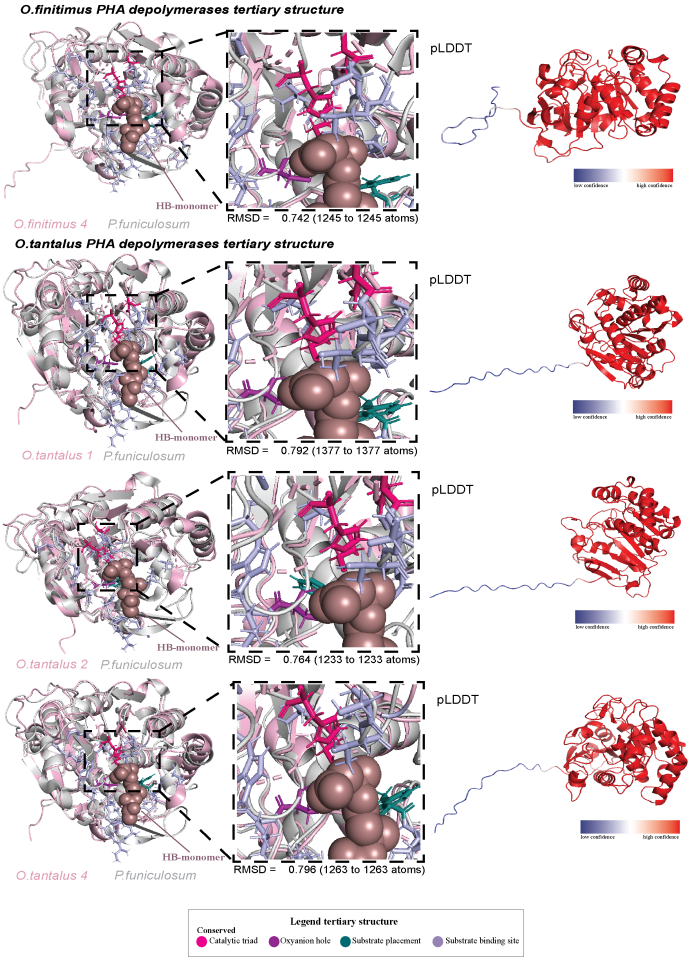
O.finitimus PHA depolymerases tertiary structure
pLDDT
HB-monomer
RMSD = 0.742 (1245 to 1245 atoms)
O.finitimus 4 P.funiculosum
O.tantalus PHA depolymerases tertiary structure
pLDDT
HB-monomer
RMSD = 0.792 (1377 to 1377 atoms)
O.tantalus 1 P.funiculosum
pLDDT
HB-monomer
RMSD = 0.764 (1233 to 1233 atoms)
O.tantalus 2 P.funiculosum
pLDDT
HB-monomer
RMSD = 0.796 (1263 to 1263 atoms)
O.tantalus 4 P.funiculosum
Legend tertiary structure
Conserved
Catalytic triad
Oxyanion hole
Substrate placement
Substrate binding site

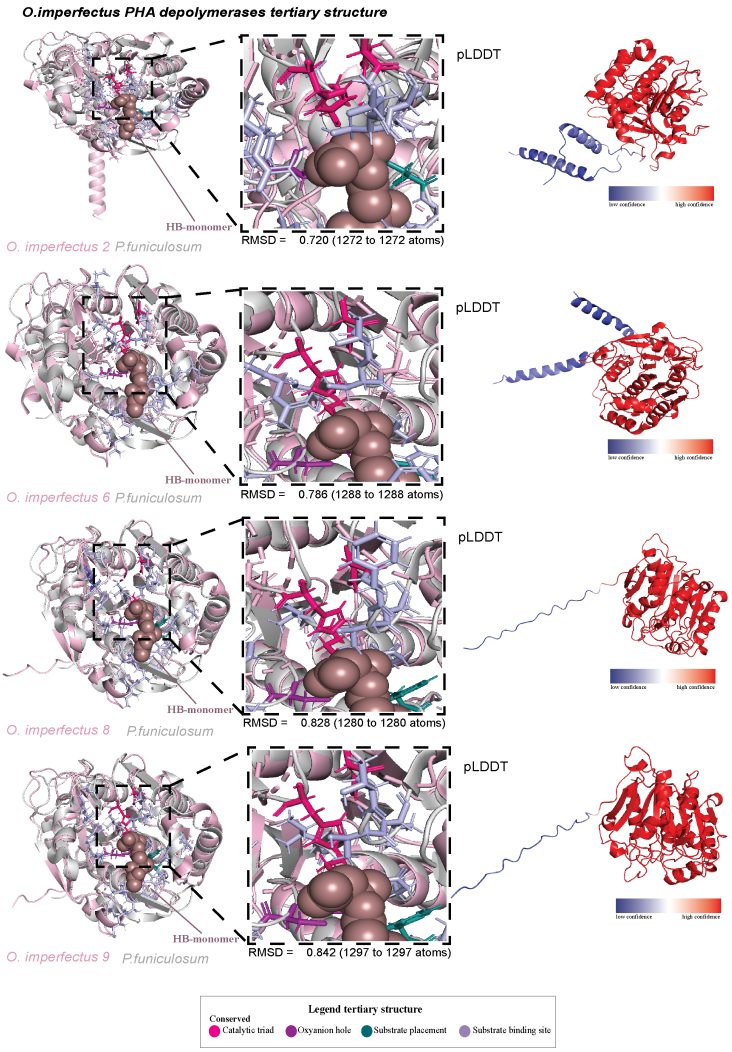
O.imperfectus PHA depolymerases tertiary structure
pLDDT
HB-monomer
O. imperfectus 2 P.funiculosum
RMSD = 0.720 (1272 to 1272 atoms)
low confidence
high confidence
pLDDT
HB-monomer
O. imperfectus 6 P.funiculosum
RMSD = 0.786 (1288 to 1288 atoms)
low confidence
high confidence
pLDDT
HB-monomer
O. imperfectus 8 P.funiculosum
RMSD = 0.828 (1280 to 1280 atoms)
low confidence
high confidence
pLDDT
HB-monomer
O. imperfectus 9 P.funiculosum
RMSD = 0.842 (1297 to 1297 atoms)
low confidence
high confidence
Legend tertiary structure
Conserved
Catalytic triad
Oxyanion hole
Substrate placement
Substrate binding site

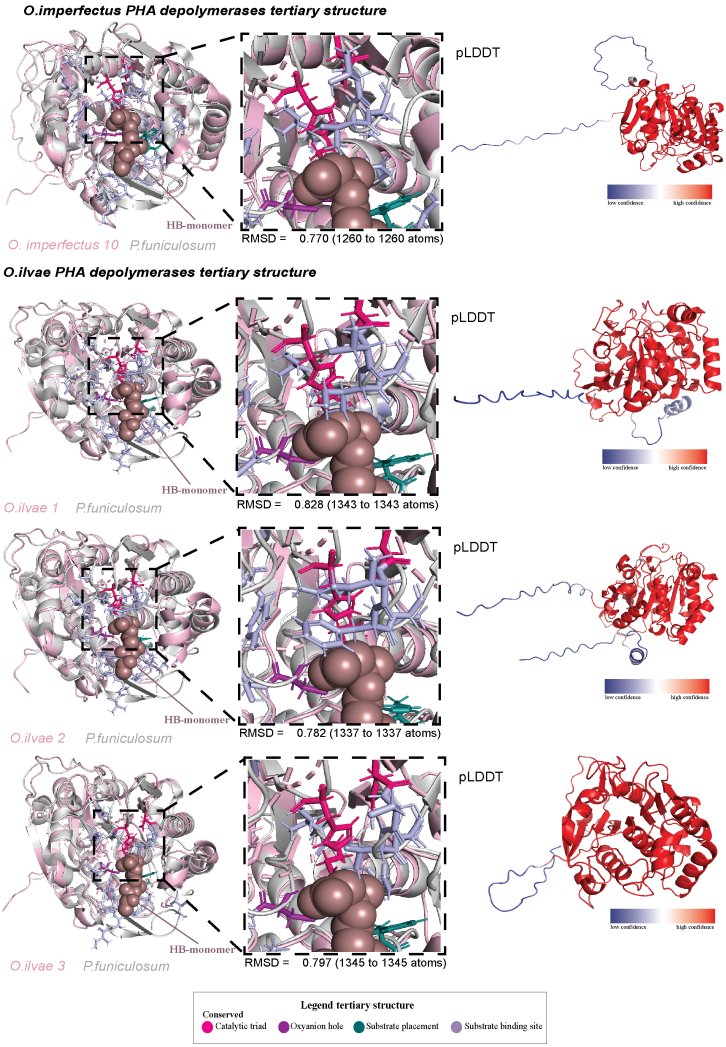
O.imperfectus PHA depolymerases tertiary structure
pLDDT
HB-monomer
O. imperfectus 10 P.funiculosum
RMSD = 0.770 (1260 to 1260 atoms)
low confidence
high confidence
O.ilvae PHA depolymerases tertiary structure
pLDDT
HB-monomer
O.ilvae 1 P.funiculosum
RMSD = 0.828 (1343 to 1343 atoms)
pLDDT
HB-monomer
O.ilvae 2 P.funiculosum
RMSD = 0.782 (1337 to 1337 atoms)
pLDDT
HB-monomer
O.ilvae 3 P.funiculosum
RMSD = 0.797 (1345 to 1345 atoms)
Legend tertiary structure
Conserved
Catalytic triad
Oxyanion hole
Substrate placement
Substrate binding site

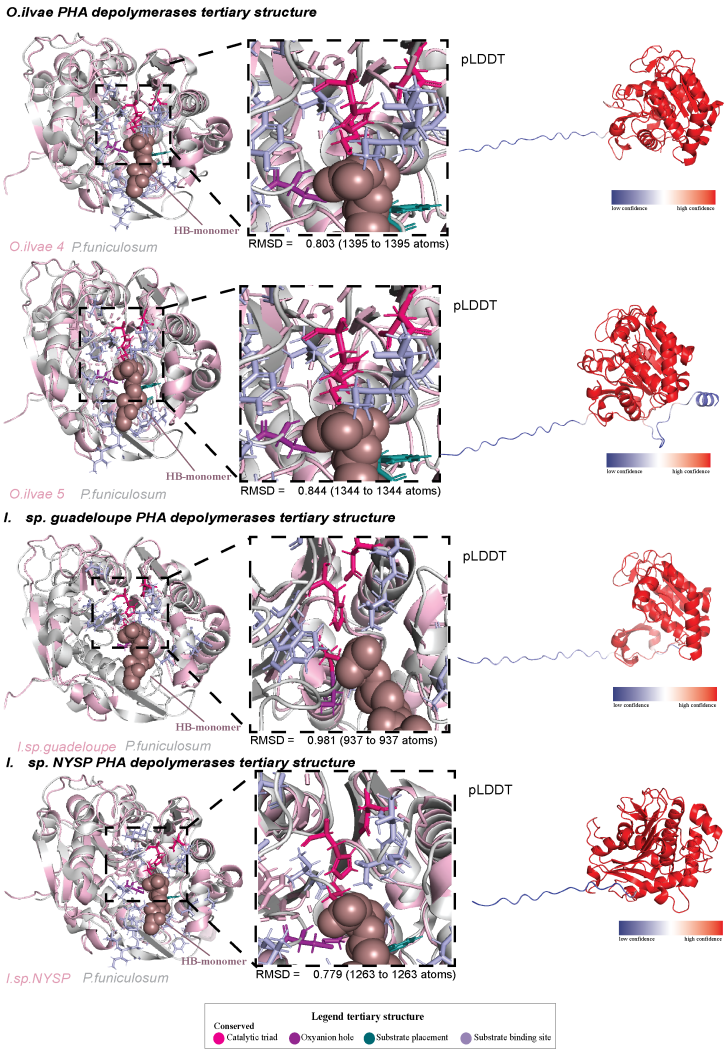
O.ilvae PHA depolymerases tertiary structure
pLDDT
HB-monomer
O.ilvae 4 P.funiculosum
RMSD = 0.803 (1395 to 1395 atoms)
low confidence
high confidence
pLDDT
HB-monomer
O.ilvae 5 P.funiculosum
RMSD = 0.844 (1344 to 1344 atoms)
low confidence
high confidence
I. sp. guadeloupe PHA depolymerases tertiary structure
pLDDT
HB-monomer
I.sp.guadeloupe P.funiculosum
RMSD = 0.981 (937 to 937 atoms)
low confidence
high confidence
I. sp. NYSP PHA depolymerases tertiary structure
pLDDT
HB-monomer
I.sp.NYSP P.funiculosum
RMSD = 0.779 (1263 to 1263 atoms)
low confidence
high confidence
Legend tertiary structure
Conserved
Catalytic triad
Oxyanion hole
Substrate placement
Substrate binding site

I. sp. ULE PHA depolymerases tertiary structure

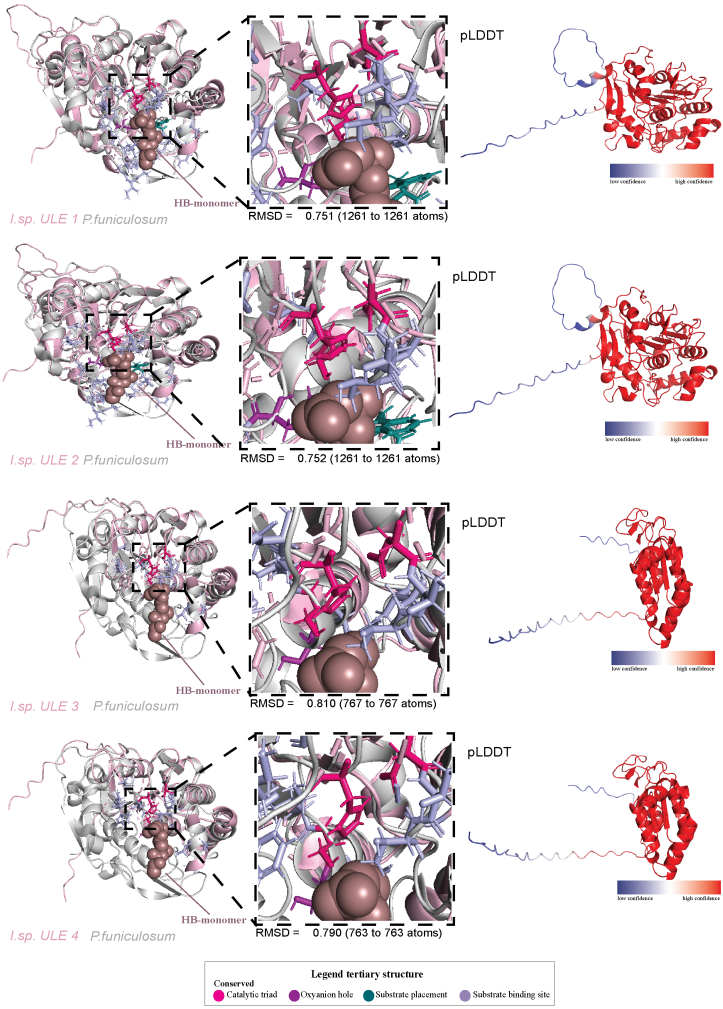

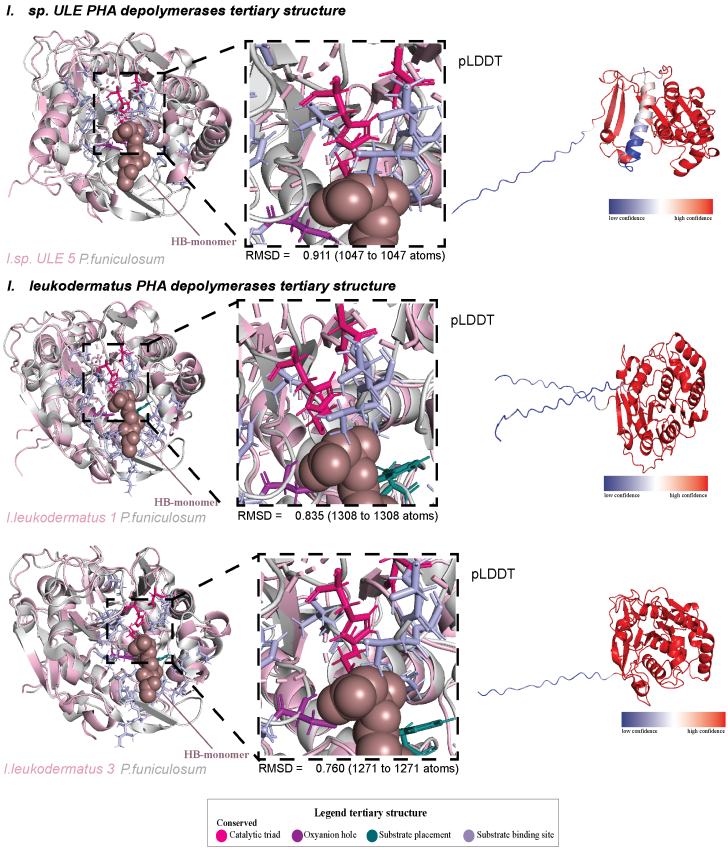
I. sp. ULE PHA depolymerases tertiary structure
pLDDT
HB-monomer
I.sp. ULE 5 P.funiculosum
RMSD = 0.911 (1047 to 1047 atoms)
low confidence
high confidence
I. leukodermatus PHA depolymerases tertiary structure
pLDDT
HB-monomer
I.leukodermatus 1 P.funiculosum
RMSD = 0.835 (1308 to 1308 atoms)
low confidence
high confidence
pLDDT
HB-monomer
I.leukodermatus 3 P.funiculosum
RMSD = 0.760 (1271 to 1271 atoms)
low confidence
high confidence
Legend tertiary structure
Conserved
Catalytic triad
Oxyanion hole
Substrate placement
Substrate binding site

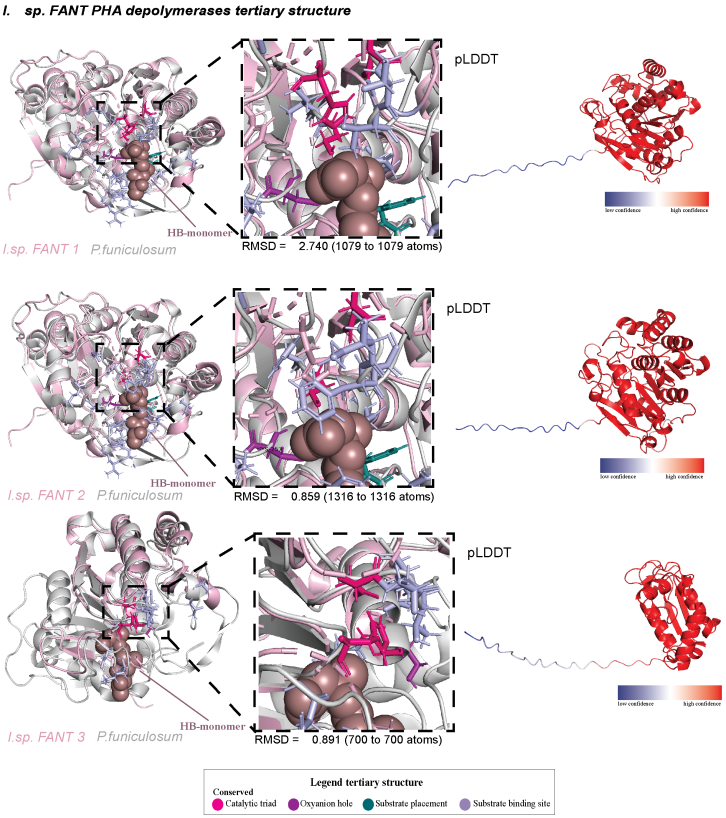

Supplementary Figure 2 | Gutless oligochaete PHADs show tertiary structure alignment to the PHAD of *P. funiculosum*. AlphaFold2[1, 2] was used to predict the structure of the gutless oligochaete PHADs, which were then aligned to the PHAD crystal structure from *P. funiculsoum's* in PyMOL. The alignments suggest that the structures of animal and fungal homologs are similar (RMSD 0.720 to 2.740 Å). Overlap between the fungal homolog and the gutless oligochaete PHADs was at the catalytic triad (pink), oxyanion hole (purple) and the residue that holds the polymer in place (teal). Even though the substrate binding site (light purple) showed little conservation in the primary structure, it overlapped with the fungal PHAD, suggesting a similar substrate binding mechanism. We aligned a monomer of PHB to the catalytic triad and oxyanion hole of the gutless oligochaete PHADs to identify its fitting in the catalytic pocket. The interaction of the catalytic site with the PHB monomer suggest that PHB could be degraded. The AlphaFold2 models were predicted for their model confidences (pLDDT). The core of the gutless oligochaete PHADs was modeled with high confidence (red; above 90%). Only the signal peptide showed poor model predictions (blue). Overall pLDDT ranged from 85 to 96.

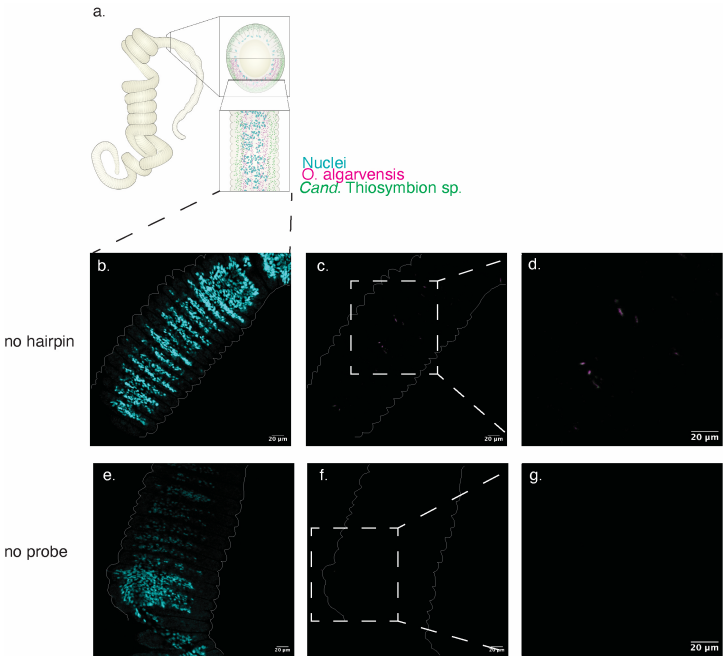

Supplementary Figure 3 | Transcripts encoding for the animal and symbiont PHADs were localized in different regions of *O. algarvensis'* symbiont layer, no labeled probes showed no signal. a, Schematic overview of the position of the signal. We identified the HCR-FISH labels in the symbiont layer that is located underneath the worm's cuticle and above the epidermis. This region harbors all symbionts, including *Ca*. T. algarvensis that synthesizes PHA. The host nuclei are drawn in cyan, the host PHAD in pink and the symbiont PHAD in green. Image courtesy of Rebekka Janke**. b,c,d,** Whole mount images of HCR-FISH of the negative control leaving out the hairpin. Labeled *O. algarvensis* (pink) and *Ca.* Thiosymbion algarvensis' (green) PHAD transcripts within a single worm showed no signal. Nuclei are shown in cyan. The signal that is seen comes from the autofluorescence of the seta. **e,f,g,** Whole mount images of HCR-FISH of the negative control leaving out the probe. Labeled *O. algarvensis* (pink) and *Ca.* Thiosymbion algarvensis' (green) PHAD transcripts within a single worm showed no signal. Nuclei are shown in cyan. No signal was observed.

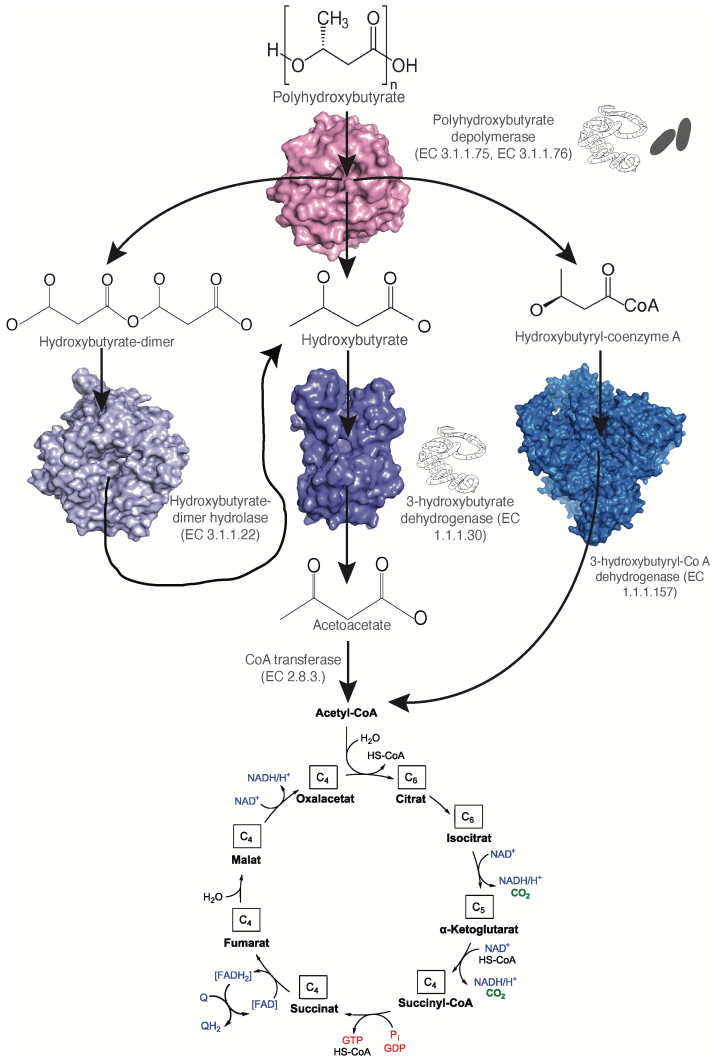
Polyhydroxybutyrate
Polyhydroxybutyrate depolymerase (EC 3.1.1.75, EC 3.1.1.76)
Hydroxybutyrate-dimer
Hydroxybutyrate
Hydroxybutyryl-coenzyme A
Hydroxybutyrate-dimer hydrolase (EC 3.1.1.22)
3-hydroxybutyrate dehydrogenase (EC 1.1.1.30)
3-hydroxybutyryl-Co A dehydrogenase (EC 1.1.1.157)
Acetoacetate
CoA transferase (EC 2.8.3.)
Acetyl-CoA
H2O
HS-CoA
C4
Oxalacetat
C6
Citrat
NADH/H+
NAD+
C6
Isocitrat
NAD+
NADH/H+
CO2
C5
α-Ketoglutarat
NAD+
HS-CoA
NADH/H+
CO2
C4
Succinyl-CoA
Pi
GDP
GTP
HS-CoA
C4
Succinat
[FADH2]
[FAD]
Q
QH2
C4
Fumarat
H2O
C4
Malat

Supplementary Figure 4 | PHADs degrade PHA to their hydroxyalkanoic monomers and dimers that can be further converted by a BHBD to acetoacetate which is used in the TCA cycle for energy generation. The PHA degradation pathway is shown at the example of the polymer polyhydroxybutyrate (PHB). PHB is degraded by the PHAD to monomers, dimers or a mix of oligomers. The dimers can be degraded to their monomers by a hydroxybutyrate-dimer hydrolase (EC 3.1.1.22). The resulting monomers are degraded by a beta-hydroxybutyrate dehydrogenase (EC 1.1.1.30) to transform the monomers into acetoacetate. Acetoacetate is then oxidized to acetyl coenzyme A, which is a key component in the citric acid cycle. Acetyl-CoA is oxidized in the citric acid cycle to release CO_2, water and under anaerobic conditions CH_4 together with reducing equivalents used for energy generation[17-27]. Alternatively, PHA degradation can result in CoA-bound monomers that can be degraded directly to Acetyl-CoA by 3-hydroxybutyryl-coenzyme A dehydrogenase (EC 1.1.1.157). While we identified in all gutless oligochaete species a PHAD and eight species had a BHBD, the primary symbiont *Ca*. Thiosymbion sp. lacked the genes to degrade PHA for energy generation. Therefore, the host might not compete with its symbionts for the energy from PHA degradation.
The enzyme structures are taken as examples from the pdb-database: PHAD (pdb 280), BHBD (pdb 3w8e), 3-hydroxybutyrylCoA dehydrogenase (pdb 6acq). The hydroxybutyric-dimer hydrolase was modeled using AlphaFold2 after the sequence from *Cuprivados nector* (NCBI accession Q0K9H3) because no structure was available. The TCA cycle was downloaded from https://www.wikipathways.org/pathways/WP78.html.

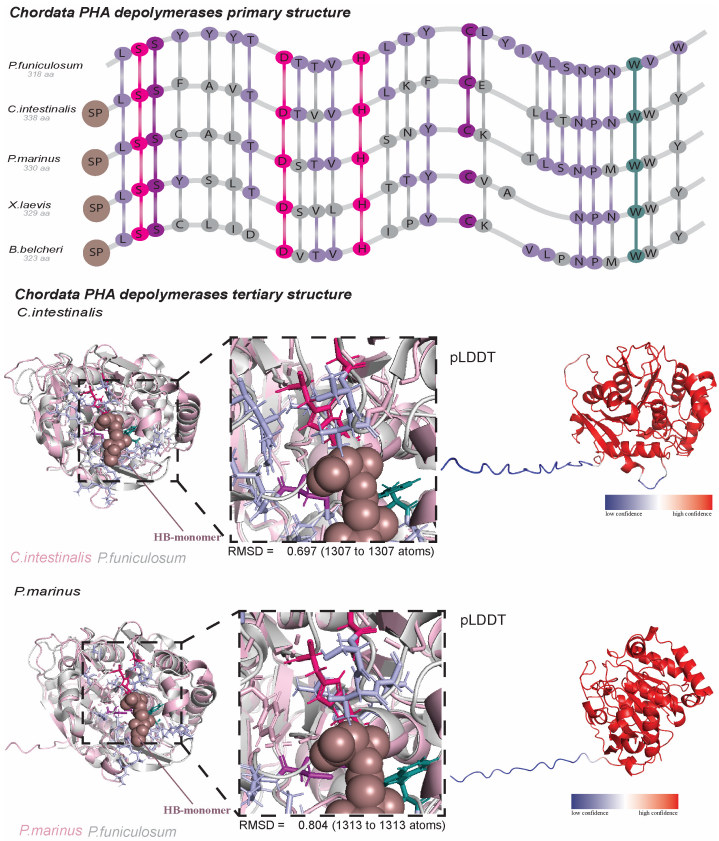
Chordata PHA depolymerases primary structure
P.funiculosum
318 aa
C.intestinalis
338 aa
P.marinus
330 aa
X.laevis
329 aa
B.belcheri
323 aa
SP
Chordata PHA depolymerases tertiary structure
C.intestinalis
pLDDT
HB-monomer
C.intestinalis P.funiculosum
RMSD = 0.697 (1307 to 1307 atoms)
low confidence
high confidence
P.marinus
pLDDT
HB-monomer
P.marinus P.funiculosum
RMSD = 0.804 (1313 to 1313 atoms)
low confidence
high confidence

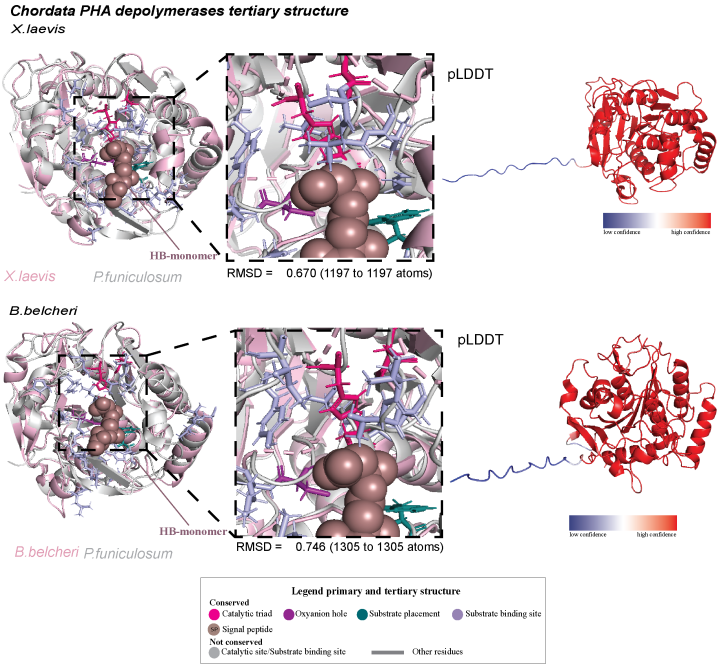

Supplementary Figure 5 | Chordata PHADs are predicted to degrade extracellular short chain PHA. Using MAFFT[16] to align the Chordata PHADs primary structure with that of homologs from *P. funiculosum* (pdb 2d81) showed 100% conservation of the catalytic site across all protein sequences. Chordata PHADs were predicted to have a signal peptide (Supplementary Table 1). Differences between the fungal PHAD and the Chordata PHADs are the substrate binding site which showed complete alignment in the tertiary structure. Colored circles show the conserved residues of the catalytic triad (pink), substrate binding site (light purple) and oxyanion hole (purple). Teal colored circles represent the residue that holds the polymer chain in place for cleavage. Gray colored circles show non-conserved residues. The regions between the circles represent all other residues.
AlphaFold2[1, 2] was used to predict the structure of the Chordata PHADs, which were then aligned to the PHAD crystal structure from *P. funiculosum* in PyMOL. The alignment suggest that the structures of animal and fungal homologs are similar (RMSD 0.670 to 0.804 Å). Overlap between the fungal homolog and the Chordata PHADs was at the catalytic triad (pink), oxyanion hole (purple) and the residue that holds the polymer in place (teal). We aligned a monomer of PHB to the catalytic triad and oxyanion hole of the Chordata PHADs to identify its fitting in the catalytic pocket. The interaction of the catalytic site with the PHB monomer suggest that PHB could be degraded. The AlphaFold2 models were predicted for their model confidences (pLDDT). The core of the Chordata PHADs was modeled with high confidence (red; above 90%). Only the signal peptide showed poor model predictions (blue).

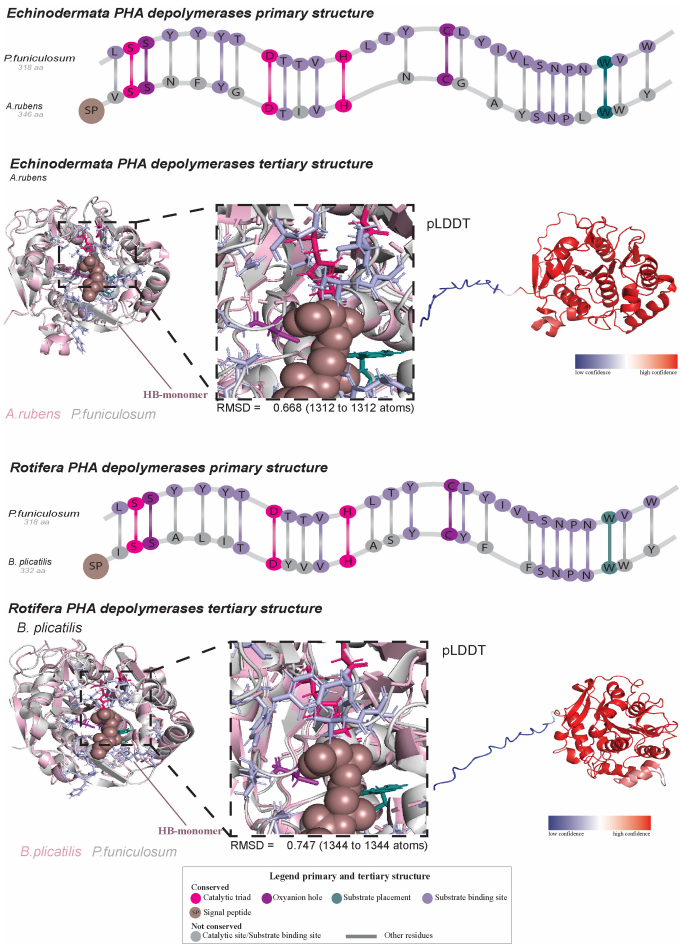
Echinodermata PHA depolymerases primary structure
P.funiculosum
318 aa
A.rubens
346 aa
SP
Echinodermata PHA depolymerases tertiary structure
A.rubens
pLDDT
HB-monomer
RMSD = 0.668 (1312 to 1312 atoms)
A.rubens P.funiculosum
low confidence
high confidence
Rotifera PHA depolymerases primary structure
P.funiculosum
318 aa
B. plicatilis
332 aa
SP
Rotifera PHA depolymerases tertiary structure
B. plicatilis
pLDDT
HB-monomer
RMSD = 0.747 (1344 to 1344 atoms)
B.plicatilis P.funiculosum
low confidence
high confidence
Legend primary and tertiary structure
Conserved
Catalytic triad
Oxyanion hole
Substrate placement
Substrate binding site
Signal peptide
Not conserved
Catalytic site/Substrate binding site
Other residues

Supplementary Figure 6 | Rotifera and Echinodermata PHADs are predicted to degrade extracellular short chain PHA. Using MAFFT[16] to align the Rotifera and Echinodermata PHADs primary structure with that of homologs from *P. funiculosum* (pdb 2d81) showed 100% conservation of the catalytic site across all protein sequences. Rotifera and Echinodermata PHADs were predicted to have a signal peptide (Supplementary Table 1). Differences between the fungal PHAD and the Rotifera and Echinodermata PHADs are the substrate binding site which showed complete alignment in the tertiary structure. Colored circles show the conserved residues of the catalytic triad (pink), substrate binding site (light purple) and oxyanion hole (purple). Teal colored circles represent the residue that holds the polymer chain in place for cleavage. Gray circles represent non-conserved residues. The regions between the circles represent all other residues.
AlphaFold2[1, 2] was used to predict the structure of the Rotifera and Echinodermata PHADs, which were then aligned to the PHAD crystal structure from *P. funiculosum* in PyMOL. The alignment suggest that the structures of animal and fungal homologs are similar (RMSD 0.747 and 0.668 Å). Overlap between the fungal homolog and the Rotifera and Echinodermata PHADs was at the catalytic triad (pink), oxyanion hole (purple) and the residue that holds the polymer in place (teal). We aligned a monomer of PHB to the catalytic triad and oxyanion hole of the Rotifera and Echinodermata PHADs to identify its fitting in the catalytic pocket. The interaction of the catalytic site with the PHB monomer suggest that PHB could be degraded. The AlphaFold2 models were predicted for their model confidences (pLDDT). The core of the Rotifera and Echinodermata PHADs was modeled with high confidence (red; above 90%). Only the signal peptide showed poor model predictions (blue).

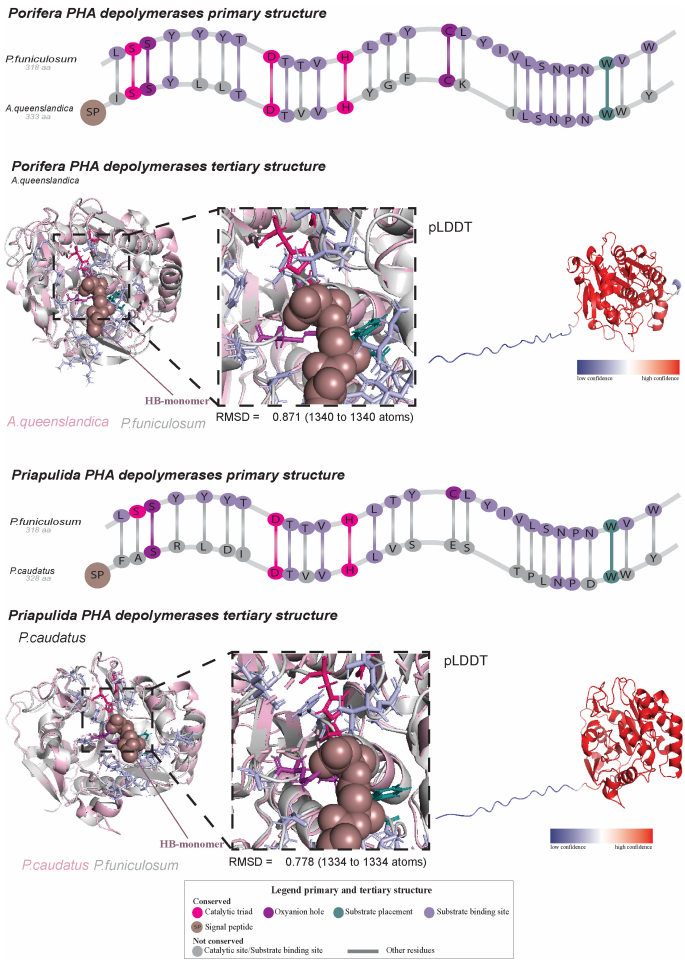
Porifera PHA depolymerases primary structure
P.funiculosum
318 aa
A.queenslandica
333 aa
SP
Porifera PHA depolymerases tertiary structure
A.queenslandica
pLDDT
HB-monomer
A.queenslandica P.funiculosum
RMSD = 0.871 (1340 to 1340 atoms)
low confidence
high confidence
Priapulida PHA depolymerases primary structure
P.funiculosum
318 aa
P.caudatus
329 aa
SP
Priapulida PHA depolymerases tertiary structure
P.caudatus
pLDDT
HB-monomer
P.caudatus P.funiculosum
RMSD = 0.778 (1334 to 1334 atoms)
low confidence
high confidence
Legend primary and tertiary structure
Conserved
Catalytic triad
Oxyanion hole
Substrate placement
Substrate binding site
Signal peptide
Not conserved
Catalytic site/Substrate binding site
Other residues

Supplementary Figure 7 | Porifera and Priapulida PHADs are predicted to degrade extracellular short chain PHA. Using MAFFT[16] to align the Porifera and Priapulida PHADs primary structure with that of homologs from *P. funiculosum* (pdb 2d81) showed 100% conservation of the catalytic site across all protein sequences. Porifera and Priapulida PHADs were predicted to have a signal peptide (Supplementary Table 1). Differences between the fungal PHAD and the Porifera and Priapulida PHADs are the substrate binding site which showed complete alignment in the tertiary structure. Colored circles show the conserved residues of the catalytic triad (pink), substrate binding site (light purple) and oxyanion hole (purple). Teal colored circles represent the residue that holds the polymer chain in place for cleavage. Gray circles show the non-conserved residues. The regions between the circles represent all other residues.
AlphaFold2[1, 2] was used to predict the structure of the Porifera and Priapulida PHADs, which were then aligned to the PHAD crystal structure from *P. funiculosum* in PyMOL. The alignment suggest that the structures of animal and fungal homologs are similar (RMSD 0.778 and 0.871 Å). Overlap between the fungal homolog and the Porifera and Priapulida PHADs was at the catalytic triad (pink), oxyanion hole (purple) and the residue that holds the polymer in place (teal). We aligned a monomer of PHB to the catalytic triad and oxyanion hole of the Porifera and Priapulida PHADs to identify its fitting in the catalytic pocket. The interaction of the catalytic site with the PHB monomer suggest that PHB could be degraded. The AlphaFold2 models were predicted for their model confidences (pLDDT). The core of the Porifera and Priapulida PHADs was modeled with high confidence (red; above 90%). Only the signal peptide showed poor model predictions (blue).

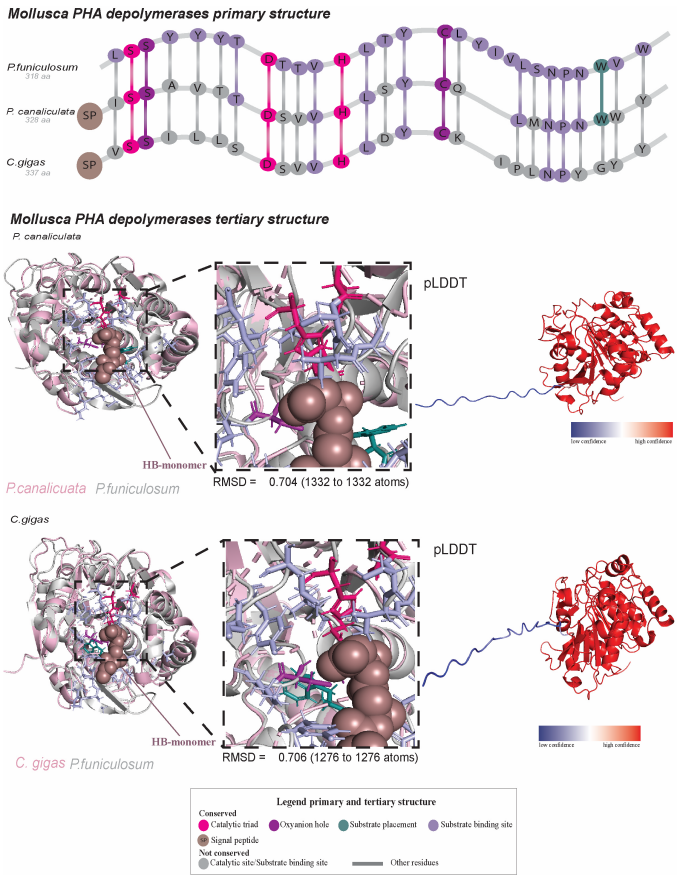
Mollusca PHA depolymerases primary structure
P.funiculosum
318 aa
P. canaliculata
328 aa
C.gigas
337 aa
SP
Mollusca PHA depolymerases tertiary structure
P. canaliculata
pLDDT
HB-monomer
RMSD = 0.704 (1332 to 1332 atoms)
P.canaliculata P.funiculosum
low confidence
high confidence
C.gigas
pLDDT
HB-monomer
RMSD = 0.706 (1276 to 1276 atoms)
C. gigas P.funiculosum
low confidence
high confidence
Legend primary and tertiary structure
Conserved
Catalytic triad
Oxyanion hole
Substrate placement
Substrate binding site
Signal peptide
Not conserved
Catalytic site/Substrate binding site
Other residues

Supplementary Figure 8 | Mollusca PHADs are predicted to degrade extracellular short chain PHA. Using MAFFT[16] to align the Mollusca PHADs primary structure with that of homologs from *P. funiculosum* (pdb 2d81) showed 100% conservation of the catalytic site across all protein sequences. Mollusca PHADs were predicted to have a signal peptide (Supplementary Table 1). Differences between the fungal PHAD and the Mollusca PHADs are the substrate binding site which showed complete alignment in the tertiary structure. Colored circles show the conserved residues of the catalytic triad (pink), substrate binding site (light purple) and oxyanion hole (purple). Teal colored circles represent the residue that holds the polymer chain in place for cleavage. *Crassostrea gigas* showed no conservation of the residue that holds the polymer chain for the nucleophilic attack. Gray circles show the non-conserved residues. The regions between the circles represent all other residues.
AlphaFold2[1, 2] was used to predict the structure of the Mollusca PHADs, which were then aligned to the PHAD crystal structure from *P. funiculosum* in PyMOL. The alignment suggest that the structures of animal and fungal homologs are similar (RMSD 0.704 and 0.706 Å). Overlap between the fungal homolog and the Mollusca PHADs was at the catalytic triad (pink), oxyanion hole (purple) and the residue that holds the polymer in place (teal). We aligned a monomer of PHB to the catalytic triad and oxyanion hole of the Mollusca PHADs to identify its fitting in the catalytic pocket. The interaction of the catalytic site with the PHB monomer suggest that PHB could be degraded. The AlphaFold2 models were predicted for their model confidences (pLDDT). The core of the Mollusca PHADs was modeled with high confidence (red; above 90%). Only the signal peptide showed poor model predictions (blue).

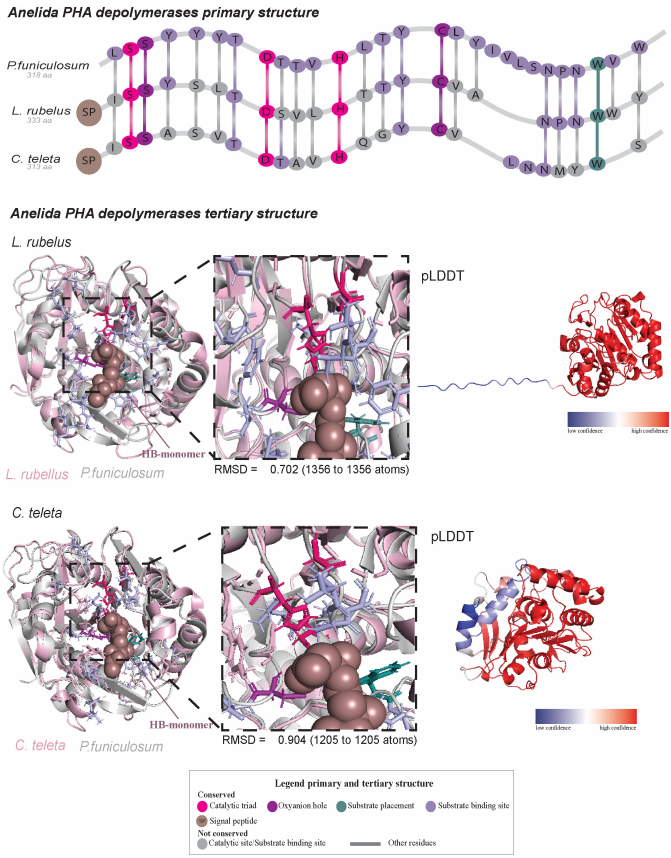
Anelida PHA depolymerases primary structure
P.funiculosum
318 aa
L. rubelus
333 aa
C. teleta
313 aa
SP
Anelida PHA depolymerases tertiary structure
L. rubelus
pLDDT
HB-monomer
L. rubellus P.funiculosum
RMSD = 0.702 (1356 to 1356 atoms)
low confidence
high confidence
C. teleta
pLDDT
HB-monomer
C. teleta P.funiculosum
RMSD = 0.904 (1205 to 1205 atoms)
low confidence
high confidence
Legend primary and tertiary structure
Conserved
Catalytic triad
Oxyanion hole
Substrate placement
Substrate binding site
Signal peptide
Not conserved
Catalytic site/Substrate binding site
Other residues

Supplementary Figure 9 | Annelida PHADs are predicted to degrade extracellular short chain PHA. Using MAFFT[16] to align the Annelida PHADs primary structure with that of homologs from *P. funiculosum* (pdb 2d81) showed 100% conservation of the catalytic site across all protein sequences. Annelida PHADs were predicted to have a signal peptide (Supplementary Table 1). Differences between the fungal PHAD and the Annelida PHADs are the substrate binding site which showed complete alignment in the tertiary structure. Colored circles show the conserved residues of the catalytic triad (pink), substrate binding site (light purple) and oxyanion hole (purple). Teal colored circles represent the residue that holds the polymer chain in place for cleavage. Gray circles represent the non-conserved residues. The regions between the circles represent all other residues.
AlphaFold2[1, 2] was used to predict the structure of the Annelida PHADs, which were then aligned to the PHAD crystal structure from *P. funiculosum* in PyMOL. The alignment suggest that the structures of animal and fungal homologs are similar (RMSD 0.702 and 0.904 Å). Overlap between the fungal homolog and the Annelida PHADs was at the catalytic triad (pink), oxyanion hole (purple) and the residue that holds the polymer in place (teal). We aligned a monomer of PHB to the catalytic triad and oxyanion hole of the Annelida PHADs to identify its fitting in the catalytic pocket. The interaction of the catalytic site with the PHB monomer suggest that PHB could be degraded. The AlphaFold2 models were predicted for their model confidences (pLDDT). The core of the Annelida PHADs was modeled with high confidence (red; above 90%). Only the signal peptide showed poor model predictions (blue).

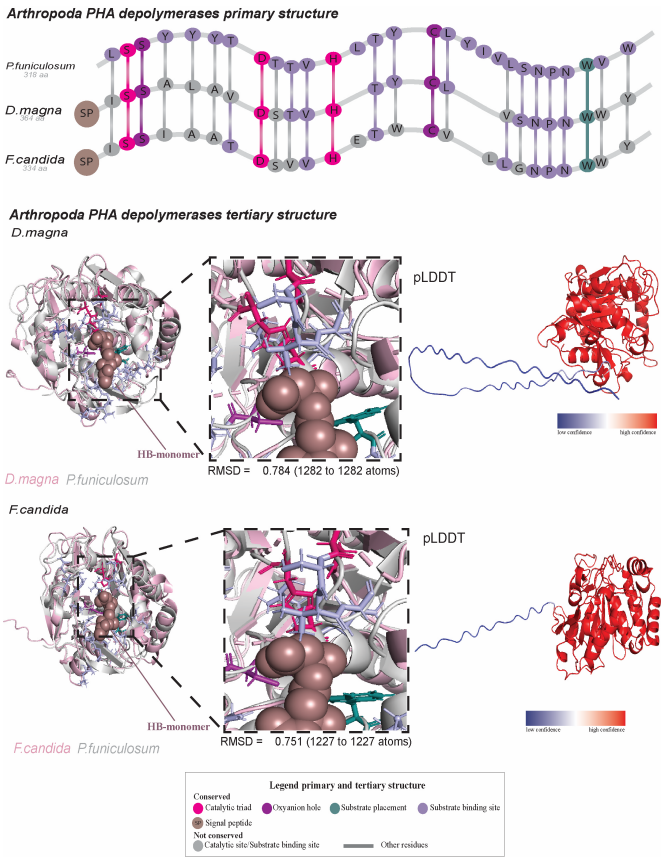
Arthropoda PHA depolymerases primary structure
P.funiculosum
D.magna
F.candida
SP
Arthropoda PHA depolymerases tertiary structure
D.magna
pLDDT
HB-monomer
RMSD = 0.784 (1282 to 1282 atoms)
D.magna P.funiculosum
F.candida
pLDDT
HB-monomer
RMSD = 0.751 (1227 to 1227 atoms)
F.candida P.funiculosum
Legend primary and tertiary structure
Conserved
Catalytic triad
Oxyanion hole
Substrate placement
Substrate binding site
Signal peptide
Not conserved
Catalytic site/Substrate binding site
Other residues

Supplementary Figure 10 | Arthropoda PHADs are predicted to degrade extracellular short chain PHA. Using MAFFT[16] to align the Arthropoda PHADs primary structure with that of homologs from *P. funiculosum* (pdb 2d81) showed 100% conservation of the catalytic site across all protein sequences. Arthropoda PHADs were predicted to have a signal peptide (Supplementary Table 1). Differences between the fungal PHAD and the Arthropoda PHADs are the substrate binding site which showed complete alignment in the tertiary structure. Colored circles show the conserved residues of the catalytic triad (pink), substrate binding site (light purple) and oxyanion hole (purple). Teal colored circles represent the residue that holds the polymer chain in place for cleavage. Gray circles represent the non-conserved residues. The regions between the circles represent all other residues.
AlphaFold2[1, 2] was used to predict the structure of the Arthropoda PHADs, which were then aligned to the PHAD crystal structure from *P. funiculosum* in PyMOL. The alignment suggest that the structures of animal and fungal homologs are similar (RMSD 0.784 and 0.751 Å). Overlap between the fungal homolog and the Arthropoda PHADs was at the catalytic triad (pink), oxyanion hole (purple) and the residue that holds the polymer in place (teal). We aligned a monomer of PHB to the catalytic triad and oxyanion hole of the Arthropoda PHADs to identify its fitting in the catalytic pocket. The interaction of the catalytic site with the PHB monomer suggest that PHB could be degraded. The AlphaFold2 models were predicted for their model confidences (pLDDT). The core of the Arthropoda PHADs was modeled with high confidence (red; above 90%). Only the signal peptide showed poor model predictions (blue).


Bacteria
Rotifera
Bacteria
Fungi
PHAD homology clade 8
PHAD homology clade 3-7
Edelfovibrionota & Provora
Evosea/Choanoflagellata/Euglenozoa/Ciliophora
Heterolobosea
Amphimedon queenslandica(Porifera, Demospongiae)
Ascidiacea (Chordata, Tunicata)
Hemichordata/Echinodermata
Nibbleromonas (Provora, Nibbleridia)
Priapulus caudatus (Priapulida, Priapulimorpha)
Rotifera
Mollusca
Chordata
Chordata
Annelida
Arthropoda
Tree scale: 1
Bootstrap > 90

Supplementary Figure 11 | Rotifera PHADs clustered with Burkholderia PHADs which could be an indication for a recent horizontal gene transfer event (HGT). Zoom in at the maximum likelihood tree (IQ TREE[28] using ultrafast bootstrap support) built from extracellular PHAD protein sequences showed that PHA degradation likely occurs across fungal, protist and animal lineages. The tree indicates that the newly discovered animal PHADs belong to the extracellular PHADs of domain type 2, which target the degradation of short chain PHAs. We observed that Rotifera PHADs clustered with *Burkholderia* sp. PHADs, representing a recent HGT event. Other Rotifera PHADs clustered in the animal PHAD clade (orange clade).

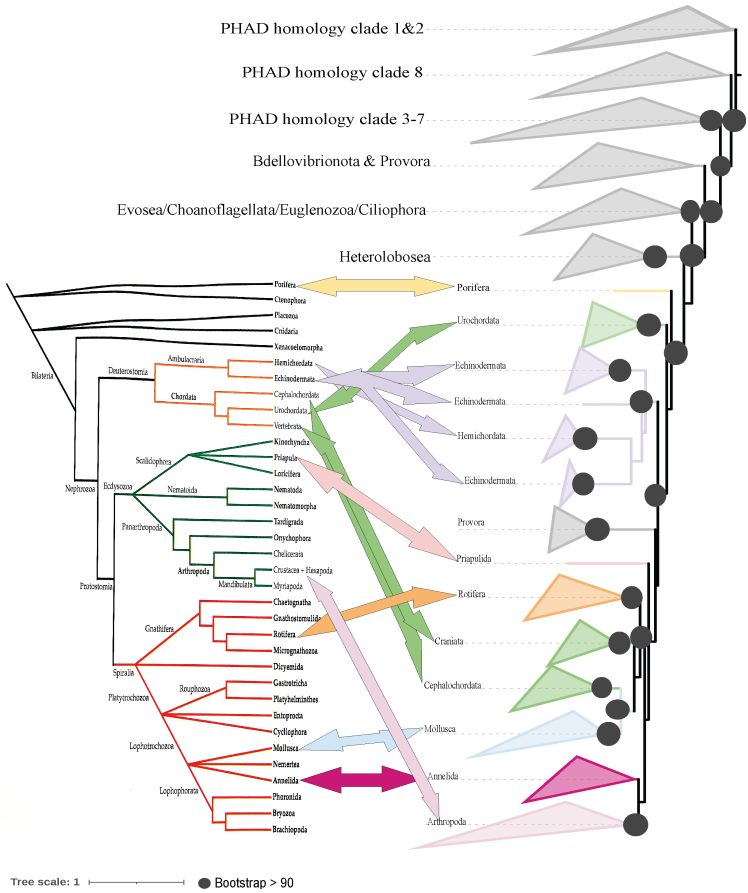

Supplementary Figure 12 | PHAD phylogeny is at some places incongruent with animal phylum phylogeny. We compared the phylogeny of animal PHADs to the species phylogeny of animals. In some cases, e.g. Echinodermata and Hemichordata, the PHAD phylogeny reflects the animal phylogeny. However, other animal PHADs, such as the Chordata PHADs, do not reflect their animal phylogeny. Animal tree taken from the book "Invertebrates" by Richard C. Brusca.

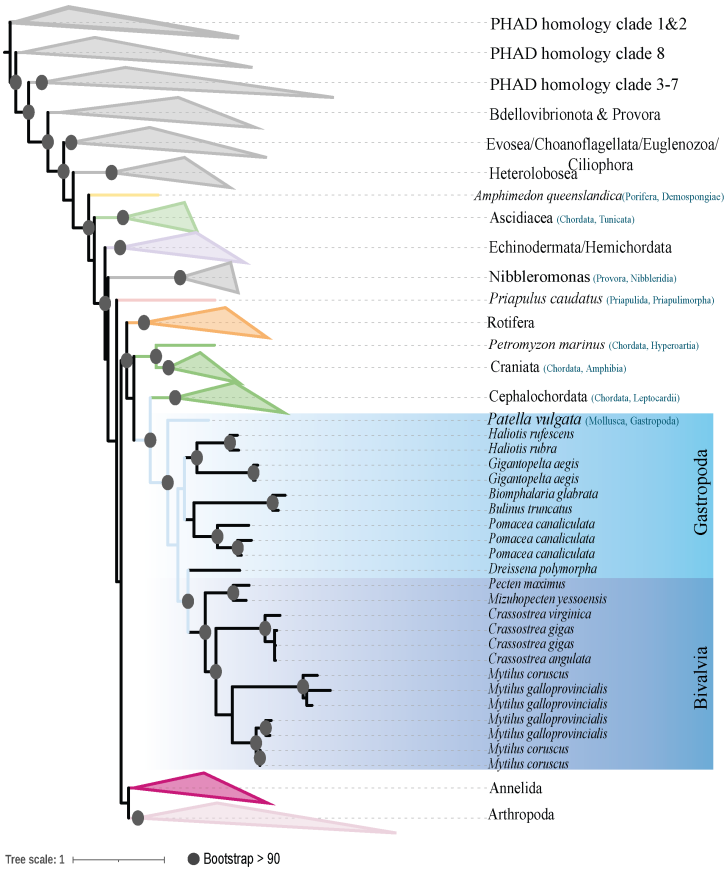

Supplementary Figure 12 | Mollusca PHADs clustered according to their phylum's class. Zoom in at the maximum likelihood tree (IQ TREE[28] using ultrafast bootstrap support) built from extracellular PHAD protein sequences showed that PHA degradation likely occurs across fungal, protist and animal lineages. The tree indicates that the newly discovered animal PHADs belong to the extracellular PHADs of domain type 2, which target the degradation of short chain PHAs. Mollusca PHADs split into two classes: Bivalvia and Gastropoda. The splitting of the two PHAD groups is in accordance with the phylum's phylogeny.

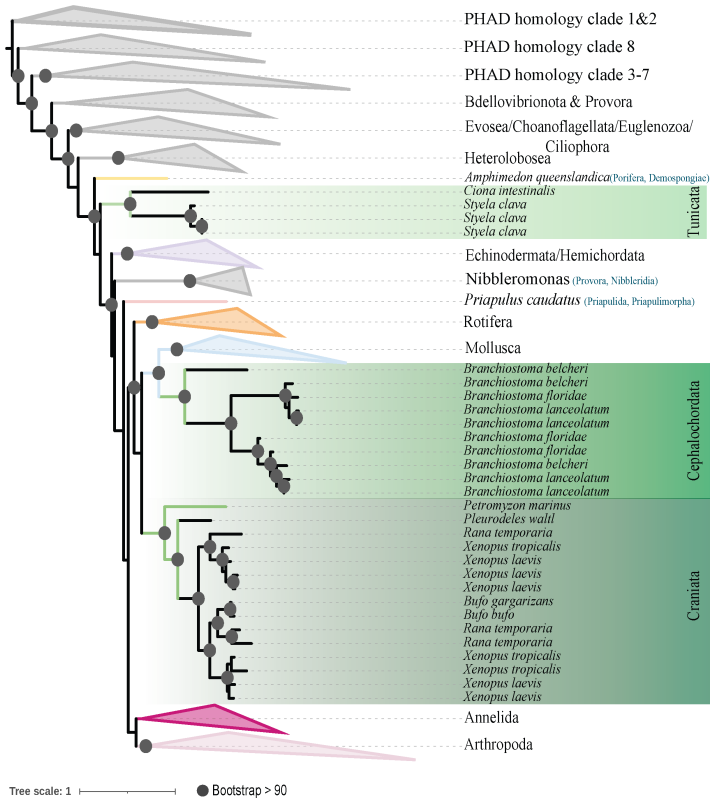

Supplementary Figure 14 | Chordata PHADs split into their proposed subclades Craniata, Cephalochordata and Tunicate but appeared in disparate branches. Zoom in at the maximum likelihood tree (IQ TREE[28] using ultrafast bootstrap support) built from extracellular PHAD protein sequences showed that PHA degradation likely occurs across fungal, protist and animal lineages. The tree indicates that the newly discovered animal PHADs belong to the extracellular PHADs of domain type 2, which target the degradation of short chain PHAs. Chordata PHADs grouped according to the Chordate subphyla of Tunicata, Craniata and Cephalochordata, but appeared in the tree as disparate branches: the Tunicata enzymes grouped as an early branching clade to all metazoan PHADs and the Craniata PHADs formed a sister clade to the Cephalochordata and Mollusca PHADs.

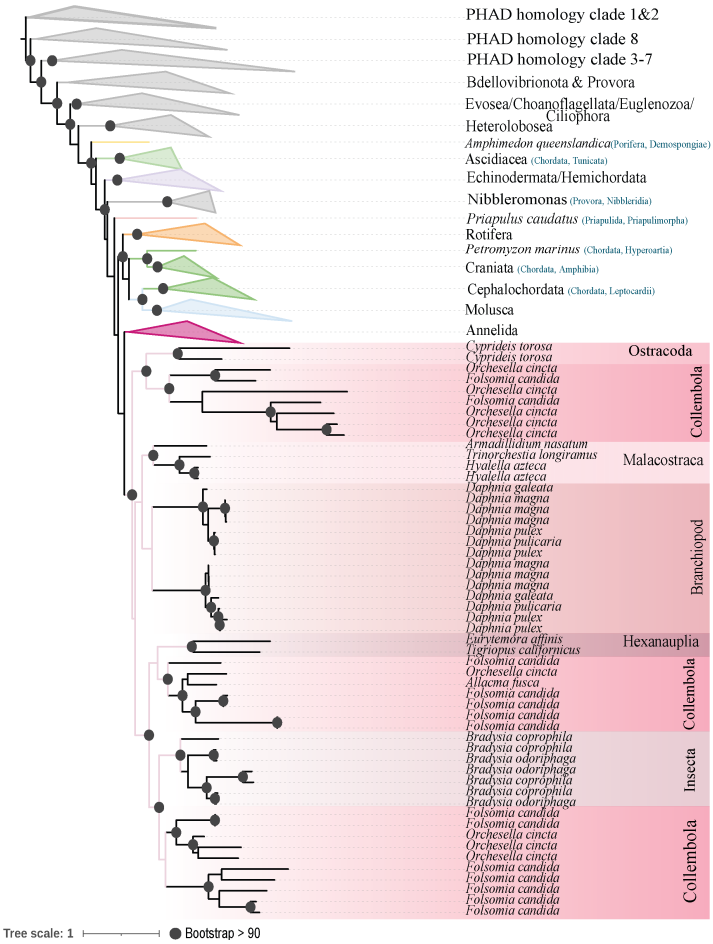
PHAD homology clade 1&2
PHAD homology clade 8
PHAD homology clade 3-7
Bdellovibrionota & Provora
Evosea/Choanoflagellata/Euglenozoa/
Ciliophora
Heterolobosea
Amphimedon queenslandica (Porifera, Demospongiae)
Ascidiacea (Chordata, Tunicata)
Echinodermata/Hemichordata
Nibbleromonas (Provora, Nibbleridia)
Priapulus caudatus (Priapulida, Priapulimorpha)
Rotifera
Petromyzon marinus (Chordata, Hyperoartia)
Craniata (Chordata, Amphibia)
Cephalochordata (Chordata, Leptocardii)
Molusca
Annelida
Cypridcis torosa
Cypridcis torosa
Ostracoda
Orchesella cincta
Folsomia candida
Orchesella cincta
Folsomia candida
Orchesella cincta
Orchesella cincta
Orchesella cincta
Collembola
Armadillidium nasatum
Trinorchestia longiramus
Hyalella azteca
Hyalella azteca
Malacostraca
Daphnia galeata
Daphnia magna
Daphnia magna
Daphnia magna
Daphnia pulex
Daphnia pulicaria
Daphnia pulex
Daphnia magna
Daphnia magna
Daphnia magna
Daphnia galeata
Daphnia pulicaria
Daphnia pulex
Daphnia pulex
Branchiopod
Eurytemora affinis
Tigriopus californicus
Hexanauplia
Folsomia candida
Orchesella cincta
Allacma fusca
Folsomia candida
Folsomia candida
Folsomia candida
Folsomia candida
Collembola
Bradysia coprophila
Bradysia coprophila
Bradysia odoriphaga
Bradysia odoriphaga
Bradysia coprophila
Bradysia coprophila
Bradysia odoriphaga
Insecta
Folsomia candida
Folsomia candida
Orchesella cincta
Orchesella cincta
Orchesella cincta
Folsomia candida
Folsomia candida
Folsomia candida
Folsomia candida
Folsomia candida
Collembola
Tree scale: 1
Bootstrap > 90

Supplementary Figure 15 | Arthropoda PHADs clustered closest to Annelida PHADs. PHADs of Collembola species had several PHAD copies that intermixed with other Arthropod PHADs. Zoom in at the maximum likelihood tree (IQ TREE[28] using ultrafast bootstrap support) built from extracellular PHAD protein sequences showed that PHA degradation likely occurs across fungal, protist and animal lineages. The tree indicates that the newly discovered animal PHADs belong to the extracellular PHADs of domain type 2, which target the degradation of short chain PHAs. Arthropoda PHADs grouped closest with homologs from Annelids, contrasting their animal phylogeny. Arthropod PHADs were split into their respective phylum classes but PHADs of Collembola intermix with those phylum class sorted PHADs. The Collembola species *Folsomia candida* and *Orchessella cincta* had several PHAD copies that intermixed with the other Arthropod PHADs (Supplementary Table 2). More PHAD copies could allow the animal species a higher metabolic flexibility to degrade PHA (Supplementary Text 3).

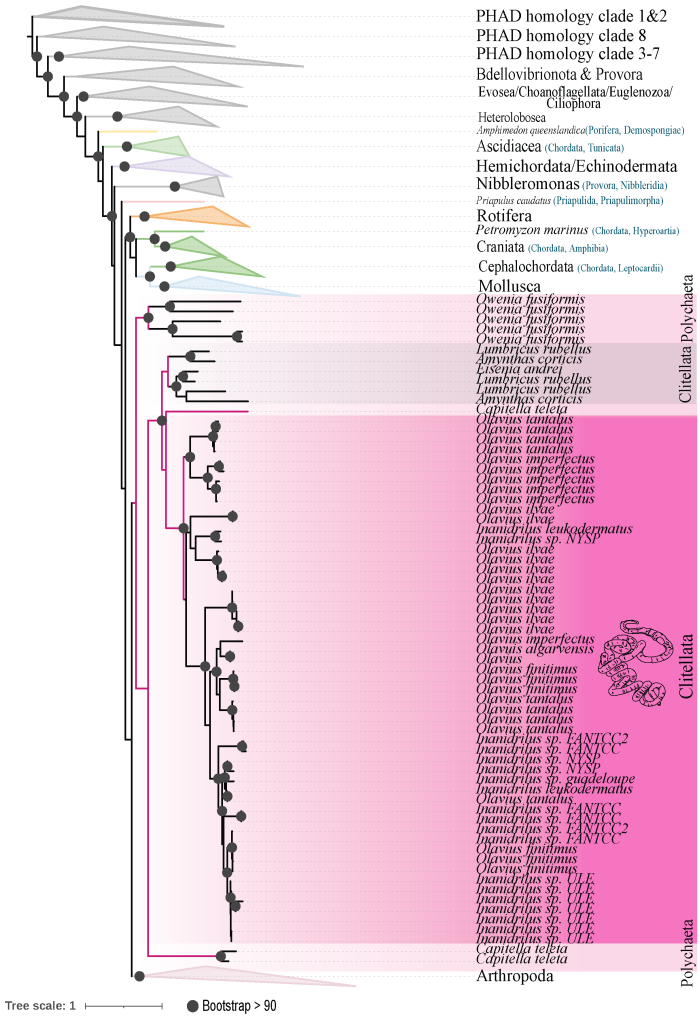

Supplementary Figure 16 | Annelids clustered closest to Arthropoda PHADs. Zoom in at the maximum likelihood tree (IQ TREE[28] using ultrafast bootstrap support) built from extracellular PHAD protein sequences showed that PHA degradation likely occurs across fungal, protist and animal lineages. The tree indicates that the newly discovered animal PHADs belong to the extracellular PHADs of domain type 2, which target the degradation of short chain PHAs. Gutless oligochaete PHADs grouped within the PHAD clade of Annelids closest to PHADs from earthworm species. Annelid PHADs grouped closest to Arthropod PHAD.

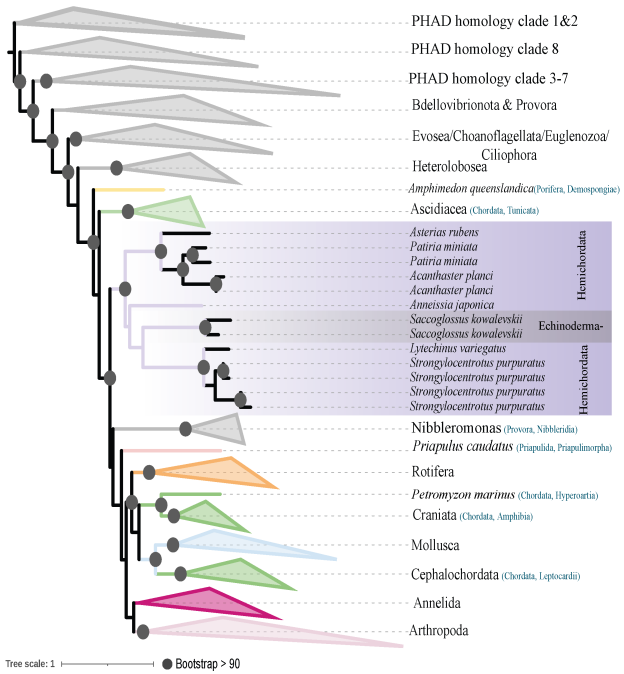

Supplementary Figure 17 | Echinodermata and Hemichordata PHADs grouped closest together according to their animals' phylogeny. Zoom in at the maximum likelihood tree (IQ TREE[28] using ultrafast bootstrap support) built from extracellular PHAD protein sequences showed that PHA degradation likely occurs across fungal, protist and animal lineages. The tree indicates that the newly discovered animal PHADs belong to the extracellular PHADs of domain type 2, which target the degradation of short chain PHAs. Echinodermata and Hemichordata grouped together according to their animal's phyla.

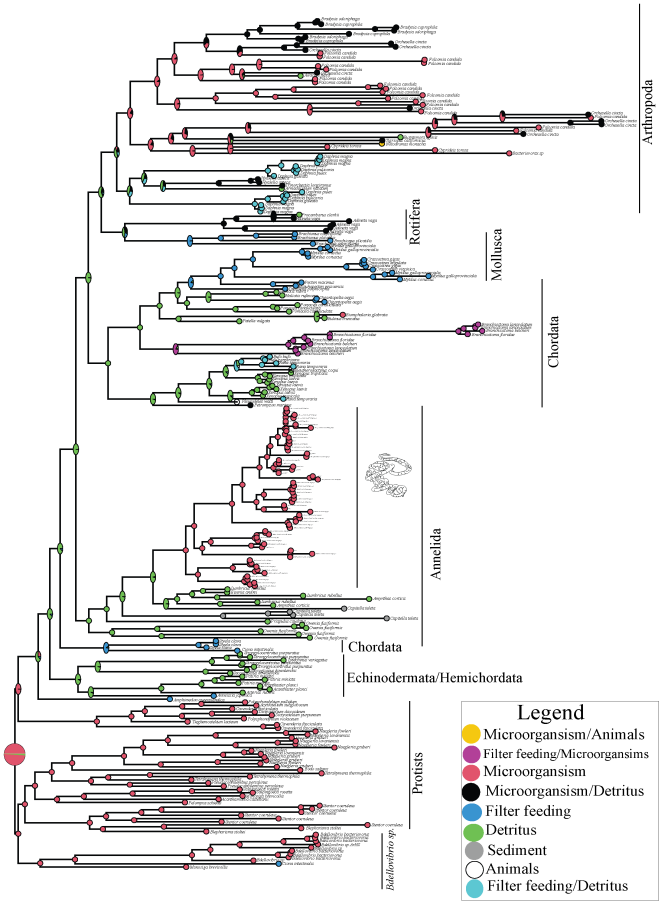

Supplementary Figure 18 | Ancestral state reconstruction of the feeding behavior of the metazoan species that retained a PHAD suggests that the LCA had a diet consisting of microorganisms and detritus. We analyzed the feeding behavior of all animals with a PHAD (Supplementary Table 2). We used these information and did an ancestral state reconstruction based on the R-package "phytools" (Revell, 2012)[29] using a tree of the animal PHAD clade. Based on the analysis, the last common ancestor of all animals is predicted to have a diet consisting of detritus and microorganisms. Animals might thus gain a nutritional advantage from PHA degradation.

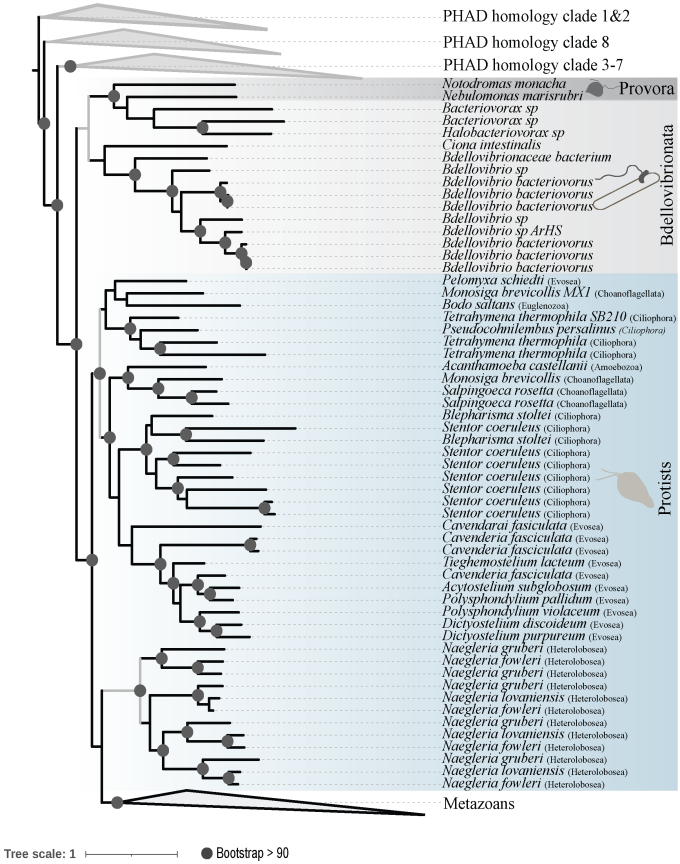

Supplementary Figure 19 | Zoom in at the protist and *Bdellovibrio* sp. PHAD clade. Zoom in at the maximum likelihood tree (IQ TREE[28] using ultrafast bootstrap support) built from extracellular PHAD protein sequences showed that PHA degradation likely occurs across fungal, protist and animal lineages. The tree indicates that the newly discovered animal PHADs belong to the extracellular PHADs of domain type 2, which target the degradation of short chain PHAs. Animal PHADs and protist PHADs formed a sister clade branching off from the *Bdellovibrio* sp. PHADs.

Supplementary Tables

Species	# ID	Prediction
Crassostrea virginica	XP0223435361 uncharacterized protein LOC111136736 Crassostrea virginica	SP
Eurytemora affinis	XP0233365361 uncharacterized protein LOC111707634 Eurytemora affinis	SP
Acanthaster planci	XP0221000541 uncharacterized protein LOC110984319 isoform X2 Acanthaster planci	OTHER
Branchiostoma belcheri	XP0196460321 PREDICTED uncharacterized protein LOC109481852 Branchiostoma belcheri	SP
Anneissia japonica	XP0331260901 uncharacterized protein LOC117124069 isoform X1 Anneissia japonica	SP
Notodromas monacha	CAD72760801 unnamed protein product Notodromas monacha	SP
Branchiostoma floridae	XP0356717041 uncharacterized protein LOC118412789 Branchiostoma floridae	SP
Branchiostoma lanceolatum	CAH12568581 Hypp1738 Branchiostoma lanceolatum	SP
Folsomia candida	XP0357041691 uncharacterized protein LOC110843519 Folsomia candida	SP
Gigantopelta aegis	XP0413718181 uncharacterized protein LOC121385275 isoform X2 Gigantopelta aegis	SP
Bulinus truncatus	KAH94948261 hypothetical protein Btru017926 Bulinus truncatus	SP
Asterias rubens	XP0336414871 uncharacterized protein LOC117301569 Asterias rubens	SP
Gigantopelta aegis	XP0413718171 uncharacterized protein LOC121385275 isoform X1 Gigantopelta aegis	OTHER
Saccoglossus kowalevskii	XP0068142251 PREDICTED uncharacterized protein LOC102801039 Saccoglossus kowalevskii	SP
Mytilus coruscus	CAC54199731 unnamed protein product Mytilus coruscus	SP
Mytilus coruscus	CAC54199721 unnamed protein product Mytilus coruscus	SP
Dreissena polymorpha	KAH37397521 hypothetical protein DPMN046439 Dreissena polymorpha	SP
Mizuhopecten yessoensis	XP0213546301 uncharacterized protein LOC110451096 Mizuhopecten yessoensis	SP
Pomacea canaliculata	XP0250834511 uncharacterized protein LOC112557674 Pomacea canaliculata	SP
Pecten maximus	XP0337318301 uncharacterized protein LOC117321514 Pecten maximus	SP
Pomacea canaliculata	PVD372561 hypothetical protein C0Q70042573 Pomacea canaliculata	OTHER
Xenopus laevis	XP0414437351 uncharacterized protein LOC121402065 Xenopus laevis	SP
Petromyzon marinus	XP0328277371 uncharacterized protein LOC116952466 Petromyzon marinus	SP
Rana temporaria	XP0402014831 uncharacterized protein LOC120932812 Rana temporaria	SP
Xenopus tropicalis	XP0029422974 uncharacterized protein LOC100498386 Xenopus tropicalis	SP
Xenopus laevis	XP0414439231 uncharacterized protein LOC108712601 Xenopus laevis	SP
Mytilus galloprovincialis	VDI220931 Hypothetical predicted protein Mytilus galloprovincialis	SP
Xenopus laevis	XP0414419481 uncharacterized protein LOC121401407 Xenopus laevis	SP
Daphnia magna	trA0A164WZR0A0A164WZR0ICRUS Uncharacterized protein OSDaphnia magna OX35525 GNAPZ42021101 PE4 SV1	SP
Crassostrea gigas	trK1QAX0K1QAX0CRAGI Uncharacterized protein OSCrassostrea gigas OX29159 GNCGI10026399 PE4 SV1	OTHER
Capitella teleta	trR7U3G8R7U3G8CAPTE Uncharacterized protein OSCapitella teleta OX283909 GNCAPTEDRAFT92319 PE4 SV1	OTHER
Olavius ilvae	LIBAE050521TRINITYDN10575c3g6i3p1	SP
Olavius ilvae	LIBAF050521TRINITYDN10541c3g6i1p1	SP
Olavius ilvae	LIBAF050521TRINITYDN10541c3g6i4p1	OTHER
Olavius ilvae	LIBK050521TRINITYDN9827c4g10i1p1	OTHER
Olavius ilvae	LIBL050521TRINITYDN4384c5g2i1p1	SP
Olavius ilvae	LIBL050521TRINITYDN4384c5g2i3p1	OTHER
Olavius ilvae	LIBL050521TRINITYDN4384c5g3i2p1	OTHER
Olavius ilvae	LIBM050521TRINITYDN7127c1g1i3p1	OTHER
Xenopus laevis	XP0414419491 uncharacterized protein LOC108710747 Xenopus laevis	SP
Rana temporaria	XP0402014811 uncharacterized protein LOC120932811 isoform X1 Rana temporaria	SP
Xenopus laevis	OCT862531 hypothetical protein XELAEV18019945mg Xenopus laevis	SP
Xenopus tropicalis	XP0317545241 uncharacterized protein LOC100497868 Xenopus tropicalis	SP
Rana temporaria	XP0402014841 uncharacterized protein LOC120932813 Rana temporaria	SP
Brachionus plicatilis	RNA003471 polyhydroxybutyrate depolymerase Brachionus plicatilis	SP
Pomacea canaliculata	XP0250834501 uncharacterized protein LOC112557673 Pomacea canaliculata	SP
Haliotis rubra	XP0465702621 uncharacterized protein LOC124278569 Haliotis rubra	SP
Haliotis rufescens	XP0463314541 uncharacterized protein LOC124114758 Haliotis rufescens	SP
Orchesella cincta	trA0A1D2MQU1A0A1D2MQU1ORCCI Poly3hydroxyalkanoate depolymerase C OSOrchesella cincta OX48709 GNOcin0111512 PE	SP
Branchiostoma belcheri	trA0A6P5AE26A0A6P5AE26BRABE uncharacterized protein LOC109481851 OSBranchiostoma belcheri OX7741 GNLOC109481	SP
Folsomia candida	trA0A226F4Z1A0A226F4Z1FOLCA Poly3hydroxyalkanoate depolymerase C OSFolsomia candida OX158441 GNFcan0100932 PE	OTHER
Tigriopus californicus	trA0A553NQ64A0A553NQ64TIGCA Uncharacterized protein Fragment OSTigriopus californicus OX6832 GNTCAL03306 PE4 SV	SP
Orchesella cincta	trA0A1D2NC91A0A1D2NC91ORCCI Poly3hydroxyalkanoate depolymerase C OSOrchesella cincta OX48709 GNOcin0103797 PE	SP
Orchesella cincta	trA0A1D2N7G8A0A1D2N7G8ORCCI Uncharacterized protein OSOrchesella cincta OX48709 GNOcin0105489 PE4 SV1	SP
Armadillidium nasatum	trA0A5N5SUW0A0A5N5SUW09CRUS Uncharacterized protein Fragment OSArmadillidium nasatum OX96803 GNAnas02819 PE4	OTHER
Folsomia candida	trA0A226F0F1A0A226F0F1FOLCA Uncharacterized protein OSFolsomia candida OX158441 GNFcan0101707 PE4 SV1	SP
Styela clava	XP0392699761 uncharacterized protein LOC120344730 Styela clava	SP
Owenia fusiformis	CAH17953251 unnamed protein product partial Owenia fusiformis	SP
Owenia fusiformis	CAH17997121 unnamed protein product Owenia fusiformis	SP
Saccoglossus kowalevskii	XP0027307001 PREDICTED uncharacterized protein LOC100371241 Saccoglossus kowalevskii	SP
Owenia fusiformis	CAH17804391 unnamed protein product Owenia fusiformis	SP
Daphnia pulicaria	XP0466566761 uncharacterized protein LOC124349832 Daphnia pulicaria	SP
Orchesella cincta	ODN050401 Poly3hydroxyalkanoate depolymerase C Orchesella cincta	SP
Amphimedon queenslandica	XP0033845101 PREDICTED uncharacterized protein LOC100634387 Amphimedon queenslandica	SP
Ciona intestinalis	XP0021192632 uncharacterized protein LOC100176456 Ciona intestinalis	SP
Bufo bufo	XP0402881601 uncharacterized protein LOC121001217 Bufo bufo	OTHER
Bufo gargarizans	XP0441334271 uncharacterized protein LOC122926106 Bufo gargarizans	SP
Trinorchestia longiramus	KAF23515371 AlphaBeta hydrolase fold partial Trinorchestia longiramus	OTHER
Daphnia pulex	XP0464543311 uncharacterized protein LOC124202104 Daphnia pulex	SP
Daphnia magna	XP0327956712 uncharacterized protein LOC116932060 Daphnia magna	SP
Bradysia odoriphaga	KAG40663391 hypothetical protein HA402000563 Bradysia odoriphaga	SP
Bradysia coprophila	XP0370453231 uncharacterized protein LOC119080854 Bradysia coprophila	SP
Branchiostoma floridae	trC3ZM4K3ZM4K4BRAFL Uncharacterized protein OSBranchiostoma floridae OX7739 GNBRAFLDRAFT97435 PE4 SV1	SP
Folsomia candida	trA0A226EBG7A0A226EBG7FOLCA Poly3hydroxyalkanoate depolymerase C OSFolsomia candida OX158441 GNFcan0110774 PE	OTHER
Folsomia candida	trA0A226F439A0A226F439FOLCA Poly3hydroxyalkanoate depolymerase C OSFolsomia candida OX158441 GNFcan0101153 PE4	SP
Ciona intestinalis	trF6Q4K1F6Q4K1CIOIN Uncharacterized protein OSCiona intestinalis OX7719 PE4 SV2	SP
Folsomia candida	XP0219489801 uncharacterized protein LOC118646509 Folsomia candida	SP
Biomphalaria glabrata	trA0A2C9LJM9A0A2C9LJM9BIOGL Uncharacterized protein OSBiomphalaria glabrata OX6526 GN106069061 PE4 SV1 PHAD	SP
Mytilus galloprovincialis	VDI072691 Hypothetical predicted protein Mytilus galloprovincialis	SP
Mytilus galloprovincialis	VDI557041 Hypothetical predicted protein Mytilus galloprovincialis	OTHER
Mytilus coruscus	CAC54165891 unnamed protein product Mytilus coruscus	SP
Mytilus galloprovincialis	VDI115391 Hypothetical predicted protein Mytilus galloprovincialis	SP
Capitella teleta	trR7T3BR7T3BCAPTE Uncharacterized protein OSCapitella teleta OX283909 GNCAPTEDRAFT207153 PE4 SV1	SP
Daphnia pulex	trE9G892E9G892DAPPU Uncharacterized protein OSDaphnia pulex OX6669 GNDAPPUDRAFT194537 PE4 SV1	SP
Daphnia pulex	trE9G893E9G893DAPPU Uncharacterized protein OSDaphnia pulex OX6669 GNDAPPUDRAFT99779 PE4 SV1	SP
Procambarus clarkii	MH1564341 Procambarus clarkii esterase PHB depolymerase mRNA partial cds	SP
Folsomia candida	trA0A226EXY5A0A226EXY5FOLCA Poly3hydroxyalkanoate depolymerase C OSFolsomia candida OX158441 GNFcan0102751 PE	SP
Orchesella cincta	trA0A1D2MDJ4A0A1D2MDJ4ORCCI Poly3hydroxyalkanoate depolymerase C OSOrchesella cincta OX48709 GNOcin0115604 PE	OTHER
Folsomia candida	trA0A226EK76A0A226EK76FOLCA Poly3hydroxyalkanoate depolymerase C OSFolsomia candida OX158441 GNFcan0107784 PE	SP
Folsomia candida	trA0A226ECK6A0A226ECK6FOLCA Poly3hydroxyalkanoate depolymerase C OSFolsomia candida OX158441 GNFcan0110652 PE	SP
Strongylocentrotus purpuratus	trW4YEN0W4YEN0STRPU Uncharacterized protein OSStrongylocentrotus purpuratus OX7668 PE4 SV1	OTHER
Capitella teleta	trR7U198R7U198CAPTE Uncharacterized protein Fragment OSCapitella teleta OX283909 GNCAPTEDRAFT107773 PE4 SV1	OTHER
Hyalella azteca	XP0180097071 PREDICTED uncharacterized protein LOC108667220 Hyalella azteca	SP
Hyalella azteca	XP0180099441 PREDICTED uncharacterized protein LOC108667432 Hyalella azteca	SP
Daphnia magna	XP0453065431 uncharacterized protein LOC116932059 Daphnia magna	SP
Daphnia galeata	CAH00985851 unnamed protein product Daphnia galeata	SP
Styela clava	XP0392698861 uncharacterized protein LOC120344660 isoform X1 Styela clava	SP
Orchesella cincta	trA0A1D2NSD0A0A1D2NSD0ORCCI Uncharacterized protein OSOrchesella cincta OX48709 GNOcin0106257 PE4 SV1	SP
Olavius finitimus	LibATRINITYDN2808c1g4i2p1	SP
Olavius finitimus	LIBATRINITYDN2808c1g1i6p1	OTHER
Olavius finitimus	LIBATRINITYDN2808c1g1i7p1	OTHER
Olavius finitimus	LIBATRINITYDN3916c0g3i10p1	SP
Inanidrilus sp. NYSP	LIBZINYSPTRINITYDN7352c0g2i4p1	SP
Olavius imperfectus	LIBACOimpTRINITYDN2799c0g2i12p1	OTHER
Olavius imperfectus	LIBACTRINITYDN2799c0g1i5p1	OTHER
Folsomia candida	XP0219531331 uncharacterized protein LOC110849958 Folsomia candida	OTHER
Daphnia galeata	CAH00985861 unnamed protein product Daphnia galeata	SP
Daphnia pulex	XP0464543301 poly3hydroxyalkanoate depolymerase Clike Daphnia pulex	SP
Daphnia pulicaria	XP0466567311 poly3hydroxyalkanoate depolymerase Clike Daphnia pulicaria	SP
Folsomia candida	XP0219683071 uncharacterized protein LOC110863333 Folsomia candida	SP
Daphnia magna	KZS137341 Uncharacterized protein APZ42021099 Daphnia magna	SP
Patiria miniata	XP0380662141 uncharacterized protein LOC119736247 Patiria miniata	SP
Cypridiels torosa	CAD72220771 unnamed protein product Cypridiels torosa	SP
Bradysia odoriphaga	KAG40681791 hypothetical protein HA402008820 Bradysia odoriphaga	SP
Bradysia coprophila	XP0370378691 uncharacterized protein LOC119075507 Bradysia coprophila	SP
Allacma fusca	CAG76840781 unnamed protein product Allacma fusca	SP
Orchesella cincta	trA0A1D2N0H2A0A1D2N0H2ORCCI Uncharacterized protein OSOrchesella cincta OX48709 GNOcin0107902 PE4 SV1	SP
Patiria miniata	XP0380652641 uncharacterized protein LOC119735575 Patiria miniata	SP

Bradysia coprophila	XP0370302231 poly3hydroxyalkanoate depolymerase Clike Bradysia coprophila	SP
Crassostrea gigas	XP0114183182 uncharacterized protein LOC105321645 Crassostrea gigas	SP
Acanthaster planci	XP0221000521 uncharacterized protein LOC110984319 isoform X1 Acanthaster planci	OTHER
Owenia fusiformis	CAH17791491 unnamed protein product Owenia fusiformis	SP
Owenia fusiformis	CAH17791521 unnamed protein product Owenia fusiformis	SP
Strongylocentrotus purpuratus	XP0308346661 uncharacterized protein LOC100888183 Strongylocentrotus purpuratus	SP
Olavius ilvae	LIBAF050521TRINITYDN10541c3g4i1p1	OTHER
Olavius ilvae	LIBAFOilvTRINITYDN11549c3g1i5p1 score6694 TRINITYDN11549c3g1i	SP
Strongylocentrotus purpuratus	XP0308341271 uncharacterized protein LOC100888362 isoform X2 Strongylocentrotus purpuratus	SP
Branchiostoma lanceolatum	CAH12568571 Hypp1737 Branchiostoma lanceolatum	SP
Folsomia candida	XP0219653091 uncharacterized protein LOC110860552 Folsomia candida	SP
Olavius tantalus	LIBETRINITYDN9281c1g1i1p1	OTHER
Olavius tantalus	LIBETRINITYDN9281c1g1i5p1	OTHER
Olavius tantalus	LIBCOtanTRINITYDN2759c0g1i3p1	OTHER
Olavius tantalus	LIBCTRINITYDN2886c0g1i44p1	OTHER
Olavius tantalus	LIBDOtanTRINITYDN8141c0g1i5p1	SP
Olavius tantalus	LIBDOtanTRINITYDN8119c0g1i2p1	SP
Olavius tantalus	LibDOtanTRINITYDN8119c0g1i1p1	SP
Olavius tantalus	LibDOtanTRINITYDN8141c0g1i4p1	SP
Inanidrilus leukodermatus	LIBQlleuTRINITYDN8853c0g8i7p1	OTHER
Inanidrilus sp. ULE	LIBTIspULETRINITYDN6378c1g4i13p1	OTHER
Strongylocentrotus purpuratus	trA0A7M7NBF9A0A7M7NBF9STRPU Uncharacterized protein OSStrongylocentrotus purpuratus OX7668 PE4 SV1	SP
Xenopus tropicalis	XP0040194973 uncharacterized protein LOC101732077 Xenopus tropicalis	OTHER
Adineta vaga	GSADVT00015692001 Adineta vaga	SP
Adineta vaga	GSADVT00046940001 Adineta vaga	SP
Adineta vaga	GSADVT00012128001 Adineta vaga	SP
Adineta vaga	GSADVT00009171001 Adineta vaga	SP
Adineta vaga	GSADVT00007586001 Adineta vaga	SP
Branchiostoma lanceolatum	BL03604evm3 Branchiostoma lanceolatum	OTHER
Inanidrilus sp. ULE	LIBTIspULETRINITYDN6792c0g2i2p1	OTHER
Inanidrilus sp. ULE	LIBUIspULETRINITYDN1596c0g1i3p1	OTHER
Inanidrilus sp. ULE	LIBTIspULETRINITYDN6792c0g2i5p1	OTHER
Inanidrilus sp. ULE	LIBTIspULETRINITYDN1596c0g1i2p1	OTHER
Inanidrilus sp. ULE	LIBUIspULETRINITYDN2171c0g2i17p1	OTHER
Inanidrilus sp. FANT	LIBYIspFANTTRINITYDN4112c0g6i6p1	SP
Inanidrilus sp. FANT	LIBYIspFANTTRINITYDN4388c2g2i1p1	SP
Inanidrilus sp. FANT	LIBYIspFANTTRINITYDN4292c0g2i20p1	OTHER
Inanidrilus sp. FANT	LIBYIspFANTTRINITYDN4292c0g2i15p1	OTHER
Olavuis algarvensis	LIBI050521TRINITYDN22120c0g1i1p1 TRINITYDN22120c0g1TRINITYDN22120c0g1i1p	SP
Styela clava	XP0392698571 uncharacterized protein LOC120344660 isoform X2 Styela clava	SP
Daphnia magna	XP0327956711 uncharacterized protein LOC116932060 Daphnia magna	SP
Brachionus calyciflorus	CAF09471221 unnamed protein product Brachionus calyciflorus	SP
Folsomia candida	XP0219618131 uncharacterized protein LOC110857529 Folsomia candida	OTHER
Brachiomas plicatilis	trA0A3M7PMK4A0A3M7PMK4BRAPC Poly3hydroxybutyrate depolymerase OSBrachionus plicatilis OX10195 GNBpHYR104674	SP
Folsomia candida	trA0A226EMS1A0A226EMS1FOLCA Uncharacterized protein OSFolsomia candida OX158441 GNFcan0108319 PE4 SV1	SP
Priapulus caudatus	XP0146755111 PREDICTED uncharacterized protein LOC106815555 Priapulus caudatus	SP
Cypridein torosa	CAD72320711 unnamed protein product Cypridein torosa	OTHER
Orchesella cincta	trA0A1D2MMN0A0A1D2MMN0ORCC1 Uncharacterized protein OSOrchesella cincta OX48709 GNOcin0112393 PE4 SV1	OTHER
Orchesella cincta	trA0A1D2MMV2A0A1D2MMV2ORCC1 Longchain fatty acid transport protein 6 OSOrchesella cincta OX48709 GNOcin0112392 PE	SP
Branchiostoma floridae	XP0356722801 uncharacterized protein LOC118413177 Branchiostoma floridae	OTHER
Bradysia coprophila	XP0370430601 uncharacterized protein LOC119079339 Bradysia coprophila	SP
Bradysia odoriphaga	KAG40767321 hypothetical protein HA402002019 Bradysia odoriphaga	OTHER
Olavius imperfectus	LIBFTRINITYDN5980c0g1i16p1	SP
Olavius imperfectus	LIBFTRINITYDN4635c1g3i1p1	SP
Brachionus calyciflorus	CAF07376411 unnamed protein product Brachionus calyciflorus	OTHER
Branchiostoma lanceolatum	BL22135evm0 Branchiostoma lanceolatum	OTHER
Olavius finitimus	Ofin1	OTHER
Olavius finitimus	Ofin2	SP
Olavius ilvae	Oilv2	SP
Daphnia magna	XP0327956701 uncharacterized protein LOC116932059 Daphnia magna	SP
Olavius imperfectus	LIBAIDOimpTRINITYDN5492c2g1i9p1	SP
Olavius imperfectus	LIBADTRINITYDN5492c2g1i1p1	OTHER
Lytechinus variegatus	XP0414709061 uncharacterized protein LOC121420369 Lytechinus variegatus	SP
Lumbricus rubellus	LRC090871 Lumbricus rubellus	OTHER
Lumbricus rubellus	C004821911 Lumbricus rubellus	SP
Lumbricus rubellus	LRP02794 1 Lumbricus rubellus	SP
Eisenia andrei	GWHPACBE025592_Eisenia andrei	SP
Patella vulgata	XP_0504418499.1 uncharacterized protein LOC126831890 _Patella vulgata_	SP
Crassostrea angulata	XP 052677101.1 uncharacterized protein LOC128158348 _Crassostrea angulata	OTHER
Branchiostoma belcheri	KAB518447.1 hypothetical protein Bbelb_044640 _Branchiostoma belcheri_	SP
Pleurodeles waltl	KAJ1165806.1 hypothetical protein NDU88_006223 _Pleurodeles waltl_	SP
Biomphalaria glabrata	XP 013084087.1 PREDICTED uncharacterized protein LOC106069061 Biomphalaria glabrata	SP
Amynthas corticis	GWHPAOSM011071.1 Amynthas corticis	SP
Amynthas corticis	GWHPAOSM008890.1 Amynthas corticis	SP

Supplementary Table 1 | Signal peptide prediction showed that almost all animals are predicted to have signal peptide. We used SignalP (Teufel et al., 2006)[6] to predict the signal peptide for the identified animal PHADs. 75% of the animal PHADs are predicted to have a signal peptide following the SecI pathway that allows their transport outside of the cell. The signal peptide is cleaved off usually before the 40's amino acid.

Animal	Phyla	Order	PHAD homol	Habitat	Habitat Citation	Feeding behavior
Amynthas corticis	Annelida	Crassiclitellata	2	Asian-Australasian soils	Wang et al.,2021	Leaf litter and soil
Eisenia andrei	Annelida	Crassiclitellata	1	Compost	Jager et al., 2003	Organic matter rich fraction soil
Lumbricus rubellus	Annelida	Crassiclitellata	3	Soil ecosystems	Greiner et al., 2012	Soil and litter
Inanidrilus leukodermatus	Annelida	Tubificida	3	Sediment; Marine habitat	Dubilier et al., 2006	Symbiont digestion; Milking for small molecules
Inanidrilus sp. FANT	Annelida	Tubificida	3	Sediment; Marine habitat	Dubilier et al., 2006	Symbiont digestion; Milking for small molecules
Inanidrilus sp. guadeloloupe	Annelida	Tubificida	1	Sediment; Marine habitat	Dubilier et al., 2006	Symbiont digestion; Milking for small molecules
Inanidrilus sp. NSSP	Annelida	Tubificida	2	Sediment; Marine habitat	Dubilier et al., 2006	Symbiont digestion; Milking for small molecules
Inanidrilus sp. ULE	Annelida	Tubificida	5	Sediment; Marine habitat	Dubilier et al., 2006	Symbiont digestion; Milking for small molecules
Olavius algarvensis	Annelida	Tubificida	1	Sediment; Marine habitat	Dubilier et al., 2006	Symbiont digestion; Milking for small molecules
Olavius finitimus	Annelida	Tubificida	4	Sediment; Marine habitat	Dubilier et al., 2006	Symbiont digestion; Milking for small molecules
Olavius ilvae	Annelida	Tubificida	5	Sediment; Marine habitat	Dubilier et al., 2006	Symbiont digestion; Milking for small molecules
Olavius imperfectus	Annelida	Tubificida	10	Sediment; Marine habitat	Dubilier et al., 2006	Symbiont digestion; Milking for small molecules
Inanidrilus reginae TC3	Annelida	Tubificida	1	Sediment; Marine habitat	Dubilier et al., 2006	Symbiont digestion; Milking for small molecules
Inanidrilus adunconsetis	Annelida	Tubificida	2	Sediment; Marine habitat	Dubilier et al., 2006	Symbiont digestion; Milking for small molecules
Inanidrilus scalprum	Annelida	Tubificida	4	Sediment; Marine habitat	Dubilier et al., 2006	Symbiont digestion; Milking for small molecules
Inanidrilus reginae TC2	Annelida	Tubificida	1	Sediment; Marine habitat	Dubilier et al., 2006	Symbiont digestion; Milking for small molecules
Inanidrilus reginae TC1	Annelida	Tubificida	1	Sediment; Marine habitat	Dubilier et al., 2006	Symbiont digestion; Milking for small molecules
Olavius tantulus	Annelida	Tubificida	5	Sediment; Marine habitat	Dubilier et al., 2006	Symbiont digestion; Milking for small molecules
Capitella teleta	Annelida	Sabellida	3	Organic enriched sediments	Blake et al., 2009	Deposit feeder
Oweniia fusiformis	Annelida	Sabellida	5	Buried in sand of marine habitats	Neal et al., 2008	Suspension feeder or deposit feeder
Daphnia galeata	Arthropoda	Diplostraca	2	Filter feeder of algea, bacteria, and detritus	Geller & Müller, 1981; Hadas et al., 1982; Porter, Orcutt & Gerritsen, 1983; Flössn	pelagic zone
Daphnia magna	Arthropoda	Diplostraca	6	Filter feeder of algea, bacteria, and detritus	Geller & Müller, 1981; Hadas et al., 1982; Porter, Orcutt & Gerritsen, 1983; Flössn	pelagic zone
Daphnia pulex	Arthropoda	Diplostraca	4	Filter feeder of algea, bacteria, and detritus	Geller & Müller, 1981; Hadas et al., 1982; Porter, Orcutt & Gerritsen, 1983; Flössn	pelagic zone
Daphnia pulicaria	Arthropoda	Diplostraca	2	Filter feeder of algea, bacteria, and detritus	Geller & Müller, 1981; Hadas et al., 1982; Porter, Orcutt & Gerritsen, 1983; Flössn	pelagic zone
Folsomia candida	Arthropoda	Entomobryomorpha	14	Soil insect	Klironomos & Ursic. 1998	Detritivores; Fungi
Orchesella cincta	Arthropoda	Entomobryomorpha	9	Surface organic layer soil	Verhoef et al., 1988	Fungi and algea
Allacma fusca	Arthropoda	Symphypleona	1	Moist terrestrial enviornments	https://en.wikipedia.org/wiki/Allacma_fusca#cite_note-Roehampton-3	Detritus
Eurytemora affinis	Arthropoda	Calanoida	1	coastal waters in the Northern hemisphere	Lee 2015	Filter feeding, Grazing, algea, ciliates
Tigriopus californicus	Arthropoda	Harpacticoida	1	High intertidal and supralittoral rock pools	Altermutt et al., 2012	Detritus and organic foos
Bradysia coprophila	Arthropoda	Diptera	4	forests, greenhouses and flower pots of ornamental plants; mushroom cellars	Shin et al., 2014; Harris et al., 1996	Green house plants; fungus
Bradysia odoriphaga	Arthropoda	Diptera	3	forests, greenhouses and flower pots of ornamental plants; mushroom cellars	Shin et al., 2014; Harris et al., 1996	Green house plants; fungus
Hyalella azteca	Arthropoda	Amphipoda	2	benthic sediments	Hargrave 1970	Sediments
Trinorchestia longiramus	Arthropoda	Amphipoda	1	sandy beaches	Pam et al., 2020	Algal ld and detritus biomass
Procambarus clarkii	Arthropoda	Decapoda	1	Swamps, sloughs and ditches in which it burrows	McDonald 1996	eating insect larvae, tadpoles, and snails, remains of dead animals and worms as well
Armadillidium nasatum	Arthropoda	Isopoda	1	Soil ecosystems	Rushton et al., 1983	Leaf litter and soil
Cyprideis torosa	Arthropoda	Podocopida	2	macrobenthos in brackish water and sediemnts	Heip, 1976	bottom sediments with bacterial-algal mats
Notodromas monacha	Arthropoda	Podocopida	1	Freshwater systems	Smith et al., 2014	Neusten feeder
Bufo bufo	Chordata	Anura	1	Terrestrial palaearctic	Crnobrnja-Isailov et al., 2012	Insects, and isopoda of terrestrial systems
Bufo gargarizans	Chordata	Anura	1	Terrestrial palaearctic	Crnobrnja-Isailov et al., 2012	Insects, and isopoda of terrestrial systems
Rana temporaria	Chordata	Anura	3	variety of freshwater habitats from ditches to temporary ponds and shallow lake shores	Fog & Schmedes de Lasson 1997; Piha *et al*. 2007	Insects; Arthanida, Isopods, Gastropods and Lumbricidae
Xenopus laevis	Chordata	Anura	5	stagnant, slow or even fastmoving water bodies	Picker, 1985	leftover plant material; smaller animals; digging trough mud to get to prey
Xenopus tropicalis	Chordata	Anura	3	stagnant, slow or even fastmoving water bodies	Picker, 1985	leftover plant material; smaller animals; digging trough mud to get to prey
Pleurodeles waltl	Chordata	Caudata	1	Aquatic: any standing water	https://www.caudata.org/cc/species/Pleurodeles/P_waltl.shtml	Opportunistic: invertebrates and small fish with carrion
Ciona intestinalis	Chordata	Phlebobranchia	2	attached to the eelgrass Zostera marine in coastal enviornments	Sugaganel et al., 2003	Suspension feeder
Styela clava	Chordata	Stolidobranchia	3	Marine habitat	Sonier et al., 2021	Filter feeder
Petromyzon marinus	Chordata	Petromyzontiformes	1	Aquatic	Silva et al.,2013	During metamophosis feeding on freshwater; hemiophagous feeding
Branchiostoma belcheri	Chordata	Amphioxiformes	2	Aquatic	Dennell, 2012	ciliary feeding enriched with detritus
Branchiostoma floridae	Chordata	Amphioxiformes	3	Aquatic	Dennell, 2012	ciliary feeding enriched with detritus
Branchiostoma lanceolatum	Chordata	Amphioxiformes	3	Aquatic	Dennell, 2012	ciliary feeding enriched with detritus
Asterias rubens	Echinodermata	Forcipulatida	1	Intertidal and subtidal population	Guillou et al., 2011	Unearth prey (eg mussels) from botting and then tube foed; infaunal benthos
Acanthaster planci	Echinodermata	Valvatida	2	Shallow coral reef	Benzie et al., 1994	Unearth prey (eg mussels) from botting and then tube foed; infaunal benthos
Patiria miniata	Echinodermata	Valvatida	2	Intertidal population	Schroeter et al., 1983	Unearth prey (eg mussels) from botting and then tube foed; infaunal benthos; bryozoans
Annenkia japonica	Echinodermata	Comatulida	1	Tropical western Atlantic and Indo-western Pacific; northeastern Atlantic; southern Australia and New Ze	Summers et al., 2014	Unearth prey (eg mussels) from botting and then tube foed; infaunal benthos; bryozoans
Strongylocentrotus purpuratus	Echinodermata	Camarodonta	4	Intertidal population	Cowie, 1972	Larvae unerdophytoplankiton; Adult herbivore grazes on algea and animals and catches floating debris
Lytechinus variegatus	Echinodermata	Temnopleuroida	1	hallow seagrass beds from the coast of North Carolina to Brazi	Watts et al., 2001	Grazing on seagrass beds; filamentous algae, sea grass epibionts, drift material, sand, shells, the mussel Modiolus americ
Saccoglossus kowalevskii	Hemichordata	-	2	marine sedimentary habitats,	Fielmann et al., 1999	Surface deposit feeder
Dreissena polymorpha	Mollusca	Mysida	1	Aquatic ecosystems	Zaiko et al., 2008	filtering suspended material
Mytilus corsicus	Mollusca	Mytilida	3	rocky intertidal zone patches	Hewatt 1935; Suchanek 1979, 1985; Tsuchiya 1979; Tsuchiya & Nishihira 198	Filter feeder
Mytilus galloprovincialis	Mollusca	Mytilida	4	rocky intertidal zone patches	Hewatt 1935; Suchanek 1979, 1985; Tsuchiya 1979; Tsuchiya & Nishihira 198	Filter feeder
Crassostrea angulata	Mollusca	Ostreida	1	Marine habitat	NA	Filter feeder
Crassostrea gigas	Mollusca	Ostreida	2	Marine habitat	NA	Filter feeder
Crassostrea virginica	Mollusca	Ostreida	1	Marine habitat	NA	Filter feeder
Mizuhopecten yessoensis	Mollusca	Pectinida	1	Marine habitat	Aya & Kudo, 2007	Detritus
Pecten maximus	Mollusca	Pectinida	1	Marine habitat	Manchais et al., 2015	phytoplankton diet
Biomphalaria glabrata	Mollusca	-	1	Freshwater systems	Duckloe et al., 1979	leaf litter and thus obtain bacterial population in their gut
Bulinus truncatus	Mollusca	-	1	Freshwater systems	Mandahl, Buth, 1957	plant, bacterial and decomposing organic materials
Gigantopelta aegis	Mollusca	-	2	Deep-sea hydrothermal vents	Copley et al., 2016	hemosymbionts for food,
Patella vulgata	Mollusca	-	1	Rocky shore associated intertidal zone	Schaal et al., 2015	Grazer
Pomacea canaliculata	Mollusca	Architaenioglossa	3	Freshwater systems	de Brito et al., 2016	polyphagous feeding habits
Haliotis rubra	Mollusca	Lepetellida	1	Aquatic ecosystems	Daume, 2006	Bacterial feeding as larvea; also macro and mercolgea food sources
Haliotis rufescens	Mollusca	Lepetellida	1	Aquatic ecosystems	Daume, 2006	Bacterial feeding as larvea; also macro and mercolgea food sources
Amphimalon queensladica	Porifera	Haplosclerida	1	Tropical coral reefs	Fieth et al., 2016	Harbors diverse microbial population; filter feeding
Priapulus candatus	Priapulida	Priapulimorphida	1	Marine habitat; burrowing in muds	Vannier et al. 2010; Sperling et al. 2013	Slow moving invertebrates
Adineta vaga	Rotifera	Adinetida	5	Transient pools where they experience periodic desiccation	Szydlowski et al., 2015	Plant and algal debris
Brachionus calyciflorus	Rotifera	Ploima	2	Freshwater, alkaline and brackish water	NA	Zooplankton (algae and bacteria) feeding
Brachionus plicatila	Rotifera	Ploima	2	Freshwater, alkaline and brackish water	NA	Zooplankton (algae and bacteria) feeding
Rotaria sp Silwood 1&2	Rotifera	Bdelloidea	8	most *Rotaria* have been recorded in aquatic habitats around the world	Donner1965	bacteria and fungi
Rotaria sordida	Rotifera	Bdelloidea	1	most *Rotaria* have been recorded in aquatic habitats around the world	Donner1965	bacteria and fungi
Rotaria magnacalcarata	Rotifera	Bdelloidea	2	most *Rotaria* have been recorded in aquatic habitats around the world	Donner1965	bacteria and fungi
Adineta ricciae	Rotifera	Adinetida	2	Transient pools where they experience periodic desiccation	Szydlowski et al., 2015	Plant and algal debris
Adineta steineri	Rotifera	Adinetida	2	Transient pools where they experience periodic desiccation	Szydlowski et al., 2015	Plant and algal debris

Supplementary Table 2 | We identified 82 animal PHADs that are all predicted to have access to PHA by their nutrition. Our database search resulted in the identification of 67 animal species with a PHAD and 15 gutless oligochaetes with a PHAD. Some of the animals, e.g. *Folsomia candida*, can have up to 14 PHAD copies. What all animals have in common is that they take up PHA with their nutrition.

Species	Phyla	Class	PHAD homologs
Salpingoeca rosetta	NA	Choanofagellata	2
Monosiga brevicollis	NA	Choanofagellata	2
Stentor coeruleus	Ciliophora	Heterotrichea	8
Tetrahymena thermophila	Ciliophora	Oligohymenophorea	3
Pseudocohnilembus persalinus	Ciliophora	Oligohymenophorea	1
Blepharisma stoltei	Ciliophora	Heterotrichea	3
Acanthamoeba castellanii	Discosea	NA	1
Bodo saltans	Eugelenozoa	Kinetoplastea	1
Cavenderia fasciculata	Evosea	Eumycetozoa	4
Polysphondylium pallidum	Evosea	Eumycetozoa	2
Polysphondylium violaceum	Evosea	Eumycetozoa	1
Tieghemostelium lacteum	Evosea	Eumycetozoa	2
Dictyostelium purpureum	Evosea	Eumycetozoa	3
Acytostelium subglobosum	Evosea	Eumycetozoa	1
Dictyostelium discoideum	Evosea	Eumycetozoa	1
Heterostelium album PN500	Evosea	Eumycetozoa	1
Pelomyxa schiedti	Evosea	NA	1
Naegleria gruberi	Heterolobosea	NA	5
Naegleria fowleri	Heterolobosea	NA	4
Naegleria lovaniensis	Heterolobosea	NA	3

Supplementary Table 3 | We identified 20 protist PHADs expanding the known diversity. Our database search resulted in the identification of 21 protist PHADs. Protist species can have up to five PHAD copies.

Species	Prediction	OTHER	SP(Sec/SPI)	CS Position
Salpingoeca rosetta	SP	0.000251	0.999708	CS pos: 21-22. Pr: 0.9767
Salpingoeca rosetta	SP	0.000019	0.999999	CS pos: 23-24. Pr: 0.9624
Monosiga brevicollis	SP	0.000238	0.999742	CS pos: 18-19. Pr: 0.9784
Monosiga brevicollis	SP	0.000235	0.999734	CS pos: 18-19. Pr: 0.9732
Stentor coeruleus	SP	0.007427	0.992545	CS pos: 14-15. Pr: 0.9490
Stentor coeruleus	SP	0.000230	0.999755	CS pos: 24-25. Pr: 0.9785
Stentor coeruleus	OTHER	0.535996	0.463990	
Stentor coeruleus	SP	0.000618	0.999344	CS pos: 12-13. Pr: 0.9653
Stentor coeruleus	SP	0.000253	0.999725	CS pos: 24-25. Pr: 0.9782
Stentor coeruleus	OTHER	0.520826	0.479171	
Stentor coeruleus	OTHER	0.520820	0.479165	
Stentor coeruleus	SP	0.000271	0.999722	CS pos: 16-17. Pr: 0.9751
Tetrahymena thermophila	SP	0.000230	0.999734	CS pos: 16-17. Pr: 0.9784
Tetrahymena thermophila	SP	0.000264	0.999725	CS pos: 18-19. Pr: 0.9793
Tetrahymena thermophila	SP	0.000342	0.999639	CS pos: 19-20. Pr: 0.9743
Tetrahymena thermophila	SP	0.001979	0.998027	CS pos: 18-19. Pr: 0.9522
Pseudocohnilembus persalinus	SP	0.000308	0.999654	CS pos: 22-23. Pr: 0.9767
Blepharisma stoltei	SP	0.000293	0.999692	CS pos: 17-18. Pr: 0.9675
Blepharisma stoltei	SP	0.002903	0.997046	CS pos: 32-33. Pr: 0.9662
Acanthamoeba castellanii	SP	0.000528	0.999446	CS pos: 18-19. Pr: 0.8709
Bodo saltans	OTHER	0.999892	0.000143	
Cavenderia fasciculata	OTHER	1.000040	0.000000	
Cavenderia fasciculata	OTHER	1.000047	0.000000	
Cavenderia fasciculata	OTHER	1.000043	0.000000	
Polysphondylium pallidum	SP	0.000197	0.999800	CS pos: 24-25. Pr: 0.9760
Polysphondylium violaceum	SP	0.107608	0.892349	CS pos: 28-29. Pr: 0.8127
Polysphondylium violaceum	SP	0.107608	0.892349	CS pos: 28-29. Pr: 0.8127
Tieghemostelium lacteum	SP	0.000225	0.999734	CS pos: 21-22. Pr: 0.9801
Tieghemostelium lacteum	SP	0.000225	0.999732	CS pos: 21-22. Pr: 0.9801
Dictyostelium purpureum	SP	0.000841	0.999136	CS pos: 22-23. Pr: 0.6989
Dictyostelium purpureum	SP	0.000841	0.999134	CS pos: 22-23. Pr: 0.6989
Acytostelium subglobosum	SP	0.000254	0.999719	CS pos: 29-30. Pr: 0.9129
Dictyostelium discoideum	OTHER	1.000029	0.000000	
Dictyostelium discoideum	OTHER	1.000029	0.000000	
Heterostelium album	SP	0.000197	0.999790	CS pos: 24-25. Pr: 0.9760
Pelomyxa schiedti	SP	0.282668	0.717314	CS pos: 63-64. Pr: 0.0013
Naegleria gruberi	SP	0.000207	0.999785	CS pos: 22-23. Pr: 0.9773
Naegleria gruberi	SP	0.000239	0.999745	CS pos: 24-25. Pr: 0.9783
Naegleria fowleri	OTHER	0.983603	0.016421	
Naegleria gruberi	SP	0.000695	0.999268	CS pos: 17-18. Pr: 0.9407
Naegleria fowleri	OTHER	1.000030	0.000015	
Naegleria fowleri	SP	0.033190	0.966773	CS pos: 25-26. Pr: 0.6590
Naegleria gruberi	SP	0.000256	0.999740	CS pos: 19-20. Pr: 0.9805
Naegleria lovaniensis	SP	0.000354	0.999620	CS pos: 25-26. Pr: 0.9779
Naegleria gruberi	SP	0.000189	0.999774	CS pos: 24-25. Pr: 0.9785
Naegleria lovaniensis	SP	0.000215	0.999772	CS pos: 24-25. Pr: 0.9746
Naegleria fowleri	OTHER	1.000035	0.000000	
Naegleria lovaniensis	OTHER	0.573103	0.426886	
Nibbleromonas arcticus	OTHER	0.999475	0.000559	
Nibbleromonas kosolapovi	OTHER	1.000035	0.000023	
Nebulomonas marisrubri	SP	0.035092	0.964888	CS pos: 32-33. Pr: 0.9312

Supplementary Table 4 | Most protist PHADs are predicted to be transported outside the cell to degrade PHA. We used SignalP (Teufel et al., 2006)[6] to predict the signal peptide for the identified protist PHADs. Most protist PHADs are predicted to have a signal peptide following the SecI pathway that allows their transport outside of the cell. The signal peptide is cleaved off usually before the 30's amino acid.

Library	Library type	Species	Extraction	Collection date	Collection place					Metadata			
				sampling_year	ocean	country	island_city	bay_spot	latitude	longitude	organic_input	sediment_type	water_depth
4514_AA	totalRNA	IregTC1	AllPrep DNA/RNA/Protein Mini Kit (modified)	2017	Atlantic	Belize	TwinCays	Fishersybeach	16,82356	-88,106	seagrass	sand	-1,5
4514_AB	totalRNA	IregTC3	AllPrep DNA/RNA/Protein Mini Kit (modified)	2017	Atlantic	Belize	TwinCays	Fishersybeach	16,82356	-88,106	seagrass	sand	-1
4514_AC	totalRNA	IregTC2	AllPrep DNA/RNA/Protein Mini Kit (modified)	2017	Atlantic	Belize	TwinCays	Fishersybeach	16,82356	-88,106	seagrass	sand	-1,5
4514_AD	totalRNA	IsaaCC1	AllPrep DNA/RNA/Protein Mini Kit (modified)	2017	Atlantic	Belize	CurlewCay	a_unknown	16,790105	-88,082	corals	sand	-2
4514_AE	totalRNA	IsaaCC2	AllPrep DNA/RNA/Protein Mini Kit (modified)	2017	Atlantic	Belize	CurlewCay	a_unknown	16,790105	-88,082	corals	sand	-2
4514_AF	totalRNA	IsaaCC3	AllPrep DNA/RNA/Protein Mini Kit (modified)	2017	Atlantic	Belize	CurlewCay	a_unknown	16,790105	-88,082	corals	sand	-2
4514_AG	totalRNA	IspNYSPCC1	AllPrep DNA/RNA/Protein Mini Kit (modified)	2017	Atlantic	Belize	CurlewCay	a_unknown	16,79	-88,083	a_unknown	sand	-1,5
4514_AH	totalRNA	IspNYSPCC2	AllPrep DNA/RNA/Protein Mini Kit (modified)	2017	Atlantic	Belize	CurlewCay	a_unknown	16,790105	-88,082	corals	sand	-2
4514_AI	totalRNA	IspINYSPCC3	AllPrep DNA/RNA/Protein Mini Kit (modified)	2017	Atlantic	Belize	CurlewCay	a_unknown	16,790135	-88,082	a_unknown	coral_sand	-2
4514_AJ	totalRNA	IspFANTCC3	AllPrep DNA/RNA/Protein Mini Kit (modified)	2017	Atlantic	Belize	CurlewCay	a_unknown	16,790105	-88,082	corals	sand	-2
4514_AK	totalRNA	IspFANTCC2	AllPrep DNA/RNA/Protein Mini Kit (modified)	2017	Atlantic	Belize	CurlewCay	a_unknown	16,790105	-88,082	corals	sand	-2
4514_AL	totalRNA	IspFANTCC1	AllPrep DNA/RNA/Protein Mini Kit (modified)	2017	Atlantic	Belize	CurlewCay	a_unknown	16,790135	-88,082	a_unknown	coral_sand	-2
4514_AM	totalRNA	IspULECC1	AllPrep DNA/RNA/Protein Mini Kit (modified)	2017	Atlantic	Belize	CurlewCay	a_unknown	16,790105	-88,082	corals	sand	-2
4514_AN	totalRNA	OimpSWC1	AllPrep DNA/RNA/Protein Mini Kit (modified)	2017	Atlantic	Belize	SouthwaterCaye	a_unknown	16,823715	-88,081	seagrass_algal_j	sand	-8
4514_AO	totalRNA	OimpSWC2	AllPrep DNA/RNA/Protein Mini Kit (modified)	2017	Atlantic	Belize	SouthwaterCaye	a_unknown	16,823715	-88,081	seagrass_algal_j	sand	-8
4514_AP	totalRNA	OimpSWC3	AllPrep DNA/RNA/Protein Mini Kit (modified)	2017	Atlantic	Belize	SouthwaterCaye	a_unknown	16,826195	-88,081	seagrass	sand	-1,5
4514_AQ	totalRNA	IspNYSP	AllPrep DNA/RNA/Protein Mini Kit (modified)	2017	Atlantic	Belize	CarnelBowCaye	a_unknown	16,8254	-88,08	seagrass	sand	-2
4514_AR	totalRNA	IspNYSP	AllPrep DNA/RNA/Protein Mini Kit (modified)	2017	Atlantic	Belize	CarnelBowCaye	a_unknown	16,8254	-88,08	seagrass	sand	-2
4514_AS	totalRNA	IspNYSPCBC1	AllPrep DNA/RNA/Protein Mini Kit (modified)	2017	Atlantic	Belize	CarnelBowCaye	a_unknown	a_unknown	a_unknown	a_unknown	sand	a_unknown
4514_M	totalRNA	IadaCC1	AllPrep DNA/RNA/Protein Mini Kit (modified)	2017	Atlantic	Belize	CurlewCay	a_unknown	16,790105	-88,082	corals	sand	-2
4514_N	totalRNA	IadaCC3	AllPrep DNA/RNA/Protein Mini Kit (modified)	2017	Atlantic	Belize	CurlewCay	a_unknown	16,790105	-88,082	corals	sand	-2
4514_O	totalRNA	IadaCC2	AllPrep DNA/RNA/Protein Mini Kit (modified)	2017	Atlantic	Belize	CurlewCay	a_unknown	16,790105	-88,082	corals	sand	-2
4514_P	totalRNA	IleaCBC2	AllPrep DNA/RNA/Protein Mini Kit (modified)	2017	Atlantic	Belize	CarnelBowCaye	a_unknown	16,8025	-88,082	seagrass	sand	a_unknown
4514_Q	totalRNA	IleaCBC3	AllPrep DNA/RNA/Protein Mini Kit (modified)	2017	Atlantic	Belize	CarnelBowCaye	a_unknown	a_unknown	a_unknown	a_unknown	sand	a_unknown
4514_R	totalRNA	IleaCBC4	AllPrep DNA/RNA/Protein Mini Kit (modified)	2017	Atlantic	Belize	CarnelBowCaye	a_unknown	a_unknown	a_unknown	seagrass	sand	-1
4514_S	totalRNA	IleaCC2	AllPrep DNA/RNA/Protein Mini Kit (modified)	2017	Atlantic	Belize	CurlewCay	a_unknown	16,790105	-88,082	corals	sand	-2
4514_T	totalRNA	IleaCC1	AllPrep DNA/RNA/Protein Mini Kit (modified)	2017	Atlantic	Belize	CurlewCay	a_unknown	16,790105	-88,082	corals	sand	-2
4514_U	totalRNA	IleaBEL2	AllPrep DNA/RNA/Protein Mini Kit (modified)	2017	Atlantic	Belize	CurlewCay	a_unknown	16,79	-88,083	a_unknown	sand	-1,5
4514_V	totalRNA	IleaSWC2	AllPrep DNA/RNA/Protein Mini Kit (modified)	2017	Atlantic	Belize	SouthwaterCaye	a_unknown	16,8265	-88,081	seagrass	sand	-2
4514_W	totalRNA	IleaSWC1	AllPrep DNA/RNA/Protein Mini Kit (modified)	2017	Atlantic	Belize	SouthwaterCaye	a_unknown	16,826195	-88,081	seagrass	sand	-1,5
4514_X	totalRNA	IleaBEL1	AllPrep DNA/RNA/Protein Mini Kit (modified)	2017	Atlantic	Belize	SouthwaterCaye	a_unknown	16,826195	-88,081	seagrass_algal_j	sand	-1,5
4514_Y	totalRNA	IleaTC1	AllPrep DNA/RNA/Protein Mini Kit (modified)	2017	Atlantic	Belize	TwinCays	a_unknown	16,831375	-88,108	seagrass	sand	-1,5
4514_Z	totalRNA	IleaTC	AllPrep DNA/RNA/Protein Mini Kit (modified)	2017	Atlantic	Belize	TwinCays	a_unknown	16,831375	-88,108	seagrass	sand	-1,5
4515_A	totalRNA	*Ispguadeloupe*	AllPrep DNA/RNA Micro Kit	a_unknown	Atlantic	Guadeloupe	IleCohon	a_unknown	16,215238	-61,537	seagrass	a_unknown	a_unknown
4515_B	totalRNA	*Ispguadeloupe*	AllPrep DNA/RNA Micro Kit	a_unknown	Atlantic	Guadeloupe	IleCohon	a_unknown	16,215238	-61,537	seagrass	a_unknown	a_unknown
4515_C	totalRNA	*Ispguadeloupe*	AllPrep DNA/RNA Micro Kit	a_unknown	Atlantic	Guadeloupe	IleCohon	a_unknown	16,215238	-61,537	seagrass	a_unknown	a_unknown
4515_D	totalRNA	*a_unknown*	AllPrep DNA/RNA Micro Kit	2015	Atlantic	Bermuda	a_unknown	HarringtonSound	a_unknown	a_unknown	a_unknown	a_unknown	a_unknown
4515_E	totalRNA	*Ileakodermatus*	AllPrep DNA/RNA Micro Kit	2015	Atlantic	Bermuda	a_unknown	HarringtonSound	a_unknown	a_unknown	a_unknown	a_unknown	a_unknown
4515_F	totalRNA	*Ileakodermatus*	AllPrep DNA/RNA Micro Kit	2015	Atlantic	Bermuda	a_unknown	HarringtonSound	a_unknown	a_unknown	a_unknown	a_unknown	a_unknown
4515_G	totalRNA	*O. ilsae*	AllPrep DNA/RNA Micro Kit	2017	Mediterranean	Italy	Elba	SantAndrea	-42,808183	10,1429	seagrass	silicate_sand	-6
4515_H	totalRNA	*O. ilsae*	AllPrep DNA/RNA Micro Kit	2017	Mediterranean	Italy	Elba	SantAndrea	-42,808183	10,1429	seagrass	silicate_sand	-6
4515_I	totalRNA	*O. ilsae*	AllPrep DNA/RNA Micro Kit	2017	Mediterranean	Italy	Elba	SantAndrea	-42,808183	10,1429	seagrass	silicate_sand	-6
4515_J	totalRNA	*I. leukodermatus*	AllPrep DNA/RNA Micro Kit	2017	Atlantic	Belize	TwinCays	a_unknown	16,831375	-88,108	seagrass	coral_sand	1,5
4515_K	totalRNA	*IspULE*	AllPrep DNA/RNA Micro Kit	2017	Atlantic	Belize	CurlewCay	a_unknown	16,790105	-88,082	corals	coral_sand	2
4515_L	totalRNA	*IspULE*	AllPrep DNA/RNA Micro Kit	2017	Atlantic	Belize	CurlewCay	a_unknown	16,790105	-88,082	corals	coral_sand	2
4731_A_662	totalRNA	*O. algarvensis*	AllPrep DNA/RNA/ATProtein Mini kit	2020	Mediterranean	Italy	Elba	SantAndrea	-42,808183	10,1429	seagrass	silicate_sand	-6
4731_A_665	totalRNA	*O. algarvensis*	AllPrep DNA/RNA/ATProtein Mini kit	2020	Mediterranean	Italy	Elba	SantAndrea	-42,808183	10,1429	seagrass	silicate_sand	-6
4731_B_662	totalRNA	*O. algarvensis*	AllPrep DNA/RNA/ATProtein Mini kit	2020	Mediterranean	Italy	Elba	SantAndrea	-42,808183	10,1429	seagrass	silicate_sand	-6
4731_B_665	totalRNA	*O. algarvensis*	AllPrep DNA/RNA/ATProtein Mini kit	2020	Mediterranean	Italy	Elba	SantAndrea	-42,808183	10,1429	seagrass	silicate_sand	-6
4731_C_662	totalRNA	*O. algarvensis*	AllPrep DNA/RNA/ATProtein Mini kit	2020	Mediterranean	Italy	Elba	SantAndrea	-42,808183	10,1429	seagrass	silicate_sand	-6
4731_C_665	totalRNA	*O. algarvensis*	AllPrep DNA/RNA/ATProtein Mini kit	2020	Mediterranean	Italy	Elba	SantAndrea	-42,808183	10,1429	seagrass	silicate_sand	-6
4731_D_662	totalRNA	*O. algarvensis*	AllPrep DNA/RNA/ATProtein Mini kit	2020	Mediterranean	Italy	Elba	SantAndrea	-42,808183	10,1429	seagrass	silicate_sand	-6
4731_D_665	totalRNA	*O. algarvensis*	AllPrep DNA/RNA/ATProtein Mini kit	2020	Mediterranean	Italy	Elba	SantAndrea	-42,808183	10,1429	seagrass	silicate_sand	-6
4731_E_662	totalRNA	*O. algarvensis*	AllPrep DNA/RNA/ATProtein Mini kit	2020	Mediterranean	Italy	Elba	SantAndrea	-42,808183	10,1429	seagrass	silicate_sand	-6
4731_E_665	totalRNA	*O. algarvensis*	AllPrep DNA/RNA/ATProtein Mini kit	2020	Mediterranean	Italy	Elba	SantAndrea	-42,808183	10,1429	seagrass	silicate_sand	-6
4731_F_662	totalRNA	*O. algarvensis*	AllPrep DNA/RNA/ATProtein Mini kit	2020	Mediterranean	Italy	Elba	SantAndrea	-42,808183	10,1429	seagrass	silicate_sand	-6
4731_F_665	totalRNA	*O. algarvensis*	AllPrep DNA/RNA/ATProtein Mini kit	2020	Mediterranean	Italy	Elba	SantAndrea	-42,808183	10,1429	seagrass	silicate_sand	-6
4732.A	polyA	*Olavius finitimus*	AllPrep DNA/RNA/Protein Mini Kit (modified)	2017	Atlantic	Belize	TwinCays	Fishersybeach	a_unknown	a_unknown	a_unknown	a_unknown	a_unknown
4732.B	polyA	*Olavius finitimus*	AllPrep DNA/RNA/Protein Mini Kit (modified)	2017	Atlantic	Belize	CurlewCay	a_unknown	16,790105	-88,082	corals	sand	-2
4732.C	polyA	*Olavius tantalus*	AllPrep DNA/RNA/Protein Mini Kit (modified)	2017	Atlantic	Belize	CarnelBowCaye	a_unknown	a_unknown	a_unknown	seagrass	sand	-1
4732.D	polyA	*Olavius tantalus*	AllPrep DNA/RNA/Protein Mini Kit (modified)	2017	Atlantic	Belize	TwinCays	Fishersybeach	a_unknown	a_unknown	a_unknown	a_unknown	a_unknown
4732.E	polyA	*Olavius tantalus*	AllPrep DNA/RNA/Protein Mini Kit (modified)	2017	Atlantic	Belize	TwinCays	Fishersybeach	a_unknown	a_unknown	a_unknown	a_unknown	a_unknown
4732.F	polyA	*Olavius imperfectus*	AllPrep DNA/RNA/Protein Mini Kit (modified)	2017	Atlantic	Belize	CarnelBowCaye	a_unknown	a_unknown	a_unknown	seagrass	sand	-1
4732.G	polyA	*Olavius imperfectus*	AllPrep DNA/RNA/Protein Mini Kit (modified)	2017	Atlantic	Belize	TwinCays	a_unknown	16,831375	-88,108	seagrass	sand	-1,5
4732.H	polyA	*Olavius algarvensis*	AllPrep DNA/RNA Micro Kit	2020	Mediterranean	Italy	Elba	SantAndrea	-42,808183	10,1429	seagrass	silicate_sand	-6
4732.I	polyA	*Olavius algarvensis*	AllPrep DNA/RNA Micro Kit	2020	Mediterranean	Italy	Elba	SantAndrea	-42,808183	10,1429	seagrass	silicate_sand	-6
4732.J	polyA	*Olavius algarvensis*	AllPrep DNA/RNA Micro Kit	2020	Mediterranean	Italy	Elba	SantAndrea	-42,808183	10,1429	seagrass	silicate_sand	-6
4732.K	polyA	*Olavius ilvae*	AllPrep DNA/RNA Micro Kit	2020	Mediterranean	Italy	Elba	SantAndrea	-42,808183	10,1429	seagrass	silicate_sand	-6
4732.L	polyA	*Olavius ilvae*	AllPrep DNA/RNA Micro Kit	2020	Mediterranean	Italy	Elba	SantAndrea	-42,808183	10,1429	seagrass	silicate_sand	-6
4732.M	polyA	*Olavius ilvae*	AllPrep DNA/RNA Micro Kit	2020	Mediterranean	Italy	Elba	SantAndrea	-42,808183	10,1429	seagrass	silicate_sand	-6
4732.N	polyA	*Inanidrilus sp. guadeloupe*	AllPrep DNA/RNA Micro Kit	a_unknown	a_unknown	a_unknown	a_unknown	a_unknown	a_unknown	unknown	a_unknown	a_unknown	a_unknown

4732.O	polyA	*Inaniidrilus sp. guadeloupe*	AllPrep DNA/RNA Micro Kit	a_unknown	a_unknown	a_unknown	a_unknown	a_unknown	a_unknown	unknown	a_unknown	a_unknown	a_unknown		
4732.P	polyA	*Inaniidrilus sp. guadeloupe*	AllPrep DNA/RNA Micro Kit	a_unknown	a_unknown	a_unknown	a_unknown	a_unknown	a_unknown	unknown	a_unknown	a_unknown	a_unknown		
4732.Q	polyA	*Inaniidrilus leukodermatus*	AllPrep DNA/RNA Micro Kit	2015	Atlantic	Bermuda	a_unknown	HarringtonSound	a_unknown	a_unknow	a_unknown	a_unknown	a_unknown		
4732.R	polyA	*Inaniidrilus leukodermatus*	AllPrep DNA/RNA Micro Kit	2015	Atlantic	Bermuda	a_unknown	HarringtonSound	a_unknown	a_unknow	a_unknown	a_unknown	a_unknown		
4732.S	polyA	*Inaniidrilus leukodermatus*	AllPrep DNA/RNA Micro Kit	2017	Atlantic	Belize	TwinCays	a_unknown	16,831375	-88,108	seagrass	coral_sand		1,5	
4732.T	polyA	*Inaniidrilus sp. ULE*	AllPrep DNA/RNA Micro Kit	2017	Atlantic	Belize	CurlewCay	a_unknown	16,790105	-88,082	corals	sand		-2	
4732.U	polyA	*Inaniidrilus sp. ULE*	AllPrep DNA/RNA Micro Kit	2017	Atlantic	Belize	CurlewCay	a_unknown	16,790105	-88,082	corals	sand		-2	
4732.V	polyA	*Inaniidrilus leukodermatusTC1*	AllPrep DNA/RNA/Protein Mini Kit (modified)	2017	Atlantic	Belize	TwinCays	a_unknown	16,831375	-88,108	seagrass	sand		-1,5	
4732.W	polyA	*Inaniidrilus leukodermatusTC*	AllPrep DNA/RNA/Protein Mini Kit (modified)	2017	Atlantic	Belize	TwinCays	a_unknown	16,831375	-88,108	seagrass	sand		-1,5	
4732.X	polyA	*Inaniidrilus sp. FANTCC3*	AllPrep DNA/RNA/Protein Mini Kit (modified)	2017	Atlantic	Belize	CurlewCay	a_unknown	16,790105	-88,082	corals	sand		-2	
4732.Y	polyA	*Inaniidrilus sp. FANTCC2*	AllPrep DNA/RNA/Protein Mini Kit (modified)	2017	Atlantic	Belize	CurlewCay	a_unknown	16,790105	-88,082	corals	sand		-2	
4732.Z	polyA	*Inaniidrilus sp. NYSP*	AllPrep DNA/RNA/Protein Mini Kit (modified)	2017	April	CentralAmerica	Belize	CarrieBowCaye	a_unknown	a_unknow	a_unknown	a_unknown	sand		
4732.AA	polyA	*Inaniidrilus sp. NYSP*	AllPrep DNA/RNA/Protein Mini Kit (modified)	2017	April	CentralAmerica	Belize	CarrieBowCaye	a_unknown	a_unknow	a_unknown	a_unknown	sand		
4732.AB	polyA	*Olavius imperfectus*	AllPrep DNA/RNA/Protein Mini Kit (modified)	2017	Atlantic	Belize	SouthwaterCaye	a_unknown	16,8265	-88,081	seagrass	sand		-2	
4732.AC	polyA	*Olavius imperfectus*	AllPrep DNA/RNA/Protein Mini Kit (modified)	2017	Atlantic	Belize	SouthwaterCaye	a_unknown	16,8265	-88,081	seagrass	sand		-2	
4732.AD	polyA	*Olavius imperfectus*	AllPrep DNA/RNA/Protein Mini Kit (modified)	2017	Atlantic	Belize	TwinCays. Northw	a_unknown	a_unknown	a_unknow	a_unknown	a_unknown	a_unknown		
4732.AE	polyA	*Olavius ilvae*	AllPrep DNA/RNA Micro Kit	2020	Mediterranean	Italy	Elba	SantAndrea	-42,808183	10,1429	seagrass	silicate_sand		-6	
4732.AF	polyA	*Olavius ilvae*	AllPrep DNA/RNA Micro Kit	2020	Mediterranean	Italy	Elba	SantAndrea	-42,808183	10,1429	seagrass	silicate_sand		-6	
4732.AG	polyA	*Olavius ilvae*	AllPrep DNA/RNA Micro Kit	2020	Mediterranean	Italy	Elba	SantAndrea	-42,808183	10,1429	seagrass	silicate_sand		-6	

Library	Reads	Coverage [Mb]	Assembly quality Total trinity 'genes	Total trinity transcripts	GC	Median contig length	Average contig	total assembled bases	N50	BUSCO (%) Complete BUSCOs	Complete and single-copy BUSCOs	Complete and duplicated BUSCOs
4514_AA	25830295	5247,621024	33938	56536	49,22	339	395,17	22341490	416	5,7	3,7	2
4514_AB	25047923	5088,676198	50559	80930	48,3	348	404,48	32734915	429	11,1	7,5	3,6
4514_AC	24499337	4977,226777	43238	72690	48,04	347	407,75	29639279	433	7	4,7	2,3
4514_AD	28024869	5693,465435	62376	100405	48,54	346	401,92	40355277	426	10,8	7,7	3,1
4514_AE	24153563	4906,980157	83754	131511	46,69	366	429,88	56534170	464	18,9	13,4	5,5
4514_AF	23668423	4808,420274	74042	119929	46,73	362	428,83	51428679	462	16,7	12,7	4
4514_AG	26120295	5306,536732	64470	105013	47,91	344	407,8	42824198	434	15,5	11,5	4
4514_AH	23783308	4831,760036	45576	63850	47,95	351	426,22	27214053	457	12,1	10,5	1,6
4514_AI	24832955	5045,003813	91375	144892	46,78	332	394,57	57169405	415	19,6	15,1	4,5
4514_AJ	23521018	4778,473826	56939	94193	48,77	342	396,8	37375887	417	11,4	9,3	2,1
4514_AK	22405251	4551,797268	55031	89220	49,49	353	414,47	36978713	442	11,6	7,7	3,9
4514_AL	32969226	6697,949192	71981	119080	47,66	341	397,07	47283514	419	10,9	9	1,9
4514_AM	22691441	4609,938944	54992	87083	47,64	345	397,01	34573003	420	13,2	8,7	4,5
4514_AN	34425514	6993,805183	45271	7896	45,62	355	422,02	33000020	453	7,5	5,9	1,6
4514_AO	23265770	4726,618252	43059	72268	46,35	362	429,67	31051616	463	9,3	6,5	2,8
4514_AP	29856064	6065,486637	30630	44690	46,2	382	447,83	20013714	486	13,5	10,8	2,7
4514_AQ	23802716	4835,702919	104933	162589	46,71	338	409,9	66644619	436	23,7	18,9	4,8
4514_AR	25747030	5230,705106	81588	135660	47,02	331	385,93	52355901	407	12	9,2	2,8
4514_AS	25426640	5165,615439	100298	162321	47,1	338	404,22	65614046	429	20,5	15,5	5
4514_M	24987160	5076,331732	68151	110875	47,29	352	413,82	45882346	443	13,9	11,1	2,8
4514_N	25279506	5135,724047	52468	88403	48,2	355	418,2	36970332	448	12	9,3	2,7
4514_O	26588436	5401,643139	82862	134460	47,6	361	434,54	58428731	471	21,1	16,2	4,9
4514_P	23568880	4788,197355	57248	89184	48,65	345	409,92	36558491	437	14,7	12,2	2,5
4514_Q	25232255	5126,124647	50822	80599	48,71	347	411,72	33184496	437	14,4	11	3,4
4514_R	25945968	5271,120875	102822	158291	46,33	364	436,42	69080787	473	25,9	20,6	5,3
4514_S	24064672	4888,921274	58856	92874	49,12	345	400,15	37163410	424	12,9	9,1	3,8
4514_T	22664047	4604,373645	46324	73376	48,4	348	403,65	29618014	429	9,5	5,7	3,8
4514_U	22391399	4548,983128	18705	26109	51,36	346	418,47	10925798	446	6,8	5,5	1,3
4514_V	24296326	4935,983547	87569	138623	47,08	333	392,34	54387256	414	15,4	11,4	4
4514_W	24514492	4980,30563	51350	82984	48,6	344	408,45	33894937	432	13,5	11	2,5
4514_X	22308173	4532,075133	43896	72195	48,8	352	413,33	29840083	443	11	8,1	2,9
4514_Y	28899666	5871,187104	28405	37850	49,68	342	425,13	16091094	452	8	6,3	1,7
4514_Z	26115144	5305,490267	26128	41134	48,66	335	381,5	15692695	399	5,5	4,1	1,4
4515_A	32257284	6553,312756	113190	197615	46,26	304	351,99	67922778	348	11,6	7,9	3,7
4515_B	23044753	4681,716966	92763	156044	45,86	305	345,16	53859425	351	9,2	7,2	2
4515_C	24484477	4974,207855	98342	173245	45,57	296	332,93	57678845	336	8,1	5,5	2,6
4515_D	23396934	4753,265217	92762	151671	46,26	387	468,8	71102997	519	29,8	21,7	8,1
4515_E	34990407	7108,567495	148788	242946	47,06	366	465,79	113161685	518	48,5	33,2	15,2
4515_F	23788274	4832,768916	108599	168726	47,45	363	452,63	76369939	498	40,8	30,5	10,3
4515_G	32986255	6701,408763	76281	90565	49,18	292	425,38	38524346	430	20,3	16,7	3,6
4515_H	32913293	6686,585977	92630	110373	49,06	290	426,75	47101987	433	23,8	17,9	5,9
4515_I	33752419	6857,06081	74875	88394	49,31	290	436,35	38570641	445	19,9	14,4	5,5
4515_J	25028450	5084,72011	37828	66228	47,37	312	351,8	23298705	360	3,5	2,6	0,9
4515_K	26158475	5314,293289	107685	181771	46,45	366	442,32	80400811	480	30,2	21,9	8,3
4515_L	25624632	5205,839021	48586	83513	48	367	435,91	36404530	471	13,4	10,2	3,2
4731_A_662	10558852	2145,111148	26579	30442	49,58	322	471,3	14347435	500	13	12,4	0,6
4731_A_665	7991270	1623,487322	19985	22752	50,14	333	489,29	11132311	529	10,6	10	0,6
4731_B_662	9133184	1855,475843	18790	21143	51,18	331	506,39	10706548	562	9,3	8,6	0,7
4731_B_665	10797779	2193,650986	19991	22657	50,79	345	533,87	12095991	606	11,7	10,8	0,9
4731_C_662	12699119	2579,922678	48846	58226	47,99	330	477,33	27793274	509	20	19,1	0,9
4731_C_665	7035570	1429,329593	28872	33991	48,89	332	482,1	16387027	516	11,6	11,3	0,3
4731_D_662	13840901	2811,884382	26363	30149	49,9	332	488,95	14741323	525	14,3	13,3	1
4731_D_665	4294836	872,5286215	9630	10625	52,32	337	473,08	5026424	511	5,6	5,5	0,1
4731_E_662	12778571	2596,063957	29456	33938	49,6	330	489,55	16614463	528	13,7	12,3	1,4
4731_E_665	6005892	1220,142671	15695	17742	51,05	331	497,75	8831132	552	8,2	7,7	0,5
4731_F_662	12313775	2501,637112	57437	67483	47,1	332	472,67	31897315	501	26,9	26,1	0,8
4731_F_665	6213396	1262,298688	32743	37565	48,08	331	464,89	17463722	486	14,5	14	0,5
4732.A	5665820	1151,054456	29480	90799	45	433	587,04	53302294	716	40,6	21,6	19
4732.B	3358895	682,3850839	25963	41271	52,17	255	299,43	12357829	282	2,2	1,7	0,5
4732.C	4547903	923,9411087	22717	91890	46,22	435	586,02	52195022	679	3,4	18,7	19,7
4732.D	5581104	1133,843756	55271	108213	43,65	411	584,05	63202290	739	50,4	23,3	27,1
4732.E	5040109	1023,936504	79135	144545	44,67	451	679,83	98266707	943	71,8	28,7	43,1
4732.F	3373188	685,2888156	53997	117392	43,5	541	742,79	87197309	1004	66,8	27,9	38,9
4732.G	3274829	665,3064362	22855	32817	54,65	262	315	10337413	302	2	1,8	0,2

4732.H	10783710	2190,792762	41181	83493	44,41	432	601,69	50237161	762	52,6	30,1	22,5
4732.I	11139002	2262,973036	57381	112491	43,51	388	534,35	60109956	639	49,3	27	22,3
4732.J	11039033	2242,663572	67908	120215	44,04	379	555,02	66721849	379	58	29,2	28,2
4732.K	11173052	2269,890552	54048	83421	44,6	367	561,05	46803212	719	55	30,4	24,6
4732.L	3581525	727,6140628	38662	70353	44,43	458	660,26	46451483	882	53,6	28,7	24,9
4732.M	5403403	1097,742445	53630	94184	44,59	421	615,08	57930669	800	58,8	30,1	28,7
4732.N	6261685	1272,108966	49089	128846	41,38	350	427,91	55133950	473	28,1	12,9	15,1
4732.O	5012229	1018,27247	44484	118088	40,59	356	438,31	51753812	491	24,1	11,5	12,6
4732.P	4351585	884,0576128	56720	116214	35,76	298	373,34	43387495	397	15,2	7,5	7,7
4732.Q	10167189	2065,541828	67825	111439	46,73	394	632,19	70450983	901	71,4	36,6	34,8
4732.R	7001557	1422,419594	66023	110992	46,33	419	661,68	73441664	956	72,6	34,8	37,8
4732.S	5696693	1156,107595	11483	45241	42,73	344	425,82	19265556	469	10	4,1	5,9
4732.T	6313565	1282,648782	56841	116558	44,94	477	701,12	81721714	972	67,3	23,7	43,6
4732.U	7558364	1535,539174	17602	45340	44,69	533	745,33	33793472	1027	42,2	22,2	20
4732.V	7894150	1603,756655	50016	102300	44,34	498,68	361	57343094	697	43,7	20,8	22,9
4732.W	5276141	1071,888201	14891	56735	43,2	382	492,63	27949281	564	21,8	11,6	10,2
4732.X	7716214	1567,607602	34212	84474	44,51	441	585,32	49443978	722	42,2	22,6	19,8
4732.Y	9200346	1869,120314	36586	92660	45,28	474	659,31	61092018	869	50,4	21,9	28,5
4732.Z	10048936	2041,517831	59873	129908	44,1	405	563,89	73253651	707	52,8	23,1	29,7
4732.AA	6865781	1394,835666	43404	136468	43,76	424	567,68	77470483	695	48,6	25,4	23,2
4732.AB	5661954	1150,269048	15946	46363	41,84	502	714,64	33132842	969	32,5	18,6	13,9
4732.AC	6427004	1305,694779	26631	73078	42,12	524	745,8	54501208	1021	47,5	25,1	22,4
4732.AD	7169671	1456,573232	50429	99280	42,07	479	703,6	69853250	976	60,4	31,7	28,7
4732.AE	12124890	2463,263686	80333	132409	45,41	435	719,33	95309994	1105	79,4	35,5	49,3
4732.AF	12325075	2503,932793	69336	112927	45,23	424	673,22	76024263	983	70,8	36,4	34,4
4732.AG	8550702	1737,140191	57686	89779	45,83	418	685,78	61568932	1029	68,2	35,1	33,1

Supplementary Table 5 | Gutless oligochaete samples used in this study. We analyzed 31 polyA libraries of gutless oligochaetes (Michellod et al., 2023)[30] and 56 totalRNA libraries. We *de novo* assembled the libraries and predicted expression of the PHAD and other PHA degradation genes.

O. algarvensis PHA depolymerases

Candidate Number	Use This Subsequence?(Y/N)	Probe-binding Sequences
1	Y	ACCgCCAAATTCTATCCAACAAAggTCgCCgTACAgCCTCTTgCAgTgTATC
2	Y	TAggCCTCgTCTACggTAACCAgAgCgTgACTgTTACgTACCgCgTCgAATg
3	Y	gAgTTCTTCCCCgTCTCTCCgCCTAgTgACTACAgTATgggCgACAgTggAT
4	Y	AATACACAAgTTggCgTTgTATAgAgCAACACAAgAAgATCTCTAACgATgC
5	Y	CggACACgAAAATTgggAAATATAAggTggACCAgAgTCAgATATCAgTAT
6	Y	ACgTTgAACTACggCAACCCATgCgTCgATACggAAAATCCgTggATTggTC
7	Y	TgTAACTTCgACggAgCTTATgCCATACTCAATCATATCTACggCAACCTAC
8	Y	TTAgCAgTTATTTgTgTTATTgTCTCCgCgCTCgCTgAACTggCgCATTgTA
9	Y	ACCgTCCTACAAggTgTCgCAAAgAAggTgCAgAAgTTTTACgAACAgTTCA
11	Y	CCgggCAATATgTCgAACgACCgCgTCCTCATTTTATCCggCATgAACgACT
12	Y	gCgTATCACggATgCCTTCAAggAAAATACCTgTTgAAAgACAAgTTTgCTC
13	Y	ACAgAAATCggTAAATAgATATAAAACAggTTTgAAgggTTTCAgTggCCTA
14	Y	gTCTACgTTCCATCCggCTgCAAgTCTggCAAAAACACgTgCAAgTTACACg
16	Y	CTCTTCATCggTgTCggACTCgTCggAggAAgTCCgTACTACTgTgCgCAgT
17	Y	gATgAAATCATCgCCACgTCCgACTgCATggATACgTATCAgAATATCAACg
18	Y	AgACCgACggCATCCACACCTACACCTggCgATTTCTACgAgTTCgATCAgg
20	Y	TCCgCTCTggCggTTTACATgCTgCAgTTCgCgTCAACCgATTTgATTgACg
21	Y	ggAATATCATCgggCgCCgAAATggCAACACAgATgCACgTTgCCTTCTCTT
22	Y	AACgCCAgCAACATCCAgACCgTCTTCAACCTCAgCgCCggACACACgTTTC
23	Y	CAggCgATTgCCATCATTgACAACCCAATgggCTgCTgggACTggTggggCT
24	Y	CATACTggCTACAACgAggTCggCgAACTgAACAACATCATCATCATCTACC

***Ca.* Thiosymbion sp. PHA depolymerases**

Candidate Number	Use This Subsequence?(Y/N)	Probe-binding Sequences
1	Y	ACCCgACTCTCATCgggAggCgCCATgACCTCCgTgATgTTggCgACCTATC
2	Y	gAgATCgTCAAgCAgTggACggACgTgCATgggTggCggACAgCCCCTgCA
3	Y	gAgCggACCCAggCgggTCATTCTCATCgggTgTggCAAgggCggACggCA
4	Y	gTgATCTATCTgTCCTgggACTCATCggACCCgATACAgCCggAggggACCA
5	Y	ggAggCgACCAAACCgCCCgTgggTCggAgCCACAAggCgggCAgggACACg
6	Y	CCCggAATTATCggCACCTCCCTggAAgCggCgggTATTCTCAgggACTTCg
7	Y	ATgCTCTTCgggCAggTATCCTCCggCCggggCCgTgAAACgggCAAACAgg
8	Y	CgATCCATgTCgCgCAAgATCgTCCTgggCCCCAggCCggAACTCAgCTATg
9	Y	gTCCTggTggATggCACgCCggTggACgAggCCgCTgCCgTCggCATggAAC
10	Y	ATCgAggCggAATggTTgCAgCgATCggAgATCgATCTTTCCCggTTTgCgg
11	Y	CggATCgTgACACTgACgTTCgAggTCgCCgCAAgCTCCAATgTCCgTACCg
12	Y	gTATCCgCCAAggCCTgggTggATCgggTCCgTATAAAATCggTTTCgCCCg
13	Y	ACCggggACCggCCCgACCAgTgCggCACCgCCgCgCCCTTCTTCAACgAgg
14	Y	CCCACCgCCgAgggATCACgCggCAgCggCggTATgCCgTTCgggATCgACg
17	Y	gTATCggTCTggCACggCgATgCCgACTCCgCggTAAAgCCCgTgAATgCCg
18	Y	ggCATCTCCTCCgCCTTCCACATCgCCgACTTCTggggTCTgCTCgAACAgg
19	Y	CgCCgACTCgATCTCAgTgCggCggTAAACgACTACACCAgCgCgAgTTTCA

Supplementary Table 6 | Binding sequences of the HCR-FISH probes designed to target the host and symbiont PHAD. We ordered specific HCR-FISH probes at the company Molecular Instruments Inc. that target the *O. algarvensis* PHAD and the symbiont PHAD of *Ca.* Thiosymbion algarvensis.

References

1. Evans, R., M. O'Neill, A. Pritzel, N. Antropova, A. Senior, T. Green, A. Žídek, R. Bates, S. Blackwell and J. Yim, *Protein complex prediction with AlphaFold-Multimer.* BioRxiv, 2021: p. 2021.10. 04.463034.
2. Jumper, J., R. Evans, A. Pritzel, T. Green, M. Figurnov, O. Ronneberger, K. Tunyasuvunakool, R. Bates, A. Žídek, A. Potapenko, A. Bridgland, C. Meyer, S.A.A. Kohl, A.J. Ballard, A. Cowie, B. Romera-Paredes, S. Nikolov, R. Jain, J. Adler, T. Back, S. Petersen, D. Reiman, E. Clancy, M. Zielinski, M. Steinegger, M. Pacholska, T. Berghammer, S. Bodenstein, D. Silver, O. Vinyals, A.W. Senior, K. Kavukcuoglu, P. Kohli and D. Hassabis, *Highly accurate protein structure prediction with AlphaFold.* Nature, 2021. **596**(7873): p. 583-589.
3. Varadi, M., S. Anyango, M. Deshpande, S. Nair, C. Natassia, G. Yordanova, D. Yuan, O. Stroe, G. Wood, A. Laydon, A. Žídek, T. Green, K. Tunyasuvunakool, S. Petersen, J. Jumper, E. Clancy, R. Green, A. Vora, M. Lutfi, M. Figurnov, A. Cowie, N. Hobbs, P. Kohli, G. Kleywegt, E. Birney, D. Hassabis and S. Velankar, *AlphaFold Protein Structure Database: massively expanding the structural coverage of protein-sequence space with high-accuracy models.* Nucleic Acids Research, 2021. **50**(D1): p. D439-D444.
4. Hisano, T., K. Kasuya, Y. Tezuka, N. Ishii, T. Kobayashi, M. Shiraki, E. Oroudjev, H. Hansma, T. Iwata, Y. Doi, T. Saito and K. Miki, *The crystal structure of polyhydroxybutyrate depolymerase from P*enicillium funiculosum *provides insights into the recognition and degradation of biopolyesters.* Journal of Molecular Biology, 2006. **356**(4): p. 993-1004.
5. Braaz, R., R. Handrick and D. Jendrossek, *Identification and characterisation of the catalytic triad of the alkaliphilic thermotolerant PHA depolymerase* PhaZ*7 of* Paucimonas lemoignei. FEMS Microbiology Letters, 2003. **224**(1): p. 107-12.
6. Teufel, F., J.J. Almagro Armenteros, A.R. Johansen, M.H. Gíslason, S.I. Pihl, K.D. Tsirigos, O. Winther, S. Brunak, G. von Heijne and H. Nielsen, *SignalP 6.0 predicts all five types of signal peptides using protein language models.* Nature Biotechnology, 2022. **40**(7): p. 1023-1025.
7. Anderson, I.J., R.F. Watkins, J. Samuelson, D.F. Spencer, W.H. Majoros, M.W. Gray and B.J. Loftus, *Gene discovery in the* Acanthamoeba castellanii *genome.* Protist, 2005. **156**(2): p. 203-14.
8. Burki, F., A.J. Roger, M.W. Brown and A.G. Simpson, *The new tree of eukaryotes.* Trends in Ecology & Evolution, 2020. **35**(1): p. 43-55.
9. Uchino, K., T. Saito, B. Gebauer and D. Jendrossek, *Isolated poly (3-hydroxybutyrate)(PHB) granules are complex bacterial organelles catalyzing formation of PHB from acetyl coenzyme A (CoA) and degradation of PHB to acetyl-CoA.* Journal of Bacteriology, 2007. **189**(22): p. 8250-8256.
10. Eggers, J. and A. Steinbüchel, *Poly (3-hydroxybutyrate) degradation in* Ralstonia eutropha *H16 is mediated stereoselectively to (S)-3-hydroxybutyryl coenzyme A (CoA) via crotonyl-CoA.* Journal of Bacteriology, 2013. **195**(14): p. 3213-3223.
11. Kobayashi, T. and T. Saito, *Catalytic triad of intracellular poly (3-hydroxybutyrate) depolymerase (*PhaZ*1) in* Ralstonia eutropha *H16.* Journal of Bioscience and Bioengineering, 2003. **96**(5): p. 487-492.

12. Uchino, K., T. Saito and D. Jendrossek, *Poly (3-hydroxybutyrate)(PHB) depolymerase* PhaZ*a1 is involved in mobilization of accumulated PHB in* Ralstonia eutropha *H16.* Applied and Environmental Microbiology, 2008. **74**(4): p. 1058-1063.
13. Sznajder, A. and D. Jendrossek, *To be or not to be a poly (3-hydroxybutyrate)(PHB) depolymerase:* PhaZ*d1 (*PhaZ*6) and* PhaZ*d2 (*PhaZ*7) of* Ralstonia eutropha*, highly active PHB depolymerases with no detectable role in mobilization of accumulated PHB.* Applied and Environmental Microbiology, 2014. **80**(16): p. 4936-4946.
14. Abe, T., T. Kobayashi and T. Saito, *Properties of a novel intracellular poly (3-hydroxybutyrate) depolymerase with high specific activity (*PhaZ*d) in* Wautersia eutropha *H16.* Journal of Bacteriology, 2005. **187**(20): p. 6982-6990.
15. Abe, H. and Y. Doi, *Side-chain effect of second monomer units on crystalline morphology, thermal properties, and enzymatic degradability for random copolyesters of (R)-3-hydroxybutyric acid with (R)-3-hydroxyalkanoic acids.* Biomacromolecules, 2002. **3**(1): p. 133-138.
16. Katoh, K. and D.M. Standley, *MAFFT multiple sequence alignment software version 7: improvements in performance and usability.* Molecular Biology and Evolution, 2013. **30**(4): p. 772-780.
17. Tanio, T., T. Fukui, Y. Shirakura, T. Saito, K. Tomita, T. Kahio and S. Masamune, *An extracellular poly (3-hydroxybutyrate) depolymerase from* Alcaligenes faecalis*.* European Journal of Biochemistry, 1982. **124**(1): p. 71-77.
18. Jendrossek, D., I. Knoke, R.B. Habibian, A. Steinbüchel and H.G. Schlegel, *Degradation of poly (3-hydroxybutyrate), PHB, by bacteria and purification of a novel PHB depolymerase from* Comamonas *sp.* Journal of Environmental Polymer Degradation, 1993. **1**(1): p. 53-63.
19. Senior, P.J. and E.A. Dawes, *The regulation of poly-beta-hydroxybutyrate metabolism in* Azotobacter beijerinckii*.* Biochemical Journal, 1973. **134**(1): p. 225-38.
20. Stuart, J., E. Ooi, J. McLeod, A. Bourns and J. Ballantyne, *D-and L-β-hydroxybutyrate dehydrogenases and the evolution of ketone body metabolism in gastropod molluscs.* The Biological Bulletin, 1998. **195**(1): p. 12-16.
21. Madison, L.L. and G.W. Huisman, *Metabolic engineering of poly (3-hydroxyalkanoates): from DNA to plastic.* Microbiology and Molecular Biology Reviews, 1999. **63**(1): p. 21-53.
22. Prieto, M.A., L.I.d. Eugenio, B. Galán, J.M. Luengo and B. Witholt, *Synthesis and degradation of polyhydroxyalkanoates*, in Pseudomonas. 2007, Springer. p. 397-428.
23. Doi, Y., Y. Kawaguchi, N. Koyama, S. Nakamura, M. Hiramitsu, Y. Yoshida and H. Kimura, *Synthesis and degradation of polyhydroxyalkanoates in* Alcaligenes eutrophus*.* FEMS Microbiology Reviews, 1992. **9**(2-4): p. 103-108.
24. Schirmer, A., D. Jendrossek and H.G. Schlegel, *Degradation of poly (3-hydroxyoctanoic acid)[P (3HO)] by bacteria: purification and properties of a P (3HO) depolymerase from* Pseudomonas fluorescens *GK13.* Applied and Environmental Microbiology, 1993. **59**(4): p. 1220-1227.
25. Nakayama, K., T. Saito, T. Fukui, Y. Shirakura and K. Tomita, *Purification and properties of extracellular poly (3-hydroxybutyrate) depolymerases*

from Pseudomonas lemoignei. Biochimica et Biophysica Acta (BBA)-Protein Structure and Molecular Enzymology, 1985. **827**(1): p. 63-72.

26. Shirakura, Y., T. Fukui, T. Tanio, K. Nakayama, R. Matsuno and K. Tomita, *An extracellular D (−)-3-hydroxybutyrate oligomer hydrolase from* Alcaligenes faecalis. Biochimica et Biophysica Acta (BBA)-Protein Structure and Molecular Enzymology, 1983. **748**(2): p. 331-339.
27. Delafield, F., K.E. Cooksey and M. Doudoroff, *β-Hydroxybutyric dehydrogenase and dimer hydrolase of* Pseudomonas lemoignei. Journal of Biological Chemistry, 1965. **240**(10): p. 4023-4028.
28. Minh, B.Q., H.A. Schmidt, O. Chernomor, D. Schrempf, M.D. Woodhams, A. von Haeseler and R. Lanfear, *IQ-TREE 2: New Models and Efficient Methods for Phylogenetic Inference in the Genomic Era.* Molecular Biology and Evolution, 2020. **37**(5): p. 1530-1534.
29. Revell, L.J., *phytools: an R package for phylogenetic comparative biology (and other things).* Methods in ecology and evolution, 2012(2): p. 217-223.
30. Michellod, D., T. Bien, D. Birgel, M. Violette, M. Kleiner, S. Fearn, C. Zeidler, H.R. Gruber-Vodicka, N. Dubilier and M. Liebeke, De novo *phytosterol synthesis in animals.* Science, 2023. **380**(6644): p. 520-526.

Chapter II

Can Chromatiales bacteria degrade their own PHA?

Chapter II | Can Chromatiales bacteria degrade their own PHA?

Caroline Zeidler[1], Nicole Dubilier[1*], Maggie Sogin[2*]

[1] Max-Planck Institute for Marine Microbiology, Celsiusstraße 1, 29395 Bremen, Germany

[2] University of California at Merced,Merced, CA 95343, USA

*Corresponding authors: **esogin@ucmerced.edu** , **ndubilie@mpi-bremen.de**

[+] *The manuscript is a draft and has not been revised by all authors.*

[+] Author contribution: C.Z. and E.S. conceived the study. C.Z. ran analysis and analyzed the data. C.Z. drafted the manuscript, with support from E.S.

Abstract

Many bacteria and halophilic archaea synthesize polyhydroxyalkanoates (PHAs) as a storage compound. PHA depolymerases (PHADs), degrade PHA into their monomers and dimers, used for energy generation. Substrate affinity for the surface structure and size of the PHA resource classifies PHADs. Intracellular PHADs function on native PHA inside the cell that have an intact surface. In contrast, extracellular PHADs degrade denatured PHA outside of the cell. While the enzyme structure of extracellular PHADs is well described, little is known about the structure of intracellular PHADs. Based on this, there are no clear hallmarks for intracellular PHADs on the protein level. Consequently, homology-based classification of PHADs is often misleading, as exemplified by the miss-classification of PHADs from Chromatiales species, including *Candidatus* Thiosymbion algarvensis and *Thiocapsa rosea*. We used phylogenetic analyses, AlphaFold2 modeling, primary structure analysis and enzyme assays to define the function of Chromatiales PHADs. While *Rheineimera* sp. PHADs are true extracellular PHADs, all other tested Chromatiales PHADs were characterized as intracellular PHADs. My results suggest that true intracellular PHADs lack a signal peptide and have an altered substrate binding site. However, experimental evidence is needed to support the initial sequence-based classification.

Introduction

Polyhydroxyalkanoates (PHAs) are carbon and energy storage compounds synthesized by many bacteria and halophilic archaea across various environments[1-5]. PHA synthesizing organisms build up PHA when nitrogen, phosphate or other nutrients are limiting despite the presence of a rich carbon source. Importantly, PHA can make up to 90% of the organism's dry weight[6, 7]. Once nutrient limiting conditions are lifted the bacterial species can use the PHA stores to jump start their metabolism[8-11]. Consequently, PHA serves as a carbon reservoir that is remobilized in the absence of an external carbon source[12]. PHA thus plays an important role for the organism's survival.

PHA is either degraded intracellularly or extracellularly using different types of PHA depolymerases (PHADs; EC 3.1.1.75, EC 3.1.1.76). Intracellular PHADs (nPHADs) are the enzymes that allow the organism to degrade the stored native PHA (nPHA).

Intracellular PHA granules have an intact surface layer consisting of proteins and phospholipids[12-17]. In contrast, extracellular PHADs (dPHADs) function on denatured PHA (dPHA). Denatured PHA results from the loss of its surface structure following the excretion from the cell[12]. The structure of most extracellular PHADs contains a N-terminal signal peptide, catalytic site, linker domain and C-terminal substrate binding domain. The catalytic serine residue is located within a lipase box. The position of the lipase box classifies extracellular PHADs into two types: Domain type 1 PHADs have the lipase box located after the oxyanion hole, whereas domain type 2 PHADs have the lipase box located before the oxyanion hole[12, 18-21]. The structure of intracellular PHADs is less understood[22] (Figure 1; Supplementary Text 1). Often intracellular PHADs do not have a lipase box motif, resulting in the replacement of the catalytic serine by a cysteine residue[10]. Due to limited characterization of intracellular PHADs, relying only on the homology-based characterization (e.g. Knoll et al., 2009[22]; Supplementary Text 2) often leads to uncertainty and incorrect assumptions of PHA degradation.

The classification of the PHAD from *Candidatus* Thiosymbion algarvensis, the primary symbiont of the gutless oligochaete *Olavius algarvensis,* was inconclusive. Under anaerobic conditions, *Ca*. T. algarvensis expresses a putative PHA synthase and a phasin enzyme that work together to build up PHA. *Ca.* T. algarvensis uses host waste products to synthesize PHA, storing excessive carbon and reducing equivalents[23]. Once nutrient limiting conditions are lifted, the symbiont could use its PHA to jump start its metabolism. When we included the *Ca*. T. algarvensis PHAD in an unrooted maximum likelihood tree built with the PHAD engineering database[22] (DED), *Ca.* T. algarvensis PHAD grouped with extracellular PHADs. Based on this tree, we hypothesized that the symbiont only degrades extracellular PHA outside their cells, rather than their own PHA. The symbiont's enzyme grouped closest to PHADs of seven other *Ca.* Thiosymbion species, that form symbiosis with other gutless oligochaete and nematode hosts, and *Candidatus* Kentron sp. (Figure 3), suggesting that there might be a restriction in the symbiosis for *Ca* T. spp. to use their own PHA.

In this chapter, we sought out to classify *Ca.* T. spp. 's and other Chromatiales PHADs. Secondly, we aimed to define characteristic differences between intracellular and extracellular PHA degrading enzymes. Using a combination of phylogenetic comparison, enzyme homology and activity assays, we argue that the classification of

PHADs should be based on a combination of homology-based classification with experimental verification.

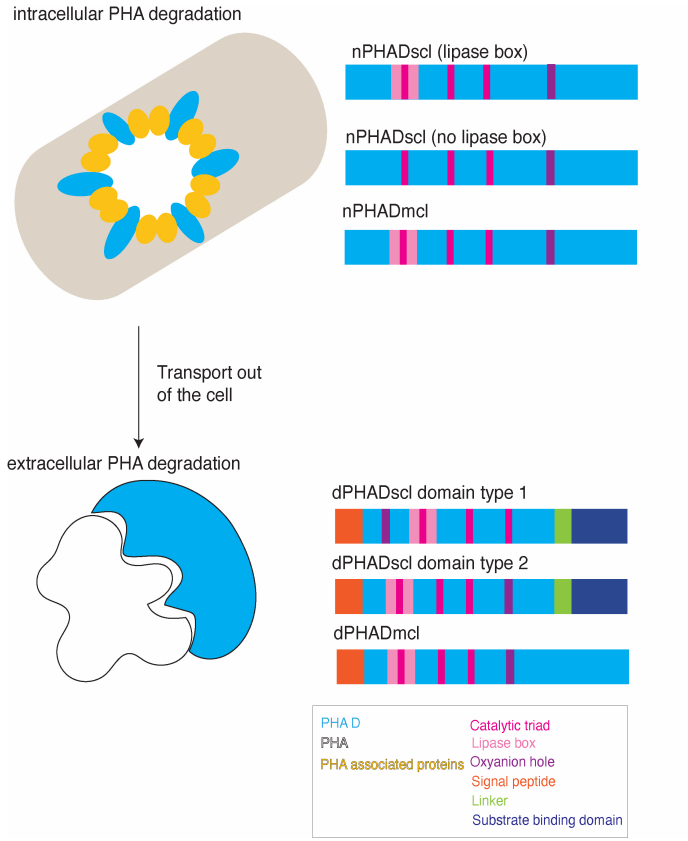

Figure 1 | PHADs that break down intracellular PHA differ in structure to those that degrade extracellular PHA. A schematic of the differences in function and structure of intracellular PHADs (nPHA) and extracellular PHADs (dPHA). Intracellular PHADs are active on native PHA, whereas extracellular PHADs function on crystalline PHA. Extracellular PHADs have a clear primary structure composed of a signal peptide, catalytic domain, linker and substrate binding site. In contrast, there is no clear structure described for intracellular PHADs, despite the presence of a catalytic domain.

Results & Discussion

Candidatus Thiosymbion algarvensis cannot degrade its own PHA

We used primary structure analysis, protein modeling and enzyme assays to investigate if *Ca*. T. algarvensis' PHAD degrades extracellular PHA, as suggested by its phylogenetic grouping. First, *Ca.* T. algarvensis' PHAD had the closest primary structure homology to the extracellular PHAD of *Lihuaxuella thermophila,* with 75% conservation of the catalytic residues (134 bits(337); Supplementary Figure 1)[24]. Second, we compared the AlphaFold2 model of the *Ca*. T. algarvensis' PHAD with the crystal structure of the extracellular PHAD of *Paucimonas lemoignei* that functions on amorphous PHA (P52090.1[25]; 99.8% coverage, 20,5% identity; Figure 2a; Supplementary Figure 2). The catalytic site aligned 100% with the *P. lemoignei*'s crystal structure. Last, *Ca.* T. algarvensis heterologously expressed PHAD showed activity on extracellular PHA. We observed clearance zones on assay plates containing the copolymer Polyhydroxybutyrate/Polyhydroxyvalerate (PHB/PHV; Figure 2b). Based on these results we first concluded that *Ca.* T. algarvensis' PHAD degrades extracellular PHA. Despite the high conservation of the catalytic triad, the substrate binding site of *Ca.* T. algarvensis' PHAD had 0% homology to that of *P. lemoignei* and *L. thermophila*. The result suggests that the substrate binding site is different from previously described extracellular PHADs. Furthermore, *Ca.* T. algarvensis' PHAD lacks a signal peptide, typical for intracellular PHADs (Figure 2a; Supplementary Table 1)[26, 27]. The lack of a signal peptide indicates that *Ca*. T. algarvensis' PHAD, is not transported outside of the cell. Instead, our AlphaFold2 models suggest that *Ca*. T. algarvensis' PHAD is a transmembrane enzyme capable of degrading intracellular PHA (Supplementary Figure 2; Supplementary Table 2)[28]. The AlphaFold2 model together with domain predictions of the *Ca*. T. algarvensis PHAD suggests that the N-terminal, along with the respective catalytic triad, is located at the inside, followed by a ten amino acid long transmembrane domain and the C-terminal on the outside. We observed the same pattern for all *Ca.* T. spp.'s PHADs (Supplementary Text 3; Supplementary Figure 3). Based on our modeling results, we reformulated our hypothesis that *Ca.* T. algarvensis' PHAD is, indeed, an intracellular enzyme that *in vivo* cannot degrade extracellular PHA.

We did not detect genes for PHA monomeric and dimeric hydroxyalkanoate degradation in the *Ca.* T. algarvensis genome and transcriptome (Figure 2c). We

searched for enzymes downstream the PHA degradation pathway, including a hydroxybutyrate-dimer hydrolase (EC 3.1.1.22) and a beta-hydroxybutyrate dehydrogenase (BHBD; EC 1.1.1.30). The former enzyme degrades PHA dimers into their hydroxyalkanoates which can be converted by the BHBD to acetoacetate. Acetoacetate is oxidized to acetyl coenzyme A (acetyl-CoA) used for energy production via the citric acid cycle[14, 29]. In intracellular PHA degradation, the PHA-monomers are coenzyme A bound for a quick re-usage of the monomers for PHA synthesis or the conversion to acetyl-CoA for energy generation by a 3-hydroxybutyryl-CoA dehydrogenase (EC 1.1.1.157)[30]. We searched for these three enzymes in all available genome bins, metatranscriptomes and metaproteomes but could not identify any of the enzymes. That we could not identify any of the enzymes could either be the result of the incomplete genomes or *Ca.* T. algarvensis does not have the ability to generate energy from PHA. Interestingly, we identified a BHBD and 3-hydroxybutyryl-CoA dehydrogenase for the secondary Deltaproteobacteria symbiont ("*Delta3*") and the eukaryotic host. Based on this we hypothesize that *Ca.* T. algarvensis cannot use its own PHA source to generate energy. Rather the bacteria require other partners to degrade PHA to generate energy.

That the *Ca.* T. spp. PHADs show characteristics of extracellular PHADs and function on denatured PHA but lack a signal peptide and substrate binding site suggests several possibilities: (1.) *Ca.* Thiosymbion spp. PHADs function *in vivo* only on intracellular PHA. (2.) Alternatively, *Ca.* Thiosymbion spp. 's PHADs could be a novel PHAD functioning on intracellular and extracellular PHA. (3.) Finally, *Ca.* Thiosymbion spp. might have lost their intracellular PHAD because the eukaryotic host and the Deltaproteobacteria symbionts are needed for the complete PHA degradation.

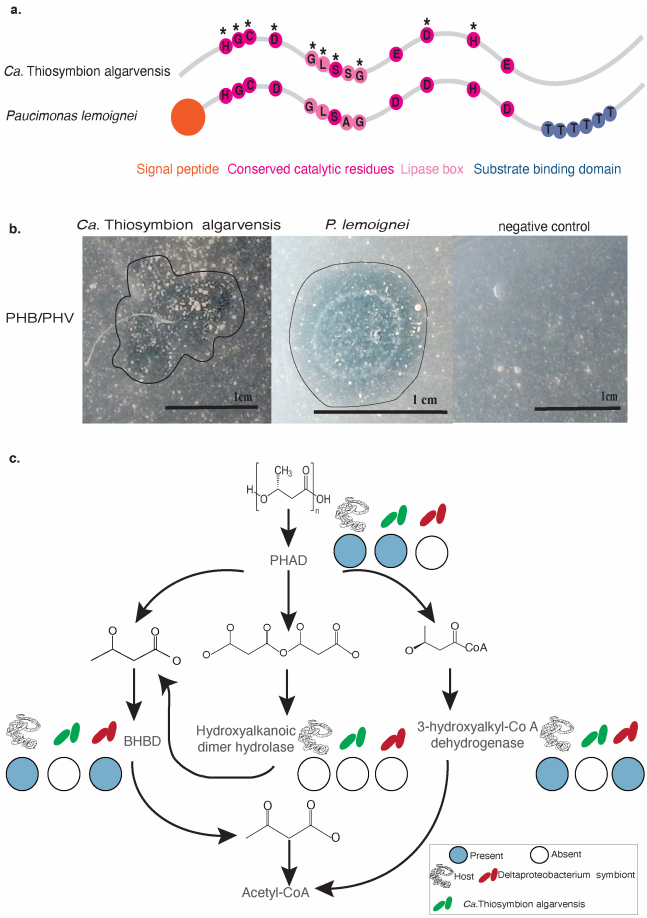

Figure 2 | PHAD of *Candidatus* Thiosymbion algarvensis shows characteristics and activity of extracellular PHADs but cannot use PHA degradation products for energy generation. a. Primary structure analysis reveals high conservation of the catalytic domain of the *Ca.* T. algarvensis PHAD in comparison to the PHAD from *P. lemoignei*. No signal peptide and substrate binding site were predicted for the *Ca.* Thiosymbion algarvensis' PHAD. Conserved residues in comparison to *P. lemoignei* PHAD are marked with an asterisk. **b.** PHAD from *Ca.* Thiosymbion algarvensis showed extracellular activity on the copolymer PHB/PHV by forming a clearance zone on PHA indicator plates. **c.** *Ca.* Thiosymbion algarvensis does not encode for the enzymes that use PHA degradation products. The Deltaproteobacterium ("*Delta3*") symbionts and the host encode for those enzymes suggesting that the complete metaorganism is needed to degrade PHA for energy generation.

Homology based classification of PHADs can be misleading

All 93 identified Chromatiales PHADs grouped with extracellular PHADs of the PHAD engineering databases (DED; Figure 3)[22]. Because some of the species produce PHA, we speculate that some of the PHADs classified as extracellular PHADs are in fact intracellular PHADs. To address this hypothesis, we investigated the phylogeny, structural homology and function of the Chromatiales PHAD enzymes.

Based on our enzyme modeling, *Rheinheimera spp.* PHADs were determined to be true extracellular PHADs (Figure 3; Clade I). The primary structure of the PHAD from *Rheinheimera aquimaris* (WP1340551281)[31] showed strong alignment to the PHAD of *Penicillium funiculosum* (basionym *Talaromyces funiculosus*; 97% coverage; 32% identity)[32]. The superposition between the AlphaFold2 model of *R. aquimaris* and the crystal structure of *P. funiculosum* (pdb: 2d81; RMSD: 0.723 (1223 to 1323 atoms); pLLDT: 92.37%; Figure 4; Supplementary Figure 4) further strengthens our hypothesis that the *R. aquimaris'* PHAD degrades extracellular PHA. Specifically, the catalytic domain showed 100% homology and the substrate binding site showed 43% conservation in comparison to the *P. funiculosum* PHAD. In particular, we saw conservation of the residue W_{302} that holds the polymer chain in place during the nucleophilic cleavage of the PHA molecule[32]. The PHAD from *R. aquimaris* was predicted to have a signal peptide, indicating that the enzyme is transported outside the cell. Lastly, *R. aquimaris* grew and formed a clearance zone on PHA plates of the homopolymer Polyhydroxybutyrate (PHB) and the copolymer Polyhydroxybutyrate/Polyhydroxyvalerate (PHB/PHV; Figure 5). When we incubated *R. aquimaris* in a medium without an external carbon source, *R. aquimaris* did not survive (Supplementary Figure 5). Taken together, *R. aquimaris* PHAD classification as an extracellular PHAD was correct given its ability to degrade extracellular PHA.

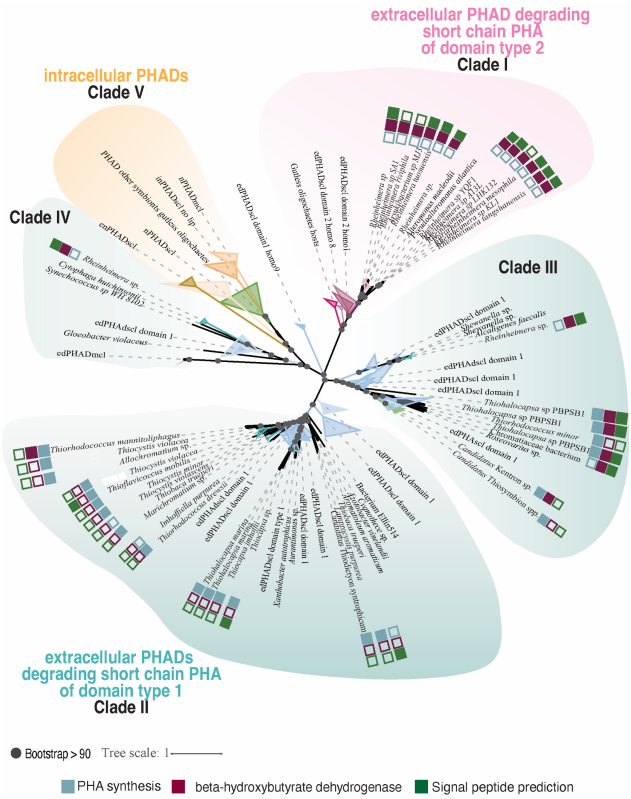

Figure 3 | Chromatiales PHADs are predicted to degrade extracellular PHA, despite their ability to synthesize PHA. Chromatiales PHADs grouped with extracellular PHADs in an unrooted maximum likelihood tree (IQTree[33], ultrafast bootstrap support). The phylogenetic tree was calculated from an alignment of 93 Chromatiales PHADs and the classified PHADs of the PHAD engineering database[22] (localpair alignment MAFFT[34]). The tree formed five subclades: One clade of extracellular PHADs degrading short chain PHA that have the lipase box located before the oxyanion hole (Clade I), three clades of extracellular PHADs degrading short chain PHA that have the lipase box located after the oxyanion hole (Clade II to IV) and one clade of intracellular PHADs (Clade V). Chromatiales species were checked for their ability to synthesize PHA (blue square), if the PHAD encoded for a signal peptide (green square) and if the organism can further generate energy from PHA degradation (purple square). If these boxes are empty, the function is not conserved. Full tree Supplementary Figure 6.

PHADs from *Allochromatium vinosum, Thiocystus violascens,* or *Thiocapsa rosea* grouped with extracellular PHADs but their enzymes structure predicts affinity for intracellular PHA (Figure 3; Clade II & III). Using an in depth primary and tertiary structure analysis (pLDDT: 81,86% - 86,81%) for each of the Chromatiales PHADs, we found that all parts of the catalytic triad including the lipase box motif located behind the oxyanion hole were 100% conserved in comparison to the PHAD from *P. lemoignei* (pdb:2x76[25]; RMSD: 14 - 19; identity 15.9% - 19.3%, coverage 73.7% - 83.4%; Figure 4; Supplementary Figure 7 & 8). We could not identify any residues of the substrate binding site motif, meaning that the substrate binding site might be different to known extracellular PHADs. None of the three Chromatiales PHADs showed a signal peptide prediction. These characteristics are typical for intracellular PHADs[28]. Lastly, the three Chromatiales species were not able to degrade extracellular PHA (Figure 5). Rather, when we incubated *T. rosea, T. violascence*, and *A. vinosum* in a medium without an external carbon source, all three species maintained cell densities or exponential growth across 72 hours (Supplementary Figure 5). Given that all three Chromatiales species cannot degrade extracellular PHA (Figure 5), we identified that their homology-based classification was misleading.

Lastly, one group of PHADs found in *Rheinheimera sp.* lacked a substrate binding site but encoded for a signal peptide, suggesting that these are extracellular PHADs without any known substrate binding site motif (Figure 3; Clade IV). This group of Rheinheimera PHADs were phylogenetically placed closer to intracellular enzymes. When we compared the primary and tertiary structure of the PHAD from *Rheinheimera riviphila* (WP1276988461)[31] to the PHAD from *P. lemoignei* (pdb:2x76[25];accession P52090.1; RMSD: 15.766 (406 to 406 atoms); pLDDT: 93.11; 69,8% coverage; 17% identity; Supplementary Figure 9)[25], we found that only the catalytic serine residue that is located in the lipase box and an asparagine residue of the

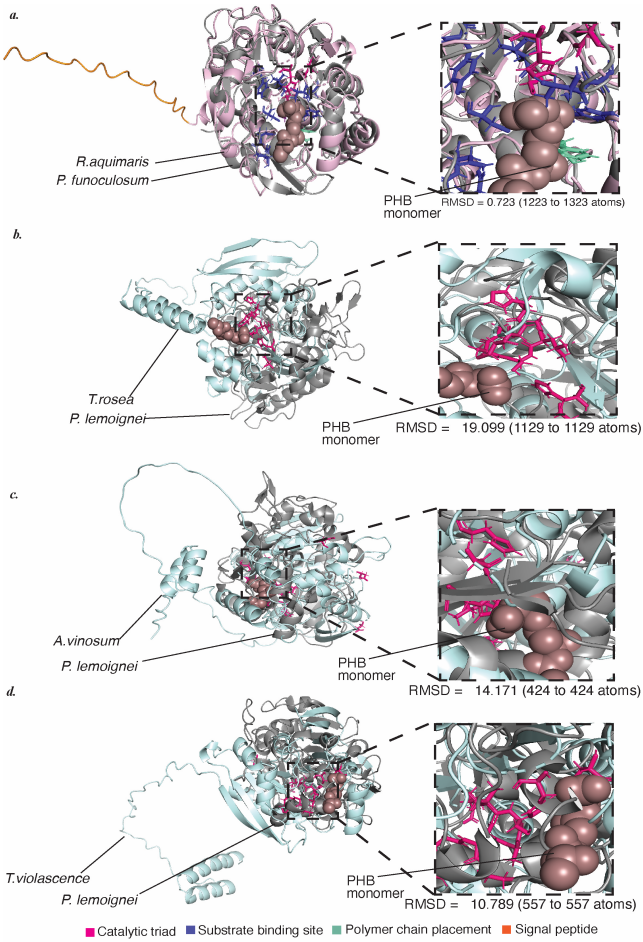

Figure 4 | Chromatiales PHADs might be mis-classified as extracellular PHADs based on their structural homology to known extracellular PHADs. We generated AlphaFold2[35-37] models of the PHADs of **a**. *R. aquimaris,* **b.** *T. rosea,* **c.** *A. vinosum* and **d.** *T. violascence.* In comparison to the homologs of *P. funiculsoum* (2d81)[32] and *P. lemoignei* (2x76)[25], only *R. aquimaris* showed characteristics of extracellular PHADs, which includes a signal peptide (orange label) and a substrate binding site (blue label and cyan label). All of the catalytic triads from Chromatiales PHADs were 100% conserved (pink label). Zoomed in regions represent the conserved residues of the catalytic site and if conserved the substrate binding domain.

catalytic domain were conserved. Thus, we concluded that the catalytic site of *R. riviphila* PHADs was not conserved in comparison to known extracellular PHADs. Based on our observations, we hypothesize that the PHADs from *Rheinheimera* sp. are a novel group of extracellular PHADs that need to be described.

We sought to identify differences in the sequence alignment between intracellular and extracellular PHADs. Intracellular PHADs are structurally separated from extracellular PHADs[12]. When we aligned the tested Chromatiales PHADs with all experimentally validated extracellular PHADs (Supplementary Figure10), we observed alignment of catalytic residues. However, the Chromatiales sequences were misaligned in the N-terminal region of the signal peptide and the C-terminal region of the substrate binding site (Supplementary Text 4; Supplementary Figure 10). We were unable to identify a common motif along the Chromatiales PHADs. In order to identify a common motif, intracellular PHADs need to be better characterized. To fully understand PHA degradation and its influence for the environment an experimental validation of these predictions is crucial.

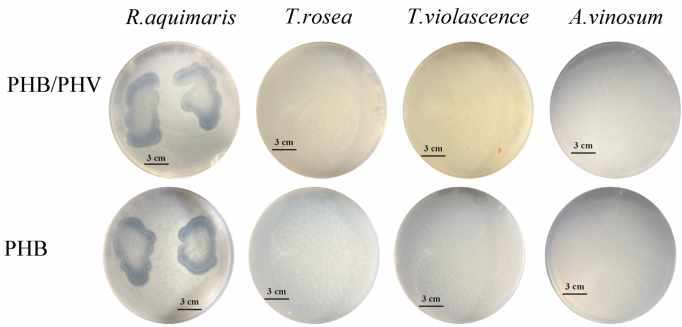

Figure 5 | Only *R. aqumaris* degrades extracellular PHA, showing that the other Chromatiales PHADs were mis-classified. We conducted extracellular PHAD assays on denatured PHA of either the homopolymer PHB or the copolymer PHB/PHV. Only *R. aquimaris* degraded PHA extracellularly by forming a clearance zone around their colonies. The other Chromatiales species *T.rosea, T. violascence, and A. vinosum* were unable to grow on extracellular PHA.

Conclusion

Our study showed that homology-based classification of PHADs can often be misleading, especially for PHA-degrading bacteria that are not yet experimentally described. When we looked into the characteristics of the PHAD from *Ca.* T. algarvensis, we found that it lacked a signal peptide and substrate binding site motif, despite its grouping with extracellular PHADs. Similarly, other Chromatiales species grouped with extracellular PHADs but all, except *R. aquimaris*, were not active on extracellular PHA. One possible explanation for the miss-classification of Chromatiales PHADs might be that intracellular PHADs are less characterized. Of the 30 described PHADs within the PHAD engineering database, only five were characterized experimentally to degrade PHA intracellularly[22]. Leading us to postulate that future work should begin to characterize intracellular PHADs.

The correct classification of PHADs is crucial as it influences our understanding of carbon cycling in the environment. Intracellular PHA serves as a sink for carbon because of the cyclic reaction of PHA build up and degradation with other storage compounds inside of the cell[12, 38]. Additionally, PHA-based plastics are considered a biodegradable alternative to common plastics and are broken down by extracellular PHADs[39]. Therefore, the correct classification of PHADs is not only important for naturally occurring PHA but also influences our thinking about the efficiency of using biodegradable PHA-based plastics.

Acknowledgements

We would like to thank Carolin Richter and Martina Meyer for the help conducting parts of the experiments. We thank the HYDRA team for their sampling support and the MPI for plant breeding for their access to the computing cluster and sequencing services. This work was funded by the Max Planck Society through Prof. N. Dubilier.

Code and data availability

Raw metatranscriptomic sequences, PHAD sequences, AlphaFold2 models and phylogenetic trees will be made publicly available upon peer-review submission on ENA, PDB and figshare. They are currently available upon request.

Materials & Methods

Metatranscriptome analysis

Sampling, extraction and sequencing. Scuba divers collected 15 different gutless oligochaete species from their natural habitats between 2015 and 2020 to generate the metatranscriptomic libraries used in this study (Supplementary Table 3). Worms were manually sorted from the sediment and were fixed directly in RNAlater (Thermo Fisher Scientific, Waltham, MA, US). The metaorganism's DNA/RNA was extracted after their storage at -80°C using either Qiagen's AllPrep DNA/RNA/Protein Mini Kit or AllPrep DNA/RNA Micro Kit (Qiagen; Supplementary Table 3). We used the following adjustments to the manufacturer's protocol: bead beating was performed using a sterilized mixture of small (approximately 20 1.2 mm ZY-S Silibeads) and large (5 2mm beads ZY-Silibeads) silicon beads in addition to Matrix B silicon sand (MP Biosystems), β-mercaptoethanol was replaced by 20 µl of 2 M DTT and 1 µl of Reagent DX (Qiagen 19088), and tissues were disrupted by bead beating using a FastPrep (MP Biomedicals™) instrument set for two cycles of at 4 m/s for 40 seconds with a 5 minutes resting of samples on ice. RNA samples were eluted in 40 µl of DEPC-treated water and stored at -80 °C until library preparation.

We send extracted RNA to the Max Planck Genome Centre (Cologne, Germany) for library generation and sequencing. The total RNA libraries were generated with the NEBNext® Ultra™ II Directional RNA Library Prep Kit for Illumina® (NEB). All metatranscriptomic libraries were sequenced on an Illumina HiSeq3000 by sequencing-by-synthesis and paired-end read mode, resulting in approximately 24296325 reads per library.

Identification of *Ca.* T. algarvensis PHAD and other PHA degradation genes in metatranscriptomes. To generate metatranscriptomic assemblies, we first trimmed raw transcriptomic reads of their adapters and quality filtered them using BBDuk[40, 41] (BBMap version 38.90; parameters: mink= 11, minlength=36, trimq=2, hdist=1). We then mapped the rRNA out by SortMeRNA[42] (version 4.3.4) using the SILVA_138_SSURef_NR99_tax_silva database. The rRNA free reads were *de novo* assembled using Trinity[43] (Trinity-v2.5.1; parameters: --max_memory 250G --normalize_reads --verbose). The quality of the assemblies was assessed by calculating the N50 values[43] (TrinityStats.pl; Trinity-v2.5.1). The coding sequences were predicted using Transdecoder (TransDecoder.Predict 5.5.0, TransDecoder.LongOrfs 5.5.0; https://github.com/TransDecoder/TransDecoder/).

We used the coding sequences of the assemblies to identify the *Ca.* T. spp.' PHADs and other PHA degradation sequences by a BLASTp search[44] (e-value 1; version Protein-Protein BLAST 2.11.0) or hmmsearch[45]. The searches were done either against the PHAD database[22] or a manual curated database consisting of bacterial hydroxybutyrate-dimer hydrolases (EC 3.1.1.22), beta-hydroxybutyrate dehydrogenases (EC 1.1.1.30) and 3-hydroxybutyryl-CoA dehydrogenases (EC 1.1.1.157). We cross checked the results using BLASTp against the non-redundant protein database on NCBI[46].

PHAD identification in metagenomes. The identified *Ca.* T. algarvensis' PHAD were used to identify the *pha*Z genes in the most recent PacBio bins published along the study by Michellod et al., 2023[47] using TBLASTN[44] (e-value 1, version Protein Query-Translated Subject BLAST 2.11.0+).

Chromatiales PHA degradation genes identification. The identified *Ca.* T. spp. PHADs were used to identify Chromatiales PHADs deposited on NCBI and UNIPROT (BLASTp search; e-value 1; version Protein-Protein BLAST 2.11.0)[44, 46, 48]. Additionally, we screened NCBI[46] manually for Chromatiales PHADs and other PHA degradation genes.

PHAD characterization

Phylogenetic reconstruction. To classify the Chromatiales and *Ca.* T. spp.' PHADs, we combined the identified sequences with the classified PHADs of the PHAD database (DED)[22]. The created dataset was aligned using the local pair alignment in MAFFT (version v7.407 (2018/Jul/23))[34]. The aligned sequences were used to calculate a maximum likelihood tree with ultrafast bootstrap support values using IQ TREE[33]. We visualized the calculated tree in iTOL[49] and Adobe Inc. Illustrator.

Primary structure analysis. In order to compare the primary structure of experimentally validated PHADs with the identified Chromatiales PHADs, we aligned the PHADs of *R. aquimaris* to the amino acid sequence of the PHADs from the fungus *Penicillium funiculosum* (basionym *Talaromyces funiculosus*; accession pdb: 2D81/2d80)[32] using the local pair alignment in MAFFT (version v7.407 (2018/Jul/23))[34]. The alignment was visualized using the MSAviewer[50]. Our analysis was based on the paper from Hisano *et al.* (2006)[32].The same analysis was repeated for the PHADs of *T. rosea, T. violascence, A.vinosum, R. aquimaris, R. riviphila* and *Ca*. T. algarvensis with the PHAD of *P. lemoignei* (accession pdb: 2x76)[25]. Additionally, we predicted the signal peptides of each of the identified Chromatiales PHADs using SignalP 6.0[51]. Transmembrane domain were predicted using TMHMM[52] and SPOCTOPUS[53].

Homologous modeling. To identify the structural alignment of the Chromatiales PHADs, we modeled the PHADs of *T. rosea, T. violascence, A.vinosum, R. aquimaris, R. riviphila* and *Ca*. T. algarvensis using the monomer prediction against the full AlphaFold2 database[35-37]. We analyzed the generated enzyme models and visualized them using PyMOL (version 2.4.0.; The PyMOL Molecular Graphics System, Version 2.0 Schrödinger, LLC). To assess the structural conservation, we aligned the AlphaFold2 models to the crystal structure of the PHAD from the fungus *P. funiculosum* (accession 2D80)[32] and of the bacterium *P. lemoignei* (accession pdb: 2x76)[25]. Based on the superposition the root-mean-square deviation (RMSD) was calculated in PyMol (version 2.4.0.; The PyMOL Molecular Graphics System, Version 2.0 Schrödinger, LLC). Additionally, we visualized the predicted local distance

difference test (pLDDT) saved in the beta spectrum of the AlphaFold2 model using PyMol.

Functionality

Heterologous gene expression and enzyme purification. To test *Ca*. T. algarvensis for its ability to degrade extracellular PHA, we expressed its PHAD in *E. coli.* As the positive control, we used an extracellular PHAD from *P. lemoignei* (accession: P52090)[54]. Genscript (Genscript®) generated pet28a(+) vectors with the sequences of interest inserted between the restriction sites NheI/XhoI. The expression vector was transformed by heat shock in *E. coli* BL21 competent cells (DE2; Theremo Fisher). The positive control was transferred into BL21 rosetta competent cells (DE3; Merck). To overexpress the enzymes, we followed the method described by Becker et al., (2018)[55]. The success of the overexpression was checked by SDS PAGE (TGX FastCast 12%, Biorad). To extract the overexpressed PHAD from the inclusion bodies and to fold the enzyme correctly, we included a refolding step following Qi *et al.* (2015)[56]. After refolding we exchanged the buffer in an overnight dialysis step using 6-8 kDa dialysis bags against SEC buffer (20 mM Tris, 0.5 M NaCl) at 4 °C stirred at 150 rpm. We analyzed the samples for their successful expression by sending them for plasmid extraction and Sanger sequencing (Microsynth AG). The recovered sequences were analyzed for the successful insertion of the *Ca.* T. algarvensis. and *P. lemoignei* PHAD sequences in *E. coli* (Supplementary Figure 11).

Enzyme assays. To test the heterologous expressed *Ca.* T. algarvensis' PHAD for its activity on crystalline PHA we performed spot assay according to the method described by Briese *et al.*, (1994)[57]. We prepared polymer plates of 0.5 mg/ml of the homopolymer PHB (Merck) and the copolymer PHB/PHV (Merck) in 100mM Tris HCl (Sigma-Aldrich). The water insoluble polymers were brought into a stable suspension by sonication of the mix at maximum intensity for 2 h at 42 °C. To this 7 g / 500 ml agar was added (Becton Dickinson). To test for the enzyme activity, we added 10 µl of the purified enzymes on the plate which we incubated at 36°C for 48h. A clearance zone showed the activity of the enzyme. To generate the negative control, we pooled the purified enzymes in a 1:1 mix which we heated at 95°C for 15 min.

Functional assays Chromatiales cultures. We obtained Chromatiales species from the DSMZ (Supplementary Table 4). To enrich the anaerobic strains in PHA, we cultivated them in a modified anaerobic Pfenning's medium[58] under light conditions at 25°C for up to 2 weeks depending on the strains growth behavior (Supplementary Table 4; Supplementary Text 5). For the *R. aquimaris* strain we used a BACTO marine broth medium (DIFCO 2216; Sigma-Aldrich) and cultivated the strain at 37°C. Subsequently, we transferred the strains in their respective medium without any carbon source for up to 72h. At the respective time points, 0h, 24h, 48h and 72h, we measured the OD at 600nm.

To test for the ability of the strains to degrade extracellular PHA, we took a 100 µl sample at the starting time point of the experiment and plated 2x 50µl on either PHB or PHB/PHV plates according to the method described by Briese *et al.,* (1994)[57]. The plates were prepared in the same way as described above for the *Ca.* T. algarvensis but we adjusted the pH according to the strains culture medium (Supplementary Table 4). The anaerobic strains were cultivated at 25°C under light conditions in anaerobic jars using the OXOID AneroGen bags (Thermo Scientific) for 1 week. *R. aquimaris* was cultured at 37°C for 2 days.

References

1. Fernandez-Castillo, R., F. Rodriguez-Valera, J. Gonzalez-Ramos and F. Ruiz-Berraquero, *Accumulation of poly (β-hydroxybutyrate) by halobacteria.* Applied and Environmental Microbiology, 1986. **51**(1): p. 214-216.
2. Steinbüchel, A. and H. Schlegel, *Physiology and molecular genetics of poly (β-hydroxyalkanoic acid) synthesis in* Alcaligenes eutrophus. Molecular Microbiology, 1991. **5**(3): p. 535-542.
3. Arun, A., R. Arthi, V. Shanmugabalaji and M. Eyini, *Microbial production of poly-β-hydroxybutyrate by marine microbes isolated from various marine environments.* Bioresource technology, 2009. **100**(7): p. 2320-2323.
4. Wang, J. and L. Bakken, *Screening of soil bacteria for poly-β-hydroxybutyric acid production and its role in the survival of starvation.* Microbial Ecology, 1998. **35**(1): p. 94-101.
5. Khardenavis, A., P. Guha, M.S. Kumar, S. Mudliar and T. Chakrabarti, *Activated sludge is a potential source for production of biodegradable plastics from wastewater.* Environmental Technology, 2005. **26**(5): p. 545-552.
6. Madison, L.L. and G.W. Huisman, *Metabolic engineering of poly (3-hydroxyalkanoates): from DNA to plastic.* Microbiology and Molecular Biology Reviews, 1999. **63**(1): p. 21-53.

7. Müller, H.M. and D. Seebach, *Poly (hydroxyalkanoates): a fifth class of physiologically important organic biopolymers?* Angewandte Chemie International Edition in English, 1993. **32**(4): p. 477-502.
8. Anderson, A.J., G.W. Haywood and E.A. Dawes, *Biosynthesis and composition of bacterial poly (hydroxyalkanoates).* International Journal of Biological Macromolecules, 1990. **12**(2): p. 102-105.
9. Kawaguchi, Y. and Y. Doi, *Kinetics and mechanism of synthesis and degradation of poly (3-hydroxybutyrate) in* Alcaligenes eutrophus. Macromolecules, 1992. **25**(9): p. 2324-2329.
10. Handrick, R., S. Reinhardt and D. Jendrossek, *Mobilization of poly (3-hydroxybutyrate) in* Ralstonia eutropha. Journal of Bacteriology, 2000. **182**(20): p. 5916-5918.
11. Ruiz, J.A., N.I. López, R.O. Fernández and B.S. Méndez, *Polyhydroxyalkanoate degradation is associated with nucleotide accumulation and enhances stress resistance and survival of* Pseudomonas oleovorans *in natural water microcosms.* Applied and Environmental Microbiology, 2001. **67**(1): p. 225-230.
12. Jendrossek, D. and R. Handrick, *Microbial degradation of polyhydroxyalkanoates.* Annual Review of Microbiology, 2002. **56**: p. 403.
13. Oeding, V. and H.G. Schlegel, *β-Ketothiolase from* Hydrogenomonas eutropha *H16 and its significance in the regulation of poly-β-hydroxybutyrate metabolism.* Biochemical Journal, 1973. **134**(1): p. 239-248.
14. Senior, P.J. and E.A. Dawes, *The regulation of poly-beta-hydroxybutyrate metabolism in* Azotobacter beijerinckii. Biochemical Journal, 1973. **134**(1): p. 225-38.
15. Griebel, R. and J. Merrick, *Metabolism of poly-β-hydroxybutyrate: effect of mild alkaline extraction on native poly-β-hydroxybutyrate granules.* Journal of Bacteriology, 1971. **108**(2): p. 782-789.
16. Mayer, F., M.H. Madkour, U. Pieper-fürst, R. Wieczorek, M. Liebergesell and A. Steinbüchel, *Electron microscopic observations on the macromolecular organization of the boundary layer of bacterial PHA inclusion bodies.* The Journal of General and Applied Microbiology, 1996. **42**(6): p. 445-455.
17. Amor, S.R., T. Rayment and J.K. Sanders, *Poly (hydroxybutyrate)* in vivo*: NMR and x-ray characterization of the elastomeric state.* Macromolecules, 1991. **24**(16): p. 4583-4588.
18. Jaeger, K.-E., A. Steinbüchel and D. Jendrossek, *Substrate specificities of bacterial polyhydroxyalkanoate depolymerases and lipases: bacterial lipases hydrolyze poly (omega-hydroxyalkanoates).* Applied and Environmental Microbiology, 1995. **61**(8): p. 3113-3118.
19. Behrends, A., B. Klingbeil and D. Jendrossek, *Poly (3-hydroxybutyrate) depolymerases bind to their substrate by a C-terminal located substrate binding site.* FEMS Microbiology Letters, 1996. **143**(2-3): p. 191-194.
20. Kasuya, K.-i., T. Ohura, K. Masuda and Y. Doi, *Substrate and binding specificities of bacterial polyhydroxybutyrate depolymerases.* International Journal of Biological Macromolecules, 1999. **24**(4): p. 329-336.
21. Ohura, T., K.-I. Kasuya and Y. Doi, *Cloning and characterization of the polyhydroxybutyrate depolymerase gene of* Pseudomonas stutzeri *and analysis of the function of substrate-binding domains.* Applied and Environmental Microbiology, 1999. **65**(1): p. 189-197.

22. Knoll, M., T.M. Hamm, F. Wagner, V. Martinez and J. Pleiss, *The PHA depolymerase engineering database: a systematic analysis tool for the diverse family of polyhydroxyalkanoate (PHA) depolymerases.* BMC Bioinformatics, 2009. **10**: p. 1-8.
23. Kleiner, M., C. Wentrup, C. Lott, H. Teeling, S. Wetzel, J. Young, Y.-J. Chang, M. Shah, N.C. VerBerkmoes and J. Zarzycki, *Metaproteomics of a gutless marine worm and its symbiotic microbial community reveal unusual pathways for carbon and energy use.* Proceedings of the National Academy of Sciences, 2012. **109**(19): p. E1173-E1182.
24. Thomas, G.M., S. Quirk, D.J. Huard and R.L. Lieberman, *Bioplastic degradation by a polyhydroxybutyrate depolymerase from a thermophilic soil bacterium.* Protein Science, 2022. **31**(11): p. e4470.
25. Wakadkar, S., S. Hermawan, D. Jendrossek and A.C. Papageorgiou, *The structure of* PhaZ*7 at atomic (1.2 Å) resolution reveals details of the active site and suggests a substrate-binding mode.* Acta Crystallographica Section F: Structural Biology and Crystallization Communications, 2010. **66**(6): p. 648-654.
26. Handrick, R., S. Reinhardt, P. Kimmig and D. Jendrossek, *The "intracellular" poly (3-hydroxybutyrate)(PHB) depolymerase of* Rhodospirillum rubrum *is a periplasm-located protein with specificity for native PHB and with structural similarity to extracellular PHB depolymerases.* Journal of Bacteriology, 2004. **186**(21): p. 7243-7253.
27. Abe, T., T. Kobayashi and T. Saito, *Properties of a novel intracellular poly (3-hydroxybutyrate) depolymerase with high specific activity (*PhaZ*d) in* Wautersia eutropha *H16.* Journal of Bacteriology, 2005. **187**(20): p. 6982-6990.
28. Uchino, K., T. Saito, B. Gebauer and D. Jendrossek, *Isolated poly (3-hydroxybutyrate)(PHB) granules are complex bacterial organelles catalyzing formation of PHB from acetyl coenzyme A (CoA) and degradation of PHB to acetyl-CoA.* Journal of Bacteriology, 2007. **189**(22): p. 8250-8256.
29. Kobayashi, T. and T. Saito, *Catalytic triad of intracellular poly (3-hydroxybutyrate) depolymerase (*PhaZ*1) in* Ralstonia eutropha *H16.* Journal of bioscience and bioengineering, 2003. **96**(5): p. 487-492.
30. Eggers, J. and A. Steinbüchel, *Poly (3-hydroxybutyrate) degradation in* Ralstonia eutropha *H16 is mediated stereoselectively to (S)-3-hydroxybutyryl coenzyme A (CoA) via crotonyl-CoA.* Journal of Bacteriology, 2013. **195**(14): p. 3213-3223.
31. Saito, T., K. Suzuki, J. Yamamoto, T. Fukui, K. Miwa, K. Tomita, S. Nakanishi, S. Odani, J.-l. Suzuki and K. Ishikawa, *Cloning, nucleotide sequence, and expression in* Escherichia coli *of the gene for poly (3-hydroxybutyrate) depolymerase from* Alcaligenes faecalis. Journal of Bacteriology, 1989. **171**(1): p. 184-189.
32. Hisano, T., K. Kasuya, Y. Tezuka, N. Ishii, T. Kobayashi, M. Shiraki, E. Oroudjev, H. Hansma, T. Iwata, Y. Doi, T. Saito and K. Miki, *The crystal structure of polyhydroxybutyrate depolymerase from* Penicillium funiculosum *provides insights into the recognition and degradation of biopolyesters.* Journal of Molecular Biology, 2006. **356**(4): p. 993-1004.
33. Minh, B.Q., H.A. Schmidt, O. Chernomor, D. Schrempf, M.D. Woodhams, A. von Haeseler and R. Lanfear, *IQ-TREE 2: New Models and Efficient Methods for Phylogenetic Inference in the Genomic Era.* Molecular Biology and Evolution, 2020. **37**(5): p. 1530-1534.

34. Katoh, K. and D.M. Standley, *MAFFT multiple sequence alignment software version 7: improvements in performance and usability.* Molecular Biology and Evolution, 2013. **30**(4): p. 772-780.
35. Evans, R., M. O'Neill, A. Pritzel, N. Antropova, A. Senior, T. Green, A. Žídek, R. Bates, S. Blackwell and J. Yim, *Protein complex prediction with AlphaFold-Multimer.* BioRxiv, 2021: p. 2021.10. 04.463034.
36. Jumper, J., R. Evans, A. Pritzel, T. Green, M. Figurnov, O. Ronneberger, K. Tunyasuvunakool, R. Bates, A. Žídek, A. Potapenko, A. Bridgland, C. Meyer, S.A.A. Kohl, A.J. Ballard, A. Cowie, B. Romera-Paredes, S. Nikolov, R. Jain, J. Adler, T. Back, S. Petersen, D. Reiman, E. Clancy, M. Zielinski, M. Steinegger, M. Pacholska, T. Berghammer, S. Bodenstein, D. Silver, O. Vinyals, A.W. Senior, K. Kavukcuoglu, P. Kohli and D. Hassabis, *Highly accurate protein structure prediction with AlphaFold.* Nature, 2021. **596**(7873): p. 583-589.
37. Varadi, M., S. Anyango, M. Deshpande, S. Nair, C. Natassia, G. Yordanova, D. Yuan, O. Stroe, G. Wood, A. Laydon, A. Žídek, T. Green, K. Tunyasuvunakool, S. Petersen, J. Jumper, E. Clancy, R. Green, A. Vora, M. Lutfi, M. Figurnov, A. Cowie, N. Hobbs, P. Kohli, G. Kleywegt, E. Birney, D. Hassabis and S. Velankar, *AlphaFold Protein Structure Database: massively expanding the structural coverage of protein-sequence space with high-accuracy models.* Nucleic Acids Research, 2021. **50**(D1): p. D439-D444.
38. Maurer, M., W. Gujer, R. Hany and S. Bachmann, *Intracellular carbon flow in phosphorus accumulating organisms from activated sludge systems.* Water Research, 1997. **31**(4): p. 907-917.
39. Morohoshi, T., K. Ogata, T. Okura and S. Sato, *Molecular characterization of the bacterial community in biofilms for degradation of poly (3-hydroxybutyrate-co-3-hydroxyhexanoate) films in seawater.* Microbes and Environments, 2018. **33**(1): p. 19-25.
40. Grigoriev, I.V., H. Nordberg, I. Shabalov, A. Aerts, M. Cantor, D. Goodstein, A. Kuo, S. Minovitsky, R. Nikitin, R.A. Ohm, R. Otillar, A. Poliakov, I. Ratnere, R. Riley, T. Smirnova, D. Rokhsar and I. Dubchak, *The Genome Portal of the Department of Energy Joint Genome Institute.* Nucleic Acids Research, 2011. **40**(D1): p. D26-D32.
41. Nordberg, H., M. Cantor, S. Dusheyko, S. Hua, A. Poliakov, I. Shabalov, T. Smirnova, I.V. Grigoriev and I. Dubchak, *The genome portal of the Department of Energy Joint Genome Institute: 2014 updates.* Nucleic Acids Research, 2014. **42**(D1): p. D26-D31.
42. Kopylova, E., L. Noé and H. Touzet, *SortMeRNA: fast and accurate filtering of ribosomal RNAs in metatranscriptomic data.* Bioinformatics, 2012. **28**(24): p. 3211-3217.
43. Haas, B.J., A. Papanicolaou, M. Yassour, M. Grabherr, P.D. Blood, J. Bowden, M.B. Couger, D. Eccles, B. Li and M. Lieber, De novo *transcript sequence reconstruction from RNA-seq using the Trinity platform for reference generation and analysis.* Nature Protocols, 2013. **8**(8): p. 1494-1512.
44. Altschul, S.F., W. Gish, W. Miller, E.W. Myers and D.J. Lipman, *Basic local alignment search tool.* Journal of Molecular Biology, 1990. **215**(3): p. 403-410.
45. Eddy, S.R., *Accelerated profile HMM searches.* PLoS Computational Biology, 2011. **7**(10): p. e1002195.

46. Sayers, E.W., M. Cavanaugh, K. Clark, K.D. Pruitt, C.L. Schoch, S.T. Sherry and I. Karsch-Mizrachi, *GenBank.* Nucleic Acids Research, 2022. **50**(D1): p. D161.
47. Michellod, D., T. Bien, D. Birgel, M. Violette, M. Kleiner, S. Fearn, C. Zeidler, H.R. Gruber-Vodicka, N. Dubilier and M. Liebeke, De novo *phytosterol synthesis in animals.* Science, 2023. **380**(6644): p. 520-526.
48. Consortium, U., *UniProt: a hub for protein information.* Nucleic Acids Research, 2015. **43**(D1): p. D204-D212.
49. Letunic, I. and P. Bork, *Interactive Tree Of Life (iTOL) v5: an online tool for phylogenetic tree display and annotation.* Nucleic Acids Research, 2021. **49**(W1): p. W293-W296.
50. Yachdav, G., S. Wilzbach, B. Rauscher, R. Sheridan, I. Sillitoe, J. Procter, S.E. Lewis, B. Rost and T. Goldberg, *MSAViewer: interactive JavaScript visualization of multiple sequence alignments.* Bioinformatics, 2016. **32**(22): p. 3501-3503.
51. Teufel, F., J.J. Almagro Armenteros, A.R. Johansen, M.H. Gíslason, S.I. Pihl, K.D. Tsirigos, O. Winther, S. Brunak, G. von Heijne and H. Nielsen, *SignalP 6.0 predicts all five types of signal peptides using protein language models.* Nature Biotechnology, 2022. **40**(7): p. 1023-1025.
52. Hallgren, J., K.D. Tsirigos, M.D. Pedersen, J.J. Almagro Armenteros, P. Marcatili, H. Nielsen, A. Krogh and O. Winther, *DeepTMHMM predicts alpha and beta transmembrane proteins using deep neural networks.* BioRxiv, 2022: p. 2022.04. 08.487609.
53. Viklund, H., A. Bernsel, M. Skwark and A. Elofsson, *SPOCTOPUS: a combined predictor of signal peptides and membrane protein topology.* Bioinformatics, 2008. **24**(24): p. 2928-2929.
54. Jendrossek, D., B. Müller and H.G. Schlegel, *Cloning and characterization of the poly (hydroxyalkanoic acid)-depolymerase gene locus,* phaZ*1, of* Pseudomonas lemoignei *and its gene product.* European Journal of Biochemistry, 1993. **218**(2): p. 701-710.
55. Becker, S. and J.-H. Hehemann, *Laminarin quantification in microalgae with enzymes from marine microbes.* Bio-protocol, 2018. **8**(8): p. e2666-e2666.
56. Qi, X., Y. Sun and S. Xiong, *A single freeze-thawing cycle for highly efficient solubilization of inclusion body proteins and its refolding into bioactive form.* Microbial Cell Factories, 2015. **14**: p. 1-12.
57. Briese, B.H., B. Schmidt and D. Jendrossek, Pseudomonas lemoignei *has five poly (hydroxyalkanoic acid)(PHA) depolymerase genes: a comparative study of bacterial and eukaryotic PHA depolymerases.* Journal of Environmental Polymer Degradation, 1994. **2**: p. 75-87.
58. Pfennig, N. and H.G. Trüper, *The family chromatiaceae*, in *The Prokaryotes: A Handbook on the Biology of Bacteria: Ecophysiology, Isolation, Identification, Applications*. 1992, Springer. p. 3200-3221.

Chapter II

Supplementary Text, Figures and Tables

Supplementary Text

Supplementary Text 1 | PHADs are classified for their substrate use

There are four known classes of PHADs described, aptly named: dPHADscl, dPHADmcl, nPHADscl and nPHADmcl (Figure 1). These classes are named based on their substrate affinity for the size and surface structure of PHA. Short chain PHA (PHAscl) has three to five carbon atoms, while medium chain length PHA (PHAmcl) has more than five carbon atoms in its backbone[1]. The surface structure of the polymer chain also plays a role in the classification of PHA. Native PHA (nPHA) is in an amorphous state with a surface layer of proteins and phospholipids[2]. Extracellular PHA has a partially crystalline surface due to its transport outside of the cell after cell death or lysis. PHADs primary structures reflect the adaptation of the enzyme to the different PHA types[1].

The most studied PHADs are extracellular PHADs that degrade short chain PHA. All experimentally validated extracellular PHADs share a common domain structure composed of a N-terminal signal peptide, a N-terminal catalytic domain formed by a catalytic triad and an oxyanion hole, a lipase box motif, a linker domain of unknown function and a C-terminal substrate binding domain. There are two types of extracellular PHADs degrading short chain PHA. Domain type 1 PHADs have the lipase box motif located behind the oxyanion hole, whereas domain type 2 PHADs have the lipase box motif located before the oxyanion hole[1, 3-6]. In contrast to extracellular PHADs degrading short chain PHA, extracellular PHADs degrading medium chain PHA do not have an identified substrate binding domain and it is assumed that the N-terminal functions to bind to the polymer chain[1, 3, 4]. 16 bacterial taxa[7], 95 genera of fungi[8] and 77 animal species (Chapter 1) encode for extracellular PHADs across ecosystems.

Little is known about intracellular PHA degradation and thus the structure of intracellular PHADs. Likely, intracellular PHA degradation is a cyclic reaction by which PHA is simultaneously built up and degraded. PHA synthesis and degradation genes are located at the outside of the PHA granule[1, 9-12]. Therefore, PHA might function as a constant carbon reservoir that can be quickly remobilized in the absence of a carbon source[1]. Most intracellular PHADs show homology to extracellular

PHADs in the catalytic triad. A serine-asparagine-histidine motif forms the catalytic triad. The catalytic serine residue lies in a lipase box. There are some intracellular PHADs that have a catalytic cysteine replacing the serine residue. In those the lipase box is missing[13]. So far, there is no identified substrate binding domain for intracellular PHADs[14]. Little hallmarks on the protein sequence makes classification of intracellular PHADs often uncertain.

Supplementary Text 2 | PHAD engineering database

Sequence-based homology is often the basis for the classification of PHADs. The most widely used PHAD database is the PHAD engineering database (DED)[14]. The database was constructed using 28 seed sequences covering all PHAD families. These seed sequences were experimentally validated for their activity on nPHAscl/mcl or dPHAscl/mcl. The database was then populated by the data warehouse system for analyzing protein families (DWARF)[15]. DWARF pooled annotated PHAD sequences from publicly available databases, resulting in 735 database entries. The database entries represent eight PHAD superfamilies and 38 homology classes. The two groups of extracellular PHADs degrading short chain PHA, differentiated by the position of the lipase box, represent two superfamilies. Extracellular PHADs degrading short chain PHA of domain type 1 were split into 16 homology classes. Extracellular PHADs degrading short chain PHA of domain type 2 were split into eight homology groups. Intracellular PHADs degrading short chain PHA were divided into two superfamilies: with and without lipase box. The intracellular PHADs degrading short chain PHA with no lipase box included nine homology groups. Intracellular PHADs degrading short chain PHA with a lipase box only included 20 identified proteins[14]. Extracellular PHADs degrading short chain PHA have the highest representation in the database. One possible explanation for this might be the easier classification due to a known protein structure.

Supplementary Text 3 | *Ca.* Thiosymbion species across gutless oligochaete and nematode hosts have a PHAD

We identified seven complete length and four partial length *Ca.* Thiosymbion spp. PHADs. Eight of these PHADs belong to *Ca*. Thiosymbion species of gutless oligochaetes hosts from various environments and two of the PHADs belong to *Ca.* Thiosymbion species of nematode hosts (Supplementary Figure 3). All of them clustered together with their closest relative *Ca.* Kentron sp., indicating structural and evolutionary conservation among *Ca.* T. spp. PHADs (Figure 3).

All *Ca.* T. spp. PHADs showed a complete conservation of the catalytic triad and oxyanion hole when compared to the PHAD from *P. lemoignei* (accession: P52090.1; 29.7-99.8% coverage, 10.4-48.3% identity; Supplementary Figure 3)[16]. We observed that the catalytic serine residue that is embedded in the lipase box was located behind the oxyanion hole. This observation aligns with the phylogenetic clustering of the *Ca.* T. spp. PHADs with extracellular PHADs that have the lipase box located after the oxyanion hole. Two asparagine catalytic residues were not conserved in all *Ca.* T. spp. PHADs in comparison to the PHAD from *P. lemoignei*. All *Ca.* T. spp. PHADs lacked a substrate binding site and signal peptide (Supplementary Figure 3; Supplementary Table 1). Given the conservation of the catalytic site and the absence of the signal peptide, we hypothesize that all *Ca.* T. spp. PHADs show major characteristics of extracellular PHADs but cannot be transported outside of the cell.

All complete-length *Ca.* T. spp. PHADs were predicted to have a transmembrane domain (Supplementary Table 2), similar to the PHAD from *Ca.* T. algarvensis. According to the prediction, the catalytic triad would be located inside the cell, whereas the C-terminal would be outside the cell. A possible explanation could be that the *Ca.* T. spp. PHADs are anchored to the PHA granule inside of the cell. Based on this, we hypothesize that all of the *Ca.* T. spp. PHADs degrade intracellular PHA.

Supplementary Text 4 | Looking for an intracellular PHAD motif

When comparing intracellular and extracellular PHADs, we identified distinct regions of misalignment. Firstly, there is a stretch located at the N-terminal which is present in Chromatiales PHADs. The stretch does not align to extracellular PHADs

(Supplementary Figure 10). The mis-aligned stretch does not show a specific motif but rather reflects the region that intracellular PHADs have instead of a signal peptide. We identified an additional mis-alignment at the C-terminal. The misalignment corresponds to parts of the substrate binding site. These observations align to the general assumptions that intracellular PHADs are different to extracellular PHADs in the substrate binding site and signal peptide[1, 17, 18]. Therefore, we propose that these two regions of misalignment might serve as an initial indicator to differentiate intracellular PHADs and extracellular PHADs. Further effort is needed to test more PHADs experimentally for their activity. Once the function is known, structural differences between intracellular and extracellular PHADs can be elucidated.

Supplementary Text 5 | Pfennig's medium (Modified medium from Eichler and Pfennig, 1988)[19]

Solution 1:

Distilled water	Up to 1000ml with all additions
KH_2PO4	0,34 g
NH_4Cl	0,34g
KCl	0,34 g
$MgSO_4*7H_2O$	0,5 g
$CaCl_2*2H_2O$	0,25 g
Ammonium chloride.	0,35g
Ammonium acetate	0,25g
Pyruvic acid sodium salt	0,25g

Solution 2:

B12	2mg
Distilled water	100ml

Add 1ml of solution 2 to solution 1.

Solution 3 Trace element solution

Distilled water up to	1000ml
Na_2-EDTA	3.00g

$FeSO_4$ x 7 H_2O	1,1g
$CoCl_2$ x 6 H_2O	190mg
$MnCl_2$ x 2 H_2O	50mg
$ZnCl_2$	42mg
$NiCl_2$ x 6 H_2O	24mg
Na_2MoO_4 x 2 H_2O	18mg
H_3BO_3	300mg
$CuCl_2$ x 2 H_2O	2mg

Add 1 ml of solution 3 to solution 1.

Solution 4 Na-bicarbonate solution

Prepare a 7,5% Na-bicarbonate solution

Add 20 ml of solution 4 to solution 1.

Solution 5 Sodium sulfide solution

Add 4 ml of sterile 10 % Na_2S*9H2O solution to solution 1

Rezazurin (see above)

0,1% Resazurin solution	0,5ml
Distilled water	450ml

After mixing and combining the medium the pH is adjusted with sterile 2 M HCl or Na2CO3 to pH 7.2

Supplementary Figures

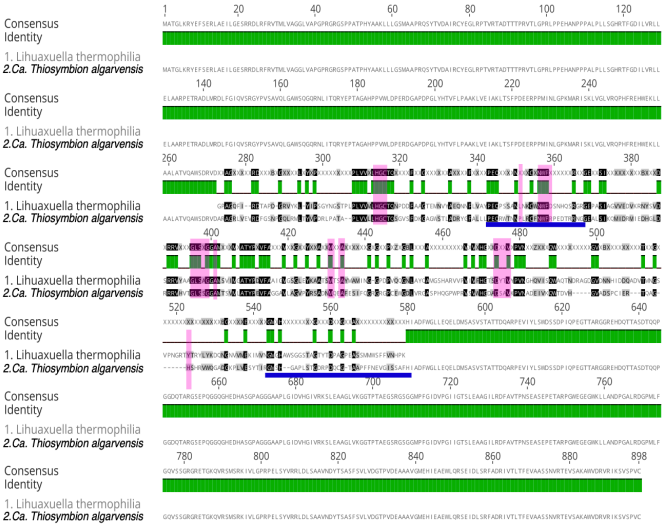

Supplementary Figure 1 | *Ca.* Thiosymbion algarvensis' PHAD showed only homology to the extracellular PHAD of *Lihuaxuella thermophilia* in the catalytic domain. We aligned the *Ca.* T. algarvensis' PHAD with the PHAD from *L. thermophilia*[20] using MAFFT[21]. The alignment was visualized using GeniousPrime (https://www.geneious.com). Alignment of the *Ca.* T. algarvensis' PHAD with the PHAD from *L. thermophilia* showed conservation of 75% of the catalytic residues (highlighted in pink). Only a few hydrophobic residues of the substrate binding site (marked by a blue line) described for *L. thermophilia* were identified in the *Ca.* T. algarvensis PHAD. This observation suggests that the substrate binding site of the *Ca.* T. algarvensis PHAD is different.

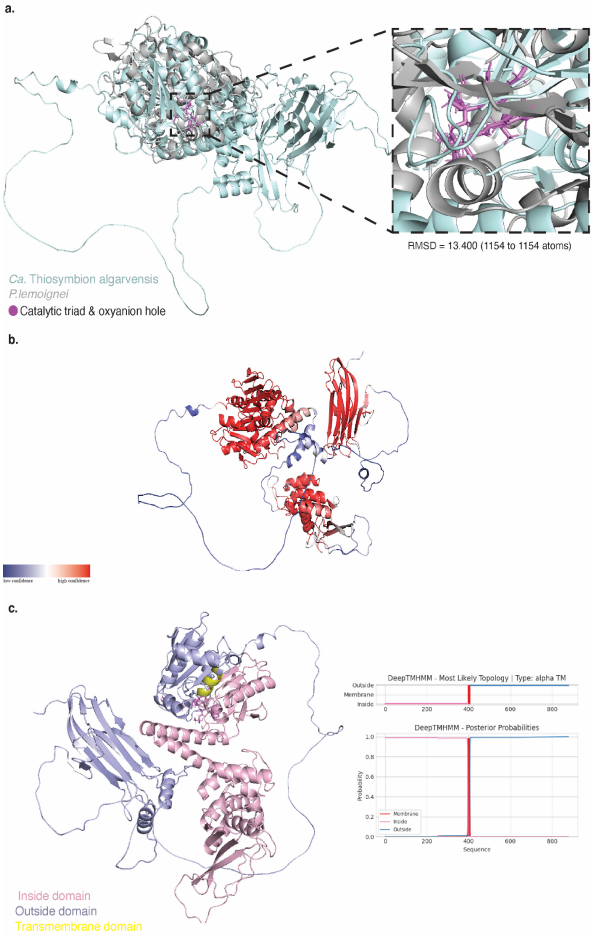
a.
RMSD = 13.400 (1154 to 1154 atoms)
Ca. Thiosymbion algarvensis
P.lemoignei
Catalytic triad & oxyanion hole
b.
low confidence
high confidence
c.
DeepTMHMM - Most Likely Topology | Type: alpha TM
Outside
Membrane
Inside
0
200
400
600
800
DeepTMHMM - Posterior Probabilities
Probability
1.0
0.8
0.6
0.4
0.2
0.0
Membrane
Inside
Outside
Sequence
Inside domain
Outside domain
Transmembrane domain

Supplementary Figure 2 | *Ca.* Thiosymbion algarvensis AlphaFold2 modeled PHAD predicts a transmembrane domain with the catalytic site located to the inside a. We modeled the *Ca.* T. algarvensis' PHAD using AlphaFold2[22-24]. The model was superposed to the crystal structure from *P. lemoignei* (pdb 2x76)[16]. *Ca.* T. algarvensis' PHAD showed good alignment in the core of the enzyme representing the catalytic triad (pink labeling) but other residues showed little homology. The *Ca.* T. algarvensis PHAD showed several subdomains in contrast to the *P. lemoignei* PHAD. **b.** Model statistics of the AlphaFold2 model (predicted local distance difference test (pLDDT)) showed that the core of the enzyme was modeled with high confidence (red color; above 90%), whereas the subdomain connections were poorly modeled (blue color). **c.** Transmembrane prediction by TMHMM[25] suggested that the *Ca.* T. algarvensis' PHAD has a transmembrane domain (yellow labeling). The catalytic domain of the enzyme (pink labeling) is predicted in the inside. Other residues are predicted to be outside (purple labeling).

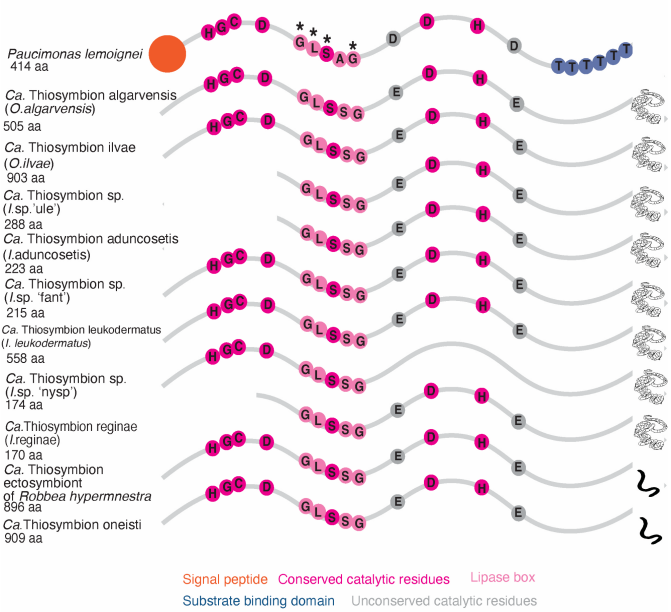

Supplementary Figure 3 | All *Ca.* Thiosymbion spp. 's PHADs showed a nearly complete conservation of the catalytic residues but lacked a substrate binding site and signal peptide. We compared the primary structure of all identified *Ca.* Thiosymbion spp. 's PHADs of the gutless oligochaetes and nematodes to the PHAD of *P. lemoignei*. The *Ca.* T. spp.'s PHADs were aligned using MAFFT[21] to the PHAD from *P. lemoignei* (pdb 2x76)[16]. All sequences showed conservation of nearly all catalytic residues (pink residues) and lipase box motif (light pink residues). The substrate binding site (blue residues) and signal peptide (orange) were missing. Conserved residues among all sequences are marked with an asterisk and non-conserved residues are labeled in gray.

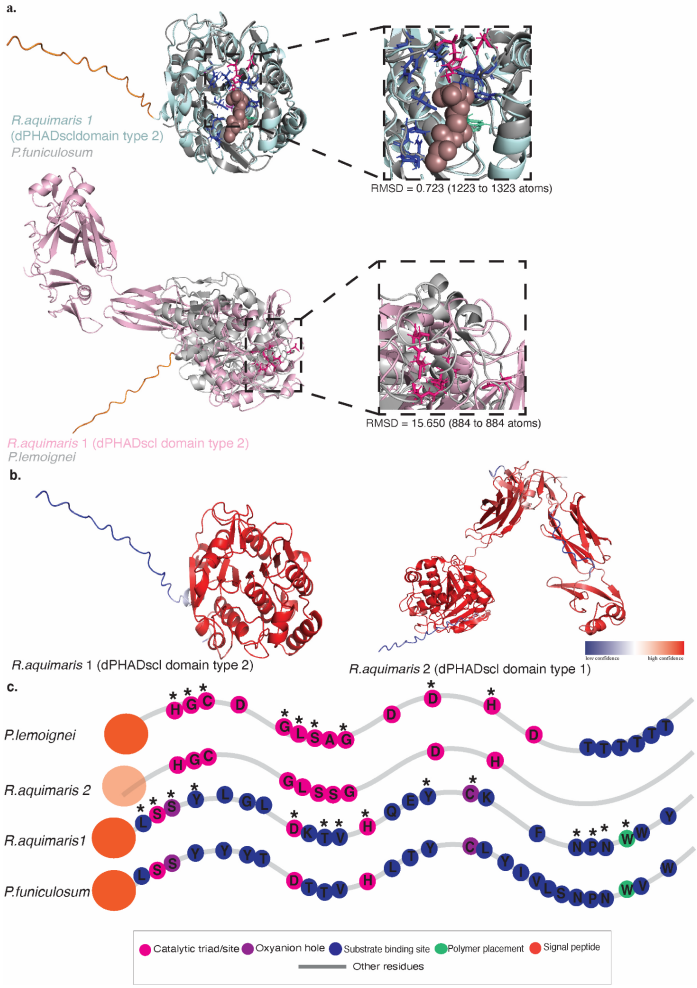
a.
R.aquimaris 1
(dPHADscldomain type 2)
P.funiculosum
RMSD = 0.723 (1223 to 1323 atoms)
RMSD = 15.650 (884 to 884 atoms)
R.aquimaris 1 (dPHADscl domain type 2)
P.lemoignei
b.
R.aquimaris 1 (dPHADscl domain type 2)
R.aquimaris 2 (dPHADscl domain type 1)
c.
P.lemoignei
R.aquimaris 2
R.aquimaris1
P.funiculosum
Catalytic triad/site
Oxyanion hole
Substrate binding site
Polymer placement
Signal peptide
Other residues

Supplementary Figure 4 | *R. aquimaris* has two extracellular PHADs. One of them showed homology to known extracellular PHADs, whereas the other did not. We modeled both *R. aquimaris* PHADs using AlphaFold2[22-24]. The models were either superposed to the PHAD from *P. funiculosum* (pdb 2d81)[26] or *P. lemoignei* (pdb 2x76)[16] in respect to their phylogeny (Figure 3). The primary structure was analyzed by aligning the *R. aquimaris* PHADs to the respective protein sequence that they were modeled to. **a.** One of the *R. aquimaris* PHADs was predicted to be an extracellular PHAD with the lipase box located before the oxyanion hole and showed respective characteristics in comparison to the fungal homolog of *P. funiculosum*. We observed conservation of a signal peptide and substrate binding site. The other *R. aquimaris* PHAD was predicted to be an extracellular PHAD with the lipase box motif behind the oxyanion hole, but showed despite the catalytic site and a low predicted signal peptide no extracellular PHAD characteristics. **b.** AlphaFold2 model statistics (pLDDT) showed that both enzymes were modeled in their core with high confidence (red labeling; above 90%). The subdomain connections of the second *R. aquimaris* PHAD were modeled with lower confidence (blue labeling). **c.** Primary structure alignments of the two *R. aquimaris* PHADs showed the same pattern as suggested by the modeled tertiary structure. Conserved residues among the two PHAD types are marked with an asterisk.

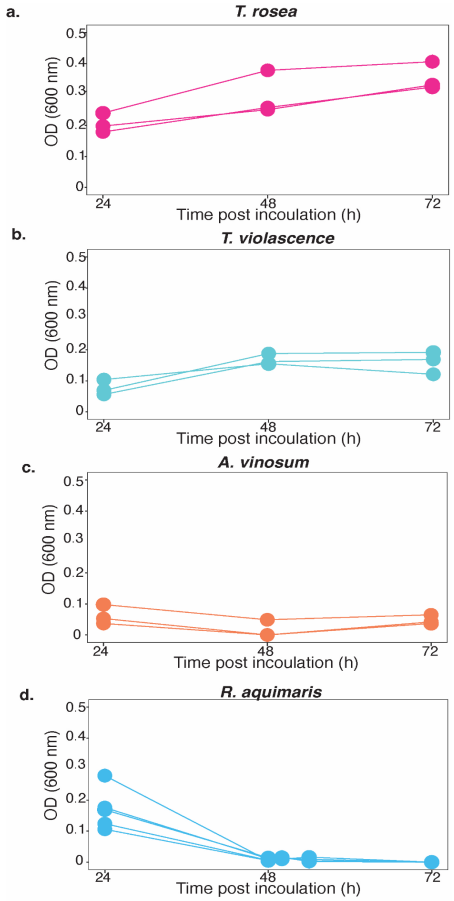
a.
T. rosea
OD (600 nm)
0.5
0.4
0.3
0.2
0.1
0
24
48
72
Time post incoulation (h)
b.
T. violascence
OD (600 nm)
0.5
0.4
0.3
0.2
0.1
0
24
48
72
Time post incoulation (h)
c.
A. vinosum
OD (600 nm)
0.5
0.4
0.3
0.2
0.1
0
24
48
72
Time post incoulation (h)
d.
R. aquimaris
OD (600 nm)
0.5
0.4
0.3
0.2
0.1
0
24
48
72
Time post incoulation (h)

Supplementary Figure 5 | Bacterial densities or exponential growth was maintained for *T. rosea*, *A. vinosum* and *T. violascence* in a medium without an external carbon source. In contrast, *R. aquimaris* did not survive without an external carbon source. a. *T. rosea* and **b**. *T. violascence* cell densities increased in the absence of an external carbon source, suggesting both bacteria used their intracellular PHA to sustain growth. **c.** *A. vinosum* maintained their cell densities. Conversely, **d.** *R. aquimaris* died off during the incubations, suggesting they cannot live without an external carbon source.

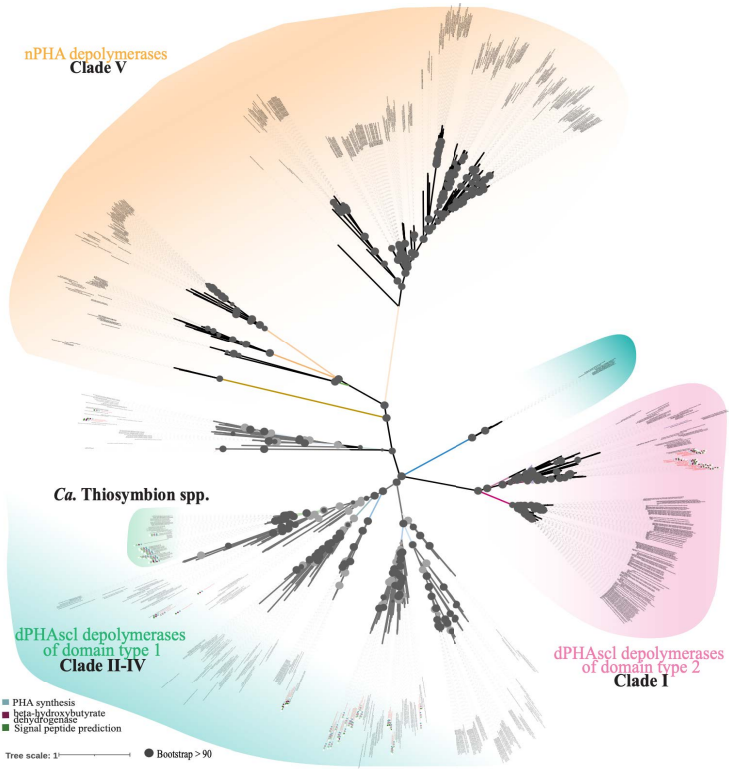

Supplementary Figure 6 | All Chromatiales PHADs grouped with extracellular PHADs. Complete unrooted maximum likelihood tree of the Chromatiales PHADs and classified PHADs according to the PHAD engineering database (DED)[14]. We aligned the identified Chromatiales PHADs with PHADs classified in the DED database using MAFFT[21] and calculated a maximum likelihood tree using IQTree[27] (ultrafast bootstrap support). All Chromatiales PHADs (labeled in Red) clustered with extracellular PHADs, despite that some of them have the ability to synthesize PHA (blue square). Additionally, some Chromatiales species were not predicted to have a signal peptide (green square), suggesting that they cannot be transported outside of the cell. Based on these observations, we hypothesize that some Chromatiales PHADs are in fact intracellular PHADs.

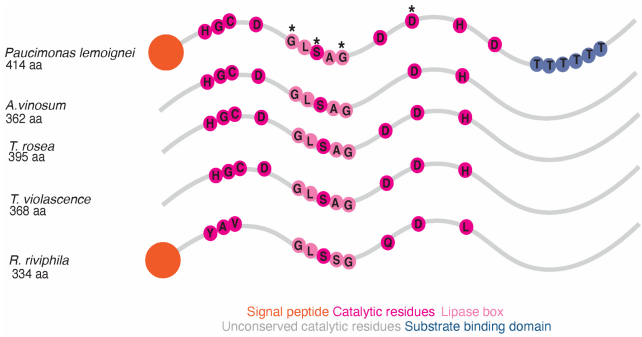

Supplementary Figure 7 | All Chromatiales PHADs are predicted to have a conserved catalytic site. The substrate binding site and signal peptide are different. Conserved residues among all sequences are marked with an asterisk. We aligned the Chromatiales PHADs with the PHAD of *P. lemoignei* (pdb 2x76)[16] using MAFFT[21]. All of the Chromatiales PHADs showed a conserved catalytic site (pink) and lipase box (light pink). We could not detect any substrate binding site motifs (blue) or predict a signal peptide (orange). Together with their experimentally shown activity, this suggests that all are mis-classified as extracellular PHADs.

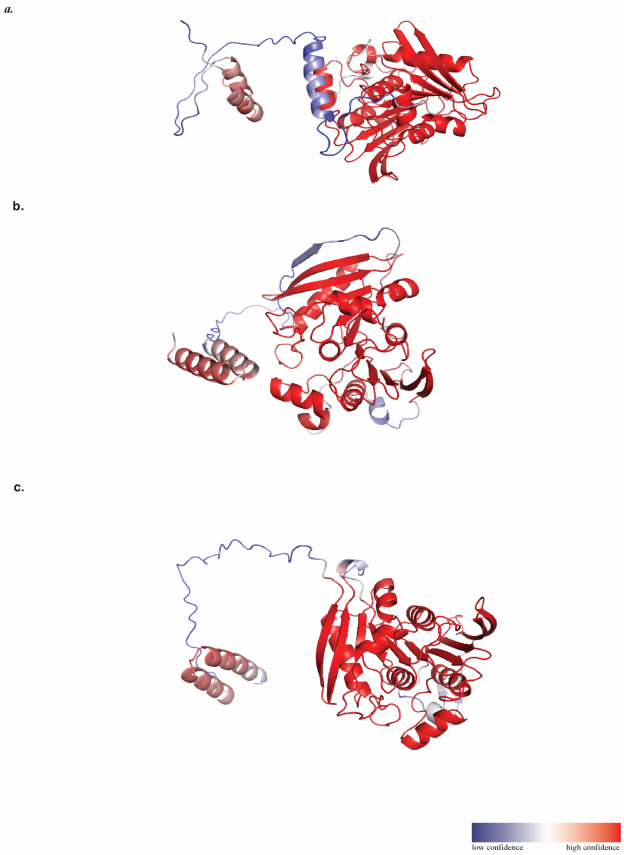

Supplementary Figure 8 | AlphaFold2 predicted local distance test (pLDDT) suggests that all Chromatiales PHADs were modeled with high confidence in the core enzyme. We used the AlphaFold2[22-24] monomer prediction against the full database to create models of the Chromatiales PHADs of **a**. *T. rosea,* **b.** *A. vinosum* and **c.** *T. violascence*. The pLDDT values were visualized in PyMol (version 2.4.0.; The PyMOL Molecular Graphics System, Version 2.0 Schrödinger, LLC) using the model statistics saved in the beta-spectrum of the model. Red color labeling indicates high model confidence (more than 90%) and blue colors indicate poor model quality (below 30%).

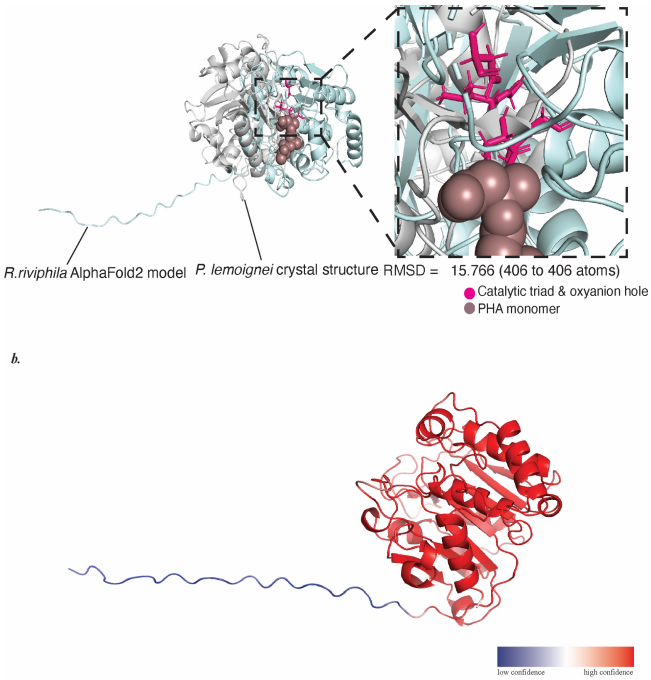

Supplementary Figure 9 | AlphaFold2 model of *R. riviphila* showed little homology to known extracellular PHADs, despite having a signal peptide. a. We used the AlphaFold2[22-24] monomer prediction against the full database to create a model of the *R. riviphila* PHAD. The PHAD showed little homology to the crystal structure of the PHAD from *P. lemoignei* (pdb 2x76)[16] after superposing the two structures. We could not detect any substrate binding site motifs and only parts of the catalytic residues are conserved (pink). **b.** The AlphaFold2 model predictions suggest that the core model was modeled with a high confidence (red labeling, above 90%), whereas the predicted signal peptide was modeled with low confidence (blue labeling) which is typical for signal peptides.

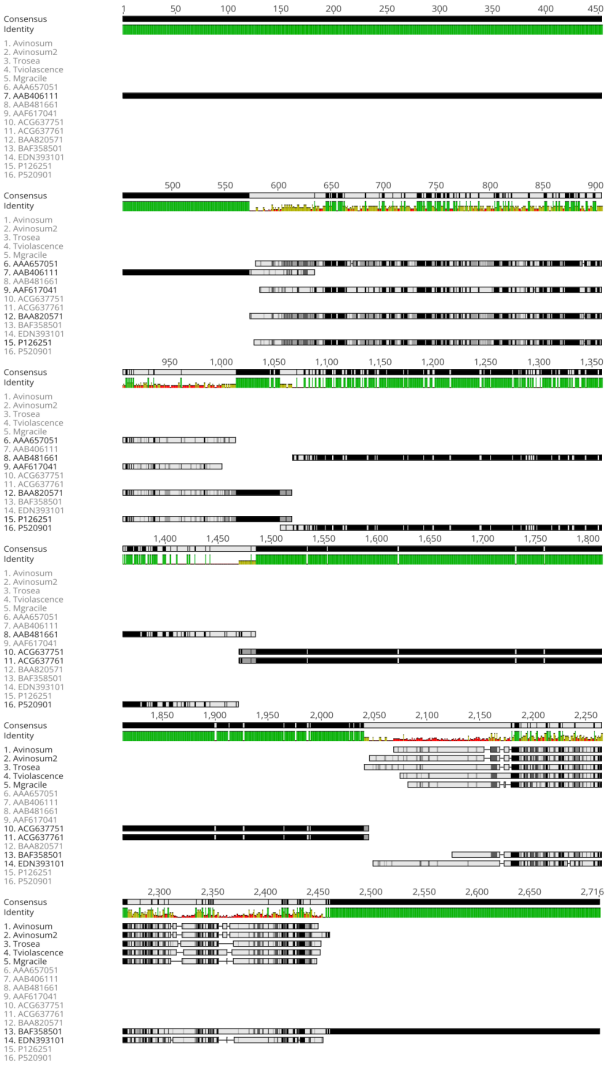
Consensus
Identity
1. Avinosum
2. Avinosum2
3. Trosea
4. Tviolascence
5. Mgracile
6. AAA657051
7. AAB406111
8. AAB481661
9. AAF617041
10. ACG637751
11. ACG637761
12. BAA820571
13. BAF358501
14. EDN393101
15. P126251
16. P520901

Supplementary Figure 10 | Intracellular Chromatiales PHADs were misaligned in the N- terminal signal peptide region and the C-terminal substrate binding site region. We aligned the experimentally verified intracellular Chromatiales PHADs with experimentally validated extracellular PHADs of the PHAD engineering database[14] using MAFFT[21]. The alignment was visualized using GeniousPrime (https://www.geneious.com). The alignment showed little homology. The catalytic residues were 100% aligned but mismatches were found at the signal peptide and substrate binding site, suggesting that these might be interesting regions to consider for the identification of motifs that can separate extracellular from intracellular PHADs.

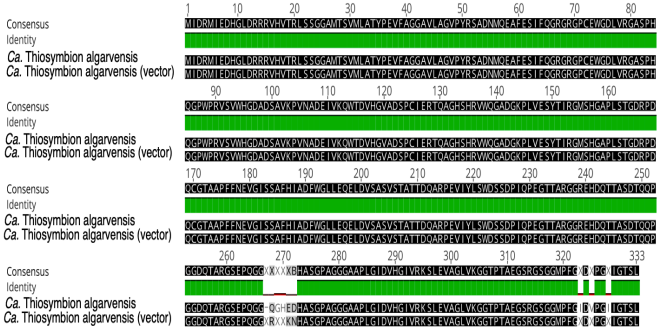

Supplementary Figure 11 | *Ca.* Thiosymbion algarvensis' PHAD was successfully inserted in *E. coli* clones used for heterologous gene expression. The *Ca.* Thiosymbion algarvensis' PHAD aligns to the sequence inserted in the expression vector. We send the expression vector of the *Ca.* Thiosymbion algarvensis' PHAD to Microsynth (Microsynth AG) for plasmid extraction and sequencing. The sequence was with over 350 amino acids too long for the full sequencing but the catalytic domain of the *Ca.* T. algarvensis' PHAD showed nearly complete alignment to the sequenced expression vector. The only mismatch was observed at position 267 to position 275.

Supplementary Tables

Accession	Species	Sec/SPI	TAT	Sec/SPII	Others	Cleavage site	Start codon?
VFK394661	*Candidatus Kentron*	0,0169	0,3658	0,0037	0,6136	No	MPS
TCT191611	*Thiobaca trueperi*	0,0672	0,169	0,0115	0,7523	No	MMM
WP1276988461	*Rheinheimera riviphila*	0,9542	0,0281	0,0051	0,0126	Yes	MDH
WP1276883231	*Rheinheimera sp YQF1*	0,9965	0,0008	0,0017	0,001	Yes	MKT
RVU344031	*Rheinheimera riviphila*	0,4353	0,0043	0,0076	0,5528	maybe	MPM
WP1270255021	*Rheinheimera sp LHK132*	0,9982	0,0004	0,0008	0,0006	Yes	MKT
RRJ209361	*Pararheinheimera mesophila*	0,988	0,0011	0,0062	0,0048	maybe	MKT
WP0897282591	*Candidatus Thiosymbion oneisti*	0,0227	0,2904	0,0053	0,6817	No	MAT
WP0437502231	*Imhoffiella purpurea*	0,0636	0,1338	0,0204	0,7822	No	MKD
WP0152800791	*Thioflavicoccus mobilis*	0,044	0,2734	0,0666	0,616	No	MRD
WP0089003141	*Rheinheimera sp A13L*	0,9969	0,0005	0,0019	0,0006	Yes	MQK
WP0070420381	*Thiorhodococcus drewsii*	0,0606	0,0977	0,0122	0,8295	No	MKD
WP1009204741	*Candidatus Thiodictyon syntrophicum*	0,0114	0,164	0,0013	0,8233	No	MNE
WP0682361741	*Rheinheimera sp EpRS3*	0,9898	0,0007	0,0087	0,0008	Yes	MKK
WP0071943001	*Thiocapsa marina*	0,0132	0,0855	0,003	0,8993	No	MAR
RNE940481	*Marichromatium sp AB32*	0,0243	0,1249	0,0016	0,8491	No	MAD
VFJ912041	*Candidatus Kentron sp H*	0,0239	0,6432	0,0029	0,3301	no	MSG
VFK592461	*Candidatus Kentron sp TUN*	0,0197	0,4755	0,0035	0,5014	no	MPG
VFK635441	*Candidatus Kentron sp TUN*	0,0197	0,4755	0,0035	0,5014	no	MPG
VFJ441611	*Candidatus Kentron sp FW*	0,0281	0,4339	0,0048	0,5332	no	MPT
VFK006791	*Candidatus Kentron sp LFY*	0,0178	0,3172	0,004	0,661	no	MPS
VFK141941	*Candidatus Kentron sp LPFa*	0,0187	0,4451	0,004	0,5322	no	MSG
VFK216981	*Candidatus Kentron sp LPFa*	0,0187	0,4451	0,004	0,5322	no	MSG
VFK659931	*Candidatus Kentron sp UNK*	0,0187	0,4451	0,004	0,5322	no	MSG
VFJ772141	*Candidatus Kentron sp FW*	0,0281	0,4339	0,0048	0,5332	no	MPT
VFK224831	*Candidatus Kentron sp LFY*	0,0178	0,3172	0,004	0,661	no	MPS
VFJ951511	*Candidatus Kentron sp LFY*	0,0178	0,3172	0,004	0,661	no	MPS
VFK282541	*Candidatus Kentron sp MB*	0,0267	0,2527	0,0044	0,7161	no	MPS
VFK508771	*Candidatus Kentron sp TC*	0,0119	0,3881	0,0025	0,5976	no	MSG
VFK639931	*Candidatus Kentron sp TC*	0,0119	0,3881	0,0025	0,5976	no	MSG
VFK419341	*Candidatus Kentron sp TC*	0,0119	0,3881	0,0025	0,5976	no	MSG
VFK792691	*Candidatus Kentron sp SD*	0,0169	0,3658	0,0037	0,6136	no	MPS
RNE905491	*Marichromatium sp AB31*	0,0246	0,1279	0,0017	0,8458	no	MAD
RKT459511	*Thiocapsa rosea*	0,0124	0,0674	0,0037	0,9164	no	MTH
SNY420621	*Rheinheimera tuosuensis*	0,995	0,0013	0,0016	0,0021	Yes	MNN
SNY496521	*Rheinheimera tuosuensis*	0,9219	0,0125	0,0168	0,0488	Yes	MKI
SNY490661	*Rheinheimera tuosuensis*	0,0006	0,0001	0,999	0,0003	Yes	MKL
WP0927938681	*Rheinheimera pacifica*	0,9413	0,0025	0,0493	0,007	Yes	MRK
SEH671221	*Rheinheimera pacifica*	0,0037	0,0001	0,995	0,0003	Yes	MKR
SDW365771	*Thiocapsa roseopersicina*	0,0076	0,0215	0,0016	0,9693	No	MKQ
SDX830831	*Allochromatium warmingii*	0,0032	0,0105	0,0008	0,9855	No	MLI
WP0700507651	*Rheinheimera salexigens*	0,9903	0,0012	0,0035	0,005	Yes	MNL
WP0682382791	*Rheinheimera sp EpRS3*	0,9295	0,0052	0,0484	0,0168	maybe	MHK
WP0680656791	*Rheinheimera sp S41*	0,9275	0,0225	0,0254	0,0247	Yes	MKK
WP2113540261	*Thiohalocapsa marina*	0,0381	0,2496	0,0058	0,7065	No	MTR
WP2053134651	*unclassified Rheinheimera*	0,9915	0,0004	0,0023	0,0058	Yes	MRP
WP2092625381	*Thiorhodococcus minor*	0,0062	0,0195	0,0017	0,9725	No	MID
WP2071685191	*Thiocystis violacea*	0,0247	0,0514	0,0064	0,9174	No	MSA
WP2061715631	*Thiorhodococcus mannitoliphagus*	0,0845	0,477	0,0064	0,4321	maybe	MID
WP2010969571	*Thiocystis minor*	0,0374	0,1339	0,0034	0,8252	No	MKD
WP2003882521	*Thiocapsa imhoffii*	0,0128	0,0653	0,0038	0,918	No	MSP
WP2003762141	*Thiocystis violacea*	0,029	0,0768	0,0049	0,8893	No	MNE
WP2001576451	*Allochromatium vinosum*	0,0061	0,0157	0,0007	0,9775	No	MNE
QQO563011	*Thiohalocapsa sp PBPSB1*	0,9289	0,0008	0,0381	0,0322	Yes	MVK
QQO555441	*Thiohalocapsa sp PBPSB1*	0,9945	0,0004	0,0035	0,0015	Yes	MHG
QQO545081	*Thiohalocapsa sp PBPSB1*	0,0424	0,0002	0,9558	0,0016	Yes	MID
WP1769746121	*Allochromatium humboldtianum*	0,0058	0,0264	0,0007	0,9671	No	MNE
WP1735012621	*Rheinheimera sp YQF2*	0,9584	0,0015	0,0294	0,0107	Yes	MSA
WP1709489641	*Rheinheimera tuosuensis*	0,9685	0,0021	0,0128	0,0166	Yes	MWL
trD3RN5SD3RN58ALLVD	*Allochromatium vinosum*	0,0047	0,0128	0,0007	0,9818	No	MNE
trA0A6G7VCU1A0A6G7VCU19GAMM	*Chromatiaceae bacterium*	0,0082	0,02	0,0018	0,9699	No	MSE
trI3Y7Q8I3Y7Q8THIV	*Thiocystis violascens*	0,0216	0,0227	0,0023	0,9534	No	MKD
trA0A4R3N6P9A0A4R3N6P99GAMM	*Thiobaca trueperi*	0,0102	0,1071	0,0015	0,8811	No	MND
trA0A6M0K396A0A6M0K3969GAMM	*Thiorhodococcus minor*	0,0076	0,0218	0,0019	0,9686	No	MDD
trW0E020W0E020MARPU	*Marichromatium purpuratum*	0,0241	0,0887	0,002	0,8852	No	MAD
VFJ453361	*Candidatus Kentron sp DK*	0,0481	0,4812	0,0058	0,4649	No	MST
VFJ618801	*Candidatus Kentron sp DK*	0,0481	0,4812	0,0058	0,4649	No	MST
WP1686695511	*Marichromatium bheemlicum*	0,0086	0,0407	0,0013	0,9495	No	MSD
WP1668394051	*Rheinheimera pleomorphica*	0,9916	0,005	0,0019	0,0015	maybe	MRL
WP1644550491	*Thiorhodococcus minor*	0,3221	0,0065	0,0489	0,6225	No	MRG
WP1554484081	*Allochromatium palmeri*	0,0076	0,0128	0,0008	0,9788	No	MNE
QGU337121	*Thermochromatium tepidum ATCC 43061*	0,0073	0,0145	0,0014	0,9768	No	MIN
WP0931913551	*Thiocapsa sp KS1*	0,0163	0,1025	0,0036	0,8776	No	MTS
WP0622718141	*Marichromatium gracile*	0,0385	0,1913	0,0033	0,7669	No	MAD
WP0205053671	*Lamprocystis purpurea*	0,0655	0,2379	0,0124	0,6843	No	MKI
WP1479041581	*Rheinheimera tangshanensis*	0,9969	0,0002	0,0024	0,0004	Yes	MKI
TXH984671	*Rheinheimera sp*	0,8117	0,0138	0,1536	0,0209	maybe	MQN
WP1340529121	*Rheinheimera aquimaris*	0,6946	0,0007	0,3031	0,0016	Yes	MKK
WP1335125141	*Candidatus Thiosymbion oneisti*	0,0237	0,2756	0,0055	0,6952	No	MAT
WP1340551281	*Rheinheimera aquimaris*	0,9869	0,0009	0,0101	0,0022	Yes	MRF
WP1325831821	*Rheinheimera sp D18*	0,9865	0,0005	0,0104	0,0027	maybe	MRV
GAB596671	*Rheinheimera nanhaiensis E4078*	0,0012	0,0001	0,9985	0,0002	Yes	MKR
GAB598021	*Rheinheimera nanhaiensis E4078*	0,9916	0,0006	0,0066	0,0013	maybe	MPR
KOO576171	*Rheinheimera sp KL1*	0,9969	0,0002	0,0024	0,0004	Yes	MKI
WP0527501201	*Arsukibacterium sp MJ3*	0,9547	0,0045	0,009	0,0318	Yes	MNN
WP0276706171	*Rheinheimera baltica*	0,9608	0,0065	0,0222	0,0105	Yes	MQA
AFJ450721	*Thiocapsa roseopersicina*	0,0161	0,1123	0,0046	0,867	No	MPR
MCB22640801	*Candidatus Thiosymbion ectosymbiont of Robbea hypermnestra*	0,0147	0,7209	0,0033	0,2511	No	MAT
VFK394661	*Candidatus Kentron sp SD*	0,0169	0,3658	0,0037	0,6136	No	MPS
TVQ861301	*Chromatiaceae bacterium*	0,4794	0,0023	0,4715	0,0469	maybe	MRR
EGM771381	*Rheinheimera sp A13L*	0,9883	0,0006	0,0104	0,0007	Yes	MKT
WP2113540531	*Thiohalocapsa marina*	0,0234	0,1664	0,0042	0,8061	No	MTR
Gamma1	*Candidatus Thiosymbion sp. (O. ilvae)*	0,0201	0,6836	0,0034	0,2928	No	MWA

Gamma1 Oalg	*Candidatus Thiosymbion sp. (O. algarvensis)*	0,0174	0,7447	0,0045	0,2334	No	MAT
MJAOBCJG_03803	*Candidatus Thiosymbion sp. (O. ilvae)*	8E-06	0	1E-06	1	No	MWA
OPDNNKOM_02752	*Candidatus Thiosymbion sp. (O. algarvensis)*	2E-05	0	1E-06	1	No	MAT
MCB22640801	*Candidatus Thiosymbion ectosymbiont of Robbea hypermnestra*	8E-06	0	1E-06	1	No	MAT
WP0897282591	*Candidatus Thiosymbion oneisti*	0	0	0	1	No	MAT
WP1335125141	*Candidatus Thiosymbion oneisti*	0	0	0	1	No	MAT
TRINITYDN15009c0g2i1p1	*Candidatus Thiosymbion sp. (I. sp. FANT)*	1E-06	0	0	1,0001	No	WFR
TRINITYDN15474c0g1i2p1	*Candidatus Thiosymbion sp. (I. sp. FANT)*	2E-05	0	1E-06	1	No	GQL
TRINITYDN30849c1g1i6p1	*Candidatus Thiosymbion sp. (I. leukodermatus)*	0	0	0	1,0001	No	MIN
TRINITYDN30849c1g1i7p1	*Candidatus Thiosymbion sp. (I. leukodermatus)*	0	0	0	1,0001	No	PGQ
TRINITYDN28792c0g1i1p1	*Candidatus Thiosymbion sp. (O. ilvae)*	4E-05	0	1E-06	1	No	GLK
TRINITYDN31819c0g1i1p1	*Candidatus Thiosymbion sp. (O. algarvensis)*	5E-05	0	2E-06	1	No	PGL
TRINITYDN13785c0g1i3p1	*Candidatus Thiosymbion sp. (I. sp. ULE)*	1E-06	0	0	1,0001	No	CPK
TRINITYDN12871c0g1i2p2	*Candidatus Thiosymbion sp. (I. adu.)*	0	0	0	1,0001	No	MAP
TRINITYDN5074c3g7i3p1	*Candidatus Thiosymbion sp. (I. adu.)*	0	0	0	1,0001	No	GFA
TRINITYDN3538c1g1i2p1	*Candidatus Thiosymbion sp. (O. algarvensis)*	3E-05	0	0	1	No	GMS
TRINITYDN6487c0g1i1p1	*Candidatus Thiosymbion sp. (O. algarvensis)*	3E-06	0	0	1,0001	No	MIE
Oalg Gamma1 PHAD	*Candidatus Thiosymbion sp. (O. algarvensis)*	1E-06	0	0	1	No	MID
TRINITY_DN8475_c0_g1_i1,p1	*Candidatus Thiosymbion sp. (I. reg)*	0,0001	0	1E-05	0,9999	No	VTL
TRINITY_DN21337_c0_g1_i1,p1	*Candidatus Thiosymbion sp. (I. sp. NYSP)*	3E-05	0	1E-06	1	No	SIR
TRINITY_DN24511_c1_g1_i3,p1	*Candidatus Thiosymbion sp. (I. sp. NYSP)*	1E-06	0	0	1,0001	No	NFV

Supplementary Table 1 | Only some Chromatiales species were predicted to have a signal peptide. We used SignalP[28] to predict signal peptides of all 93 Chromatiales PHADs and PHADs of *Ca.* Thiosymbion spp. The *Ca.* T. spp. PHADs were not predicted to have a signal peptide.

			THMM			SPOCTOPUS
Accession	**Species**	**Length**	**Inside**	**Transmembrane**	**Outside**	
MJAOBCJG_03803	*Cand. Thiosymbion sp. (O. ilvae)*	903	1-400	401-410	411-903	Outside - Transmembrane - Outside
OPDNNKOM_02752	*Cand. Thiosymbion sp. (O. algarvensis)*	878	1-396	397-406	407-878	Outside - Transmembrane - Outside
MCB22640801	*Cand.Thiosymbion ectosymbiont of Robbea hypermnestra*	869	1-398	399-408	409-869	Outside - Transmembrane - Outside
WP0897282591	*Cand. Thiosymbion oneisti*	909	1-396	397-406	407-909	Outside - Transmembrane - Outside
WP1335125141	*Cand. Thiosymbion oneisti*	909	1-396	397-406	407-909	Outside - Transmembrane - Outside
TRINITYDN15009c0g2i1p1	*Cand. Thiosymbion sp. (I.sp. FANT)*	215			1-215	Outside
TRINITYDN15474c0g1i2p1	*Cand. Thiosymbion sp. (I.sp. FANT)*	235			1-235	Signal Peptide - Outside - Transmembrane - Outside
TRINITYDN30849c1g1i6p1	*Cand. Thiosymbion sp. (I. leukodermatus)*	558	1-558			Outside - Transmembrane - Outside
TRINITYDN30849c1g1i7p1	*Cand. Thiosymbion sp. (I. leukodermatus)*	558	1-558			Outside - Transmembrane - Outside
TRINITYDN28792c0g1i1p1	*Cand. Thiosymbion sp. (O. ilvae)*	897	1-394	395-404	405-897	Outside - Transmembrane - Outside
TRINITYDN31819c0g1i1p1	*Cand. Thiosymbion sp. (O. ilvae)*	898	1-395	396-405	406-898	Outside - Transmembrane - Outside
TRINITYDN13785c0g1i3p1	*Cand. Thiosymbion sp. (I. sp. ULE)*	288			1-288	Outside - Transmembrane - Outside
TRINITYDN12871c0g1i2p2	*Cand. Thiosymbion sp. (I. adu.)*	223			1-223	Outside
TRINITYDN5074c3g7i3p1	*Cand. Thiosymbion sp. (O. algarvensis)*	554			1-554	Outside - Transmembrane - Outside
TRINITYDN3538c1g1i2p1	*Cand. Thiosymbion sp. (O. algarvensis)*	352			1-352	Outside
TRINITYDN6487c0g1i1p1	*Cand. Thiosymbion sp. (O. algarvensis)*	500			1-500	Outside - Transmembrane - Outside
Oalg	*Cand. Thiosymbion sp. (O. algarvensis)*	505			1-505	Outside - Transmembrane - Outside
TRINITY_DN8475_c0_g1_i1,p1	*Candidatus Thiosymbion sp. (I. reg)*	169			1-169	Outside - Transmembrane - Outside
TRINITY_DN21337_c0_g1_i1,p1	*Candidatus Thiosymbion sp. (I. sp. NYSP)*	151			1-151	Outside - Transmembrane - Outside
TRINITY_DN24511_c1_g1_i3,p1	*Candidatus Thiosymbion sp. (I. sp. NYSP)*	173			36-173	Outside - Transmembrane

Supplementary Table 2 | All full-length *Ca*. Thiosymbion spp. PHADs were predicted to have a transmembrane domain. We used TMHMM[25] and SPOCTOPUS[29] to predict transmembrane regions. According to the prediction all full-length *Ca*. Thiosymbion spp. PHADs have a transmembrane region following the catalytic domain. Thus, the catalytic domain is predicted to be inside. A possible explanation could be the anchoring to the PHA granule or the *Ca*. Thiosymbion spp. membrane.

Library	Library type	Species	Extraction	Fixation	Collectiondate sampling_year	sampling_month	Collectionplace ocean	continent	country	island_city	bay_spot	latitude	longitude	Metadata organic_input	sediment_ty	water_depth
4514_AA	totalRNA	*I. reginae*	AllPrep DNA/RNA/Protein Mini Kit (modified)	RNAlater	2017	April	Atlantic	CentralAmerica	Belize	TwinCays	Fishersybeach	16,82356	-88,10617	seagrass	sand	-1,5
4514_AB	totalRNA	*I. reginae*	AllPrep DNA/RNA/Protein Mini Kit (modified)	RNAlater	2017	April	Atlantic	CentralAmerica	Belize	TwinCays	Fishersybeach	16,82356	-88,10617	seagrass	sand	-1
4514_AC	totalRNA	*I. reginae*	AllPrep DNA/RNA/Protein Mini Kit (modified)	RNAlater	2017	April	Atlantic	CentralAmerica	Belize	TwinCays	Fishersybeach	16,82356	-88,10617	seagrass	sand	-1,5
4514_AD	totalRNA	*I. aduncosetis*	AllPrep DNA/RNA/Protein Mini Kit (modified)	RNAlater	2017	April	Atlantic	CentralAmerica	Belize	CurlewCay	a_unknown	16,79011	-88,08201	corals	sand	-2
4514_AE	totalRNA	*I. aduncosetis*	AllPrep DNA/RNA/Protein Mini Kit (modified)	RNAlater	2017	April	Atlantic	CentralAmerica	Belize	CurlewCay	a_unknown	16,79011	-88,08201	corals	sand	-2
4514_AF	totalRNA	*I. aduncosetis*	AllPrep DNA/RNA/Protein Mini Kit (modified)	RNAlater	2017	April	Atlantic	CentralAmerica	Belize	CurlewCay	a_unknown	16,79011	-88,08201	corals	sand	-2
4514_AG	totalRNA	I. sp. 'nyspf	AllPrep DNA/RNA/Protein Mini Kit (modified)	RNAlater	2017	April	Atlantic	CentralAmerica	Belize	CurlewCay	a_unknown	16,79	-88,0826	a_unknown	sand	-1,5
4514_AH	totalRNA	I. sp. 'nyspf	AllPrep DNA/RNA/Protein Mini Kit (modified)	RNAlater	2017	April	Atlantic	CentralAmerica	Belize	CurlewCay	a_unknown	16,79011	-88,08201	corals	sand	-2
4514_AI	totalRNA	I. sp. 'nyspf	AllPrep DNA/RNA/Protein Mini Kit (modified)	RNAlater	2017	April	Atlantic	CentralAmerica	Belize	CurlewCay	a_unknown	16,79014	-88,0818	a_unknown	coral_sand	-2
4514_AJ	totalRNA	I. sp. 'fanf	AllPrep DNA/RNA/Protein Mini Kit (modified)	RNAlater	2017	April	Atlantic	CentralAmerica	Belize	CurlewCay	a_unknown	16,79011	-88,08201	corals	sand	-2
4514_AK	totalRNA	I. sp. 'fanf	AllPrep DNA/RNA/Protein Mini Kit (modified)	RNAlater	2017	April	Atlantic	CentralAmerica	Belize	CurlewCay	a_unknown	16,79011	-88,08201	corals	sand	-2
4514_AL	totalRNA	I. sp. 'fanf	AllPrep DNA/RNA/Protein Mini Kit (modified)	RNAlater	2017	April	Atlantic	CentralAmerica	Belize	CurlewCay	a_unknown	16,79014	-88,0818	a_unknown	coral_sand	-2
4514_AM	totalRNA	I. sp. 'ule'	AllPrep DNA/RNA/Protein Mini Kit (modified)	RNAlater	2017	April	Atlantic	CentralAmerica	Belize	CurlewCay	a_unknown	16,79011	-88,08201	corals	sand	-2
4514_AN	totalRNA	*O. imperfectus*	AllPrep DNA/RNA/Protein Mini Kit (modified)	RNAlater	2017	April	Atlantic	CentralAmerica	Belize	SouthwaterCaye	a_unknown	16,82372	-88,08144	seagrass_algal_plumbs	sand	-8
4514_AO	totalRNA	*O. imperfectus*	AllPrep DNA/RNA/Protein Mini Kit (modified)	RNAlater	2017	April	Atlantic	CentralAmerica	Belize	SouthwaterCaye	a_unknown	16,82372	-88,08144	seagrass_algal_plumbs	sand	-8
4514_AP	totalRNA	*O. imperfectus*	AllPrep DNA/RNA/Protein Mini Kit (modified)	RNAlater	2017	April	Atlantic	CentralAmerica	Belize	SouthwaterCaye	a_unknown	16,8262	-88,0813	seagrass	sand	-1,5
4514_AQ	totalRNA	I. sp. 'nyspf	AllPrep DNA/RNA/Protein Mini Kit (modified)	RNAlater	2017	April	Atlantic	CentralAmerica	Belize	CarrieBowCaye	a_unknown	16,8254	-88,08	seagrass	sand	-2
4514_AR	totalRNA	I. sp. 'nyspf	AllPrep DNA/RNA/Protein Mini Kit (modified)	RNAlater	2017	April	Atlantic	CentralAmerica	Belize	CarrieBowCaye	a_unknown	16,8254	-88,08	seagrass	sand	-2
4514_AS	totalRNA	I. sp. 'nyspf	AllPrep DNA/RNA/Protein Mini Kit (modified)	RNAlater	2017	April	Atlantic	CentralAmerica	Belize	CarrieBowCaye	a_unknown	a_unknown	a_unknown	a_unknown	sand	a_unknown
4514_M	totalRNA	*I. aduncosetis*	AllPrep DNA/RNA/Protein Mini Kit (modified)	RNAlater	2017	April	Atlantic	CentralAmerica	Belize	CurlewCay	a_unknown	16,79011	-88,08201	corals	sand	-2
4514_N	totalRNA	*I. aduncosetis*	AllPrep DNA/RNA/Protein Mini Kit (modified)	RNAlater	2017	April	Atlantic	CentralAmerica	Belize	CurlewCay	a_unknown	16,79011	-88,08201	corals	sand	-2
4514_O	totalRNA	*I. aduncosetis*	AllPrep DNA/RNA/Protein Mini Kit (modified)	RNAlater	2017	April	Atlantic	CentralAmerica	Belize	CurlewCay	a_unknown	16,79011	-88,08201	corals	sand	-2
4514_P	totalRNA	*I. leukodermatus*	AllPrep DNA/RNA/Protein Mini Kit (modified)	RNAlater	2017	April	Atlantic	CentralAmerica	Belize	CarrieBowCaye	a_unknown	16,8025	-88,0822	seagrass	sand	a_unknown
4514_Q	totalRNA	*I. leukodermatus*	AllPrep DNA/RNA/Protein Mini Kit (modified)	RNAlater	2017	April	Atlantic	CentralAmerica	Belize	CarrieBowCaye	a_unknown	a_unknown	a_unknown	a_unknown	sand	a_unknown
4514_R	totalRNA	*I. leukodermatus*	AllPrep DNA/RNA/Protein Mini Kit (modified)	RNAlater	2017	March	Atlantic	CentralAmerica	Belize	CarrieBowCaye	a_unknown	a_unknown	a_unknown	seagrass	sand	-1
4514_S	totalRNA	*I. leukodermatus*	AllPrep DNA/RNA/Protein Mini Kit (modified)	RNAlater	2017	April	Atlantic	CentralAmerica	Belize	CurlewCay	a_unknown	16,79011	-88,08201	corals	sand	-2
4514_T	totalRNA	*I. leukodermatus*	AllPrep DNA/RNA/Protein Mini Kit (modified)	RNAlater	2017	April	Atlantic	CentralAmerica	Belize	CurlewCay	a_unknown	16,79011	-88,08201	corals	sand	-2
4514_U	totalRNA	*I. leukodermatus*	AllPrep DNA/RNA/Protein Mini Kit (modified)	RNAlater	2017	April	Atlantic	CentralAmerica	Belize	CurlewCay	a_unknown	16,79	-88,0826	a_unknown	sand	-1,5
4514_V	totalRNA	*I. leukodermatus*	AllPrep DNA/RNA/Protein Mini Kit (modified)	RNAlater	2017	April	Atlantic	CentralAmerica	Belize	SouthwaterCaye	a_unknown	16,8265	-88,0807	seagrass	sand	-2
4514_W	totalRNA	*I. leukodermatus*	AllPrep DNA/RNA/Protein Mini Kit (modified)	RNAlater	2017	April	Atlantic	CentralAmerica	Belize	SouthwaterCaye	a_unknown	16,8262	-88,0813	seagrass	sand	-1,5
4514_X	totalRNA	*I. leukodermatus*	AllPrep DNA/RNA/Protein Mini Kit (modified)	RNAlater	2017	April	Atlantic	CentralAmerica	Belize	SouthwaterCaye	a_unknown	16,8262	-88,0813	seagrass_algal_plumbs	sand	-1,5
4514_Y	totalRNA	*I. leukodermatus*	AllPrep DNA/RNA/Protein Mini Kit (modified)	RNAlater	2017	April	Atlantic	CentralAmerica	Belize	TwinCays	a_unknown	16,83138	-88,10835	seagrass	sand	-1,5
4514_Z	totalRNA	*I. leukodermatus*	AllPrep DNA/RNA/Protein Mini Kit (modified)	RNAlater	2017	April	Atlantic	CentralAmerica	Belize	TwinCays	a_unknown	16,83138	-88,10835	seagrass	sand	-1,5
4515_A	totalRNA	I. sp. 'guadeloupe'	AllPrep DNA/RNA Micro Kit	RNAlater	a_unknown	a_unknown	Atlantic	CentralAmerica	Guadeloupe	IletCohon	a_unknown	16,21524	-61,53657	seagrass	a_unknown	a_unknown
4515_B	totalRNA	I. sp. 'guadeloupe'	AllPrep DNA/RNA Micro Kit	RNAlater	a_unknown	a_unknown	Atlantic	CentralAmerica	Guadeloupe	IletCohon	a_unknown	16,21524	-61,53657	seagrass	a_unknown	a_unknown
4515_C	totalRNA	I. sp. 'guadeloupe'	AllPrep DNA/RNA Micro Kit	RNAlater	a_unknown	a_unknown	Atlantic	CentralAmerica	Guadeloupe	IletCohon	a_unknown	16,21524	-61,53657	seagrass	a_unknown	a_unknown
4515_D	totalRNA	a_unkown	AllPrep DNA/RNA Micro Kit	RNAlater	2015	May	Atlantic	CentralAmerica	Bermuda	a_unknown	HarringtonSound	a_unknown	a_unknown	a_unknown	a_unknown	a_unknown
4515_E	totalRNA	*I. leukodermatus*	AllPrep DNA/RNA Micro Kit	RNAlater	2015	May	Atlantic	CentralAmerica	Bermuda	a_unknown	HarringtonSound	a_unknown	a_unknown	a_unknown	a_unknown	a_unknown
4515_F	totalRNA	*I. leukodermatus*	AllPrep DNA/RNA Micro Kit	RNAlater	2015	May	Atlantic	CentralAmerica	Bermuda	a_unknown	HarringtonSound	a_unknown	a_unknown	a_unknown	a_unknown	a_unknown
4515_G	totalRNA	*O. ilvae*	AllPrep DNA/RNA Micro Kit	RNAlater	2017	May	Mediterr	Europe	Italy	Elba	SantAndrea	-42,80818	10,1429	seagrass	silicate_sand	-6
4515_H	totalRNA	*O. ilvae*	AllPrep DNA/RNA Micro Kit	RNAlater	2017	May	Mediterr	Europe	Italy	Elba	SantAndrea	-42,80818	10,1429	seagrass	silicate_sand	-6
4515_I	totalRNA	*O. ilvae*	AllPrep DNA/RNA Micro Kit	RNAlater	2017	May	Mediterr	Europe	Italy	Elba	SantAndrea	-42,80818	10,1429	seagrass	silicate_sand	-6
4515_J	totalRNA	*I. leukodermatus*	AllPrep DNA/RNA Micro Kit	RNAlater	2017	April	Atlantic	CentralAmerica	Belize	TwinCays	a_unknown	16,83138	-88,10835	seagrass	coral_sand	1,5
4515_K	totalRNA	I. sp. 'ule'	AllPrep DNA/RNA Micro Kit	RNAlater	2017	April	Atlantic	CentralAmerica	Belize	CurlewCay	a_unknown	16,79011	-88,08201	corals	coral_sand	2
4515_L	totalRNA	I. sp. 'ule'	AllPrep DNA/RNA Micro Kit	RNAlater	2017	April	Atlantic	CentralAmerica	Belize	CurlewCay	a_unknown	16,79011	-88,08201	corals	coral_sand	2
4731_A_662	totalRNA	*O. algarvensis*	AllPrep DNA/RNATProtein Mini kit	RNAlater	2020	a_unknown	Mediterr	Europe	Italy	Elba	SantAndrea	-42,80818	10,1429	seagrass	silicate_sand	-6
4731_A_665	totalRNA	*O. algarvensis*	AllPrep DNA/RNATProtein Mini kit	RNAlater	2020	a_unknown	Mediterr	Europe	Italy	Elba	SantAndrea	-42,80818	10,1429	seagrass	silicate_sand	-6
4731_B_662	totalRNA	*O. algarvensis*	AllPrep DNA/RNATProtein Mini kit	RNAlater	2020	a_unknown	Mediterr	Europe	Italy	Elba	SantAndrea	-42,80818	10,1429	seagrass	silicate_sand	-6
4731_B_665	totalRNA	*O. algarvensis*	AllPrep DNA/RNATProtein Mini kit	RNAlater	2020	a_unknown	Mediterr	Europe	Italy	Elba	SantAndrea	-42,80818	10,1429	seagrass	silicate_sand	-6
4731_C_662	totalRNA	*O. algarvensis*	AllPrep DNA/RNATProtein Mini kit	RNAlater	2020	a_unknown	Mediterr	Europe	Italy	Elba	SantAndrea	-42,80818	10,1429	seagrass	silicate_sand	-6
4731_C_665	totalRNA	*O. algarvensis*	AllPrep DNA/RNATProtein Mini kit	RNAlater	2020	a_unknown	Mediterr	Europe	Italy	Elba	SantAndrea	-42,80818	10,1429	seagrass	silicate_sand	-6
4731_D_662	totalRNA	*O. algarvensis*	AllPrep DNA/RNATProtein Mini kit	RNAlater	2020	a_unknown	Mediterr	Europe	Italy	Elba	SantAndrea	-42,80818	10,1429	seagrass	silicate_sand	-6
4731_D_665	totalRNA	*O. algarvensis*	AllPrep DNA/RNATProtein Mini kit	RNAlater	2020	a_unknown	Mediterr	Europe	Italy	Elba	SantAndrea	-42,80818	10,1429	seagrass	silicate_sand	-6
4731_E_662	totalRNA	*O. algarvensis*	AllPrep DNA/RNATProtein Mini kit	RNAlater	2020	a_unknown	Mediterr	Europe	Italy	Elba	SantAndrea	-42,80818	10,1429	seagrass	silicate_sand	-6
4731_E_665	totalRNA	*O. algarvensis*	AllPrep DNA/RNATProtein Mini kit	RNAlater	2020	a_unknown	Mediterr	Europe	Italy	Elba	SantAndrea	-42,80818	10,1429	seagrass	silicate_sand	-6
4731_F_662	totalRNA	*O. algarvensis*	AllPrep DNA/RNATProtein Mini kit	RNAlater	2020	a_unknown	Mediterr	Europe	Italy	Elba	SantAndrea	-42,80818	10,1429	seagrass	silicate_sand	-6
4731_F_665	totalRNA	*O. algarvensis*	AllPrep DNA/RNATProtein Mini kit	RNAlater	2020	a_unknown	Mediterr	Europe	Italy	Elba	SantAndrea	-42,80818	10,1429	seagrass	silicate_sand	-6

Library	Reads	Coverag [Mb]	Assembly quality Total trinity 'genes'	Total trinity transcripts	GC	Median contig lengt	Average contig	total assembled bases	N50
4514_AA	25830295	5247,6	33938	56536	49,22	339	395,17	22341490	416
4514_AB	25047923	5088,7	50559	80930	48,3	348	404,48	32734915	429
4514_AC	24499337	4977,2	43238	72690	48,04	347	407,75	29639279	433
4514_AD	28024869	5693,5	62376	100405	48,54	346	401,92	40355277	426
4514_AE	24153563	4907	83754	131511	46,69	366	429,88	56534170	464
4514_AF	23668423	4808,4	74042	119929	46,73	362	428,83	51428679	462
4514_AG	26120295	5306,5	64470	105013	47,91	344	407,8	42824198	434
4514_AH	23783308	4831,8	45576	63850	47,95	351	426,22	27214053	457
4514_AI	24832955	5045	91375	144892	46,78	332	394,57	57169405	415
4514_AJ	23521018	4778,5	56939	94193	48,77	342	396,8	37375887	417
4514_AK	22405251	4551,8	55031	89220	49,49	353	414,47	36978713	442
4514_AL	32969226	6697,9	71981	119080	47,66	341	397,07	47283514	419
4514_AM	22691441	4609,9	54992	87083	47,64	345	397,01	34573003	420
4514_AN	34425514	6993,8	45271	7896	45,62	355	422,02	33000020	453
4514_AO	23265770	4726,6	43059	72268	46,35	362	429,67	31051616	463
4514_AP	29856064	6065,5	30630	44690	46,2	382	447,83	20013714	486
4514_AQ	23802716	4835,7	104933	162589	46,71	338	409,9	66644619	436
4514_AR	25747030	5230,7	81588	135660	47,02	331	385,93	52355901	407
4514_AS	25426640	5165,6	100298	162321	47,1	338	404,22	65614046	429
4514_M	24987160	5076,3	68151	110875	47,29	352	413,82	45882346	443
4514_N	25279506	5135,7	52468	88403	48,2	355	418,2	36970332	448
4514_O	26588436	5401,6	82862	134460	47,6	361	434,54	58428731	471
4514_P	23568880	4788,2	57248	89184	48,65	345	409,92	36558491	437
4514_Q	25232255	5126,1	50822	80599	48,71	347	411,72	33184496	437
4514_R	25945968	5271,1	102822	158291	46,33	364	436,42	69080787	473
4514_S	24064672	4888,9	58856	92874	49,12	345	400,15	37163410	424
4514_T	22664047	4604,4	46324	73376	48,4	348	403,65	29618014	429
4514_U	22391399	4549	18705	26109	51,36	346	418,47	10925798	446
4514_V	24296326	4936	87569	138623	47,08	333	392,34	54387256	414
4514_W	24514492	4980,3	51350	82984	48,6	344	408,45	33894937	432
4514_X	22308173	4532,1	43896	72195	48,8	352	413,33	29840083	443

4514_Y	28899666	5871,2	28405	37850	49,68	342	425,13	16091094	452
4514_Z	26115144	5305,5	26128	41134	48,66	335	381,5	15692695	399
4515_A	32257284	6553,3	113190	197615	46,26	304	351,99	67922778	348
4515_B	23044753	4681,7	92763	156044	45,86	305	345,16	53859425	351
4515_C	24484477	4974,2	98342	173245	45,57	296	332,93	57678845	336
4515_D	23396934	4753,3	92762	151671	46,26	387	468,8	71102997	519
4515_E	34990407	7108,6	148788	242946	47,06	366	465,79	113161685	518
4515_F	23788274	4832,8	108599	168726	47,45	363	452,63	76369939	498
4515_G	32986255	6701,4	76281	90565	49,18	292	425,38	38524346	430
4515_H	32913293	6686,6	92630	110373	49,06	290	426,75	47101987	433
4515_I	33752419	6857,1	74875	88394	49,31	290	436,35	38570641	445
4515_J	25028450	5084,7	37828	66228	47,37	312	351,8	23298705	360
4515_K	26158475	5314,3	107685	181771	46,45	366	442,32	80400811	480
4515_L	25624632	5205,8	48586	83513	48	367	435,91	36404530	471
4731_A_662	10558852	2145,1	26579	30442	49,58	322	471,3	14347435	500
4731_A_665	7991270	1623,5	19985	22752	50,14	333	489,29	11132311	529
4731_B_662	9133184	1855,5	18790	21143	51,18	331	506,39	10706548	562
4731_B_665	10797779	2193,7	19991	22657	50,79	345	533,87	12095991	606
4731_C_662	12699119	2579,9	48846	58226	47,99	330	477,33	27793274	509
4731_C_665	7035570	1429,3	28872	33991	48,89	332	482,1	16387027	516
4731_D_662	13840901	2811,9	26363	30149	49,9	332	488,95	14741323	525
4731_D_665	4294836	872,53	9630	10625	52,32	337	473,08	5026424	511
4731_E_662	12778571	2596,1	29456	33938	49,6	330	489,55	16614463	528
4731_E_665	6005892	1220,1	15695	17742	51,05	331	497,75	8831132	552
4731_F_662	12313775	2501,6	57437	67483	47,1	332	472,67	31897315	501
4731_F_665	6213396	1262,3	32743	37565	48,08	331	464,89	174637422	486

Supplementary Table 3 | We used 56 total RNA libraries of various gutless oligochaete hosts in this study. Between 2015 and 2020 we sampled 15 gutless oligochaete hosts across ecosystems. We generated total RNA libraries that we assembled using Trinity[30]. The assembly resulted in a N50 value ranging from 348 bp to 606 bp.

Species	DSMZ Accession	Culture medium	Culture Temperature	PHA enrichment culture time	Light conditions?
Allochromatium vinosum	183	Anaerobic Pfennigs medium	25°C	2 weeks	Yes
Thiocpasa rosea	6611	Anaerobic Pfennigs medium	25°C	1 week	Yes
Thiocystis violascens	198	Anaerobic Pfennigs medium	25°C	2 weeks +	Yes
Rheinheimera aquimaris	22681	Aerobic BACTO marine broth medium	37°C	2 days	No

Supplementary Table 4 | We cultured four Chromatiales strains obtained from the DSMZ. We first enriched Chromatiales in PHA using either an anaerobic Pfennig's medium (Supplementary Text 5)[19] or aerobic BACTO marine broth. The anaerobic cultures were incubated for more than 2 weeks at 25°C under light conditions. The aerobic strain *R. aquimaris* was cultured for two days at 37°C without light.

References

1. Jendrossek, D. and R. Handrick, *Microbial degradation of polyhydroxyalkanoates.* Annual Review of Microbiology, 2002. **56**: p. 403.
2. Amor, S.R., T. Rayment and J.K. Sanders, *Poly (hydroxybutyrate)* in vivo*: NMR and x-ray characterization of the elastomeric state.* Macromolecules, 1991. **24**(16): p. 4583-4588.
3. Jaeger, K.-E., A. Steinbüchel and D. Jendrossek, *Substrate specificities of bacterial polyhydroxyalkanoate depolymerases and lipases: bacterial lipases hydrolyze poly (omega-hydroxyalkanoates).* Applied and Environmental Microbiology, 1995. **61**(8): p. 3113-3118.
4. Behrends, A., B. Klingbeil and D. Jendrossek, *Poly (3-hydroxybutyrate) depolymerases bind to their substrate by a C-terminal located substrate binding site.* FEMS Microbiology Letters, 1996. **143**(2-3): p. 191-194.
5. Kasuya, K.-i., T. Ohura, K. Masuda and Y. Doi, *Substrate and binding specificities of bacterial polyhydroxybutyrate depolymerases.* International Journal of Biological Macromolecules, 1999. **24**(4): p. 329-336.
6. Ohura, T., K.-I. Kasuya and Y. Doi, *Cloning and characterization of the polyhydroxybutyrate depolymerase gene of* Pseudomonas stutzeri *and analysis of the function of substrate-binding domains.* Applied and Environmental Microbiology, 1999. **65**(1): p. 189-197.
7. Viljakainen, V. and L. Hug, *The phylogenetic and global distribution of bacterial polyhydroxyalkanoate bioplastic-degrading genes.* Environmental Microbiology, 2021. **23**(3): p. 1717-1731.
8. Neumeier, S., *Abbau thermoplastischer Biopolymere auf Poly-β-Hydroxyalkanoat-Basis durch terrestrische und marine Pilze*. 1994, Diplomarbeit, Universität Regensburg: 99 pp.
9. Oeding, V. and H.G. Schlegel, *β-Ketothiolase from* Hydrogenomonas eutropha *H16 and its significance in the regulation of poly-β-hydroxybutyrate metabolism.* Biochemical Journal, 1973. **134**(1): p. 239-248.
10. Senior, P.J. and E.A. Dawes, *The regulation of poly-beta-hydroxybutyrate metabolism in* Azotobacter beijerinckii. Biochemical Journal, 1973. **134**(1): p. 225-38.
11. Griebel, R. and J. Merrick, *Metabolism of poly-β-hydroxybutyrate: effect of mild alkaline extraction on native poly-β-hydroxybutyrate granules.* Journal of Bacteriology, 1971. **108**(2): p. 782-789.
12. Mayer, F., M.H. Madkour, U. Pieper-fürst, R. Wieczorek, M. Liebergesell and A. Steinbüchel, *Electron microscopic observations on the macromolecular organization of the boundary layer of bacterial PHA inclusion bodies.* The Journal of General and Applied Microbiology, 1996. **42**(6): p. 445-455.
13. Handrick, R., S. Reinhardt and D. Jendrossek, *Mobilization of poly (3-hydroxybutyrate) in* Ralstonia eutropha. Journal of Bacteriology, 2000. **182**(20): p. 5916-5918.
14. Knoll, M., T.M. Hamm, F. Wagner, V. Martinez and J. Pleiss, *The PHA depolymerase engineering database: a systematic analysis tool for the diverse family of polyhydroxyalkanoate (PHA) depolymerases.* BMC Bioinformatics, 2009. **10**: p. 1-8.

15. Fischer, M., Q.K. Thai, M. Grieb and J. Pleiss, *DWARF–a data warehouse system for analyzing protein families.* BMC Bioinformatics, 2006. **7**: p. 1-10.
16. Wakadkar, S., S. Hermawan, D. Jendrossek and A.C. Papageorgiou, *The structure of* PhaZ*7 at atomic (1.2 Å) resolution reveals details of the active site and suggests a substrate-binding mode.* Acta Crystallographica Section F: Structural Biology and Crystallization Communications, 2010. **66**(6): p. 648-654.
17. Abe, T., T. Kobayashi and T. Saito, *Properties of a novel intracellular poly (3-hydroxybutyrate) depolymerase with high specific activity (*PhaZ*d) in* Wautersia eutropha *H16.* Journal of Bacteriology, 2005. **187**(20): p. 6982-6990.
18. Handrick, R., S. Reinhardt, P. Kimmig and D. Jendrossek, *The "intracellular" poly (3-hydroxybutyrate)(PHB) depolymerase of* Rhodospirillum rubrum *is a periplasm-located protein with specificity for native PHB and with structural similarity to extracellular PHB depolymerases.* Journal of Bacteriology, 2004. **186**(21): p. 7243-7253.
19. Pfennig, N. and H.G. Trüper, *The family chromatiaceae*, in *The Prokaryotes: A Handbook on the Biology of Bacteria: Ecophysiology, Isolation, Identification, Applications*. 1992, Springer. p. 3200-3221.
20. Thomas, G.M., S. Quirk, D.J. Huard and R.L. Lieberman, *Bioplastic degradation by a polyhydroxybutyrate depolymerase from a thermophilic soil bacterium.* Protein Science, 2022. **31**(11): p. e4470.
21. Katoh, K. and D.M. Standley, *MAFFT multiple sequence alignment software version 7: improvements in performance and usability.* Molecular Biology and Evolution, 2013. **30**(4): p. 772-780.
22. Evans, R., M. O'Neill, A. Pritzel, N. Antropova, A. Senior, T. Green, A. Žídek, R. Bates, S. Blackwell and J. Yim, *Protein complex prediction with AlphaFold-Multimer.* BioRxiv, 2021: p. 2021.10. 04.463034.
23. Jumper, J., R. Evans, A. Pritzel, T. Green, M. Figurnov, O. Ronneberger, K. Tunyasuvunakool, R. Bates, A. Žídek, A. Potapenko, A. Bridgland, C. Meyer, S.A.A. Kohl, A.J. Ballard, A. Cowie, B. Romera-Paredes, S. Nikolov, R. Jain, J. Adler, T. Back, S. Petersen, D. Reiman, E. Clancy, M. Zielinski, M. Steinegger, M. Pacholska, T. Berghammer, S. Bodenstein, D. Silver, O. Vinyals, A.W. Senior, K. Kavukcuoglu, P. Kohli and D. Hassabis, *Highly accurate protein structure prediction with AlphaFold.* Nature, 2021. **596**(7873): p. 583-589.
24. Varadi, M., S. Anyango, M. Deshpande, S. Nair, C. Natassia, G. Yordanova, D. Yuan, O. Stroe, G. Wood, A. Laydon, A. Žídek, T. Green, K. Tunyasuvunakool, S. Petersen, J. Jumper, E. Clancy, R. Green, A. Vora, M. Lutfi, M. Figurnov, A. Cowie, N. Hobbs, P. Kohli, G. Kleywegt, E. Birney, D. Hassabis and S. Velankar, *AlphaFold Protein Structure Database: massively expanding the structural coverage of protein-sequence space with high-accuracy models.* Nucleic Acids Research, 2021. **50**(D1): p. D439-D444.
25. Hallgren, J., K.D. Tsirigos, M.D. Pedersen, J.J. Almagro Armenteros, P. Marcatili, H. Nielsen, A. Krogh and O. Winther, *DeepTMHMM predicts alpha and beta transmembrane proteins using deep neural networks.* BioRxiv, 2022: p. 2022.04. 08.487609.
26. Hisano, T., K. Kasuya, Y. Tezuka, N. Ishii, T. Kobayashi, M. Shiraki, E. Oroudjev, H. Hansma, T. Iwata, Y. Doi, T. Saito and K. Miki, *The crystal structure of polyhydroxybutyrate depolymerase from* Penicillium

funiculosum *provides insights into the recognition and degradation of biopolyesters.* Journal of Molecular Biology, 2006. **356**(4): p. 993-1004.

27. Minh, B.Q., H.A. Schmidt, O. Chernomor, D. Schrempf, M.D. Woodhams, A. von Haeseler and R. Lanfear, *IQ-TREE 2: New Models and Efficient Methods for Phylogenetic Inference in the Genomic Era.* Molecular Biology and Evolution, 2020. **37**(5): p. 1530-1534.
28. Teufel, F., J.J. Almagro Armenteros, A.R. Johansen, M.H. Gíslason, S.I. Pihl, K.D. Tsirigos, O. Winther, S. Brunak, G. von Heijne and H. Nielsen, *SignalP 6.0 predicts all five types of signal peptides using protein language models.* Nature Biotechnology, 2022. **40**(7): p. 1023-1025.
29. Viklund, H., A. Bernsel, M. Skwark and A. Elofsson, *SPOCTOPUS: a combined predictor of signal peptides and membrane protein topology.* Bioinformatics, 2008. **24**(24): p. 2928-2929.
30. Haas, B.J., A. Papanicolaou, M. Yassour, M. Grabherr, P.D. Blood, J. Bowden, M.B. Couger, D. Eccles, B. Li and M. Lieber, De novo *transcript sequence reconstruction from RNA-seq using the Trinity platform for reference generation and analysis.* Nature protocols, 2013. **8**(8): p. 1494-1512.

Chapter III

Earthworms degrade the bioplastic polyhydroxyalkanoate

Chapter III | Earthworms degrade the bioplastic polyhydroxyalkanoate

Caroline Zeidler[1], Nicole Dubilier[1*], Maggie Sogin[2*]

[1] Max-Planck Institute for Marine Microbiology, Celsiusstraße 1, 29395 Bremen, Germany

[2] University of California at Merced,Merced, CA 95343, USA

*Corresponding authors: **esogin@ucmerced.edu**, **ndubilier@mpi-bremen.de**

[+] *The manuscript is a draft and has not been revised by all authors.*

[+] Author contribution: C.Z. and E.S. conceived the study. C.Z. ran analysis and analyzed the data. C.Z. drafted the manuscript, with support from E.S.

Abstract

Terrestrial soil systems store more carbon than the vegetation and atmosphere combined. Polyhydroxyalkanoates (PHAs) are an important storage compound found in terrestrial soil systems, ranging from 1.2 µg C g-1 to 4.3 µg C g-1 (soil). In a previous study we showed that 77 animal species representing nine animal phyla encode for a PHA depolymerase (PHAD). These animal species likely gain a nutritional advantage from PHA degradation. Among the animal PHADs were five earthworm PHAD homologs representing three globally distributed species. We analyzed the earthworm PHADs for their ability to degrade PHA, the localization of the expression and the benefit for the earthworms. The *Lumbricus rubellus* PHAD showed activity on extracellular PHA, suggesting that it can lyse PHA taken up with its nutrition. However, the earthworm expressed the PHAD protein in the epidermis, contradicting our initial hypothesis. Based on the localization of the PHAD, we hypothesized that *L. rubellus* might excrete the PHAD through the gland cells. The PHAD could degrade PHA of invading bacteria after their lysis. Alternatively, *L. rubellus* excretes the PHAD into the burrowed casts to degrade extracellular PHA found in soil. We could not identify if earthworm PHA degradation provides a nutritional benefit for the earthworms. Therefore, we propose that future studies should focus on the benefits for animals from PHA degradation.

Introduction

Globally, soil organic matter (SOM) contributes to more carbon than found in vegetation and atmosphere. A large fraction of SOM is formed by the microbial biomass[1-4]. In soils, polyhydroxyalkanoate (PHA) concentrations range between 1.2 µg C g-1 (soil) in forest soils and 4.3 µg C g-1 (soil) in agricultural land, constituting approximately 2.5% to 4.2% of the microbial carbon pool[5, 6]. PHAs are naturally occurring carbon storage compounds synthesized by many bacteria and halophilic archaea in various environments, including terrestrial soil systems[7-10]. Within organisms, PHA can make up to 90% of the organism's dry weight. PHA is built up when carbon is in excess but nutrients, e.g. nitrogen or phosphate, are limiting[11, 12]. Once nutrient limiting conditions are lifted, PHA can provide carbon and energy to fuel the organism's metabolism[13-15]. PHA depolymerases (PHADs;

EC 3.1.1.75, EC 3.1.1.76) degrade PHA into monomeric and dimeric hydroxyalkanoates[16-18]. Bacteria, archaea, fungi, protist and as our previous study showed 77 metazoan species representing nine animal phyla encode for PHADs[16, 19-22]. Given that PHA degradation is widespread across animals, they ultimately influence the release of carbon across ecosystems.

Given that in Chapter I we showed that earthworms encode for a PHAD, we hypothesized that earthworms may contribute to PHA degradation in soil systems. Earthworms feed on soil microbial communities by burrowing their casts. By burrowing casts, earthworms break down organic matter that microbial species can use for their metabolism (Supplementary Text 1)[23, 24]. By feeding on soils, earthworms ingest PHA-synthesizing organisms. Using their PHAD, they could degrade the ingested bacteria to gain carbon and energy. Additionally, PHA is commercially used as a bio-plastics sharing many characteristics to thermoplastics but can be fully degraded by PHADs. Therefore, earthworms may contribute to the degradation of PHA-based plastics (Supplementary Text 2)[25-29]. Based on this, we hypothesize that earthworms can use both naturally occurring PHA and PHA-based plastics for their nutrition.

The aim of this study was to show that earthworms degrade PHA found in their habitat. PHA synthesizing bacteria were found in earthworm's guts[30]. Additionally, earthworm's nephridial symbionts *Verminephrobacter* sp. synthesize PHA, which earthworms could degrade. Therefore, earthworms have access to two extracellular PHA sources (Supplementary Text 3)[31-33]. We showed that the PHAD of the earthworm species *Lumbricus rubellus* can degrade extracellular PHA. Re-analysis of a cDNA microarray study[34] indicated that *L. rubellus* expressed the PHAD and a beta-hydroxybutyrate dehydrogenase (BHBD; EC 1.1.1.30). The earthworm could thus degrade the resulting hydroxyalkanoic monomers and likely use them for energy generation[35, 36]. Contradicting our initial hypothesis, *L. rubellus* expressed the PHAD protein in the epidermis. The observation suggests that the earthworm does not degrade PHA taken up by its nutrition or from its symbionts. Based on the expression of the PHAD in the epidermis, we hypothesize that all globally distributed earthworm species might benefit from PHA in a yet unknown way.

Results & Discussion

Earthworms can degrade extracellular PHA

All earthworm PHADs grouped with PHADs from Annelids in the animal PHAD clade (Chapter I), suggesting their eukaryotic origin. The symbiont PHADs of *Verminephrobacter eiseniae* grouped separated from their host PHADs with intracellular PHADs according to the PHAD engineering database (DED)[37]. This further confirms the eukaryotic origin of the earthworm PHADs. The earthworm PHADs shared less than 6.8% to 16.2% amino acid identity to the symbiont PHAD. Specifically, the symbiont PHADs lacked a lipase box motif which is typical for intracellular PHADs (Supplementary Figure 1)[14]. The phylogenetic and structural differences between the earthworm and symbiont PHADs, suggest that the earthworm PHADs were not horizontally transferred from the symbionts. It rather indicates that the animal PHADs are evolutionary conserved.

Re-analysis of a cDNA microarray study suggests that the *L. rubellus* PHAD is expressed together with a beta-hydroxybutyrate dehydrogenase (BHBD; EC 1.1.1.30). We screened the published dataset of 2-log fold changed transcripts and identified expression of a putative PHAD and BHBD[34]. In bacteria, PHADs break PHA molecules into hydroxyalkanoic monomeric and oligomeric units. Oligomers are further broken down into monomers by a hydroxybutyrate-dimer hydrolase (EC 3.1.1.22). The monomers are subsequently converted into acetoacetate by a BHBD. Acetoacetate is then oxidized to acetyl-coenzyme A, which is used to generate energy via the citric acid cycle[35, 38-41]. Taken together, the expression data suggests that the earthworm species *L. rubellus* likely derives energy from PHA degradation.

All five identified earthworm PHADs had a conserved catalytic triad, 100% identical to the PHAD of the fungal homolog of *Penicillium funiculosum* (basionym *Talaromyces funiculosus;* pdb: 2d81; coverage: 69% to 965; identity: 11% to 37%; RMSD: 0,702 to 1,067; pLLDT: 68 to 94; Figure 1a; Supplementary Figure 2)[42]. The high degree of homology suggests that all earthworm PHADs have the same function as the fungal PHAD, namely to degrade PHA. We identified that all earthworm PHADs have the lipase box motif with the catalytic serine at the beginning of the catalytic site. These characteristics suggest that the earthworm PHADs degrade short chain extracellular PHA. This assumption is further supported because the substrate

binding site of the earthworm PHADs showed 17%-56% conservation in comparison to the extracellular PHAD of *P. funiculosum*. In particular, we identified conservation of the residue $W_{299-302}$, that holds the polymer chain in place. Lastly, all earthworm PHADs were predicted to have a signal peptide (Supplementary Table 1). We thus hypothesize that the earthworm PHADs function on extracellular PHA by being transported outside of the cell.

We hypothesized that the earthworm PHADs function on extracellular PHA. To examine this hypothesis, we heterologously expressed the *L. rubellus* PHAD in *E. coli* (Figure 1c; Supplementary Figure 3). Activity assays on crystalline PHA showed that the purified *L. rubellus* PHAD is able to degrade extracellular PHA (Figure 1b). We tested the *L. rubellus* PHAD both on the homopolymer Polyhydroxybutyrate (PHB) and the copolymer Polyhydroxybutyrate/Polyhydroxyvalerate (PHB/PHV). We observed a clearance zone forming around the spotted enzyme after 24 h, which suggested that the *L. rubellus* PHAD degraded PHA. Interestingly, the *L. rubellus* PHAD showed a higher activity for PHB with 25 out of 30 PHB assays resulting in a clearance zone, compared to 2 out of 25 PHB/PHV assays. Our results suggest that the earthworm PHAD is adapted to degrade the most common PHA source, PHB[43].

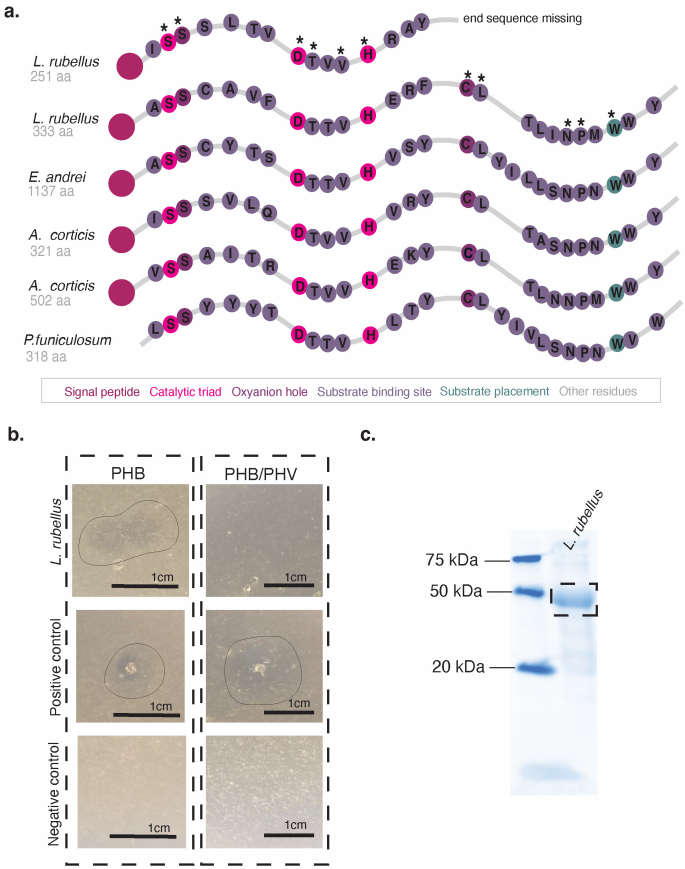

Figure 1 | *L. rubellus* PHAD degraded extracellular PHA as predicted by its primary enzyme structure. a. Primary structure alignment (localpair alignment MAFFT)[44] of all five earthworm PHADs in comparison to the PHAD from *P. funiculosum* (pdb: 2d81)[42]. All conserved regions are denoted by an asterisk. The earthworm PHADs showed 100% conservation of the catalytic site and conservation of parts of the substrate binding site, indicating that they degrade extracellular PHA. **b.** Enzyme assays of the *L. rubellus* PHAD on PHA plates of the homopolymer PHB and the copolymer PHB/PHV showed PHA degradation by a clearance zone. Only two out of 25 assays of the *L. rubellus* PHAD on PHB/PHV showed activity, suggesting a higher activity for PHB. **c.** SDS PAGE gel confirming the purification of the heterologously expressed *L. rubellus* PHAD.

L. rubellus expresses its PHAD at the worm's epidermis

We sought out to localize the expression of the *L. rubellus* PHAD by designing antibodies that target the *L. rubellus* PHAD (Supplementary Figure 4; Supplementary Table 2). *L. rubellus* expressed the PHAD protein in epidermal cells shown by immunohistochemistry staining (Figure 2). The observation is contradicting our initial hypothesis that earthworms use PHA taken up with their diet. *L. rubellus* likely expressed the PHAD at the worm's basal cells. The basal cells are underneath the cuticle and above the circular muscles. Based on this we hypothesize that the earthworm's PHAD might be excreted with gland cell produced mucus. One possible scenario could be that the earthworm's PHAD degrades the PHA of invading bacteria. The epidermis of earthworms functions as an antibacterial barrier, removing bacteria through phagocytosis during wound healing[45]. We observed that the earthworm PHAD formed round structures. These round structures could be an indication for phago-lysosomes found in the epidermis, similar to the ones described for *Dendrobaena veneta*[46]. To test this hypothesis, a double labeling of the PHAD and lysozyme by specific antibodies could be done. Additionally, the earthworm's PHAD could function on excreted PHA from its nephridial symbionts. The earthworm's nephridia are paired excretory organs connected to the body wall. The nephridia function to release invading bacteria[47]. Potentially not only PHA of invading bacteria could be released via the nephridia but also the extracellular PHA of lysed or dead symbionts. The earthworm might thus get access to the excreted PHA. Additionally, the earthworm's epidermis produces mucus that helps the body movement and protects from soil particles[48]. The mucus is not only beneficial to the earthworm but also enhances the microbial biomass in the earthworm's burrows[49, 50]. The microbial biomass increase might be because the protein rich mucus leads to microbial activity in the otherwise mostly dormant soil bacterial population[51]. Based on this we hypothesize that earthworms might excrete their PHAD with their mucus. The excreted PHAD breaks down PHA into its monomers and dimers that can benefit the microbial community around the earthworm. The increased microbial activity might have an indirect effect on the earthworm's growth[52]. Alternatively, the water soluble monomeric and dimeric hydroxyalkanoates diffuse through the earthworm's epidermis. Further analysis that colocalize the presence of PHA and the PHAD should be done to look into these hypotheses. Lastly, *L. rubellus* has two PHADs. Localizing

the second PHAD by immunohistochemistry might help to further confirm the hypothesis that earthworms cannot degrade PHA taken up by their nutrition.

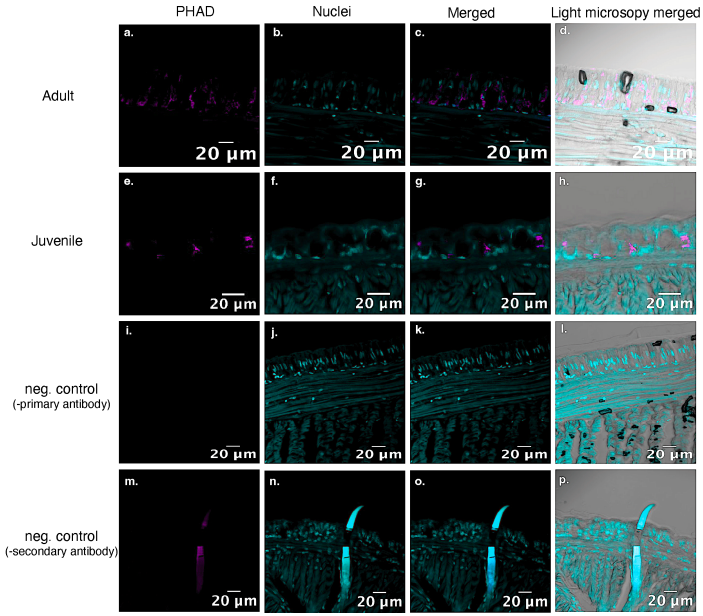

Figure 2 | *L. rubellus* PHAD was expressed at the epidermis, suggesting its transport out to the earthworm's surrounding. We used a specific antibody for the *L. rubellus* PHAD (**a,e**) and tested it with a DAPI counterstaining (**b,f,j,n**) on 18µm sections of an adult (**a-d**) and a juvenile worm (**e-h**). As our negative controls, we either left out the primary antibody (**i-l**) or the secondary antibody (**m-p**). With both negative controls we did not see a signal, confirming the specific binding of the antibody. Signal seen in panel **m** comes from the autofluorescence of the setae.

Do earthworms benefit from PHA degradation?

Based on the expression of the PHAD and the BHBD, we hypothesized that *L. rubellus* benefits from PHA degradation. That is why we incubated individuals of *L. rubellus*, *L. terrestris* and several non-speciated garden-collected earthworms for 21 days in soil. We supplemented the soil every two days with a larger concentration of PHA than naturally occurring (Figure 3). In all three incubations, we observed reduction in body

weight of the earthworms independent of their incubation conditions. Additionally, individuals of both experimental groups died throughout the experiment. *L. rubellus* and *L. terrestris* individuals that did not get PHA addition showed a more frequent increase in body weight. All garden collected earthworms reduced their body size over a period of 21 days. Based on this, we hypothesize that the incubation conditions were not favorable for the earthworms.

These results could be explained by several reasons. One possible explanation is that the earthworms experienced stress throughout the experiment. The stress likely made it difficult to observe the benefits of PHA addition. Another possibility might be that the addition of PHA to soil that already includes a large fraction of organic matter, microbial biomass and thus PHA addition does not have an effect. Additionally, PHA as a nutritional source might be more beneficial during maturation. We observed PHAD expression in a juvenile earthworm (Figure 3). Therefore, we propose to repeat the experiment using juvenile worms. Given the epidermal localization of the PHAD, an alternative hypothesis is that the PHAD is secreted to the surrounding soil. PHA degradation might thus stimulate the bacterial community but not lead to a direct benefit for the earthworm. Therefore, the activity of the soil microorganisms should be analyzed.

These experiments are especially important because we hypothesize that earthworm PHADs cannot only use naturally occurring PHA but completely degrade PHA-based bioplastics to CO_2. This hypothesis is contrasting to what is known about earthworm's plastic degradation. Earthworms ingest bio-plastics like poly lactic acid (PLA)[53]. The plastic digestion led to a reduction in size of the plastics but never in the complete removal[54]. The accumulation of plastics in organisms' gut has harmful effects such as the inflammation of the gut and thus changing of the feeding behavior[55]. It could lead to burns and lesions on the earthworm's skin[56]. Additionally, it could change the earthworm's soil aggregation behavior[57]. Previous feeding studies with the earthworm *Eisenia fetida* showed that a combination of PLA and PHA had no significant negative effect on the earthworm[58], suggesting that PHA-based plastics might not be harmful for earthworms. Given that earthworms are effective decomposers in soil environments, it is essential to consider their influence for the use of PHA-based plastics degradation. Based on this, we postulate that there needs to be more studies investigating the effects of PHA-based plastics in the earthworm's diet.

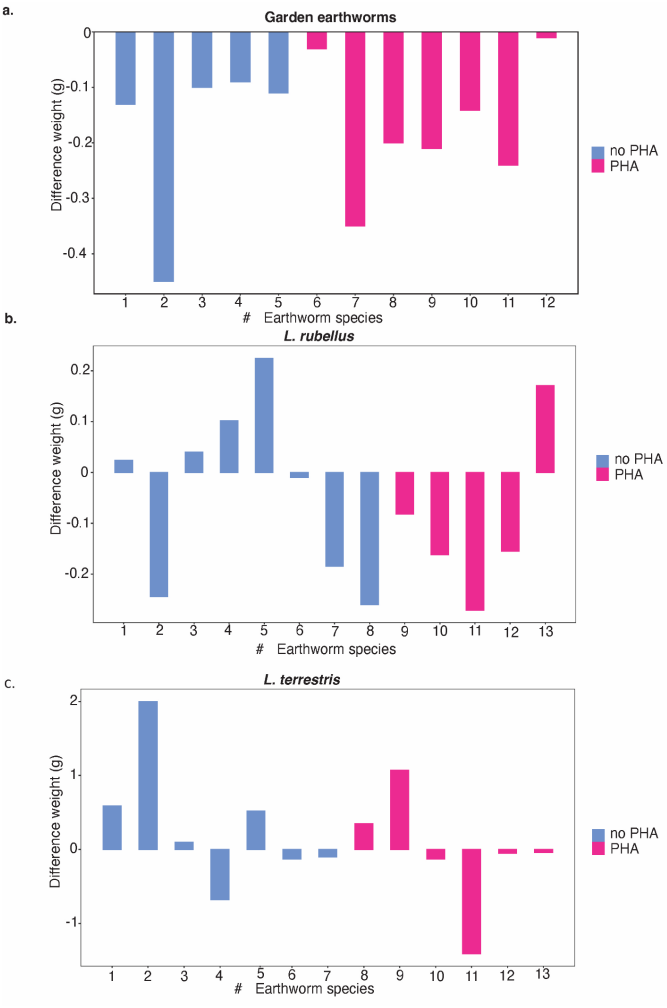
a.
Garden earthworms
Difference weight (g)
0
-0.1
-0.2
-0.3
-0.4
1 2 3 4 5 6 7 8 9 10 11 12
Earthworm species
no PHA
PHA
b.
L. rubellus
Difference weight (g)
0.2
0.1
0
-0.1
-0.2
1 2 3 4 5 6 7 8 9 10 11 12 13
Earthworm species
no PHA
PHA
c.
L. terrestris
Difference weight (g)
2
1
0
-1
1 2 3 4 5 6 7 8 9 10 11 12 13
Earthworm species
no PHA
PHA

Figure 3 | PHA addition to the earthworm's soil did not lead to a benefit for the earthworms. Earthworms were incubated in natural soil, supplemented every two days with PHA of a concentration of 4 mg. Both PHA fed (pink bars) and not PHA fed (blue bars) worms showed a decrease in body weight. Individuals that died throughout the experiment are not shown **a.** Garden collected earthworms representing various non- speciated worms showed a general decrease in body weight, suggesting that the PHA treatment was neither beneficial nor harmful but that the culture conditions were not favorable **b.** *L. rubellus* earthworms showed similar to the garden collected earthworms a general decrease in body weight. Four worms that did not get PHA increased in body weight, whereas only one worm that got PHA **c.** *L. terrestris* worms showed a mixed pattern of weight differences. Four worms that did not get PHA showed a body weight increase, whereas only two worms that got the PHA addition. The other worms decreased in body weight.

Conclusion

Our study showed that earthworm species can degrade PHA. These findings imply that earthworms influence PHA degradation in terrestrial systems. *L. rubellus* expressed the PHAD in epidermal cells, suggesting a transport to the soil environment. Potentially, the earthworms PHADs function on PHA of invading microbial species. These are lysed by phago-lysosomes in the earthworm's cuticle during wound healing[45], allowing access to PHA. Alternatively, *L. rubellus* degrades PHA found in their burrowed casts. The resulting water soluble hydroxyalkanoates could be used for energy generation by the earthworms or the surrounding microorganisms. If used by the microbial community, their metabolisms could be stimulated. In our previous study (Chapter 1), we hypothesized that 77 animals gain an additional nutritional source by PHA degradation. Most of the animals gain access to PHA through their microorganism rich diet (Chapter 1). While we were unable to show that earthworms use PHA in their diet, we propose that PHA degradation by animal species might be more complex. Future research should focus on the role of PHA degradation for animals.

Earthworms are considered to be ecosystem engineers that stimulate ecosystem health through soil aggregation and soil organic carbon degradation[23, 24]. It is thus important to investigate how they influence PHA degradation. Our hypothesis is that by expressing a functional PHAD, globally earthworms can tap into microbial stored PHA and release carbon. The carbon released from PHA degradation by earthworms would impact carbon emission from terrestrial soils. Therefore, future studies should focus

on how earthworms influence PHA degradation in soil systems by analyzing the rates of PHA degradation and comparing them to those of microbial PHA degraders.

Acknowledgements

We would like to thank Carolin Richter, Martina Meyer and Silke Wetzel for their help in the lab. We thank Alexander Robinson for the earthworms used in this study. We thank the MPI for plant breeding for their access to the computing cluster. This work was funded by the Max Planck Society through Prof. N. Dubilier.

Code and data availability

PHAD sequences are from public databases. The codes used to analyze them will be made publicly available upon peer-review submission and are currently available upon request.

Materials & Methods

Identification

Identification of earthworm PHADs. To identify earthworm PHADs we screened publicly available resources. For the identification of the *A. corticis* and *E. andrei* PHAD, we BLASTed (BLASTp) the *Olavius algarvensis* PHAD (Chapter 1) against the coding sequences of the earthworm's genomes[59-61]. We identified the *L. rubellus* PHAD by BLASTing the *O. algarvensis* PHAD against the *L. rubellus* metatranscriptome using LumbriBASE (Earthworms.org: home of the *Lumbricus rubellus* genome project). We aligned the retrieved sequences using the local pair alignment in MAFFT [44](version v7.407 (2018/Jul/23)). We checked for the conservation of the catalytic site. Earthworm sequences that had conservation of these identifiers were further used in this study.

Sequence comparison

Primary structure analysis. To identify conserved regions in the earthworms PHADs, we aligned the five identified earthworm PHADs with the amino acid sequence of the PHAD from the fungus *Penicillium funiculosum* (basionym *Talaromyces funiculosus*; accession 2D80/2D81)[42] using the local pair alignment in MAFFT[44](version v7.407 (2018/Jul/23). The alignment was then visualized using the MSAviewer[62]. The identification of conserved sites was based on the paper from Hisano *et al*. (2006)[42]. We predicted the signal peptides of individual enzymes using SignalP 6.0[63].

The earthworm PHADs were also compared to the *V. eiseniae* PHADs[64] by aligning them using the local pair alignment in MAFFT(version v7.407 (2018/Jul/23)[44]. We visualized the alignment using the Geneious (Geneious Prime® 2022.0.1; https://www.geneious.com).

Homologous modeling. We were interested if the earthworm PHADs showed structural conservation to the fungal homolog. We modeled all of the identified earthworm PHADs using the monomer prediction against the full AlphaFold2 database[65-67]. We analyzed and visualized the generated models using PyMOL (version 2.4.0.; The PyMOL Molecular Graphics System, Version 2.0 Schrödinger, LLC). First, we checked the quality of the models by visualizing the results of the predicted local distance difference test (pLDDT) saved in the beta spectrum of the AlphaFold2 models. Next, to identify the structural conservation of the earthworm PHADs, we compared the AlphaFold2 models to the crystal structure of the PHAD from the fungus *P. funiculosum* (accession 2D80/2D81)[42]. We superposed the models with the crystal structure. This enabled us to calculate the root-mean-square deviation (RMSD).

L. rubellus PHAD activity

Heterologous gene expression and enzyme purification. To analyze the function of the *L. rubellus* PHAD, we expressed the *L. rubellus* PHAD in *E. coli*. As our positive control we expressed an extracellular PHAD from *Paucimons lemoignei* (accession:

P52090). We ordered the pet28a(+) expression vectors at Genscript (Genscript®) with the sequences of interest inserted between the restriction sites NheI/XhoI. We transformed the *L. rubellus* PHAD vector by heat shock into E. *coli* Lemo21 competent cells (DE3; Theremo Fisher). The *P. lemoignei* vector was transformed into BL21 rosetta competent cells (DE3; Merck). For the enzyme overexpression and purification we followed the method described by Becker *et al.* (2018)[68]. The success of the enzyme overexpression and purification was checked by SDS PAGE (TGX FastCast 12%, Biorad). We exchanged the buffer of the purified enzymes by an overnight dialysis using 6-8 kDa dialysis bags against SEC buffer (20 mM Tris, 0.5 M NaCl) at 4 °C stirred at 150 rpm. To determine if we successfully expressed the *L. rubellus* PHAD we sent samples of the *E. coli* clones for plasmid extraction and Sanger sequencing (Microsynth AG).

Enzyme assays. Using the purified enzymes, we tested enzyme activity by spot assays according to the method described by Briese *et al.* (1994)[69]. We prepared polymer plates containing 0.5 mg/ml of the homopolymer PHB (Merck) and the copolymer PHB/PHV (Merck; 3% PHV). PHA was brought to a stable suspension in a 100 mM Tris HCl (Sigma-Aldrich) solution by sonication of the mix at maximum intensity for 3 h at 42 °C. We added 7 g / 500 ml agar (Becton Dickinson) to the polymers. We then added 10 µl droplets of the purified *L. rubellus* PHAD to the plate. We incubated the plates at 36 °C for 24 h. The activity of the enzyme was determined by a clearance zone. As a negative control we used a heat-denatured 1:1 enzyme mix (95 °C for 15 min) of the purified enzymes.

PHAD Expression

Earthworm dissection, fixation and embedding. We narcotised earthworms in a 1% to 10% ethanol (Carl Roth) series. We slowly increased the ethanol concentration until worms were motionless, following Julka et al. (1993)[70]. Lastly, we added 90% ethanol to kill the worms. We dissected the worm using eye scissors by taking small sections along the earthworm's gut (Supplementary Figure 4a). These sections were fixed in 4% Paraformaldehyde (Electron Microscopy Sciences) in PBS (Phosphate Buffered Saline) at 4°C overnight. Respectively, earthworm pieces were embedded in paraffin (Carl Roth).

Paraformaldehyde fixed samples were dehydrated in an ethanol series ranging from 60% to 100% for six days. The ethanol was gradiently exchanged with Rotihistol (Carl Roth) for two days. Rotihistol was gradiently exchanged for four days by Paraffin to allow complete infiltration of the tissue. Samples were then embedded in paraffin. We prepared sections of 18 µm thickness. The sections were first backed for 4 h at 60°C. Next, they were de-waxed in a Rotihistol to 50% ethanol series with each step for 10 minutes. To thoroughly attach the earthworm sections to the glass slide, we embedded them in a 0.2% agarose solution (Carl Roth).

Immunohistochemistry. We used the deparaffinized sections for the indirect immunofluorescence method (Vector Lab, Burlingham, CA, USA). We designed a specific *L. rubellus* PHAD antibody (Supplementary Figure 4; Supplementary Table 2; Eurogentec; prepared in rabbit; 15-25 mg each). We first blocked nonspecific bindings by pre-incubating the sections in the blocking buffer (2.5% BSA, 1x PBS, 0.05% Triton X-100) for 30 minutes at room temperature. Subsequently, we added the primary antibody (concentration: 1:50) in the blocking buffer to the blocked sections and incubated them overnight at 4°C. Thereafter, we washed the sections three times in PBS for ten minutes before applying the secondary antibody in a 1:100 dilution in blocking buffer. The sections were incubated for two hours with the secondary antibody (Anti-Rabbit IgG (H+L), highly cross-adsorbed, CF™ 633 antibody produced in goat; Merck) at room temperature. The secondary antibody was washed out three times in PBS for 30 minutes. Before mounting the sections in Electron Microscopy Sciences Citifluor™, we counterstained the samples with 2 µM DAPI for ten minutes. Sections were washed for ten minutes in PBS. We visualized the hybridizations using confocal microscopy (Zeiss LSM 780 with Airyscan and ELYRA PS.1).

Western Blots to test the specificity of the earthworm PHAD antibody. To test the specificity of the *L. rubellus* PHAD antibody we prepared Western Blots. Therefore, earthworms were frozen in liquid nitrogen and dissected into pieces along the intestine (Supplementary Figure 4a). These sections were ground with a pestle in three parts Bolt LDS 4x sample buffer (Thermo Fisher Scientific, B0007) with one parts Bolt LDS 10x reducing agent (Thermo Fisher Scientific, B0009). The samples were then heated

for 5 minutes at 95°C and subsequently cooled for 2 minutes on ice to allow denaturation of the proteins. The samples were centrifuged at 14.000 rpm for 10 minutes and the supernatant which included the extracted proteins was transferred to a new tube. We applied 15µl of the extracted proteins to a SDS gel (Bolt 4-12% Bis-Tris-Plus Mini Gel (Thermo Fisher Scientific, NW04120BOX)) following the manufacturer's description. The resulting SDS PAGE was transferred to a membrane (Amersham ProTran 0.2 µm NC membrane 0,2µm, 8x9cm (Merck, GE10600094)) following the manufacturer's instructions. The membrane was stained with a Ponceau S solution (1% Ponceau S, 5% acetic acid) to monitor the efficiency of the protein transfer. Before blocking, the Ponceau staining was washed off in PBS. The membrane was blocked using a blocking solution (1x PBS; 1 % TritonX-100; 5 % milk powder) in two steps: Firstly 60 minutes at room temperature and then two hours at 4°C. The primary antibody (Supplementary Table 2) was added in a 1:100 dilution in blocking solution to the membrane and incubated for 45 minutes. Subsequently, we washed the membrane in the blocking buffer for two times 30 minutes and one time for sixty minutes. Lastly, we incubated the membrane in the secondary antibody (1:1000 dilution; Anti rabbit lgG alkaline phosphatase antibody produced in goat; Merck) in the blocking buffer. The detection was done in a solution of 33 µl NBT (Nitro Blue Tetrazolium (NBT), (Roche, 11383213001)) and 33 µl BCIP (Roche, 11383221001) in 10 ml AP buffer (1M Tris pH 9.5, 2M NaCl, 1M $MgCl_2$, Tween-20) for 260 min.

Benefit of PHA for earthworms

Earthworm PHA incubations. To test if earthworms benefit from PHA addition in their nutrition, we incubated earthworm species for up to 21 days in natural soil that we supplemented every two days with 4 mg PHB (Merck). We collected 12 earthworms from their natural habitat (Wichdorf, Germany; 51° 13' 0" North, 9° 18' 0" East) and incubated them individually upon their arrival in petri dishes with their natural soil for 21 days. Every two days we added 4 mg PHB in MQ water to the soil. The control group got only MiliQ water. We exchanged the soil every week to reduce the humus formation. Earthworms were weighed at the beginning and at the end of the experiment. We repeated the experiment with 13 *L. rubellus* individuals (UK Centre for Ecology & Hydrology (UKCEH)). Lastly, we incubated 13 *L. terrestris* worms (b.t.b.e. Insektenzucht GmbH) in the same way.

References

1. Eswaran, H., E. Van Den Berg and P. Reich, *Organic carbon in soils of the world.* Soil Science Society of America Journal, 1993. **57**(1): p. 192-194.
2. Kästner, M. and A. Miltner, *SOM and microbes—What is left from microbial life*, in *The future of soil carbon*. 2018, Elsevier. p. 125-163.
3. Liang, C. and T.C. Balser, *Preferential sequestration of microbial carbon in subsoils of a glacial-landscape toposequence, Dane County, WI, USA.* Geoderma, 2008. **148**(1): p. 113-119.
4. Ciais, P., C. Sabine, G. Bala, L. Bopp, V. Brovkin, J. Canadell, A. Chhabra, R. DeFries, J. Galloway and M. Heimann, *Carbon and other biogeochemical cycles*, in *Climate change 2013: the physical science basis.* Contribution of Working Group I to the Fifth Assessment Report of the Intergovernmental Panel on Climate Change. 2014, Cambridge University Press. p. 465-570.
5. Mason-Jones, K., S.L. Robinson, G. Veen, S. Manzoni and W.H. van der Putten, *Microbial storage and its implications for soil ecology.* The ISME Journal, 2022. **16**(3): p. 617-629.
6. Mason-Jones, K., C.C. Banfield and M.A. Dippold, *Compound-specific 13C stable isotope probing confirms synthesis of polyhydroxybutyrate by soil bacteria.* Rapid Communications in Mass Spectrometry, 2019. **33**(8): p. 795-802.
7. Fernandez-Castillo, R., F. Rodriguez-Valera, J. Gonzalez-Ramos and F. Ruiz-Berraquero, *Accumulation of poly (β-hydroxybutyrate) by halobacteria.* Applied and Environmental Microbiology, 1986. **51**(1): p. 214-216.
8. Steinbüchel, A. and H. Schlegel, *Physiology and molecular genetics of poly (β-hydroxyalkanoic acid) synthesis in* Alcaligenes eutrophus. Molecular Microbiology, 1991. **5**(3): p. 535-542.
9. Arun, A., R. Arthi, V. Shanmugabalaji and M. Eyini, *Microbial production of poly-β-hydroxybutyrate by marine microbes isolated from various marine environments.* Bioresource Technology, 2009. **100**(7): p. 2320-2323.
10. Wang, J. and L.R. Bakken, *Screening of soil bacteria for poly-β-hydroxybutyric acid production and its role in the survival of starvation.* Microbial Ecology, 1998. **35**: p. 94-101.
11. Madison, L.L. and G.W. Huisman, *Metabolic engineering of poly (3-hydroxyalkanoates): from DNA to plastic.* Microbiology and Molecular Biology Reviews, 1999. **63**(1): p. 21-53.
12. Müller, H.M. and D. Seebach, *Poly (hydroxyalkanoates): a fifth class of physiologically important organic biopolymers?* Angewandte Chemie International Edition in English, 1993. **32**(4): p. 477-502.
13. Kawaguchi, Y. and Y. Doi, *Kinetics and mechanism of synthesis and degradation of poly (3-hydroxybutyrate) in* Alcaligenes eutrophus. Macromolecules, 1992. **25**(9): p. 2324-2329.
14. Handrick, R., S. Reinhardt and D. Jendrossek, *Mobilization of poly (3-hydroxybutyrate) in* Ralstonia eutropha. Journal of Bacteriology, 2000. **182**(20): p. 5916-5918.
15. Ruiz, J.A., N.I. López, R.O. Fernández and B.S. Méndez, *Polyhydroxyalkanoate degradation is associated with nucleotide accumulation and enhances stress resistance and survival of* Pseudomonas

oleovorans *in natural water microcosms.* Applied and Environmental Microbiology, 2001. **67**(1): p. 225-230.

16. Jendrossek, D. and R. Handrick, *Microbial degradation of polyhydroxyalkanoates.* Annual Review of Microbiology, 2002. **56**: p. 403.
17. Lee, S.Y. and J.-i. Choi, *Production and degradation of polyhydroxyalkanoates in waste environment.* Waste Management, 1999. **19**(2): p. 133-139.
18. Jendrossek, D., *Extracellular polyhydroxyalkanoate (PHA) depolymerases: the key enzymes of PHA degradation.* Biopolymers Online: Biology Chemistry Biotechnology Applications, 2005. **3**.
19. Gonda, K., D. Jendrossek and H.-P. Molitoris, *Fungal degradation of the thermoplastic polymer poly-ß-hydroxybutyric acid (PHB) under simulated deep sea pressure*, in *Life at Interfaces and Under Extreme Conditions*. 2000, Springer. p. 173-183.
20. Kim, D. and Y. Rhee, *Biodegradation of microbial and synthetic polyesters by fungi.* Applied Microbiology and Biotechnology, 2003. **61**(4): p. 300-308.
21. Anderson, I.J., R.F. Watkins, J. Samuelson, D.F. Spencer, W.H. Majoros, M.W. Gray and B.J. Loftus, *Gene discovery in the* Acanthamoeba castellanii *genome.* Protist, 2005. **156**(2): p. 203-14.
22. Viljakainen, V. and L. Hug, *The phylogenetic and global distribution of bacterial polyhydroxyalkanoate bioplastic-degrading genes.* Environmental Microbiology, 2021. **23**(3): p. 1717-1731.
23. Angst, G., C.W. Mueller, I. Prater, Š. Angst, J. Frouz, V. Jílková, F. Peterse and K.G. Nierop, *Earthworms act as biochemical reactors to convert labile plant compounds into stabilized soil microbial necromass.* Communications Biology, 2019. **2**(1): p. 441.
24. Jones, C.G., J.H. Lawton and M. Shachak, *Organisms as ecosystem engineers.* Oikos, 1994: p. 373-386.
25. Steinbüchel, A. and B. Füchtenbusch, *Bacterial and other biological systems for polyester production.* Trends in Biotechnology, 1998. **16**(10): p. 419-427.
26. Van-Thuoc, D., T. Huu-Phong, N. Thi-Binh, N. Thi-Tho, D. Minh-Lam and J. Quillaguaman, *Polyester production by halophilic and halotolerant bacterial strains obtained from mangrove soil samples located in N orthern V ietnam.* Microbiologyopen, 2012. **1**(4): p. 395-406.
27. Ho, Y.-H., S.-N. Gan and I.K. Tan, *Biodegradation of a medium-chain-length polyhydroxyalkanoate in tropical river water.* Applied Biochemistry and Biotechnology, 2002. **102**: p. 337-347.
28. Lenz, R.W. and R.H. Marchessault, *Bacterial polyesters: biosynthesis, biodegradable plastics and biotechnology.* Biomacromolecules, 2005. **6**(1): p. 1-8.
29. Lim, S.-P., S.-N. Gan and I.K. Tan, *Degradation of medium-chain-length polyhydroxyalkanoates in tropical forest and mangrove soils.* Applied Biochemistry and Biotechnology, 2005. **126**: p. 23-33.
30. Ponnusamy, S., S. Viswanathan, A. Periyasamy and S. Rajaiah, *Production and characterization of PHB-HV copolymer by* Bacillus thuringiensis *isolated from* Eisenia foetida. Biotechnology and Applied Biochemistry, 2019. **66**(3): p. 340-352.
31. Cheema, S., M. Bassas-Galia, P.M. Sarma, B. Lal and S. Arias, *Exploiting metagenomic diversity for novel polyhydroxyalkanoate synthases: production of a terpolymer poly (3-hydroxybutyrate-co-3-*

hydroxyhexanoate-co-3-hydroxyoctanoate) with a recombinant Pseudomonas putida *strain.* Bioresource Technology, 2012. **103**(1): p. 322-328.

32. Lund, M.B., M.F. Mogensen, I.P. Marshall, M. Albertsen, F. Viana and A. Schramm, *Genomic insights into the Agromyces-like symbiont of earthworms and its distribution among host species.* FEMS Microbiology Ecology, 2018. **94**(6): p. fiy068.
33. Møller, P., M.B. Lund and A. Schramm, *Evolution of the tripartite symbiosis between earthworms,* Verminephrobacter *and* Flexibacter-*like bacteria.* Frontiers in Microbiology, 2015. **6**: p. 529.
34. Bundy, J.G., J.K. Sidhu, F. Rana, D.J. Spurgeon, C. Svendsen, J.F. Wren, S.R. Stürzenbaum, A.J. Morgan and P. Kille, *'Systems toxicology'approach identifies coordinated metabolic responses to copper in a terrestrial non-model invertebrate, the earthworm* Lumbricus rubellus*.* BMC Biology, 2008. **6**: p. 1-21.
35. Senior, P.J. and E.A. Dawes, *The regulation of poly-beta-hydroxybutyrate metabolism in* Azotobacter beijerinckii*.* Biochemical Journal, 1973. **134**(1): p. 225-38.
36. Kobayashi, T. and T. Saito, *Catalytic triad of intracellular poly (3-hydroxybutyrate) depolymerase (*PhaZ*1) in* Ralstonia eutropha *H16.* Journal of Bioscience and Bioengineering, 2003. **96**(5): p. 487-492.
37. Knoll, M., T.M. Hamm, F. Wagner, V. Martinez and J. Pleiss, *The PHA depolymerase engineering database: a systematic analysis tool for the diverse family of polyhydroxyalkanoate (PHA) depolymerases.* BMC Bioinformatics, 2009. **10**: p. 1-8.
38. Tanio, T., T. Fukui, Y. Shirakura, T. Saito, K. Tomita, T. Kahio and S. Masamune, *An extracellular poly (3-hydroxybutyrate) depolymerase from* Alcaligenes faecalis*.* European Journal of Biochemistry, 1982. **124**(1): p. 71-77.
39. Jendrossek, D., I. Knoke, R.B. Habibian, A. Steinbüchel and H.G. Schlegel, *Degradation of poly (3-hydroxybutyrate), PHB, by bacteria and purification of a novel PHB depolymerase from* Comamonas *sp.* Journal of Environmental Polymer Degradation, 1993. **1**(1): p. 53-63.
40. Stuart, J., E. Ooi, J. McLeod, A. Bourns and J. Ballantyne, *D-and L-β-hydroxybutyrate dehydrogenases and the evolution of ketone body metabolism in gastropod molluscs.* The Biological Bulletin, 1998. **195**(1): p. 12-16.
41. Shiraki, M., T. Endo and T. Saito, *Fermentative production of (R)-(-)-3-hydroxybutyrate using 3-hydroxybutyrate dehydrogenase null mutant of* Ralstonia eutropha *and recombinant* Escherichia coli*.* Journal of Bioscience and Bioengineering, 2006. **102**(6): p. 529-34.
42. Hisano, T., K. Kasuya, Y. Tezuka, N. Ishii, T. Kobayashi, M. Shiraki, E. Oroudjev, H. Hansma, T. Iwata, Y. Doi, T. Saito and K. Miki, *The crystal structure of polyhydroxybutyrate depolymerase from* Penicillium funiculosum *provides insights into the recognition and degradation of biopolyesters.* Journal of Molecular Biology, 2006. **356**(4): p. 993-1004.
43. Jendrossek, D., *Peculiarities of PHA granules preparation and PHA depolymerase activity determination.* Applied Microbiology and Biotechnology, 2007. **74**: p. 1186-1196.
44. Katoh, K. and D.M. Standley, *MAFFT multiple sequence alignment software version 7: improvements in performance and usability.* Molecular Biology and Evolution, 2013. **30**(4): p. 772-780.

45. Burke, J.M., *Wound healing in* Eisenia foetida *(Oligochaeta) II. A fine structural study of the role of the epidermis.* Cell and Tissue Research, 1974. **154**: p. 61-82.
46. Fiołka, M.J., M.P. Zagaja, M. Hułas-Stasiak and J. Wielbo, *Activity and immunodetection of lysozyme in earthworm* Dendrobaena veneta *(Annelida).* Journal of Invertebrate Pathology, 2012. **109**(1): p. 83-90.
47. Ratcliffe, N., A. Rowley, S. Fitzgerald and C. Rhodes, *Invertebrate immunity: basic concepts and recent advances.* International Review of Cytology, 1985. **97**: p. 183-350.
48. Lee, K.E., *Earthworms: their ecology and relationships with soils and land use*. 1985: Academic Press Inc.
49. Scheu, S., N. Schlitt, A.V. Tiunov, J.E. Newington and H.T. Jones, *Effects of the presence and community composition of earthworms on microbial community functioning.* Oecologia, 2002. **133**: p. 254-260.
50. Heděnec, P., T. Cajthaml, V. Pižl, K. Márialigeti, E. Tóth, A.K. Borsodi, A. Chroňáková, V. Krištůfek and J. Frouz, *Long-term effects of earthworms (*Lumbricus rubellus *Hoffmeister, 1843) on activity and composition of soil microbial community under laboratory conditions.* Applied Soil Ecology, 2020. **150**: p. 103463.
51. Lavelle, P., *The structure of earthworm communities*, in *Earthworm ecology: from Darwin to vermiculture*. 1983, Springer. p. 449-466.
52. Pižl, V. and A. Nováková, *Interactions between microfungi and* Eisenia andrei *(Oligochaeta) during cattle manure vermicomposting: The 7th international symposium on earthworm ecology· Cardiff· Wales· 2002.* Pedobiologia, 2003. **47**(5-6): p. 895-899.
53. Kim, H., *A study on the utilization of the earthworms* Eisenia fetida *and* Eisenia andrei *for the disposal of polymers.* International Journal of Environmental Science and Development, 2016. **7**(5): p. 355-358.
54. Lwanga, E.H., B. Thapa, X. Yang, H. Gertsen, T. Salánki, V. Geissen and P. Garbeva, *Decay of low-density polyethylene by bacteria extracted from earthworm's guts: A potential for soil restoration.* Science of the Total Environment, 2018. **624**: p. 753-757.
55. Eltemsah, Y.S. and T. Bøhn, *Acute and chronic effects of polystyrene microplastics on juvenile and adult* Daphnia magna. Environmental Pollution, 2019. **254**: p. 112919.
56. Baeza, C., C. Cifuentes, P. González, A. Araneda and R. Barra, *Experimental exposure of* Lumbricus terrestris *to microplastics.* Water, Air, & Soil Pollution, 2020. **231**: p. 1-10.
57. Huerta Lwanga, E., H. Gertsen, H. Gooren, P. Peters, T. Salánki, M. Van Der Ploeg, E. Besseling, A.A. Koelmans and V. Geissen, *Microplastics in the terrestrial ecosystem: implications for* Lumbricus terrestris *(Oligochaeta, Lumbricidae).* Environmental Science & Technology, 2016. **50**(5): p. 2685-2691.
58. Rodríguez, T., D. Represas and E.V. Carral, *Ecotoxicity of Single-Use Plastics to Earthworms.* Environments, 2023. **10**(3): p. 41.
59. Wang, X., Y. Zhang, Y. Zhang, M. Kang, Y. Li, S.W. James, Y. Yang, Y. Bi, H. Jiang and Y. Zhao, Amynthas corticis *genome reveals molecular mechanisms behind global distribution.* Communications Biology, 2021. **4**(1): p. 135.
60. Shao, Y., X.-B. Wang, J.-J. Zhang, M.-L. Li, S.-S. Wu, X.-Y. Ma, X. Wang, H.-F. Zhao, Y. Li and H.H. Zhu, *Genome and single-cell RNA-sequencing*

of the earthworm Eisenia andrei *identifies cellular mechanisms underlying regeneration.* Nature Communications, 2020. **11**(1): p. 1-15.

61. Altschul, S.F., W. Gish, W. Miller, E.W. Myers and D.J. Lipman, *Basic local alignment search tool.* Journal of Molecular Biology, 1990. **215**(3): p. 403-410.
62. Yachdav, G., S. Wilzbach, B. Rauscher, R. Sheridan, I. Sillitoe, J. Procter, S.E. Lewis, B. Rost and T. Goldberg, *MSAViewer: interactive JavaScript visualization of multiple sequence alignments.* Bioinformatics, 2016. **32**(22): p. 3501-3503.
63. Teufel, F., J.J. Almagro Armenteros, A.R. Johansen, M.H. Gíslason, S.I. Pihl, K.D. Tsirigos, O. Winther, S. Brunak, G. von Heijne and H. Nielsen, *SignalP 6.0 predicts all five types of signal peptides using protein language models.* Nature Biotechnology, 2022. **40**(7): p. 1023-1025.
64. Saegusa, H., M. Shiraki, C. Kanai and T. Saito, *Cloning of an intracellular poly [d (−)-3-hydroxybutyrate] depolymerase gene from* Ralstonia eutropha *H16 and characterization of the gene product.* Journal of bacteriology, 2001. **183**(1): p. 94-100.
65. Evans, R., M. O'Neill, A. Pritzel, N. Antropova, A. Senior, T. Green, A. Žídek, R. Bates, S. Blackwell and J. Yim, *Protein complex prediction with AlphaFold-Multimer.* BioRxiv, 2021: p. 2021.10. 04.463034.
66. Jumper, J., R. Evans, A. Pritzel, T. Green, M. Figurnov, O. Ronneberger, K. Tunyasuvunakool, R. Bates, A. Žídek, A. Potapenko, A. Bridgland, C. Meyer, S.A.A. Kohl, A.J. Ballard, A. Cowie, B. Romera-Paredes, S. Nikolov, R. Jain, J. Adler, T. Back, S. Petersen, D. Reiman, E. Clancy, M. Zielinski, M. Steinegger, M. Pacholska, T. Berghammer, S. Bodenstein, D. Silver, O. Vinyals, A.W. Senior, K. Kavukcuoglu, P. Kohli and D. Hassabis, *Highly accurate protein structure prediction with AlphaFold.* Nature, 2021. **596**(7873): p. 583-589.
67. Varadi, M., S. Anyango, M. Deshpande, S. Nair, C. Natassia, G. Yordanova, D. Yuan, O. Stroe, G. Wood, A. Laydon, A. Žídek, T. Green, K. Tunyasuvunakool, S. Petersen, J. Jumper, E. Clancy, R. Green, A. Vora, M. Lutfi, M. Figurnov, A. Cowie, N. Hobbs, P. Kohli, G. Kleywegt, E. Birney, D. Hassabis and S. Velankar, *AlphaFold Protein Structure Database: massively expanding the structural coverage of protein-sequence space with high-accuracy models.* Nucleic Acids Research, 2021. **50**(D1): p. D439-D444.
68. Becker, S. and J.-H. Hehemann, *Laminarin quantification in microalgae with enzymes from marine microbes.* Bio-protocol, 2018. **8**(8): p. e2666-e2666.
69. Briese, B.H., B. Schmidt and D. Jendrossek, Pseudomonas lemoignei *has five poly (hydroxyalkanoic acid)(PHA) depolymerase genes: a comparative study of bacterial and eukaryotic PHA depolymerases.* Journal of Environmental Polymer degradation, 1994. **2**: p. 75-87.
70. Julka, J.M., *Earthworm resources and vermiculture*. 1993: The Survey.

Chapter III

Supplementary Text, Figures and Tables

Supplementary Text

Supplementary Text 1 | Earthworm's influence in the environment

Earthworms play an important role in soil systems, influencing whether soils represent a sink or source of soil organic carbon (SOC). They stabilize the labile SOC by forming aggregates - storing carbon. Additionally, they transform plant materials to be usable by microorganisms. The feeding, burrowing and casting behavior of earthworms creates a favorable environment for the breakdown of SOC by microorganisms, thus stimulating the release of carbon to the atmospheres[1]. Earthworms are generally used as a bioindicator and ecosystem engineer[2, 3].

Supplementary Text 2 | PHA as a biodegradable plastic by animal species

High molecular weight PHAs are biodegradable polymers used to produce thermoplastics[4-7]. The use of plastics is a worldwide problem affecting every known environment (e.g. Dris et al., 2015[8]; Lebreton et al., 2017[9]; Brandon et al., 2019[10]; Hurley et al., 2020[11]). Petroleum-based plastics further degrade into microplastics which can enter the food chain[12-17]. These problems lead to the higher interest in biodegradable plastics. Microbial activity degrades bio-plastics completely to CO_2[18]. PHA-based bioplastics gained attention because they are not only synthesized by bacteria but are also fully biodegradable, making them and alternative to traditional petrochemical plastics.

PHA-based bioplastics are directly extracted from PHA-synthesizing bacteria after they have been incubated in the presence of a rich carbon source[19]. These PHA-based bioplastics are broken down by PHADs synthesized in bacteria, fungi and some protist species[20-24]. For example, in shallow water environments, PHA-based bottles are estimated to be degraded after 1.5-3.5 years[25]. 77 animal species representing nine animal phyla across diverse habitats can degrade PHA (Chapter 1). The PHADs of these animals might contribute to the degradation of PHA-based bioplastics to their monomers. The complete PHA degradation might help to reduce plastic waste and the

microplastic problem. Earthworm species, in particular, play a role in plastic degradation as they were shown to ingest bioplastics such as poly lactic acid (PLA) and other plastics[26]. The ingestion of these plastics by earthworm species always led to a reduction in size of the plastics but not in their complete degradation[27]. Given that earthworm species expressed a PHAD, it seems likely that they can degrade PHA-based plastic. Therefore, earthworms could help along with other animal species to reduce the (micro-)plastic contamination.

Supplementary Text 3 | Earthworm symbiosis

I hypothesized that earthworms have access to PHA from their nephridial symbionts or the bacteria they regularly ingest.

Nephridial symbionts are commonly found in earthworms[28]. Nephridia are paired excretory organs for nitrogenous waste products, coiled into three loops at each segment[29, 30]. The nephridial symbionts formed a monophyletic clade of the symbiont specific genus *Verminephrobacter*[31]. *Verminephrobacter* symbionts were found in 19 out of 23 earthworm species, including *Lumbricus terrestris*. *Verminephrobacter* symbionts are species-specific to the earthworm host. While distinct earthworm species harbor different symbiont genotypes, the same species from different regions have more closely related symbiont genotypes[32]. *Verminephrobacter* symbionts have the ability to synthesize PHA as they have the PHA synthase (*phaC*) gene[33]. Given that most earthworm species harbor *Verminephrobacter* symbionts, we hypothesize that the PHA synthesized by the nephridial symbionts could serve as a PHA source for earthworms.

The existence of symbionts in the gut is debated[34]. One argument against the existence of gut symbionts is the similarity between the gut bacteria and the bacteria found in fresh casts[35]. However, there is evidence for specific gut bacteria, such as *Acinetobacte*r sp. and *Aeromonas* sp., which were not found in the surrounding soil[36]. Additionally, certain gut bacteria are persistent in the epithelium of the hind gut. They likely attach by physical links[37, 38]. Soil bacteria, including *Pseudomonas* and *Firmicute* species, have also been shown to enrich along the digestive tract [39]. It is not yet known what benefits might arise from these potential gut symbionts. Conditions are favorable for N_2O-producing bacteria[40, 41]. Based on the ability of many soil bacteria

to synthesize PHA, we hypothesize that the gut microbiota might deliver PHA to the earthworm through their diet.

Supplementary Figures

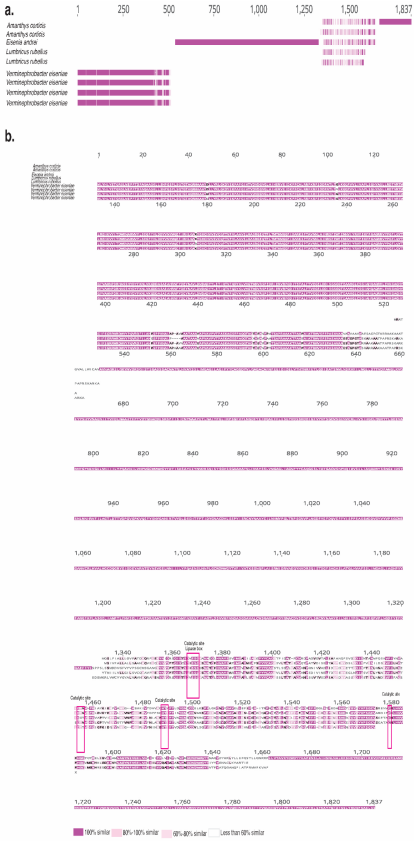

Supplementary Figure 1 | Earthworm PHADs are different to the symbiont PHADs of *V. eisenia*. We aligned the protein sequences of the earthworm PHADs with the PHADs of the symbiont *V. eisenia* using MAFFT[42]. The alignment was visualized using GeniousPrime (https://www.geneious.com). **a.** Overview of the alignment showed no overlap between the symbiont and earthworm PHADs. **b.** By zooming in the alignment, we identified that the symbiont PHADs do not show alignment to the catalytic site and lipase box because the symbionts lacked the lipase box. A missing lipase box is typical for intracellular PHADs. Symbiont PHADs are predicted to be intracellular PHADs based on the PHAD engineering database [43-45].

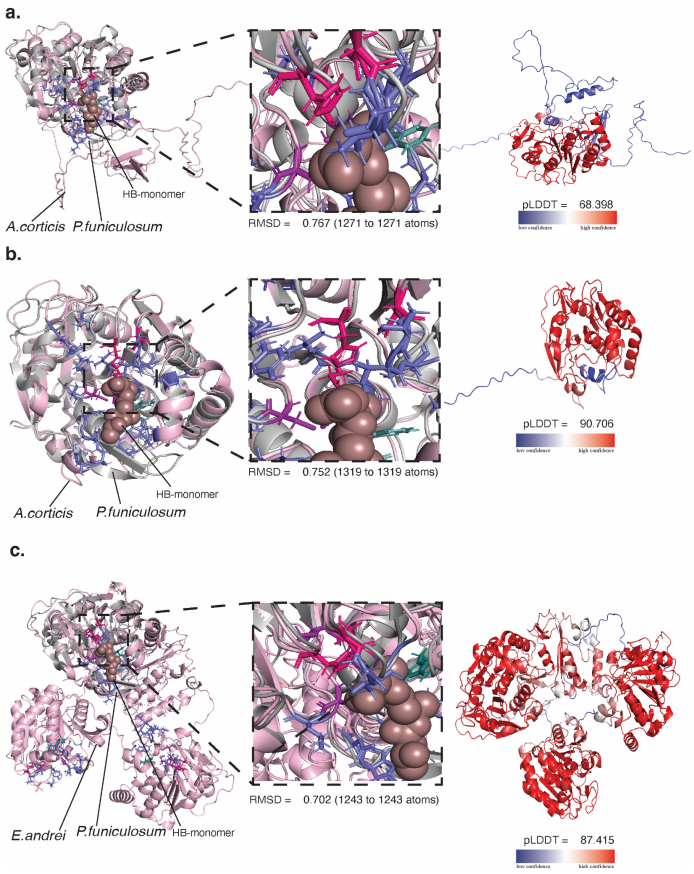
a.
HB-monomer
A.corticis
P.funiculosum
RMSD = 0.767 (1271 to 1271 atoms)
pLDDT = 68.398
low confidence
high confidence
b.
HB-monomer
A.corticis
P.funiculosum
RMSD = 0.752 (1319 to 1319 atoms)
pLDDT = 90.706
low confidence
high confidence
c.
E.andrei
P.funiculosum
HB-monomer
RMSD = 0.702 (1243 to 1243 atoms)
pLDDT = 87.415
low confidence
high confidence

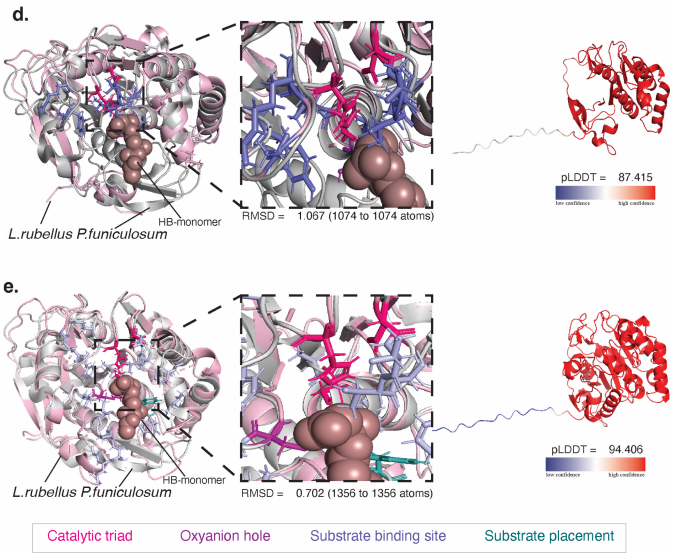

Supplementary Figure 2 | AlphaFold2 models of all five earthworm PHADs showed structural conservation of the catalytic and substrate binding site. We created AlphaFold2[46-48] models of all five earthworm PHADs. **a.** *A. corticis* PHAD showed structural alignment to the PHAD of the fungus *P. funiculosum* (RMSD: 0.867 (1271 to 1271 atoms; pdb 2d81)[49]. The *A. corticis* PHAD showed an external loop formation that is different to the one domain enzyme of the fungal homolog. This extra loop showed poor model prediction. **b.** The second *A. corticis* PHAD was modeled as one globular domain enzyme that aligned to the fungal homolog (RMSD: 0.752 (1319 to 1319 atoms). Especially the catalytic site and the substrate binding site were conserved. **c.** The *E. andrei* PHADs was modeled as a three-subdomain enzyme. When we looked into each of the subdomains, each of the domains showed 100% conservation of the catalytic site and the substrate binding site, suggesting that each subdomain can degrade PHA. As there are no described PHAD multimers, we hypothesized that *E. andrei* has three PHADs that were assembled together. **d.** The *L. rubellus* PHAD was not complete, lacking parts of the C-terminal substrate binding site. The catalytic site showed complete alignment to the fungal homolog (RMSD: 10.067 (1074 to 1074 atoms). **e.** The second *L. rubellus* PHAD showed good alignment to the fungal homolog (RMSD: 0.702 (1356 to 1356 atoms), especially at the catalytic site and substrate binding site. Both *L. rubellus* PHADs were modeled as a globular enzyme.

```
Lumbricus rubellus   MIILVLLGILSVCQAAVPLEKYNVDPTQISCSGISSGASMASQFHVAYSARIMGVGMIAG
Expression vector    MIILVLLGILSVCQAAVPLEKYNVDPTQISCSGISSGASMASQFHVAYSARIMGVGMIAG
                     MIILVLLGILSVCQAAVPLEKYNVDPTQISCSGISSGASMASQFHVAYSARIMGVGMIAG

                     SPYYCAQGVLLTALGACMVNPEDIVISELTDQTERYEGLNDIDSVSNLYNARVFILHGTE
                     SPYYCAQGVLLTALGACMVNPEDIVISELTDQTERYEGLNDIDSVSNLYNARVFILHGTE
                     SPYYCAQGVLLTALGACMVNPEDIVISELTDQTERYEGLNDIDSVSNLYNARVFILHGTE

                     DTVVDPGLGPTVVEYYQTYVNPANIETVFNLAAEHTFPTLNYGNACDRAASPYISDCDYD
                     DTVVDPGLGPTVVEYYQTYVNPANIETVFNLAAEHTFPTLNYGNACDRAASPYISDCDYD
                     DTVVDPGLGPTVVEYYQTYVNPANIETVFNLAAEHTFPTLNYGNACDRAASPYISDCDYD

                     GAYAILNSIYGGNLVAPGGTVPLNGEFYEFDQVEFFYISPPSLSSMDEVGYVYVPSGCVS
                     GAYAILNSIYGGNLVAPGGTVPLNGEFYEFDQVEFFYISPPSLSSMDEVGYVYVPSGCVS
                     GAYAILNSIYGGNLVAPGGTVPLNGEFYEFDQVEFFYISPPSLSSMDEVGYVYVPSGCVS

                     GATACRLHVVFHGCVMGRHRIEDEFARNAGYNEVGELNNIIILYPQAIATASNPNGCWDW
                     GATACRLHVVFHGCVMGRHRIEDEFARNAGYNEVGELNNIIILYPQAIATASNPNGCWDW
                     GATACRLHVVFHGCVMGRHRIEDEFARNAGYNEVGELNNIIILYPQAIATASNPNGCWDW

                     WGYTIYYYATQGANQPLATIR
                     WGYTIYYYATQGANQPLATIR
                     WGYTIYYYATQGANQPLATIR

                     100% similar   80%-100% similar   60%-80% similar   Less than 60% similar
```

Supplementary Figure 3 | The *L. rubellus* PHAD was successfully inserted in the expression vector. We inserted the *L. rubellus* PHAD in a pet28(+) expression vector between the sites NheI/XhoI. The expression vector was transferred to *E.coli* clones which we used to overexpress the *L. rubellus* PHAD. We send the *E.coli* clones with the expression vector to Microsynth AG for plasmid sequencing. The resulting sequences showed a 100% match to the original *L. rubellus* PHAD.

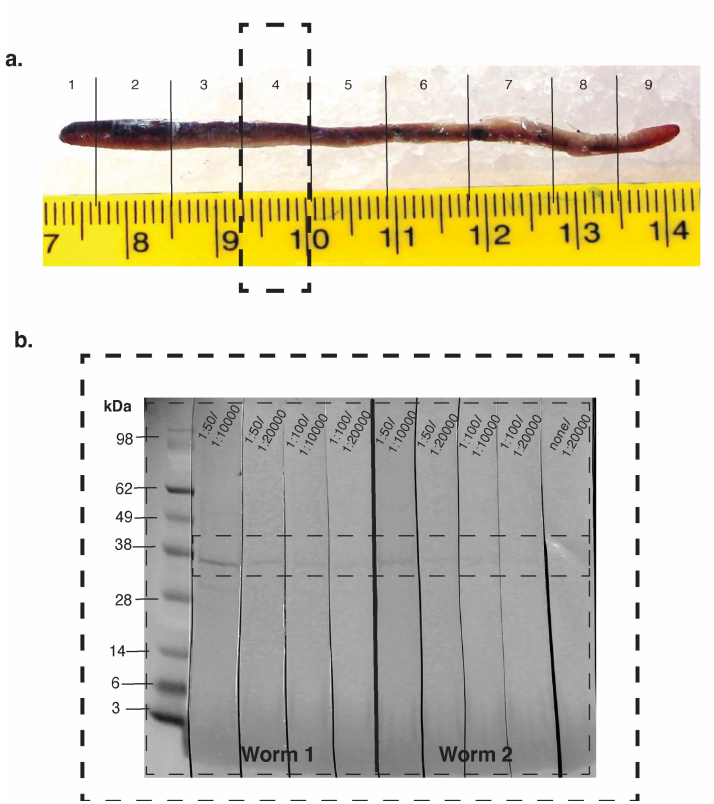

Supplementary Figure 4 | The *L. rubellus* PHAD antibody binds specifically. a. We dissected *L. rubellus* individuals in nine sections following the earthworm's intestine to localize the expression of the PHAD. **b.** The sections were then tested for the specific binding of the *L. rubellus* PHAD antibody which we found to be expressed at the start of the intestine following the earthworm's hearts (section 4 labeled by a square). In this region we tested the antibody for the best concentration in two different worms. The best antibody concentration ranges from 1:50 -1:100 dilution of the primary antibody and a 1:10000 - 1:20000 dilution of the secondary antibody which we used for the testing of the immunohistochemistry on sections.

Supplementary Tables

Species	Prediction	Other	SP (Sec/SPI)	Cleavage site position
Lumbricus rubellus	Signal peptide	0.000244	0.999748	CS pos: 17-18. Pr: 0.9735
Lumbricus rubellus	Signal peptide	0.311439	0.688541	CS pos: 18-19. Pr: 0.7973
Eisenia andrei	Signal peptide	0.248412	0.751586	CS pos: 18-19. Pr: 0.8262
Amynthas corticis	Signal peptide	0.000248	0.999724	CS pos: 16-17. Pr: 0.9792
Amynthas corticis	Signal peptide	0.000507	0.999502	CS pos: 17-18. Pr: 0.9581

Supplementary Table 1 | All earthworm PHADs are predicted to have a signal peptide and are likely transported out of the cell. We used SignalP (6.0)[50] to predict if the earthworm's PHADs have a signal peptide which would allow their transport outside of the cell. All five earthworm PHADs have with high probability a signal peptide that is cleaved between amino acid position 16-19. We therefore hypothesize that the earthworm PHADs can degrade extracellular PHA.

***L. rubellus* antibody**	**Sequence**	**Antibody programm**
Peptide 1	nh2-C+ELTDQTERYEGLNDI – conh2	AS-SUPR-DXP · Speedy 28-Day programme · 2 Rabbits · 2 peptides synthesized at Eurogentec · ELISA Guarantee · Affinity Purif.
Peptide 2	nh2-C+GTEDTVVDPGLGPTV – conh2	AS-SUPR-DXP · Speedy 28-Day programme · 2 Rabbits · 2 peptides synthesized at Eurogentec · ELISA Guarantee · Affinity Purif.

Supplementary Table 2 | The *L. rubellus* specific PHAD antibody was synthesized by the company Eurogentec in a rabbit host system. We designed two peptides that target the *L. rubellus* PHAD. Both were synthesized using Eurogentec's speedy 28-day program in a rabbit system. The yield of the enzyme was between 15 and 25mg. Both antibodies were pooled.

References

1. Angst, G., C.W. Mueller, I. Prater, Š. Angst, J. Frouz, V. Jílková, F. Peterse and K.G. Nierop, *Earthworms act as biochemical reactors to convert labile plant compounds into stabilized soil microbial necromass.* Communications Biology, 2019. **2**(1): p. 441.
2. Jones, C.G., J.H. Lawton and M. Shachak, *Organisms as ecosystem engineers.* Oikos, 1994: p. 373-386.
3. Fusaro, S., F. Gavinelli, F. Lazzarini and M.G. Paoletti, *Soil Biological Quality Index based on earthworms (QBS-e). A new way to use earthworms as bioindicators in agroecosystems.* Ecological Indicators, 2018. **93**: p. 1276-1292.
4. Steinbüchel, A. and T. Lütke-Eversloh, *Metabolic engineering and pathway construction for biotechnological production of relevant polyhydroxyalkanoates in microorganisms.* Biochemical Engineering Journal, 2003. **16**(2): p. 81-96.
5. Snell, K.D. and O.P. Peoples, *PHA bioplastic: A value-added coproduct for biomass biorefineries.* Biofuels, Bioproducts and Biorefining: Innovation for a Sustainable Economy, 2009. **3**(4): p. 456-467.
6. Keshavarz, T. and I. Roy, *Polyhydroxyalkanoates: bioplastics with a green agenda.* Current Opinion in Microbiology, 2010. **13**(3): p. 321-326.
7. Pratt, S., L.-J. Vandi, D. Gapes, A. Werker, A. Oehmen and B. Laycock, *Polyhydroxyalkanoate (PHA) bioplastics from organic waste.* Biorefinery: Integrated Sustainable Processes for Biomass Conversion to Biomaterials, Biofuels, and Fertilizers, 2019: p. 615-638.
8. Dris, R., H. Imhof, W. Sanchez, J. Gasperi, F. Galgani, B. Tassin and C. Laforsch, *Beyond the ocean: contamination of freshwater ecosystems with (micro-) plastic particles.* Environmental Chemistry, 2015. **12**(5): p. 539-550.
9. Lebreton, L.C., J. Van Der Zwet, J.-W. Damsteeg, B. Slat, A. Andrady and J. Reisser, *River plastic emissions to the world's oceans.* Nature Communications, 2017. **8**(1): p. 15611.
10. Brandon, J.A., W. Jones and M.D. Ohman, *Multidecadal increase in plastic particles in coastal ocean sediments.* Science Advances, 2019. **5**(9): p. eaax0587.
11. Hurley, R., A. Horton, A. Lusher and L. Nizzetto, *Plastic waste in the terrestrial environment*, in *Plastic Waste and Recycling*. 2020, Elsevier. p. 163-193.
12. Steinmetz, Z., C. Wollmann, M. Schaefer, C. Buchmann, J. David, J. Tröger, K. Muñoz, O. Frör and G.E. Schaumann, *Plastic mulching in agriculture. Trading short-term agronomic benefits for long-term soil degradation?* Science of the Total Environment, 2016. **550**: p. 690-705.
13. Ammala, A., S. Bateman, K. Dean, E. Petinakis, P. Sangwan, S. Wong, Q. Yuan, L. Yu, C. Patrick and K. Leong, *An overview of degradable and biodegradable polyolefins.* Progress in Polymer Science, 2011. **36**(8): p. 1015-1049.
14. Laycock, B., M. Nikolić, J.M. Colwell, E. Gauthier, P. Halley, S. Bottle and G. George, *Lifetime prediction of biodegradable polymers.* Progress in Polymer Science, 2017. **71**: p. 144-189.

15. Qi, R., D.L. Jones, Z. Li, Q. Liu and C. Yan, *Behavior of microplastics and plastic film residues in the soil environment: A critical review.* Science of the Total Environment, 2020. **703**: p. 134722.
16. Qian, J., S. Tang, P. Wang, B. Lu, K. Li, W. Jin and X. He, *From source to sink: Review and prospects of microplastics in wetland ecosystems.* Science of The Total Environment, 2021. **758**: p. 143633.
17. Rillig, M.C., *Microplastic in terrestrial ecosystems and the soil?* 2012, ACS Publications.
18. Rodríguez, T., D. Represas and E.V. Carral, *Ecotoxicity of Single-Use Plastics to Earthworms.* Environments, 2023. **10**(3): p. 41.
19. Holmes, P., *Applications of PHB-a microbially produced biodegradable thermoplastic.* Physics in Technology, 1985. **16**(1): p. 32.
20. Jendrossek, D. and R. Handrick, *Microbial degradation of polyhydroxyalkanoates.* Annual Review of Microbiology, 2002. **56**: p. 403.
21. Gonda, K., D. Jendrossek and H.-P. Molitoris, *Fungal degradation of the thermoplastic polymer poly-ß-hydroxybutyric acid (PHB) under simulated deep sea pressure*, in *Life at Interfaces and Under Extreme Conditions*. 2000, Springer. p. 173-183.
22. Kim, D. and Y. Rhee, *Biodegradation of microbial and synthetic polyesters by fungi.* Applied Microbiology and Biotechnology, 2003. **61**(4): p. 300-308.
23. Anderson, I.J., R.F. Watkins, J. Samuelson, D.F. Spencer, W.H. Majoros, M.W. Gray and B.J. Loftus, *Gene discovery in the* Acanthamoeba castellanii *genome.* Protist, 2005. **156**(2): p. 203-14.
24. Viljakainen, V. and L. Hug, *The phylogenetic and global distribution of bacterial polyhydroxyalkanoate bioplastic-degrading genes.* Environmental Microbiology, 2021. **23**(3): p. 1717-1731.
25. Dilkes-Hoffman, L.S., P.A. Lant, B. Laycock and S. Pratt, *The rate of biodegradation of PHA bioplastics in the marine environment: A meta-study.* Marine Pollution Bulletin, 2019. **142**: p. 15-24.
26. Kim, H., *A study on the utilization of the earthworms* Eisenia fetida *and* Eisenia andrei *for the disposal of polymers.* International Journal of Environmental Science and Development, 2016. **7**(5): p. 355-358.
27. Lwanga, E.H., B. Thapa, X. Yang, H. Gertsen, T. Salánki, V. Geissen and P. Garbeva, *Decay of low-density polyethylene by bacteria extracted from earthworm's guts: A potential for soil restoration.* Science of the Total Environment, 2018. **624**: p. 753-757.
28. Knop, J. and J. Knop, *Bakterien und Bakteroiden bei Oligochaeten: Inaugural-Dissertation zur Erlangung der Doktorwürde der Hohen Philosophischen Fakultät der Universität zu Greifswald*. 1926: Springer.
29. Edwards, C.A. and P.J. Bohlen, *Biology and ecology of earthworms*. Vol. 3. 1996: Springer Science & Business Media.
30. Dales, R.P., *Earthworm Physiology*. 1963, Nature Publishing Group UK London.
31. Pinel, N., S.K. Davidson and D.A. Stahl, *Verminephrobacter eiseniae gen. nov., sp. nov., a nephridial symbiont of the earthworm* Eisenia foetida *(Savigny).* International Journal of Systematic and Evolutionary Microbiology, 2008. **58**(9): p. 2147-2157.
32. Schramm, A., S.K. Davidson, J.A. Dodsworth, H.L. Drake, D.A. Stahl and N. Dubilier, Acidovorax*-like symbionts in the nephridia of earthworms.* Environmental Microbiology, 2003. **5**(9): p. 804-809.

33. Cheema, S., M. Bassas-Galia, P.M. Sarma, B. Lal and S. Arias, *Exploiting metagenomic diversity for novel polyhydroxyalkanoate synthases: production of a terpolymer poly (3-hydroxybutyrate-co-3-hydroxyhexanoate-co-3-hydroxyoctanoate) with a recombinant* Pseudomonas putida *strain.* Bioresource Technology, 2012. **103**(1): p. 322-328.
34. Curry, J.P. and O. Schmidt, *The feeding ecology of earthworms – a review.* Pedobiologia, 2007. **50**(6): p. 463-477.
35. Egert, M., S. Marhan, B. Wagner, S. Scheu and M.W. Friedrich, *Molecular profiling of 16S rRNA genes reveals diet-related differences of microbial communities in soil, gut, and casts of* Lumbricus terrestris *L.(Oligochaeta: Lumbricidae).* FEMS Microbiology Ecology, 2004. **48**(2): p. 187-197.
36. Byzov, B., T.Y. Nechitaylo, B. Bumazhkin, A. Kurakov, P. Golyshin and D. Zvyagintsev, *Culturable microorganisms from the earthworm digestive tract.* Microbiology, 2009. **78**: p. 360-368.
37. Jolly, J., H. Lappin-Scott, J. Anderson and C. Clegg, *Scanning electron microscopy of the gut microflora of two earthworms:* Lumbricus terrestris *and* Octolasion cyaneum*.* Microbial Ecology, 1993. **26**: p. 235-245.
38. Lavelle, P. and A. Spain, *Soil ecology*. 2002: Springer Science & Business Media.
39. Furlong, M.A., D.R. Singleton, D.C. Coleman and W.B. Whitman, *Molecular and culture-based analyses of prokaryotic communities from an agricultural soil and the burrows and casts of the earthworm* Lumbricus rubellus*.* Applied and Environmental Microbiology, 2002. **68**(3): p. 1265-1279.
40. Horn, M.A., A. Schramm and H.L. Drake, *The earthworm gut: an ideal habitat for ingested N2O-producing microorganisms.* Applied and Environmental Microbiology, 2003. **69**(3): p. 1662-1669.
41. Ihssen, J., M.A. Horn, C. Matthies, A. Gößner, A. Schramm and H.L. Drake, *N2O-producing microorganisms in the gut of the earthworm* Aporrectodea caliginosa *are indicative of ingested soil bacteria.* Applied and Environmental Microbiology, 2003. **69**(3): p. 1655-1661.
42. Katoh, K. and D.M. Standley, *MAFFT multiple sequence alignment software version 7: improvements in performance and usability.* Molecular Biology and Evolution, 2013. **30**(4): p. 772-780.
43. Handrick, R., S. Reinhardt and D. Jendrossek, *Mobilization of poly (3-hydroxybutyrate) in* Ralstonia eutropha*.* Journal of Bacteriology, 2000. **182**(20): p. 5916-5918.
44. Knoll, M., T.M. Hamm, F. Wagner, V. Martinez and J. Pleiss, *The PHA depolymerase engineering database: a systematic analysis tool for the diverse family of polyhydroxyalkanoate (PHA) depolymerases.* BMC Bioinformatics, 2009. **10**: p. 1-8.
45. Saegusa, H., M. Shiraki, C. Kanai and T. Saito, *Cloning of an intracellular poly [d (−)-3-hydroxybutyrate] depolymerase gene from* Ralstonia eutropha *H16 and characterization of the gene product.* Journal of Bacteriology, 2001. **183**(1): p. 94-100.
46. Evans, R., M. O'Neill, A. Pritzel, N. Antropova, A. Senior, T. Green, A. Žídek, R. Bates, S. Blackwell and J. Yim, *Protein complex prediction with AlphaFold-Multimer.* BioRxiv, 2021: p. 2021.10. 04.463034.
47. Jumper, J., R. Evans, A. Pritzel, T. Green, M. Figurnov, O. Ronneberger, K. Tunyasuvunakool, R. Bates, A. Žídek, A. Potapenko, A. Bridgland, C. Meyer, S.A.A. Kohl, A.J. Ballard, A. Cowie, B. Romera-Paredes, S.

Nikolov, R. Jain, J. Adler, T. Back, S. Petersen, D. Reiman, E. Clancy, M. Zielinski, M. Steinegger, M. Pacholska, T. Berghammer, S. Bodenstein, D. Silver, O. Vinyals, A.W. Senior, K. Kavukcuoglu, P. Kohli and D. Hassabis, *Highly accurate protein structure prediction with AlphaFold*. Nature, 2021. **596**(7873): p. 583-589.

48. Varadi, M., S. Anyango, M. Deshpande, S. Nair, C. Natassia, G. Yordanova, D. Yuan, O. Stroe, G. Wood, A. Laydon, A. Žídek, T. Green, K. Tunyasuvunakool, S. Petersen, J. Jumper, E. Clancy, R. Green, A. Vora, M. Lutfi, M. Figurnov, A. Cowie, N. Hobbs, P. Kohli, G. Kleywegt, E. Birney, D. Hassabis and S. Velankar, *AlphaFold Protein Structure Database: massively expanding the structural coverage of protein-sequence space with high-accuracy models.* Nucleic Acids Research, 2021. **50**(D1): p. D439-D444.

49. Hisano, T., K. Kasuya, Y. Tezuka, N. Ishii, T. Kobayashi, M. Shiraki, E. Oroudjev, H. Hansma, T. Iwata, Y. Doi, T. Saito and K. Miki, *The crystal structure of polyhydroxybutyrate depolymerase from* Penicillium funiculosum *provides insights into the recognition and degradation of biopolyesters*. Jornal of Molecular Biology, 2006. **356**(4): p. 993-1004.

50. Teufel, F., J.J. Almagro Armenteros, A.R. Johansen, M.H. Gíslason, S.I. Pihl, K.D. Tsirigos, O. Winther, S. Brunak, G. von Heijne and H. Nielsen, *SignalP 6.0 predicts all five types of signal peptides using protein language models.* Nature Biotechnology, 2022. **40**(7): p. 1023-1025.

Discussion

General discussion and future directions

During my studies, I worked with the marine worm *Olavius algarvensis*, a non-model organism that is in symbiosis with up to five symbiont types. *O. algarvensis* does not have a digestive tract including a mouth, gut, anus and nephridial organs. Consequently, the host depends on its extracellular symbionts for nutrition and waste management[1]. Under anaerobic conditions, the primary symbiont *Candidatus* Thiosymbion algarvensis synthesizes polyhydroxyalkanoates (PHAs) from host waste products, representing 42% of the saved carbon[2] (Kleiner et al., unpublished). PHAs are carbon and energy storage compounds synthesized by many bacteria and halophilic archaea[3-8]. Once conditions become unfavorable, *Ca.* T. algarvensis could degrade PHA to gain carbon and energy. However, during my dissertation, I identified that the symbiont lacks key genes that would allow *Ca.* T. algarvensis to generate energy after PHA degradation (**Chapter II**). Due to the dependency of the host on its symbionts, I asked the question if *O. algarvensis* can use its symbiont's produced PHA as a carbon and energy source.

Until now, PHA depolymerases (PHADs), the enzymes degrading PHA, were only identified in bacteria, fungi and some archaea and protist species[9-13]. In my dissertation, I identified the first animal PHAD in the gutless oligochaete *O. algarvensis* (**Chapter I**). I also discovered 195 animal PHAD homologs in 67 animal species spanning nine metazoan phyla (**Chapter I & III**). Animal PHA degradation is not linked to symbiotic associations. All of the animals that encode for a PHAD access PHA through their microbial rich diets. Based on my initial findings, I hypothesized that PHA plays a nutritional role in animals (**Chapter I**). However, my detailed investigation into the earthworm PHAD revealed that there might be another advantage of encoding for a PHAD. I observed that *L. rubellus* expressed its PHAD protein in the epidermis which suggests that the earthworm secrets its PHAD either to degrade PHA of invading bacteria or to the soil environment (**Chapter III**).

Taken together, my dissertation allowed me to identify animal PHADs in a wide variety of metazoan species across ecosystems. The identification of this novel group of enzymes opened up new questions (Figure 1) which I would like to discuss in the following.

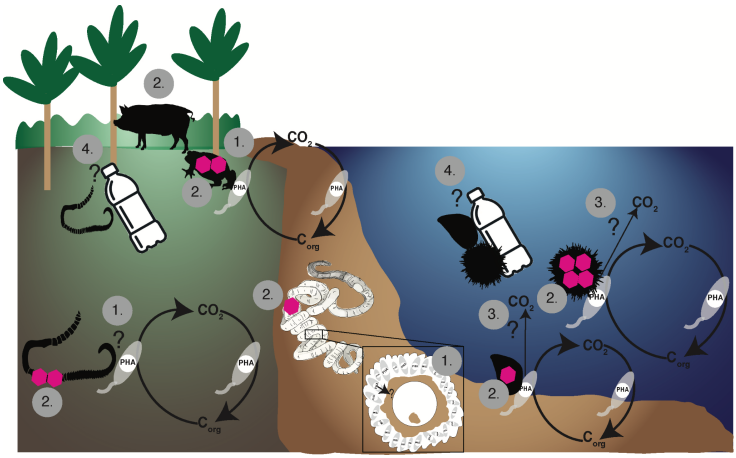

Figure 1 | During my studies, I identified that animals can degrade PHA. The identification opened up new questions and hypotheses. 1. Animals encode for PHADs that degrade PHA into its monomers and dimers used for energy generation. Future research should focus on the question "What is the benefit for animals to degrade PHA?" **2.** "Why are PHADs conserved in some animals but not in others?" I identified that 77 animals encode for PHADs across ecosystems. PHADs likely allow animals to gain a nutritional benefit from PHA. PHAD copy numbers can vary from one to up to 14, likely allowing animals with higher PHAD copy numbers more metabolic flexibility. **3.** I hypothesize that animal species across ecosystems can use the natural stored PHA from microbes and degrade it, respiring it to CO_2. We currently lack the understanding on the efficiency of animal PHADs and thus their influence on the carbon cycle. Future research should focus on the question: "How efficient are animal PHADs?" **4.** My analyses showed that animals in terrestrial, freshwater and marine habitats have PHADs. As PHADs degrade PHA-based plastics, I hypothesize that animals influence the degradation of PHA-based plastics. Leading to the question "Do animal PHADs contribute to the degradation of PHA-based plastics?"

1. What is the benefit for animals to degrade PHA?

PHA-producing symbionts have higher stress resistance, leading to an indirect fitness benefit for the host. The bean bug *Riptortus pedestris* had a shorter time until adulthood and larger body size, likely due to enhanced symbiont colonization and proliferation[14]. In contrast, *O. algarvensis* encodes and expresses a PHAD that degrades PHA extracellularly. The PHAD likely allows the host to use its symbionts stored PHA as a nutritional source, thus the host gains a direct benefit from PHA.

In my dissertation I hypothesized that the gutless oligochaetes acquire PHA by digesting their symbionts, which provides the worm with nutrition (**Chapter I**). Evidence for this hypothesis included (1) expression of an animal-specific PHAD, (2) functionality of the PHAD on extracellular PHA, and (3) imaging showing that *Ca.* T. algarvensis is often digested with intact PHA (Figure 2a). These observations make it likely that the hosts digest their symbionts, secrete their PHAD in the phago-lysosome and can take up the water-soluble monomers and dimers[15]. Alternatively, the hosts secrete the PHAD into the symbiont layer where it would come into contact with the PHA released following symbiont digestion. (Figure 2b).

PHA degradation might be important during the worm's movement to the oxic layers. Under oxic conditions, *Ca.* T. algarvensis is more frequently digested to overcome nutrient limitations. Worms incubated for eight days under oxic conditions showed depletion of symbiont proteins indicating symbiont digestion [16]. Given the hypothesis that the host gains access to PHA by symbiont digestion, PHA might play a role once the worm moves to the oxic sediment layers, helping the host to overcome nutrient limitation.

To test what benefits gutless oligochaetes get from PHA degradation, one possible approach is to create *Ca.* T. algarvensis mutants that do not synthesize PHA, similar as described for the bean bug *R. pedestris*[14]. However, we are currently limited in the creation of mutants due to the inability to culture the symbionts. Another possibility to identify the role of PHA for the symbiosis is to leverage metabolic modeling approaches (e.g.[17]) that aim to identify the carbon and energy transfer from the symbionts to the host. The symbiont-produced PHA makes up 42% of the stored carbon of the symbionts, representing more than a third of the carbon stored in the symbionts (Kleiner et al., unpublished). Previous modeling attempts suggest that likely symbiont digestion led to ^{13}C-enrichments in the host tissue. However, the rate and amount of the transferred carbon is not known (Kleiner et al., unpublished). Future metabolic models should capture the transfer of energy and carbon to the host to identify the benefit from degrading PHA. The experiment needed to create this model is a ^{13}C-labeling pulse-chase experiment, to identify the yield of carbon transfer during symbiont digestion.

Ca. Thiosymbion spp. appear to be limited in their ability to use their own PHA resource. I analyzed both the genome bins and metatranscriptomes of several *Ca.* Thiosymbion spp. for the enzymes needed for energy generation from PHA

degradation products and could not identify any of the respective enzymes (**Chapter II**). PHADs degrade PHA into monomers and dimers. Dimers are broken down by a hydroxybutyrate-dimer hydrolase (EC 3.1.1.22) and monomers by a beta-hydroxybutyrate dehydrogenase (EC 1.1.1.30). The degradation of the monomers yields acetoacetate, which is oxidized to acetyl-coenzyme A (acetyl-CoA) and then used in the citric acid cycle for energy generation[18, 19]. For intracellular PHA degradation, PHA-monomers are often coenzyme-A bound. It allows a quick usage of monomers for PHA synthesis or the degradation by a 3-hydroxybutyryl-CoA dehydrogenase producing acetyl-CoA (EC 1.1.1.157)[20]. The absence of these enzymes in *Ca*. Thiosymbion spp. suggests that the primary symbionts cannot generate energy from their own PHA resource. Only *Ca*. Thiosymbion spp. are unable to generate energy from PHA as other Chromatiales species can use their intracellular PHA to generate energy (**Chapter II**). Based on this, I hypothesize that there might be an adaptation of the primary symbiont to the ability of the host to use PHA for energy generation.

My analyses revealed that a secondary symbiont, the Deltaproteobacterium "Delta3", expressed homologs of the 3-hydroxybutyryl-CoA dehydrogenase and beta-hydroxybutyrate dehydrogenase (**Chapter II**). These results suggested that the "Delta3"-symbionts can also take up the water soluble PHA monomers through their cell membrane, and use them to generate energy. Based on my observations, I hypothesized that the entire metaorganism is needed to degrade PHA. Considering that the primary symbiont has an excess of carbon and energy under anaerobic conditions[2], PHA-degradation might redistribute the excess carbon and energy across symbiotic partners.

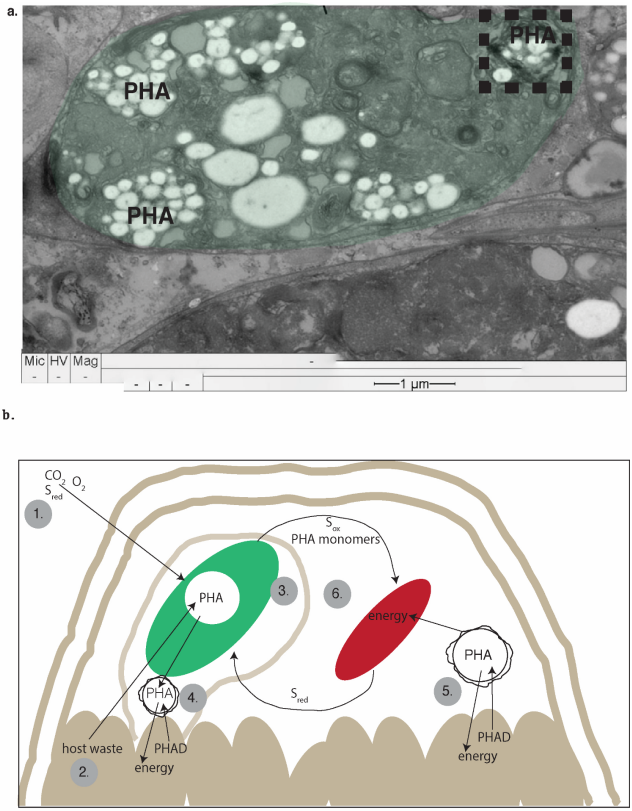

Figure 2 | Gutless oligochaetes gain access to the PHA stored by their symbionts through digestion. a. A TEM image of *O. algarvensis* host cells in the symbiont layer shows that *Ca*. Thiosymbion algarvensis symbionts (area labeled in green) are digested through phago-lysosomal digestion. Intact PHA in the form of white granules are in the phago-lysosome (highlighted in the square). Image courtesy of Mario Schimak. **b.** A diagram highlighting the major predictions developed from my dissertation. (1.) *Ca.* T. sp. (green) fixes CO_2 using chemical energy. (2.) Under anaerobic conditions the animal produces host waste products that the symbiont uses to build up PHA. (3.) *Ca.* T. sp. is digested by the host through phago-lysosomal digestion, which gives the host access to the symbiont's stored PHA. (4.) The host degrades PHA by its PHAD excreted to the phago-lysosome and takes up the resulting monomers to gain energy. (5.) Alternatively, lysed symbiont cells released extracellular PHA to the symbiont layer. The host degrades the PHA via PHAD activity and takes up the water-soluble monomers to generate energy. (6.) The "Delta3"-symbionts (red) likely use the resulting PHA monomers for energy generation. The "Delta3"-symbionts provide *Ca.* T. sp. with reduced sulfur species.

Other animal species either partially or fully feed on PHA-synthesizing organisms. For example, filter feeding molluscan species ingest water that contains PHA-synthesizing organisms[21, 22]. Collembola species feed on plant and detritus that likely contains PHA[23]. Animal PHADs together with protist PHADs branched off from a clade of bacteria from the *Bdellovibrio* genus (**Chapter I**). *Bdellovibrio* bacteria feed on Gram-negative bacteria after lysing them in the periplasm gaining access to bacterial synthesized PHA[24-27]. *Bdellovibrio* species feeding on PHA-synthesizing bacteria increased in predation motility and efficiency[25]. Animal species might take up PHA-synthesizing organisms with their diet and lyse them. The water-soluble monomers and dimers diffuse through the cell membrane and are used for energy generation. The generated energy likely leads to a fitness advantage for the animals. I analyzed the feeding behavior of all animal species using an ancestral state reconstruction. The results suggest that the last common ancestor of animals (LCA) had a diet consisting of microorganisms (**Chapter I, Supplementary Figure 18**). The "microvorous" nutrition of animals, protist and *Bdellovibrio* species likely results in a nutritional benefit from PHA degradation.

One exception to this hypothesis, is my observation that *L. rubellus* expressed the PHAD protein in the epidermis and not in the gut (**Chapter III**). The earthworm's cuticle functions to exclude invading bacteria by digesting them through phagocytosis[28]. It is possible that upon bacterial digestion, PHA will be released making it accessible to the degradation by the animal specific PHAD. However, in contrast to gutless worms, earthworms obtain most of their nutrition within their gut. It is thus not clear if PHA degradation would lead to increased nutrition. Alternatively, the earthworm could secrete the PHAD to their environment where it would work to degrade PHA found in the soil. The resulting monomers are either taken up by the earthworm or, more likely, by microorganisms living in the soil. The bacteria can then use the PHA monomers and dimers to promote their growth and metabolism. The enhanced microbial metabolism might help to improve microbial colonization in the earthworm burrows, instead of serving as a nutrient to support worm metabolism.

Future experiments should focus on (1) the location of the expressed PHAD transcripts and proteins and (2) determine the benefit of PHA supplemented in the animals' nutrition. Across animal species PHAD expression is localized using specific antibodies. The localization of PHAD expression is combined with applying a Nile Red staining on consecutive sections to show the site of PHA[29]. The combined labeling

would allow to link the site of PHA degradation to that of PHA molecules. In the second experiment, animals are fed with PHA to identify if an increase in PHA in their nutrition leads to a fitness benefit. Following the supplementation of PHA in the diet, I would monitor animal body weight, size, reproduction and survival to determine impacts on animal fitness. In parallel, metaproteomics analysis of individual species would allow me to correlate PHAD expression to an increase of PHA. I attempted this experiment with different earthworm species (*L. rubellus*, *L. terrestris* and several non-speciated individuals; **Chapter III**), but I was not able to detect an effect of PHA addition on earthworm fitness. During the experiment, I observed that earthworms of both experimental groups decreased in body weight and died. A possible explanation was high stress during the incubations. A last experiment that I would do to assess the benefit of PHA degradation, is to knock down the PHADs using RNAi. RNAi systems have recently been established for *Folsomia candida*[30] and would allow me to explore the fitness benefit from PHA degradation in animals.

2. Why are animal PHADs conserved in some animals but not in others?

Why did we identify animal PHADs in some animal species but not in others? In the first chapter of my dissertation I proposed that animal PHADs were present in the last common ancestor of animals (LCA), due to the monophyletic clustering of animal PHADs. The LCA either had one or multiple PHADs that diversified within the metazoans, with losses in some animal lineages (**Chapter I**). Some animal species, like the freshwater prawn *Macrobrachium rosenbergii* and domesticated pigs, do not have a PHAD in their genomes. Both of the species benefited from PHA supplementation in their nutrition but relied on their microbiome that degraded PHA[31, 32]. Alternatively, animals with a more complex diet might have lost their PHADs due to a lower benefit. Moving forward, it is important to determine the benefit of animal PHAD degradation in order to develop hypotheses about the evolutionary history of this enzyme group.

In my analysis, I showed that PHAD copy number varies across animal species. For example, *O. algarvensis* has only one PHAD copy, while *F. candida* has 14 PHAD copies (**Chapter I**). In bacteria, different PHADs allow them to use different PHA sources or will result in the formation of different PHA degradation products. For

example, the Betaproteobacterium, *Ralstonia eutropha,* encodes for nine PHADs. Each of the PHADs has a different function. Either they release CoA-bound monomers[20, 33], or hydrolyze PHA either into its hydroxycarboxylic monomers[19, 34] or oligomers[35, 36]. Similarly, the different PHAD copies likely allows metazoans to degrade different PHA sources or lead to the formation of different degradation products.

Intriguingly, gutless oligochaetes species often expressed more than one PHAD. While *O. algarvensis* only expressed one PHAD, its conspecific *Olavius ilvae* expressed five different copies (**Chapter I**). Therefore, it is possible that *O. ilvae* uses different PHA sources or degrades PHA into different reaction products. While it is known that *O. algarvensis* symbionts produce a copolymer of polyhydroxybutyrate/polyhydroxyvalerate/polyhydroxymethyl-valerate (PHB/PHV/PHMV), the PHA source found in other gutless oligochaetes remains unclear. Based on this, future experiments should focus on the identification of PHA found in other gutless oligochaetes by gas chromatography [37]. The identification of the PHA source might allow to better understand the role of PHAD copies. Additionally, it would allow to test each of the PHAD copies for the adaptation of a specific PHA source present in the symbiosis. Similarly, *L. rubellus* hast two PHADs. One showed a higher activity for PHB than for the copolymer PHB/PHV (**Chapter III**). It would thus be intriguing to heterologously express the second *L. rubellus* PHAD and test it on a variety of different PHA sources to determine if the earthworm can degrade different types of PHA.

The Arthropoda species, *Daphnia magna* has four PHAD copies that are likely adapted to the PHA sources that *D. magna* takes up by filter feeding[38]. To test this hypothesis, I chose to model *D. magnas* PHADs using AlphaFold2[39-41] (**Chapter I**; Figure 3). In Pymol, I measured the size range of their catalytic pockets. The catalytic site ranged from 3.8 x 2.5 x 7.0 Å to 4.7 x 4.4 x 8.5 Å. The variation in size could come from the substitution following the catalytic asparagine of $SV_{140\text{-}141}$ or $ST_{124\text{-}125/158\text{-}159}$ and could lead to degradation of different PHA sources. Enzyme assays should be done to support the hypothesis drawn from the AlphaFold2 predictions.

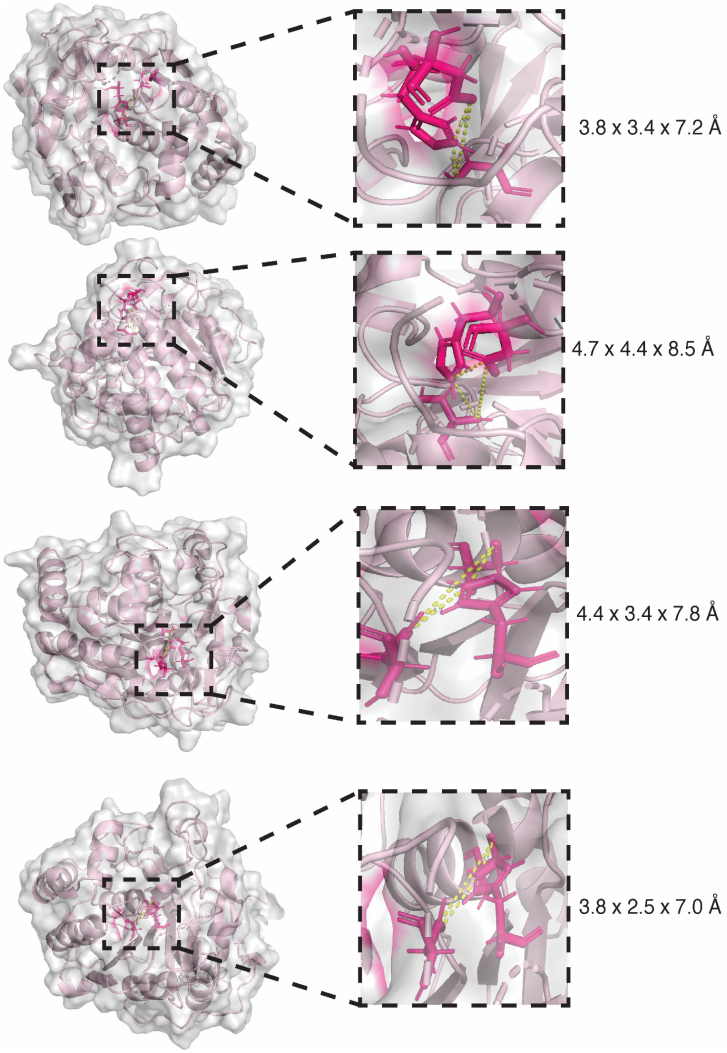

Figure 3 | *D. magna* PHADs have a different size range in their catalytic triads. AlphaFold2 models of the *D. magna* PHAD coupled with Pymol measurement of the pocket showed a variation in size of the catalytic triad. The size of the catalytic triad ranged from 2.5 x 7.0 Å to 4.7 x 4.4 x 8.5 Å. The variation in size of the catalytic triad could allow the binding of different PHA substrates.

3. What are the degradation efficiencies of animal PHADs?

Fungi have a higher efficiency to degrade PHA than bacterial PHADs due to the mobility of the enzyme[42]. The animal PHADs showed high homology to the fungal PHAD of *Penicillium funiculosum* (basionym *Talaromyces funiculosus*; pdb:2d81; 60-95% coverage, 22-43% identity)[43]. All of the identified sequences shared the common architecture of extracellular PHADs, including a signal peptide, followed by the catalytic site and substrate binding site. What differentiates animal PHADs from the fungal PHAD was the replacement of a beta-sheet (residues 295-299) by a loop. By looking into the surface structure of the *O. algarvensis* PHAD, the missing beta-sheet creates a channel to the catalytic crevice (Figure 4). I thus predicted the structure of the ancestral PHAD of the microvorous PHAD clade using a combination of ancestral reconstruction of proteins (GRASP)[44] and AlphaFold2 modeling[39-41] (Figure 4). The predicted ancestral PHAD lacked the beta-sheet suggesting that this is a trait conserved in "microvorous" PHADs.

Along the missing beta-sheet are several hydrophobic residues of the substrate binding site that allow the attachment to PHA. The channel of the "microvorous" PHADs might thus compensate for the missing hydrophobic residues by helping to direct the PHA to the catalytic site[45]. To test this hypothesis, the "microvorous" PHADs are heterologously expressed in *E. coli.* PHA degradation kinetics of animal PHADs in comparison to the fungal homolog are determined. Understanding the efficiency of the animal PHADs might help to identify the rate at which they degrade naturally occurring PHA.

In soil environments, the concentration of PHA ranges between 1.2 to 4.3 µg C/g of soil, depending on the soil type[46]. PHA serves as an internal storage compound once essential nutrients like oxygen, nitrogen or phosphate are scarce relative to an abundant carbon source - contributing to the storage of carbon[47, 48]. Extracellular PHADs act on denatured PHA released after the cell death or lysis of PHA-synthesizers[11]. PHADs degrade PHA into monomers and dimers, yielding energy. The hydroxyalkanoic monomers and dimers are respired to CO_2, CH_4 and water[49-51] - releasing carbon. For the reason that animals encode for extracellular PHADs, they likely influence carbon cycling across ecosystems. Future studies should thus focus on the rate of PHA degradation by animals.

One approach to determine the rate of PHA degradation is to use nanoSIMS. For example, ^{13}C-labeled bacteria are added to sterile water in which *D. magna* species are incubated. The ^{13}C of the bacteria nutrition incorporated into the animal tissue is quantified by normalizing with the ^{12}C. Additionally, it allows to localize the uptake (e.g. [52]). A second approach to determine the contribution of the carbon released from animal PHA degradation are respiration experiments using ^{13}C-labeling.

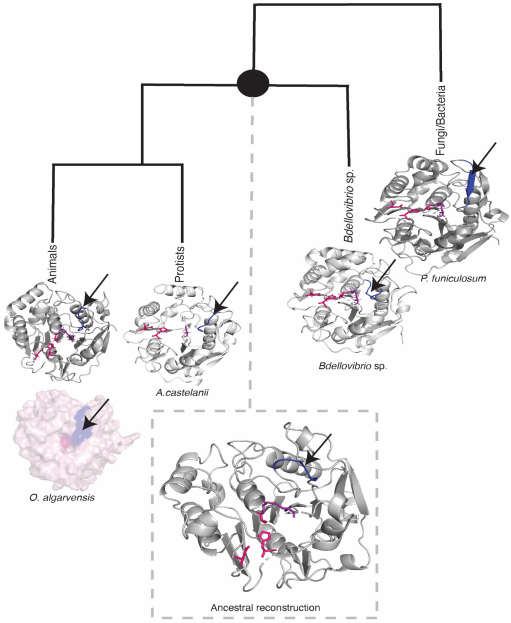

Figure 4 | Animal, protist and Bdellovibrio PHADs show a channel formation of the substrate binding site. The crystal structure of the fungal PHAD from *P. funiculosum* (pdb: 2d81) showed a beta-sheet (blue colored) between the residues 296 to 299. The predicted AlphaFold2 models of *O. algarvensis*, *A. castelanii* and *Bdellovibrio* sp. show a replacement by a loop (blue colored). The loop formation leads to a channel formation as shown by the surface structure of the *O. algarvensis* PHAD. The ancestral reconstructed structure of the microvorous PHADs shows the same replacement, suggesting that this is a common adaptation of the microvorous PHADs. All enzymes show conservation of the catalytic site (pink) and oxyanion hole (purple). The places of the amino acid replacements are labeled by an arrow.

4. Do animal PHADs contribute to the degradation of PHA-based biodegradable plastics?

We are currently facing a global plastic problem leading to plastic accumulation and microplastic formation (e.g. Dris et al.,2015[53]; Lebreton et al., 2017[54]; Brandon et al., 2019[55]; Hurley et al., 2020[56]). Interest in bio-degradable plastics, such as PHA, has increased. PHA is both biosynthesized by bacteria and biodegraded in the environment. For example, the degradation rates of PHA-based water bottles deposited in shallow water systems ranged from 0.04 to 0.09 mg/day/cm^2, resulting in a total length of PHA degradation of 1.5 to 3.5 years [57]. These results raise the question to what extent animals contribute to PHA-based plastic degradation in nature.

Given that animals encode for a PHAD it is likely that they have the ability to degrade PHA-based plastics. It is not clear what the effect of PHA-based plastics is on the animal's health. One hypothesis is that animals can degrade PHA-based plastics using their PHAD. The resulting monomers and dimers are used for energy generation. In this scenario PHA-based plastics would represent a nutritional advantage for the animals. Feeding studies with the earthworm *Eisenia fetida* suggest that a combination of the plastics poly-lactic acid and PHA did not have a harmful effect on the worms, but also did not confer a benefit[58]. In the other extreme, PHA could have harmful effects as was shown for the wax moth larvae. Wax moth larvae are predicted to degrade polypropylene (PE) based of the observation that PE bags reduced by 13% in weight after 14 hours[59]. However, the larvae's survival rate and weight decreased after ingestion of PE, suggesting that they cannot live from PE. A possible explanation is that they are not able to degrade PE but only mechanically disrupt the PE bags[60]. Taken together, future experiments should focus on the ability of animal species to degrade PHA-based plastics.

One approach to identify the ability of animals to degrade PHA is to incubate them in the presence of PHA-based plastics. In the first step, the surface of PHAs is analyzed by atomic force microscopy (AFM) after the PHA incubations. As a second step, fourier transform infrared spectroscopy (FTIR) and high-performance liquid chromatography coupled with mass spectrometry (HPLC–MS) are used to identify if animals can fully degrade PHA-based plastics to monomers and dimers (e.g [59]). During these experiments, animal fitness needs to be monitored in terms of survival rate, body mass and size, time until adulthood and reproduction efficiency. These experiments will help

to answer the question if animals can eat PHA-based plastics and therefore help to degrade plastics in the environment.

Concluding remarks

The data and analysis presented in my thesis show that the classification of PHADs is not as straightforward as previously assumed. Using a non-model organism, like *O. algarvensis*, I was able to identify the first animal PHAD which enabled me to find PHADs in 67 animal species (**Chapter I**). Furthermore, my research highlighted the limitations of homology-based classification for novel PHADs, as exemplified by the misclassification of certain Chromatiales PHADs (**Chapter II**). Lastly, PHA degradation in earthworms might not yield a nutritional advantage given the expression of the PHAD in the worm's epidermis (**Chapter III**). These findings throughout my thesis emphasize the importance of exploring the unusual results, even if they do not align with our initial expectations.

While additional work is needed to identify the benefits for animals from the degradation of naturally occurring PHA and PHA-based plastics, my analyses provided the basis for studying these questions. Throughout my thesis I employed a toolbox composed of computational analysis, such as metatranscriptomics, AlphaFold2 modeling and phylogenetic analysis, to wet-lab based techniques, ranging from fluorescent labeling of PHADs to enzyme assays after enzyme overexpression and purification. These methods allowed me to identify a novel group of animal PHADs. Lastly, my thesis showed that animals can use a microbial storage compound and degrade it to release carbon. Leaving us with the most important question: How does animal PHA degradation influence global carbon cycles?

References

1. Dubilier, N., C. Mülders, T. Ferdelman, D. de Beer, A. Pernthaler, M. Klein, M. Wagner, C. Erséus, F. Thiermann and J. Krieger, *Endosymbiotic sulphate-reducing and sulphide-oxidizing bacteria in an oligochaete worm.* Nature, 2001. **411**(6835): p. 298-302.
2. Kleiner, M., C. Wentrup, C. Lott, H. Teeling, S. Wetzel, J. Young, Y.-J. Chang, M. Shah, N.C. VerBerkmoes and J. Zarzycki, *Metaproteomics of a gutless marine worm and its symbiotic microbial community reveal unusual pathways for carbon and energy use.* Proceedings of the National Academy of Sciences, 2012. **109**(19): p. E1173-E1182.
3. Koller, M., L. Maršálek, M.M. de Sousa Dias and G. Braunegg, *Producing microbial polyhydroxyalkanoate (PHA) biopolyesters in a sustainable manner.* New biotechnology, 2017. **37**: p. 24-38.
4. Fernandez-Castillo, R., F. Rodriguez-Valera, J. Gonzalez-Ramos and F. Ruiz-Berraquero, *Accumulation of poly (β-hydroxybutyrate) by halobacteria.* Applied and Environmental Microbiology, 1986. **51**(1): p. 214-216.
5. Steinbüchel, A. and H. Schlegel, *Physiology and molecular genetics of poly (β-hydroxyalkanoic acid) synthesis in* Alcaligenes eutrophus. Molecular Microbiology, 1991. **5**(3): p. 535-542.
6. Arun, A., R. Arthi, V. Shanmugabalaji and M. Eyini, *Microbial production of poly-β-hydroxybutyrate by marine microbes isolated from various marine environments.* Bioresource Technology, 2009. **100**(7): p. 2320-2323.
7. Wang, J. and L.R. Bakken, *Screening of soil bacteria for poly-β-hydroxybutyric acid production and its role in the survival of starvation.* Microbial Ecology, 1998. **35**: p. 94-101.
8. Khardenavis, A., P. Guha, M.S. Kumar, S. Mudliar and T. Chakrabarti, *Activated sludge is a potential source for production of biodegradable plastics from wastewater.* Environmental Technology, 2005. **26**(5): p. 545-552.
9. Viljakainen, V. and L. Hug, *The phylogenetic and global distribution of bacterial polyhydroxyalkanoate bioplastic-degrading genes.* Environmental Microbiology, 2021. **23**(3): p. 1717-1731.
10. Anderson, I.J., R.F. Watkins, J. Samuelson, D.F. Spencer, W.H. Majoros, M.W. Gray and B.J. Loftus, *Gene discovery in the* Acanthamoeba castellanii *genome.* Protist, 2005. **156**(2): p. 203-14.
11. Jendrossek, D. and R. Handrick, *Microbial degradation of polyhydroxyalkanoates.* Annual Review of Microbiology, 2002. **56**: p. 403.
12. Gonda, K., D. Jendrossek and H.-P. Molitoris, *Fungal degradation of the thermoplastic polymer poly-β-hydroxybutyric acid (PHB) under simulated deep sea pressure*, in *Life at Interfaces and Under Extreme Conditions*. 2000, Springer. p. 173-183.
13. Kim, D. and Y. Rhee, *Biodegradation of microbial and synthetic polyesters by fungi.* Applied Microbiology and Biotechnology, 2003. **61**(4): p. 300-308.
14. Kim, J.K., Y.J. Won, N. Nikoh, H. Nakayama, S.H. Han, Y. Kikuchi, Y.H. Rhee, H.Y. Park, J.Y. Kwon and K. Kurokawa, *Polyester synthesis genes associated with stress resistance are involved in an insect–bacterium symbiosis.* Proceedings of the National Academy of Sciences, 2013. **110**(26): p. E2381-E2389.

15. Lucas, N., C. Bienaime, C. Belloy, M. Queneudec, F. Silvestre and J.-E. Nava-Saucedo, *Polymer biodegradation: Mechanisms and estimation techniques–A review.* Chemosphere, 2008. **73**(4): p. 429-442.
16. Wippler, J., M. Kleiner, C. Lott, A. Gruhl, P.E. Abraham, R.J. Giannone, J.C. Young, R.L. Hettich and N. Dubilier, *Transcriptomic and proteomic insights into innate immunity and adaptations to a symbiotic lifestyle in the gutless marine worm* Olavius algarvensis. BMC Genomics, 2016. **17**(1): p. 1-19.
17. Pfau, T., N. Christian, S.K. Masakapalli, L.J. Sweetlove, M.G. Poolman and O. Ebenhöh, *The intertwined metabolism during symbiotic nitrogen fixation elucidated by metabolic modelling.* Scientific Reports, 2018. **8**(1): p. 12504.
18. Senior, P.J. and E.A. Dawes, *The regulation of poly-beta-hydroxybutyrate metabolism in* Azotobacter beijerinckii. Biochemical Journal, 1973. **134**(1): p. 225-38.
19. Kobayashi, T. and T. Saito, *Catalytic triad of intracellular poly (3-hydroxybutyrate) depolymerase (*PhaZ*1) in* Ralstonia eutropha *H16.* Journal of Bioscience and Bioengineering, 2003. **96**(5): p. 487-492.
20. Eggers, J. and A. Steinbüchel, *Poly (3-hydroxybutyrate) degradation in* Ralstonia eutropha *H16 is mediated stereoselectively to (S)-3-hydroxybutyryl coenzyme A (CoA) via crotonyl-CoA.* Journal of Bacteriology, 2013. **195**(14): p. 3213-3223.
21. Suzuki, M., Y. Tachibana and K.-i. Kasuya, *Biodegradability of poly (3-hydroxyalkanoate) and poly (ε-caprolactone) via biological carbon cycles in marine environments.* Polymer Journal, 2021. **53**(1): p. 47-66.
22. Shrivastav, A., S.K. Mishra, B. Shethia, I. Pancha, D. Jain and S. Mishra, *Isolation of promising bacterial strains from soil and marine environment for polyhydroxyalkanoates (PHAs) production utilizing Jatropha biodiesel byproduct.* International Journal of Biological Macromolecules, 2010. **47**(2): p. 283-287.
23. Rusek, J., *Biodiversity of Collembola and their functional role in the ecosystem.* Biodiversity & Conservation, 1998. **7**: p. 1207-1219.
24. Jurkevitch, E. and Y. Davidov, *Phylogenetic diversity and evolution of predatory prokaryotes*, in *Predatory prokaryotes*. 2006, Springer. p. 11-56.
25. Martínez, V., E. Jurkevitch, J.L. García and M.A. Prieto, *Reward for* Bdellovibrio bacteriovorus *for preying on a polyhydroxyalkanoate producer.* Environmental Microbiology, 2013. **15**(4): p. 1204-1215.
26. Sockett, R.E., *Predatory lifestyle of* Bdellovibrio bacteriovorus. Annual Review of Microbiology, 2009. **63**: p. 523-539.
27. Martínez, V., F. de la Peña, J. García-Hidalgo, I. de la Mata, J.L. García and M.A. Prieto, *Identification and biochemical evidence of a medium-chain-length polyhydroxyalkanoate depolymerase in the* Bdellovibrio bacteriovorus *predatory hydrolytic arsenal.* Applied and Environmental Microbiology, 2012. **78**(17): p. 6017-6026.
28. Burke, J.M., *Wound healing in* Eisenia foetida *(Oligochaeta) II. A fine structural study of the role of the epidermis.* Cell and Tissue Research, 1974. **154**: p. 61-82.
29. Zuriani, R., S. Vigneswari, M. Azizan, M. Majid and A. Amirul, *A high throughput Nile red fluorescence method for rapid quantification of intracellular bacterial polyhydroxyalkanoates.* Biotechnology and Bioprocess Engineering, 2013. **18**: p. 472-478.

30. Konopova, B. and M. Akam, *The Hox genes Ultrabithorax and abdominal-A specify three different types of abdominal appendage in the springtail* Orchesella cincta *(Collembola)*. EvoDevo, 2014. **5**(1): p. 1-14.
31. Nhan, D.T., M. Wille, P. De Schryver, T. Defoirdt, P. Bossier and P. Sorgeloos, *The effect of poly β-hydroxybutyrate on larviculture of the giant freshwater prawn* Macrobrachium rosenbergii. Aquaculture, 2010. **302**(1-2): p. 76-81.
32. Forni, D., C. Wenk and G. Bee, *Digestive utilization of novel biodegradable plastic in growing pigs.* Annales De Zootechnie, 1999. **48**: p. 163-171.
33. Uchino, K., T. Saito, B. Gebauer and D. Jendrossek, *Isolated poly (3-hydroxybutyrate)(PHB) granules are complex bacterial organelles catalyzing formation of PHB from acetyl coenzyme A (CoA) and degradation of PHB to acetyl-CoA.* Journal of Bacteriology, 2007. **189**(22): p. 8250-8256.
34. Uchino, K., T. Saito and D. Jendrossek, *Poly (3-hydroxybutyrate)(PHB) depolymerase* PhaZ*a1 is involved in mobilization of accumulated PHB in* Ralstonia eutropha *H16.* Applied and Environmental Microbiology, 2008. **74**(4): p. 1058-1063.
35. Sznajder, A. and D. Jendrossek, *To be or not to be a poly (3-hydroxybutyrate)(PHB) depolymerase:* PhaZ*d1 (*PhaZ*6) and* PhaZ*d2 (*PhaZ*7) of* Ralstonia eutropha*, highly active PHB depolymerases with no detectable role in mobilization of accumulated PHB.* Applied and Environmental Microbiology, 2014. **80**(16): p. 4936-4946.
36. Abe, T., T. Kobayashi and T. Saito, *Properties of a novel intracellular poly (3-hydroxybutyrate) depolymerase with high specific activity (*PhaZ*d) in* Wautersia eutropha *H16.* Journal of Bacteriology, 2005. **187**(20): p. 6982-6990.
37. Braunegg, G., B. Sonnleitner and R. Lafferty, *A rapid gas chromatographic method for the determination of poly-β-hydroxybutyric acid in microbial biomass.* European Journal of Applied Microbiology and Biotechnology, 1978. **6**: p. 29-37.
38. Porter, K., J. Orcutt Jr and J. Gerritsen, *Functional response and fitness in a generalist filter feeder,* Daphnia magna *(Cladocera: Crustacea).* Ecology, 1983. **64**(4): p. 735-742.
39. Evans, R., M. O'Neill, A. Pritzel, N. Antropova, A. Senior, T. Green, A. Žídek, R. Bates, S. Blackwell and J. Yim, *Protein complex prediction with AlphaFold-Multimer.* BioRxiv, 2021: p. 2021.10. 04.463034.
40. Jumper, J., R. Evans, A. Pritzel, T. Green, M. Figurnov, O. Ronneberger, K. Tunyasuvunakool, R. Bates, A. Žídek, A. Potapenko, A. Bridgland, C. Meyer, S.A.A. Kohl, A.J. Ballard, A. Cowie, B. Romera-Paredes, S. Nikolov, R. Jain, J. Adler, T. Back, S. Petersen, D. Reiman, E. Clancy, M. Zielinski, M. Steinegger, M. Pacholska, T. Berghammer, S. Bodenstein, D. Silver, O. Vinyals, A.W. Senior, K. Kavukcuoglu, P. Kohli and D. Hassabis, *Highly accurate protein structure prediction with AlphaFold.* Nature, 2021. **596**(7873): p. 583-589.
41. Varadi, M., S. Anyango, M. Deshpande, S. Nair, C. Natassia, G. Yordanova, D. Yuan, O. Stroe, G. Wood, A. Laydon, A. Žídek, T. Green, K. Tunyasuvunakool, S. Petersen, J. Jumper, E. Clancy, R. Green, A. Vora, M. Lutfi, M. Figurnov, A. Cowie, N. Hobbs, P. Kohli, G. Kleywegt, E. Birney, D. Hassabis and S. Velankar, *AlphaFold Protein Structure Database: massively expanding the structural coverage of protein-sequence space with*

high-accuracy models. Nucleic Acids Research, 2021. **50**(D1): p. D439-D444.

42. Reddy, C., R. Ghai and V.C. Kalia, *Polyhydroxyalkanoates: an overview.* Bioresource Technology, 2003. **87**(2): p. 137-146.
43. Hisano, T., K. Kasuya, Y. Tezuka, N. Ishii, T. Kobayashi, M. Shiraki, E. Oroudjev, H. Hansma, T. Iwata, Y. Doi, T. Saito and K. Miki, *The crystal structure of polyhydroxybutyrate depolymerase from* Penicillium funiculosum *provides insights into the recognition and degradation of biopolyesters.* Journal of Molecular Biology, 2006. **356**(4): p. 993-1004.
44. Ross, C.M., G. Foley, M. Boden and E.M. Gillam, *Using the evolutionary history of proteins to engineer insertion-deletion mutants from robust, ancestral templates using graphical representation of ancestral sequence predictions (GRASP).* Enzyme Engineering: Methods and Protocols, 2022: p. 85-110.
45. Lautier, T., P. Ezanno, C. Baffert, V. Fourmond, L. Cournac, J.C. Fontecilla-Camps, P. Soucaille, P. Bertrand, I. Meynial-Salles and C. Léger, *The quest for a functional substrate access tunnel in FeFe hydrogenase.* Faraday Discussions, 2011. **148**: p. 385-407.
46. Mason-Jones, K., C.C. Banfield and M.A. Dippold, *Compound-specific 13C stable isotope probing confirms synthesis of polyhydroxybutyrate by soil bacteria.* Rapid Communications in Mass Spectrometry, 2019. **33**(8): p. 795-802.
47. Madison, L.L. and G.W. Huisman, *Metabolic engineering of poly (3-hydroxyalkanoates): from DNA to plastic.* Microbiology and Molecular Biology Reviews, 1999. **63**(1): p. 21-53.
48. Müller, H.M. and D. Seebach, *Poly (hydroxyalkanoates): a fifth class of physiologically important organic biopolymers?* Angewandte Chemie International Edition in English, 1993. **32**(4): p. 477-502.
49. Lee, S.Y. and J.-i. Choi, *Production and degradation of polyhydroxyalkanoates in waste environment.* Waste Management, 1999. **19**(2): p. 133-139.
50. Jendrossek, D., *Extracellular polyhydroxyalkanoate (PHA) depolymerases: the key enzymes of PHA degradation.* Biopolymers Online: Biology Chemistry Biotechnology Applications, 2005. **3**.
51. Volova, T., A. Boyandin, A. Vasiliev, V. Karpov, S. Prudnikova, O. Mishukova, U. Boyarskikh, M. Filipenko, V. Rudnev and B.B. Xuân, *Biodegradation of polyhydroxyalkanoates (PHAs) in tropical coastal waters and identification of PHA-degrading bacteria.* Polymer Degradation and Stability, 2010. **95**(12): p. 2350-2359.
52. Eybe, T., T. Bohn, J. Audinot, T. Udelhoven, H. Cauchie, H. Migeon and L. Hoffmann, *Uptake visualization of deltamethrin by NanoSIMS and acute toxicity to the water flea* Daphnia magna. Chemosphere, 2009. **76**(1): p. 134-140.
53. Dris, R., H. Imhof, W. Sanchez, J. Gasperi, F. Galgani, B. Tassin and C. Laforsch, *Beyond the ocean: contamination of freshwater ecosystems with (micro-) plastic particles.* Environmental Chemistry, 2015. **12**(5): p. 539-550.
54. Lebreton, L.C., J. Van Der Zwet, J.-W. Damsteeg, B. Slat, A. Andrady and J. Reisser, *River plastic emissions to the world's oceans.* Nature Communications, 2017. **8**(1): p. 15611.

55. Brandon, J.A., W. Jones and M.D. Ohman, *Multidecadal increase in plastic particles in coastal ocean sediments.* Science Advances, 2019. **5**(9): p. eaax0587.
56. Hurley, R., A. Horton, A. Lusher and L. Nizzetto, *Plastic waste in the terrestrial environment*, in *Plastic Waste and Recycling*. 2020, Elsevier. p. 163-193.
57. Dilkes-Hoffman, L.S., P.A. Lant, B. Laycock and S. Pratt, *The rate of biodegradation of PHA bioplastics in the marine environment: A meta-study*. Marine Pollution Bulletin, 2019. **142**: p. 15-24.
58. Rodríguez, T., D. Represas and E.V. Carral, *Ecotoxicity of Single-Use Plastics to Earthworms.* Environments, 2023. **10**(3): p. 41.
59. Bombelli, P., C.J. Howe and F. Bertocchini, *Polyethylene bio-degradation by caterpillars of the wax moth* Galleria mellonella. Current Biology, 2017. **27**(8): p. R292-R293.
60. Billen, P., L. Khalifa, F. Van Gerven, S. Tavernier and S. Spatari, *Technological application potential of polyethylene and polystyrene biodegradation by macro-organisms such as mealworms and wax moth larvae.* Science of the Total Environment, 2020. **735**: p. 139521.

Acknowledgements

My thesis would not have been possible without the support and love from my family, colleagues and friends over the past years.

I would like to start by thanking **Prof. Dr. Nicole Dubilier** for the chance to work in your Department. Thank you for the support throughout the years! Thank you for giving me the chance to work on such an interesting project, for giving me the opportunity to go on field trips and conferences, and thank you for reviewing my thesis.

Dr. Maggie Sogin thank you for supervising me over the years even though starting your own group in the US. Thank you for always being there for my question, going through my super long and wordy sentences and for getting up early for our meetings. Thank you for the wonderful discussions we had.

Many thanks to **Prof. Dr. Tilmann Harder** and **Assoc. Prof. Dr. Jillian Petersen** for agreeing to review my thesis and for joining my examination board.

I would also like to thank **Prof. Dr. Michael Friedrich, Dr. Luis Humberto Orellana** and **Guillermo Cera** for being in my thesis committee.

Dr. Tristan Wagner, thank you for showing me a glimpse of your knowledge about enzyme structures.

Thank you to current and past members at the MPI for organizing field trip and other everyday life challenges. Thank you to **Alexandra Krüger, Susanne Krüger, Ulrike Tietjen, Tina Peters, Gabriele Lothringer, Ralf Schwenke, Dr. Christiane Glöckner, Anita Tingeberg** and **Martina Patze.**

I would like to thank former and present members of the **Symbiosis Department**. Thank you for so many fruit full discussions that helped to improve my sciences and that helped me to grow as a scientist.

Special thanks to all the technicians that accompanied me throughout the years. Thanks to **Miriam, Silke, Anja, Wiebke, Janine** and **Tomasz**. Thank you **Carolin,** for being my queen of earthworms and keeping them alive. Team Caro! Thanks to **Martina** for your help and wisdom in anaerobic culturing. Without your help I would not have been able to finish the last experiment.

Dolma, thank you for your advice throughout the years. Thank you for many discussions concerning the strange things that *Olavius* does. Thanks for proofreading parts of my thesis.

Tina and **Anna,** thank you for welcoming me five years ago in your office. Thank you for your advice throughout the years, for the nice office cooking evenings and the discussions about gutless oligochaetes.

Grace, thank you for being such a nice office mate and for all the fun. Thanks for being there for me when I needed you.

Jero, thank you for always being so kind, your positivity and support.

Alex, thank you for introducing me to the zoology of gutless oligochaetes and imaging.

Harald, I really enjoyed learning your wisdom about phylogenies and discussing the evolution of PHADs.

Manuel, thank you for so many questions and insights in the metabolism of gutless oligochaetes.

Manuel and **Marlene**, thank you for all your efforts in trying to find the PHAD in the metaproteomes and the critical discussions during my thesis committee meetings.

I would like to thank **Miriam Weber, Christian Lott** and the **HYDRA-team,** for their support during field trips. Thanks to **Dr. Bruno Hüttel** and **Roland Dietrich** for the sequencing support and the help at the cologne cluster.

Without the love of my friends I would not have been able to finish my PhD. **Johanna** and (Jan von) **Arx** thank you for always supporting me. Thanks for the brunches that ended up in dinners and the laughters we had. Thanks for proofreading parts of my thesis. **Linda**, I am so happy we met again in Bremen. Thanks for the cooking evenings we had with all the memories from our time at the Schutzstation.

Finally, the biggest thank you goes to my family.
Danke **Mama** und **Papa**, dass ihr immer an mich Glaubt. Danke, dass ihr mich in allem Unterstützt habt, selbst wenn es noch so eine Schnapsidee war. Danke, dass ich immer ein offenes Ohr bei euch habe und ihr mein Drama ganz schnell auffangt. Ich verdanke euch soviel!

Oma und **Opa**, danke dass ihr immer an mich geglaubt habt. Danke für eure Unterstützung und eure Liebe. Danke, dass ihr immer da seid für mich.

Oma Nantsche, danke für all deine Liebe und Stärke die du mir gegeben hast. Du bist der ehrgeizigste Mensch den ich kenne. Danke, dass du davon nur ein bisschen an mich abgegeben hast.

Danke an **Opa Rudel** und **Onkel Herbert**. Leider seid ihr nicht mehr bei mir aber ihr habt mich in meinem Leben inspiriert.

Last but not least, **David**, danke dass du der beste Bruder der Welt bist. Danke, dass du mich immer zum Lachen bringst und immer für mich da bist. Danke, dass du mich in der letzten Phase der Doktorarbeit so unterstützt hast und mein Life-Manager warst.

Contributions to manuscripts and co-authorships

First author manuscripts

Name of the candidate: Caroline Zeidler

Title of the thesis: "Bioplastic-eating animals: Polyhydroxyalkanoate degrading enzymes in a chemosymbiotic worm"

Contribution of the candidate in percentage of the total workload (up to 100% for each of the following categories):

Chapter I "Animals degrade the bioplastic polyhydroxyalkanoate"

Manuscript in preparation

Contribution

Conceptual design: ca. 80%

Data acquisition and experiments: ca. 85%

Analysis and interpretation of results: ca. 90%

Preparation of figures and tables: ca. 90%

Writing the manuscript: ca. 80%

Chapter II "Can Chromatiales bacteria degrade their own PHA?"

Manuscript in preparation

Contribution

Conceptual design: ca. 90%

Data acquisition and experiments: ca. 90%

Analysis and interpretation of results: ca. 95%

Preparation of figures and tables: ca. 90%

Writing the manuscript: ca. 90%

Chapter III "Earthworms degrade the bioplastic polyhydroxyalkanoate"

Manuscript in preparation

Contribution

Conceptual design: ca 90%

Data acquisition and experiments: ca 90%

Analysis and interpretation of results: ca 95%

Preparation of figures and tables: ca 95%

Writing the manuscript: ca 95%

Co-authorships (not included in the thesis):

Michellod, Dolma, Tanja Bien, Daniel Birgel, Marlene Violette, Manuel Kleiner, Sarah Fearn, **Caroline Zeidler**, Harald R. Gruber-Vodicka, Nicole Dubilier, and Manuel Liebeke. "De novo phytosterol synthesis in animals." *Science* 380, no. 6644 (2023): 520-526.

Contribution: Contribution to collection and preparation of the metatranscriptomes and heterologous expression and protein purification.

Insurance in Lieu of oath

Universität Bremen

Universität Bremen | Fachbereich 02 | Postfach 33 04 40, 28334 Bremen

Universität Bremen
Fachbereich 2
Prüfungsamt Chemie
z. Hd. Frau Frauke Ernst
Leobener Straße

28359 Bremen
Deutschland

Prüfungsamt
Chemie

Frauke Ernst
Geschäftsstelle
Fachbereich 02
Leobener Str. / NW2
D-28359 Bremen

Verwaltungspavillon 06
Tel. 0421 218-62802
Fax 0421 218-9862802
frauke.ernst@uni-bremen.de
www.fb2.uni-bremen.de

Versicherung an Eides Statt

Name, Vorname	Zeidler, Caroline
Matrikel-Nr.	3118248
Straße	
Ort, PLZ	

Ich, Caroline, Zeidler (Vorname, Name)

versichere an Eides Statt durch meine Unterschrift, dass ich die vorstehende Arbeit selbständig und ohne fremde Hilfe angefertigt und alle Stellen, die ich wörtlich dem Sinne nach aus Veröffentlichungen entnommen habe, als solche kenntlich gemacht habe, mich auch keiner anderen als der angegebenen Literatur oder sonstiger Hilfsmittel bedient habe.
Ich versichere an Eides Statt, dass ich die vorgenannten Angaben nach bestem Wissen und Gewissen gemacht habe und dass die Angaben der Wahrheit entsprechen und ich nichts verschwiegen habe.
Die Strafbarkeit einer falschen eidesstattlichen Versicherung ist mir bekannt, namentlich die Strafandrohung gemäß § 156 StGB bis zu drei Jahren Freiheitsstrafe oder Geldstrafe bei vorsätzlicher Begehung der Tat bzw. gemäß § 161 Abs. 1 StGB bis zu einem Jahr Freiheitsstrafe oder Geldstrafe bei fahrlässiger Begehung.

_____

Ort, Datum/Unterschrift